THE UNIVERSITY OF HULL

# On the transport mechanisms, ecological interactions, and fate of microplastics in aquatic environments

A Thesis submitted for the

Degree of Doctor of Philosophy (PhD)

Energy and Environment Institute,

University of Hull

By

Freija Mendrik BSc. MSc.

June 2022

[Page intentionally left blank]

# Thesis Abstract

Degree of Doctor of Philosophy (PhD)

UNIVERSITY OF HULL

## On the transport mechanisms, ecological interactions, and fate of microplastics in aquatic environments

By Freija Mendrik

Microplastics are now persistent throughout aquatic systems globally and can cause a range of ecological damage. The transport of microplastics is influenced by the polymer type, in addition to physical, biological, and chemical gradients plastic particles move through as they are transported across freshwater to marine environments. The combined influence of these mechanisms on microplastic fate is largely unquantified, which prevents the accurate identification of accumulation zones and the related development of effective mitigation measures. This research applies a multidisciplinary approach that combines innovative experiments and physical modelling with detailed fieldwork to quantify the main factors influencing microplastic transport and fate. Using a suite of novel settling experiments, biofouling is shown to be a principal factor affecting microplastic deposition through changes in specific density. Yet settling regimes differ depending on polymer and shape as well as ambient sediment and salinity concentrations. To understand particle distribution further, abundances and fluxes of microplastics within a large river system are coupled with hydrological data to explore how microplastics are transported through the vertical water column, finding that most are dispersed below the water surface, yet concentration is dependent on seasonal discharge. Finally, the role of complex coastal ecosystems as a sink for microplastics is investigated in a hydraulic flume under a range of flow conditions. It is shown, for the first time, that microplastic trapping efficiency could be high for both sparse and dense coral canopies due to a reduction in streamwise velocities causing settling on, within, and behind coral structures. It is concluded that although sediment laws can provide a basic understanding of microplastic transport, a new generation of microplastic transport regimes is needed. The findings from the thesis enhance our knowledge of the complex mechanisms that govern microplastic transport and fate in aquatic environments and this new understanding is contextualised in terms of their broad ecological implications.

Total word count (not including reference list) 51,298.

[Page intentionally left blank]

# Acknowledgements

This research would not have been possible without the support of many people. First and foremost, I would like to thank my supervisors, Prof. Dan Parsons, Dr. Chris Hackney, and Dr. Cath Waller for their continuous support, invaluable advice, and guidance throughout my PhD. Dan, you gave me this opportunity in the first place for which I will be forever grateful. Your ambition has made me believe I can do so much more than I ever imagined with this research. Chris, you have always had so many brilliant ideas and great advice to assist me through all the stages of this work. Thank you for giving me the opportunity to be part of the River of Plastic Project, which has led to so many exciting opportunities. Cath, your continued support and words of encouragement, especially during lockdown, spurred me on during the hardest moments. I feel so fortunate to have had such a great team, thank you!

To our colleagues overseas at the Southern Institute of Water Resources Research and Can Tho University, Vietnam, and the Institute of Technology of Cambodia, especially of course to wonderful Ben for your kindness and wisdom. Thank you all for your hospitality and support that enabled me to do my fieldwork.

It's been such a pleasure to be a part of the Energy and Environment Institute, from day one I have felt welcomed and I have made friends that I'm sure will be with me for life. There are far too many of you to name individually, but you all know who you are and that I couldn't have done it without you! I do have to mention Dr. Flo though, for your endless positivity, helping me believe in myself, and continuously inspiring me. Our daily catchups have helped me in so many ways. Then of course Jack, we started this microplastics PhD journey (ha!) together and I can't imagine it without you. From the beach cleans, to Earth2050 and venting about long hours on the FT-IR.

To friends and family, thank you for your patience and understanding over these four years and for providing a much-needed escape!

To mum, your sacrifices have enabled me to achieve this. Thank you for sharing your love of the ocean and your creativity with me. It hasn't been easy, but you have always made me believe I could do anything if I put my mind to it. You are the strongest person that I know and have taught me since I was little to never give up. This is for you.

Finally, to Eric. For the endless cups of tea, consoling me when it's all gotten too much, and reassuring me I've done my maths right! You have never questioned the long nights or moving halfway across the country for me to do this. I can't thank you enough for your endless support, encouragement, and patience.

[Page intentionally left blank]

# COVID-19 impact statement

This PhD was intended to be substantially fieldwork-based, with the main focus on the Mekong River of Cambodia and Vietnam. Data collection was to include sampling water further north in Tonlé Sap Lake, Cambodia, and south in the Mekong Delta, in addition to collecting various fish species to be analysed for microplastic ingestion allowing ecological analysis. The COVID-19 pandemic began during the second year of my PhD, with the final two field trips of my project planned for March and July 2020 having to be cancelled. Thankfully, one field trip had already been completed in 2019, with enough data to form Chapter 5 of this thesis.

As a core part of my PhD was planned to be field-based, we had to change a substantial part of the project in response to COVID-19, adding more laboratory experiments and computer-based work to the project. During the first lockdown (March 2020 onwards) the microplastic settling experiments of Chapter 3 were conceptualised and developed and began once laboratories were open (September 2020). The settling experiments were completed in February 2021. During that time, there was still a lot of uncertainty surrounding COVID-19 and travel restrictions, so fieldwork plans remained for the summer of 2021 with the hope of forming a second research chapter. However, it soon became apparent that this would not be possible, so the microplastic trapping experiments (Chapter 6) were developed and began in November 2021.

COVID-19 also caused several other delays within the laboratory. New equipment that was ordered during this time and was necessary for polymer analysis of microplastic samples (FT-IR spectroscopy) was delayed in getting to the University. Furthermore, once it had arrived it was in such high demand it resulted in further delays to the analysis of my Mekong samples, which were not completed until April 2022.

I am very grateful that I was awarded an extension from the University of Hull that allowed me to complete this thesis.

# Contribution statement

Chapter 4 “The shifting settling regimes of aquatic microplastics” has been accepted to Nature Communications Earth & Environment subject to revisions and therefore a contribution statement is necessary for this chapter. The PhD candidate led the experimental design, experimental process, data analysis, writing, and review. Dr. Roberto Fernández supported the experimental design and process and designed the code for the data analysis that the PhD candidate led in utilising. Dr. Christopher Hackney and Prof. Daniel Parsons also aided in the experimental design. All authors, including Dr. Catherine Waller, commented on the manuscript and helped shape the narrative.

I would also like to thank my examiners Prof. Jamie Woodward and Dr. Katherina Wollenberg Valero for their time, insightful comments, questions and discussion of this thesis, which very much helped improve it.

# Contents

# Nomenclature

| Symbol | Unit | Description |
|---|---|---|
| $A$ | $m^2$ | Cross-sectional area |
| ADV | - | Acoustic Doppler current profiler |
| $C_{mp}$ | # per $m^3$ | Concentration of microplastics |
| $D$ | mm | Diameter |
| DI | - | Deionised |
| $d_s$ | mm | Base diameter |
| EPS | - | Extracellular polymeric substance |
| $D_e$ | mm | Equivalent diameter |
| FT-IR | - | Fourier transform infrared |
| $g$ | $m/s^2$ | Acceleration due to gravity |
| $h_c$ | m | Canopy height |
| HDPE | - | High-density polyethylene |
| $h_v$ | m | Overall height |
| $h_v/h_w$ | - | Submergence ratio |
| $h_w$ | m | Standing water depth |
| LabSFLOC | - | Laboratory Spectral Flocculation Characteristics |
| LDPE | - | Low-density polyethylene |
| $n_{mp}$ | - | Number of microplastics |
| NP&A | - | Nylon, polyester, and acrylic |
| PAN | - | Polyacrylonitrile |
| PET | - | Polyethylene terephthalate |
| PP | - | Polypropylene |
| PS | - | Polystyrene |
| PTV | - | Particle Tracking Velocimetry |
| PVC | - | Polyvinyl chloride |
| Q | $m^3/s$ | Discharge, $m^3/s$ |
| $R$ | - | Submerged specific gravity |
| SAL | ppm | Salinity |
| SEM | - | Scanning electron microscope |
| $t$ | s | Length of sampling |
| TKE | J/Kg | Turbulent kinetic energy |
| $U$ | m/s | Bulk incoming velocities |
| $V$ | $m^3$ | Volume of water |
| $v$ | m/s, | Flow velocity |
| v | $m^2/s$ | Kinematic viscosity |
| WWTP | - | Wastewater treatment plant |
| $w$ | mm/s | Settling velocity of microplastic |

[Page intentionally left blank]

# Chapter 1.

# Introduction

## 1.1 Research context and rationale

Global environmental changes caused by human activity suggests that the Earth has entered the Anthropocene, a new geological epoch (Lewis and Maslin, 2015). A key geological indicator of the Anthropocene is plastic pollution as it is now so abundant and widespread (Zalasiewicz et al., 2016). Plastic is a lightweight and durable material that is cheap to manufacture and has become a favourable every-day commodity, resulting in the "age of plastics" (Avio *et al.,* 2017). Most societies worldwide rely on plastic products and there is currently no indication that the production of these synthetic polymers, derived from crude oil, will decline (Mendoza and Balcer, 2018). As plastics are both easily discarded and durable, a worldwide environmental threat has emerged, with marine plastic pollution gaining a high amount of public attention. Marine plastic debris was first reported in the 1970s but has been researched extensively since the early 2000s ( e.g. Thompson *et al.,* 2004; do Sul and Costa, 2007). While maritime activities such as recreational and commercial fishing contribute a large amount to marine plastic debris, the majority arrive from land-based sources, with rivers acting as an important transport pathway (Schmidt *et al.,* 2017). Mismanaged waste highly influences both macroplastic (>5 mm) and microplastic (<5 mm) riverine load (Schmidt et al., 2017). As a result, ecosystems are being contaminated worldwide with numerous adverse repercussions for organisms including entanglement and reduced survival rates (Chiba *et al.,* 2018; Derraik, 2002; Munari *et al.,* 2017). Furthermore, plastic pollution directly impacts economies, with the Asia-Pacific Economic Cooperation (APEC) estimating that marine plastic pollution has created a cost to shipping, fishing, and tourism in the region of $1.3bn, for example when debris becomes entangled in a ship's propellers (UNEP, 2014).

There remains a lack of international regulation concerning the prevention of plastic pollution. Despite the 1994 United Nations Convention on the Law of the Sea (UNCLOS) recognising six different sources of marine pollution, including land-based, States are directed to adopt their own regulations, leading to considerable discrepancy. In terms of plastic pollution generated at sea, the 1973 International Convention for the Prevention of Pollution from Ships (MARPOL) and the 1978 Protocol to MARPOL were created to address gaps in previous instruments regarding marine pollution and has 160 signatories. Annex V of MARPOL (revised in 2011, entering into force in 2013) specifically prohibits the disposal of plastics anywhere at sea. However, compliance remains a concern, with a lack of implementation and regulation in numerous countries. The United Nations Environmental Program (UNEP), has identified marine plastic pollution as one of the most critical risks to the environment (UNEP, 2014), yet although none of the Sustainable Development Goals (SDGs) has plastic pollution as the main focus, several SDGs include preventing plastic pollution entering the environment, the associated health risks and absolute reduction in plastic pollution. Examples of SDGs that indirectly deal with plastic pollution are: no poverty (SDG 1), promotion of good health and well-being (SDG 3), clean water and sanitation (SDG 6), industry, innovation and infrastructure (SDG 9), reduced inequality (SDG 10), responsible consumption and production (SDG 12) and climate action (SDG 13). Yet SDG 14 particularly addresses plastic pollution with its aim to conserve and sustainably use marine resources. Recently, at the UN Environment Assembly (UNEA) in Nairobi, 175 nations agreed to develop a global plastics treaty to end plastic pollution and encourage a circular economy.

Despite the growing research regarding plastic debris and governance structures, there are significant knowledge gaps concerning the understanding of the main sources and movement of plastic pollution within riverine settings, which therefore hinders the development of mitigation measures. A strong bias towards marine plastic research remains with many knowledge gaps in regards to sources, transport, flux, sinks, and ecological risk in

riverine and delta systems and how the transition from freshwater to marine influences plastic movement.

### 1.1.2 Riverine input of plastic debris

Land-based sources and rivers are considered the dominant pathways of plastics into the sea and therefore transport mechanisms within rivers must be fully understood to curtail the plastic pollution crisis (Hurley et al., 2018; Lebreton et al., 2017; Meijer et al., 2021)**.** Population density, urban land use and the characteristics of a catchment strongly influence plastic pollution concentration and loads within a river (Schmidt, *et al.,* 2017). Buoyant and non-buoyant plastics can be suspended throughout the river water column and transported to the ocean due to large flood events and turbulent river flows (Hurley *et al.,* 2018; Nizzetto *et al.,* 2016a). However, there is a lack of information to link sources, riverine transport, and deposition processes in the plastic pathway and distribution to the oceans (Eerkes-Medrano, *et al.,* 2015; Besseling *et al.,* 2017; Kataoka *et al.,* 2019). To develop effective mitigation measures and prevention strategies, an understanding of the role of rivers in plastic transport is vital. The “missing plastic” problem still exists whereby there is a mismatch between a large amount of estimated plastic input into the oceans and the low numbers actually observed during field campaigns (Thompson, *et al.,* 2004). Therefore, there remains many unanswered questions on the fate of plastic pollution in aquatic environments and the key factors that influence plastic transport.

There have been attempts to quantify the abundance of plastics being discharged by rivers into the ocean globally, some of which relied on empirical indications that represent waste generation within river basins (Lebreton *et al.,* 2017; Schmidt *et al.,* 2017). Lebreton *et al.,* (2017) estimated that the global annual input of plastic from rivers to be 1.15-2.41 million tonnes with the majority from 20 top polluting rivers. However, predictions have contradicted one another, with a more recent model estimating that more than 1,000 rivers are accountable for 80% of plastic waste entering the ocean and that small urban rivers

contribute the most (Meijer *et al.,* 2021). Both Lebreton *et al.,* (2017) and Schmidt, Krauth, and Wagner, (2017) concluded the disproportional contribution from Asian rivers. Relatively large mismanaged plastic waste (MPW) production rates, a considerably high population density, and episodes of heavy rainfall driven by the East Asian monsoon are speculated to cause this overriding contribution from Asia (Lebreton *et al.,* 2017). In addition, the Western world continues to ship plastic waste to developing countries, including those in Southeast Asia despite several bans being in place (Uhm, 2020). Most riverine plastic studies have not been carried out in this area and there is therefore a lack of data to inform policy and decision-makers. Furthermore, studies do not consider macro- and microplastic fallout such as settling on the riverbed or entrapment in vegetation and other complex structures on the coast such as coral reefs. Recently, studies have begun to investigate the role of aquatic ecosystems including seagrass meadows, mangroves, saltmarshes, and corals in retaining microplastics, through field measurements and experiments (Cozzolino *et al.,* 2020; de los Santos *et al.,* 2021a; Y. Huang *et al.,* 2021; Li *et al.,* 2018; Stead *et al.,* 2020; Unsworth *et al.,* 2021). This research demonstrated how these various ecosystems could trap microplastics and act as potential sinks, yet the transport and depositional processes that determine the trapping efficiency of aquatic canopies are very limited. This highlights the scarcity of data on microplastic transport from rivers to coastal regions and the ocean and the need for further research in these areas.

As the majority of riverine plastic input is often predicted to originate from Asia and as rapid population growth and poor waste management continue, it is paramount that more research and effective monitoring and mitigation efforts are formed there. The field component of this research focuses on one such river: the Mekong. The Mekong River is the 10$^{th}$ largest river in the world by volume of discharge, flowing for more than 4,000 km but has also been predicted to be one of the top riverine plastic contributors to the ocean with an upper mass input estimate of 3.76x10$^{4}$ tonnes/year (Kummu and Sarkkula, 2008; Lebreton *et al.,* 2017). Originating in the Tibetan Plateau, over 5,100 m above sea level, the Mekong

River flows through China's Yunnan Province into Myanmar, Laos, Thailand, and Cambodia before discharging in the South China Sea via numerous distributaries within its delta which is predominantly in Vietnam (Ziv *et al.,* 2012). The annual Mekong flood pulse is the driving force of the highly productive ecological area of the Mekong delta (Campbell, 2009). The Lower Mekong Basin is strongly influenced by two distinct monsoon seasons: the dry north-east monsoon season, from November to May, and the rainy south-west monsoon season from June to October (Xue *et al.,* 2011). It is therefore expected that the largest plastic flux in the Mekong River will occur during the rainy monsoon season.

The Mekong Basin is also socioeconomically important, home to more than 70 million people, and continues to undergo rapid economic development and population growth (Xue *et al.,* 2011). Furthermore, the Mekong is one of the world's most important rivers due to the vast ecological resources it contains, supporting some of the highest diversities of fish globally with more than 1,000 species, and one of the world's largest inland fisheries (Campbell, 2009). The area is highly dependent on the river for its economy, supporting numerous livelihoods with agriculture and energy production through hydropower (Li *et al.,* 2017). The Mekong River's most basic hydrological feature is the flood pulse with a dominance of a large mean annual discharge that is concentrated in a single wet season peak. It is also highly influenced by Tonlé Sap Lake (Cambodia), the largest freshwater lake in Southeast Asia, with over a million people relying on its natural resources (Campbell, 2009; Kummu and Sarkkula, 2008; Räsänen *et al.,* 2017). Tonlé Sap Lake is a dynamic flood-pulsed ecosystem as a result of the seasonal flooding of the Mekong River and annually increases from 2,500 $km^2$ to over 12,500 $km^2$ (Holtgrieve *et al.,* 2013). The annual fish migration between Tonlé Sap and the Mekong River provides communities throughout the Mekong Basin with a reliable source of nutrition and protein (Li *et al.,* 2017).

The amount of plastic discharged from the Mekong River is likely to grow as the population increases in the future will drive the use of plastics in countries where effective waste management, recycling, and alternative materials are lacking. Although predictions

have been made concerning the high amount of plastic discharge from the Mekong, only one study has been conducted around Phnom Penh, Cambodia (Haberstroh *et al.,* 2021a). No systematic study of plastic transport and its ecological effects exists at multiple points throughout the Mekong River, in addition to a general lack of research conducted in freshwater and delta systems**.**

Despite the widespread recognition that rivers dominate the global flux of plastics to the ocean, there is a key knowledge gap regarding the nature of the flux, the behaviour of microplastics in transport, and pathways from rivers into the ocean (Horton et al., 2017c). To predict the transport, fate, and ecological risk of microplastics in aquatic environments at a global scale, the factors that control these processes must be identified and understood. This includes quantifying the drivers that may affect particle density, such as biofouling, salinity, and aggregation as a microplastic moves from freshwater to marine environments. Increased monitoring of microplastic abundance throughout riverine systems is needed worldwide to fully understand plastic discharge into the ocean. Furthermore, the role of coastal ecosystems such as mangroves and coral reefs as sinks for microplastics remains largely unknown. This prevents progress in understanding microplastic accumulation and fate, as well as curtailing the development of effective mitigation and policy measures.

## 1.2 Research aims and objectives

To understand the movement and fate of microplastics in aquatic environments, a multidisciplinary approach is necessary, which should include fieldwork, laboratory analysis, and experimental aspects. The previous sections revealed several research gaps, which are related to the following main research aim and aligned questions of this thesis. The overarching research aim of this thesis is to:

*Evaluate and determine the key controlling factors that influence microplastic fate in aquatic environments.*

This overarching aim will be delivered by addressing a set of 4 interrelated research questions:

**Research question 1:** How does polymer type and biofilm formation affect the transport of microplastics through influences on density?

**Research question 2:** How do changes in water conditions (such as freshwater to marine salinity gradients) and suspended sediment alter how microplastics settle?

**Research question 3:** How are microplastics distributed throughout major rivers and how does this influence ecological risk?

**Research question 4:** How do structurally complex ecosystems such as coral reefs control the transport, fate, and sinking dynamics of microplastics from a riverine environment?

## 1.3 Thesis structure

This thesis contains seven chapters; this introduction is followed by a literature review (Chapter 2), laboratory and field methodology (Chapter 3), and experimental and fieldwork-based research that systematically investigates the settling and transport dynamics of microplastics. These results are detailed in Chapters 4, 5, and 6, which each contain focused literature reviews aligned with the content of each chapter. Concluding remarks and a synthesis of the research are given in Chapter 7. Comprehensive introductions are provided for each research chapter and are briefly introduced here:

**Chapter 4: The shifting settling regimes of aquatic microplastics**

To predict the transport, fate, and biological interactions of microplastics in aquatic environments at a global scale, the factors that control these processes must be identified and understood. It is assumed that plastic pollution persists for decades due to its durability and the fact that more than 50% of produced polymers are less dense than seawater (Andrady, 2011). However, the observed global load of floating plastics on the ocean surface

is much lower than predicted (Cózar et al., 2014; Eriksen et al., 2014). It has been argued that microplastics are deposited in a similar way to other well-studied particles such as sediments; but compared to sediment mobility, microplastic transport and deposition behaviour varies in terms of polymer density, particle shape, and other mechanisms including biofouling (Stock *et al.,* 2019). Although it is known that biota ingest and egest microplastics, in addition to acting as a vector for bioaccumulation through food webs, research into the impacts of biofouling is still developing. Biofouling is the accumulation of organisms on submerged surfaces and when occurring on microplastics can affect the buoyancy and hydrophobicity of the particle (Lobelle and Cunliffe, 2011). A plausible explanation for the “missing” plastic is that fouling by macro and microorganisms can increase the average material density of plastic fragments, overcoming the positive buoyance and causing them to sink (Fazey and Ryan, 2016). In addition, biofouling formation and sinking velocities are highly dependent on salinity and therefore will vary between freshwater, delta, and marine environments (Kaiser et al., 2017). A settling experiment is therefore proposed measuring the settling velocity of “clean” and biofilmed (community of microorganisms adhered to a surface) microplastics of various polymers under different salinities that replicate a particle moving from a freshwater to a marine environment, in addition to several concentrations of suspended sediment. This will address research questions 1 and 2.

**Chapter 5**: **The transport and vertical distribution of microplastics in a major delta: a case study in the Mekong River, Southeast Asia**

Currently, there is a large knowledge gap for measuring and predicting the transport of microplastics in major rivers, despite riverine transport being identified as a key source of marine microplastic pollution. The results from the physical settling experiments will provide an understanding of the transport mechanisms that influence microplastic fate, which can be used to predict microplastic distribution in aquatic systems. However, the distribution of

microplastics in the water column is also highly influenced by environmental factors such as turbulence, discharge, currents, and wind (Prata *et al.,* 2019), and therefore more *in situ* studies are necessary. As the Mekong River has been identified as a key source of plastic pollution that has been understudied, this chapter aims to document microplastics throughout the Mekong. Microplastic concentrations and fluxes are determined within the water column at several sites of the Mekong River in Cambodia and Vietnam. The relationship between microplastic concentration and discharge is discussed and compared to known sediment dynamics within rivers. The distribution of microplastics is also used to gain an insight into ecological risk throughout the Mekong, therefore answering research question 3.

**Chapter 6. Transport and trapping in complex aquatic canopies: how do coral reefs act as sinks for microplastics?**

This chapter investigates the role complex ecosystem structures (canopies) play in the fate of microplastic pollution. Ecosystems with complex structures such as mangroves and coral reefs are often in coastal settlings influences by fluvial discharge and therefore plastic discharge and have the potential to trap microplastics, acting as a sink. This may be important in explaining how microplastics are “missing” from observations of the ocean environment. There are significant knowledge gaps associated with coral reefs and plastic pollution, with a lack of understanding of the patterns, concentrations, and impacts of microplastics on reef ecosystems. Corals are vulnerable to environmental change and are particularly at risk of ingesting microplastic particles (<5 mm) as the size range of the polyps' normal diet corresponds to that of microplastics (Axworthy and Padilla-Gamiño, 2019; Mouchi *et al.,* 2019; Reichert *et al.,* 2019; Zink and Smith, 2016). However, the role of the complex corallite structure of corals in trapping microplastics is yet to be studied, in addition to the potential ecological risk areas of such accumulation could cause. Using a hydraulic flume under several unidirectional flow conditions, the prevalence of microplastic retention

by branching coral canopies was tested. Corals were created using 3D-printed models of staghorn coral, *Acropora* genus, an important reef-building species found globally. The relationship between canopy hydrodynamics and microplastic distribution and trapping was also investigated, providing an insight into microplastic transport dynamics and physical entrapment mechanisms within coral canopies. The trapping and accumulation of microplastics within a coral reef has implications for the ecological health of reef systems and is discussed. This will answer research question 4.

**Chapter 7: Synthesis and Conclusions**

This chapter provides a combined synthesis of the three substantive chapters that thematically address the overall research aim of this thesis. The synthesis draws the results together across the chapters and considers the wider context and the implications for the findings for microplastic transport projections, in addition to considerations of future research directions.

[Page intentionally left blank]

# Chapter 2.

# Literature Review

## 2.1 Introduction

This chapter presents current literature for each research chapter and provides an insight into the gaps of knowledge that must be addressed. An overview of the interconnected issues that will be addressed in this thesis is shown in Figure 2.1.

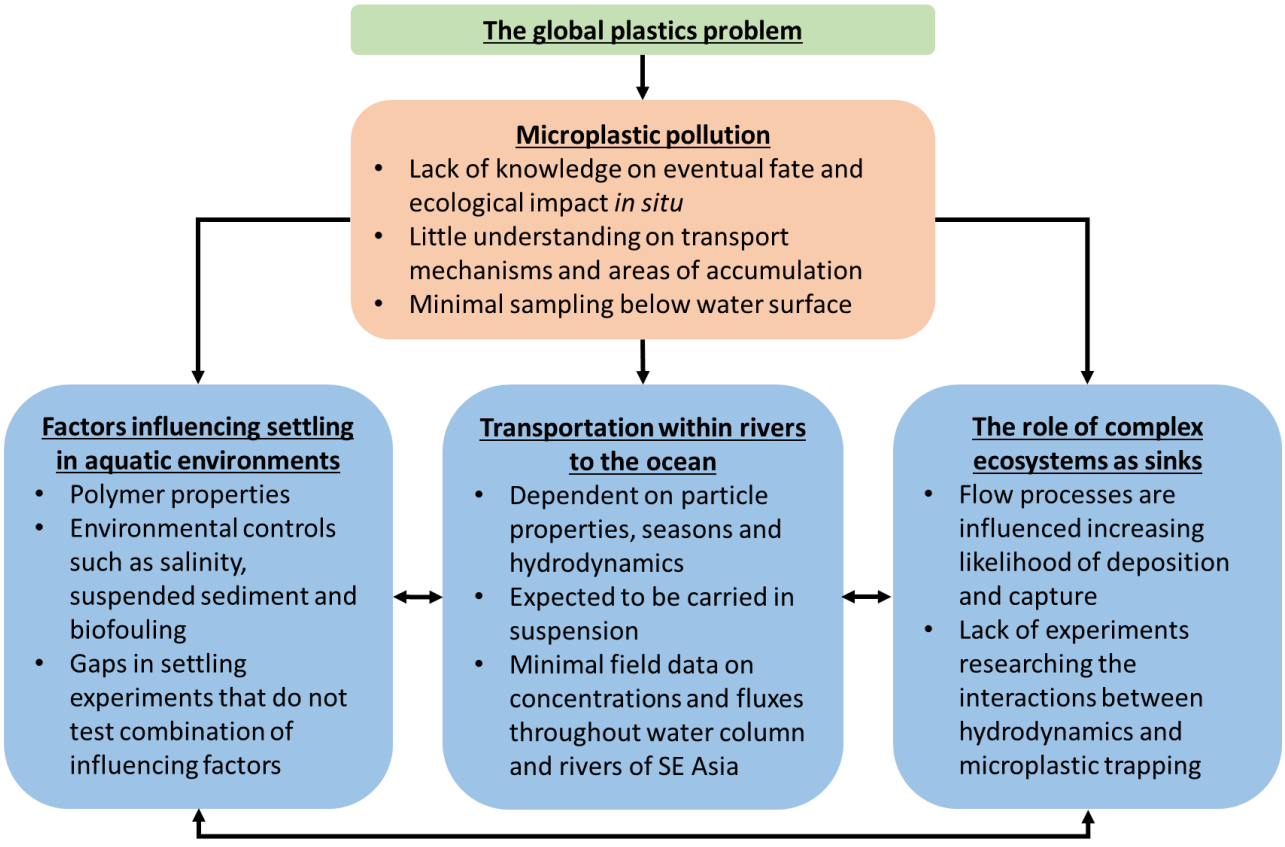


Figure 2.1: Schematic overview of the interlinked topics covered in this literature review

### 2.1.1 The global plastics problem

Plastic production began commercially in the 1950s and has since grown considerably worldwide, increasing from 1.5 million tonnes/year in 1960 to 367 million tonnes/year in 2020

(Fig 2.2) (PlasticsEurope, 2021). Yet the plastic industry failed to predict the rapid growth in demand, use, and therefore the production of plastic, with the adverse environmental impacts overlooked for decades (Derraik, 2002; Fergusson, 1974). The same properties that make plastic such a successful material have resulted in plastic becoming a serious threat to aquatic environments (Derraik, 2002; Ryan *et al.,* 2009). The buoyancy of many plastics allows them to be carried over long distances due to currents and winds, in addition to the chemical properties of polymers allowing plastics to persist for decades (Derraik, 2002; Thompson, *et al.,* 2004; Eriksen *et al.,* 2014a). Plastic pollution has now contaminated the world's most remote locations including the Arctic and Antarctica, in addition to the Mariana Trench, with plastic debris being found at a depth of 10,898 m (Chiba *et al.,* 2018; Cincinelli *et al.,* 2017; Lusher *et al.,* 2015). However, the amount of plastics observed on the surface of the world's oceans is lower than predicted based on estimated outputs (Cózar et al., 2014; Eriksen et al., 2014).

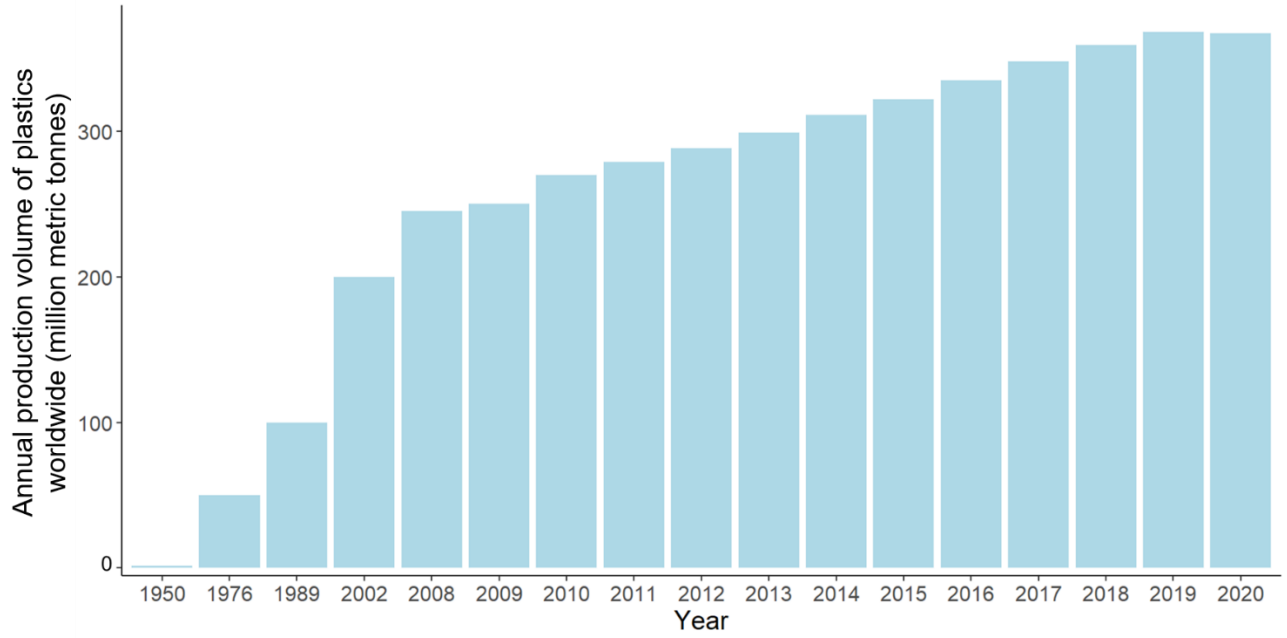


Figure 2.2 : Annual production of plastics worldwide from 1950 to 2020. Source PlasticsEurope (2021)

The amount of plastic waste available to enter the oceans has been estimated by Jambeck *et al.,* 2015 by utilising global data on population density, economic status and solid waste. It was estimated that in 2020, 192 countries generated a total of 275 million

metric tons with 4.8-12.7 million metric tons entering the ocean (Jambeck et al., 2015). The quality of waste management and population size have been identified as a key determiner in which countries contribute the highest amount of uncaptured waste that can become marine debris (Jambeck et al., 2015). The top five contributing countries were in Asia, namely China, Indonesia, the Philippines, Vietnam and Sri Lanka (Fig. 2.3) (Jambeck et al., 2015). There are many reasons for this; with annual waste generation often being mainly a function of population size and the top contributing countries having large coastal populations, in addition to lack of waste management systems (Jambeck et al., 2015). In addition, the Western world continues to ship plastic waste to developing countries, including those in Southeast Asia despite several bans being in place (Uhm, 2020).

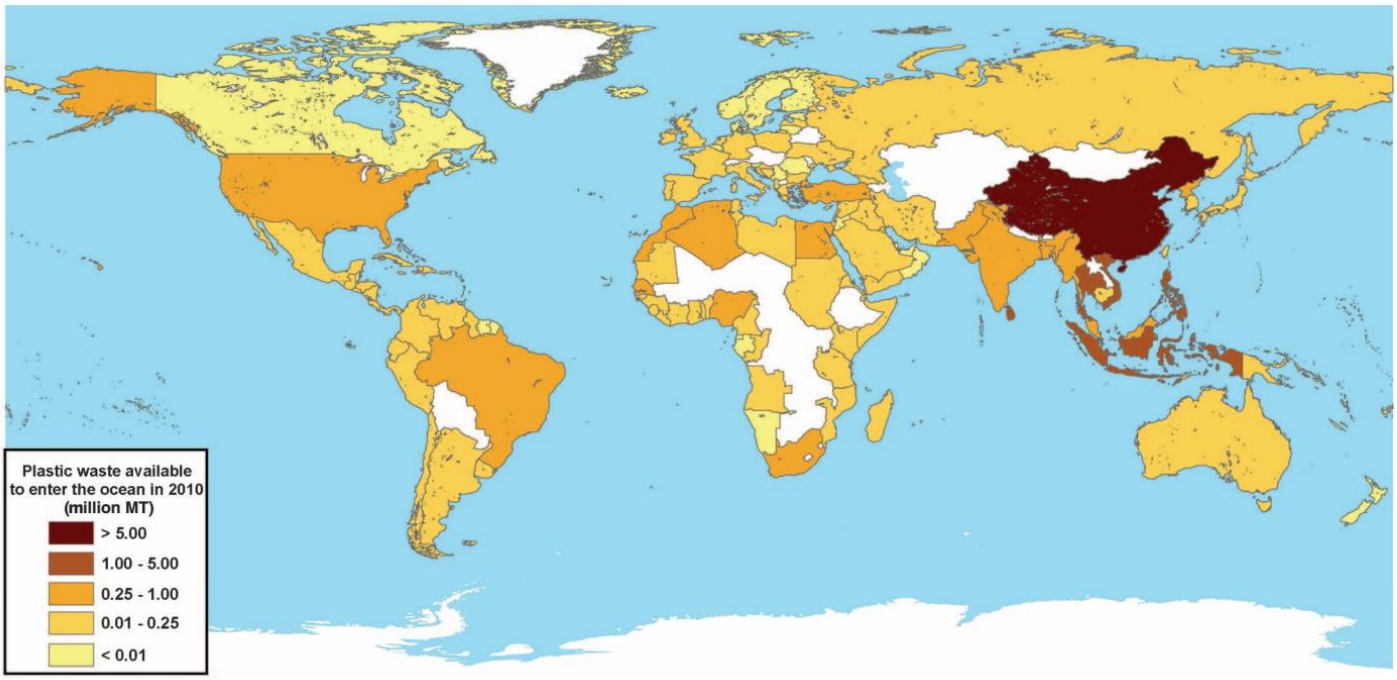


Figure 2.3: Global map denoting the estimated mass of mismanaged plastic waste [million metric tons (MT)] in 2010 by populations living within 50km of the coast, with each country shaded accordingly. Credit: Jambeck *et al.,* 2015

Once plastic waste enters the environment, it can cause a number of problems and persist for hundreds of years. There continues to be growing evidence that plastics are a threat to aquatic organisms, with reports of marine biota ingesting plastics emerging as early as the 70s, where Carpenter *et al.,* (1972) observed plastic within the gut of numerous fish species. Macroplastics have been observed to entangle and cause the death of numerous

marine and terrestrial species (Ryan *et al.,* 2009). Ingestion of large fragments often prevents animals from ingesting normal sources of food or gives a false sense of satiety ultimately leading to starvation (Pierce *et al.,* 2004). Macroplastic litter can also cause economic losses through the lower aesthetic quality of aquatic environments leading to reduced tourism and increased cost of mitigation measures such as beach cleaning (Newman, 2015). Plastics not only physically harm organisms but can redistribute non-indigenous species to new locations, spread pathogens, and distribute persistent organic pollutants (Barnes, 2002; Yukie Mato et al., 2000). Furthermore, to enhance their performance, such as increased heat resistance, plastics contain chemical additives that can leach into the environment and are often toxic, persistent, and bioaccumulative (Oehlmann *et al.,* 2008; UNEP, 2014).

### 2.1.2 Microplastics

Microplastics are defined as particles <5 mm and, due to their size and the vast nature of the world's seas, are much more difficult to study and control than larger fragments, with there being little knowledge about their transport globally (Avio *et al.,* 2015; Cincinelli *et al.,* 2017; Wright *et al.,* 2013). Primarily, microplastics have been manufactured by industry, often in the form of nurdles used to make larger plastic items, microbeads typically found in cosmetics and industrial abrasives or synthetic fibres for textiles (Barnes *et al.,* 2009). However, the majority of microplastics are secondary, produced from the degradation of macroplastics that have broken down through mechanical abrasion and weathering, and come in many forms such as fragments and films (Thompson, *et al.,* 2004; Cole *et al.,* 2011; Avio, Gorbi and Regoli, 2017). Consequently, microplastics are numerically more abundant that macroplastics within the water column and sea surface, with the number of particles in the ocean increasing exponentially as size decreases (Cózar *et al.,* 2014). Many studies have reported that the most abundant type of microplastic observed in aquatic environments are fibres, with a large amount expected to arise from wastewater from washing clothes

(Browne et al., 2011; Napper and Thompson, 2016; Thompson et al., 2004; Wright et al., 2013). For example, Napper and Thompson (2016), estimated that over 700,000 fibres can be released from an average 6kg wash of acrylic fabrics and as fibres are reported in effluent from sewage treatment plants, clothes washing may be a major source of microplastics in aquatic environments. However, there is a lack of small particles being observed at the ocean surface compared to predicted amounts, with microplastics <1mm considered “lost” (Eriksen et al., 2014). This may be due to a lack of sampling below the water surface, and limited understanding of the transport mechanisms that influence microplastic fate. Microplastic distribution is first influenced by the polymer properties including density, shape, and size. Yet once a piece of plastic enters the aquatic environment, a biofilm will begin to grow on the particle surface within minutes to hours, affecting density (Zettler et al., 2013a). Furthermore, microplastic transport will be influenced by the salinity of the aquatic system, turbulence, and suspended sediment. In turn, this will affect microplastic ecological risk, as different species will be exposed as a plastic particle floats, settles, or is resuspended. In addition, the extensive body of research on sediment dynamics can provide basic insights into the transport of microplastics due to the similar properties of both types of particles (Waldschläger *et al.,* 2022).

There are several different exposure pathways for organisms to interact with microplastics, such as direct consumption, scavenging detrital matter (faecal pellets, carcasses, marine snow), and trophic transfer (Waldschläger et al., 2020b). Microplastics are now associated with several negative health effects when ingested by organisms including reduced fecundity, growth, and survival rates (Reichert *et al.,* 2018; Sussarellu *et al.,* 2016). Thompson, *et al.,* (2004) published the first report on microplastics globally, quantifying abundance within UK beach sediment. In addition, plankton samples collected since the 1960s were analysed from Scotland and Iceland showing microplastics archived amongst plankton with a significant increase over time. Microplastics have since been found in several different species such as phytoplankton (Setälä, *et al.,* 2014), bivalves (Sussarellu

*et al.,* 2016), crustaceans (Murray and Cowie, 2011), fish (Lusher *et al.,* 2013), marine mammals (Fossi *et al.,* 2012) and birds (Provencher, *et al.,* 2014), and often found to have harmful effects. In addition, it has been demonstrated that organisms can act as a vector for microplastics to transfer to higher trophic levels and have the potential to bioaccumulate though food webs (Galloway *et al.,* 2017; Murray and Cowie, 2011). Although the amount of literature regarding microplastic pollution in aquatic environments has grown significantly over the past few decades, a marine bias remains over riverine studies, with microplastic pollution abundance and effects in freshwater and estuarine systems being much more limited.

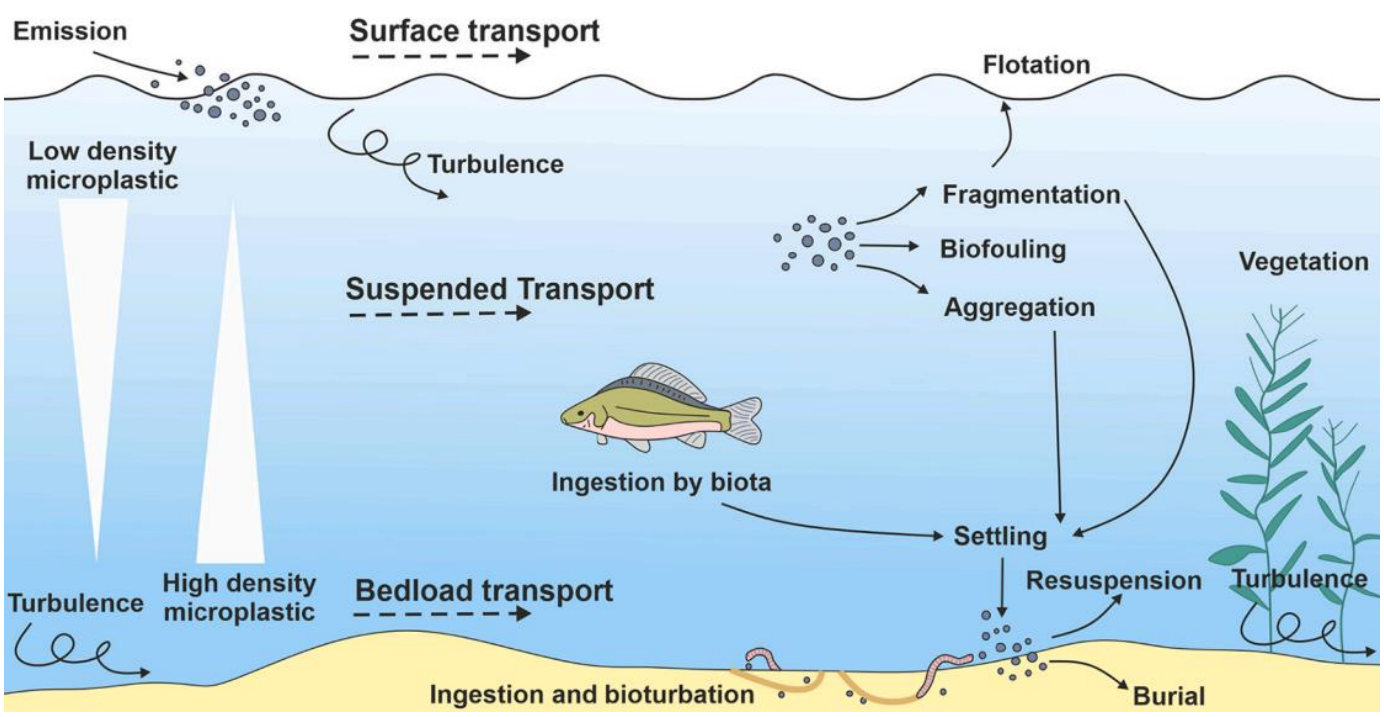


Figure 2.4: The various process that impact microplastic transport and settling in aquatic environments. Source Waldschläger *et al.,* 2022.

Currently, there remains a lack of knowledge on the eventual fate and ecological impact of microplastics in aquatic environments. There is little understanding of the processes that affect microplastic transport and subsequent areas of accumulation. Minimal sampling has been undertaken below the surface within the water column to understand these processes. To address these knowledge gaps, this thesis will present settling

experiments highlighting the main environmental facts that influence microplastic settling from rivers to marine environments (Chapter 4), fieldwork sampling for microplastics throughout the water column of a major river (Chapter 5) and physical modelling on how complex ecosystems (coral reefs) trap microplastics (Chapter 6). Academic context is given for each of the data chapters in the following sections.

## 2.2 Microplastic settling experiments

Estimates of plastic flux entering the ocean annually vary between 4.8 to 12.7 million metric tons, while floating marine plastic is calculated to be only 268,940 tons, accounting for just 2-6% of the estimated plastic entering aquatic systems every year (Eriksen et al., 2014; Jambeck et al., 2015). Land-based sources such as mismanaged waste, have resulted in rivers becoming a major pathway for macro- (>5mm) and micro- (< 5mm) plastic pollution to enter the marine environment (Jambeck et al., 2015; Lebreton et al., 2017). Yet, as microplastics, move through a river basin and transfer to the marine environment, they will undergo a range of environmental gradients and physical, biological and chemical transitions, including changes in salinity and sediment concentrations. Additionally, weathering, such as fragmentation through physical stress and UV exposure, and biofilm growth will also impact the vertical distribution of microplastics through the water column (Duan et al., 2021; Hoellein et al., 2019; Vroom et al., 2017).

The likelihood that a given microplastic particle will settle out of suspension when entering an aquatic system varies depending on the physicochemical, hydrodynamic and biological conditions of the environment (Hoellein et al., 2014; Zhang, 2017). First, microplastic distribution is dependent on the polymer properties (such as density, shape, size), but as subsequent growth of surficial biofilm occurs within minutes to hours of entering an aquatic system (Amaral-Zettler et al., 2020; Zettler et al., 2013b) (Fig.2.5), the density of the microplastic particle can change rapidly. This results in alterations to particle buoyancy and thus relative density to the ambient fluid, which has considerable implications in varying

a particle's trajectory in the water column (Chubarenko et al., 2016; Cooksey and Wigglesworth-Cooksey, 1995; Fazey and Ryan, 2016; Lagarde et al., 2016; Rummel et al., 2017). Furthermore, the development of flocs, and further associated changes in density and particle size, is known to affect the settling velocity of particles (Manning et al., 2010a). While silts and clays that undergo flocculation are typically 0.06 mm or smaller in size, flocculation can occur at larger grain sizes, including sand (Cuthbertson et al., 2018; Manning et al., 2010b). With surficial biofilms, microplastic particles can also become part of hetero-aggregates (or flocs), which includes other naturally suspended sediment (Cunha et al., 2019; Long et al., 2015). Indeed, Besseling et al., (2017) has demonstrated the aggregation of 70 nm and 1050 nm polystyrene particles with clay in natural freshwaters (Besseling et al., 2017b). However, the impact of floc formation on microplastic distribution, settling and fate is currently unquantified for larger particles (Andersen et al., 2021; Long et al., 2015; Möhlenkamp et al., 2018).

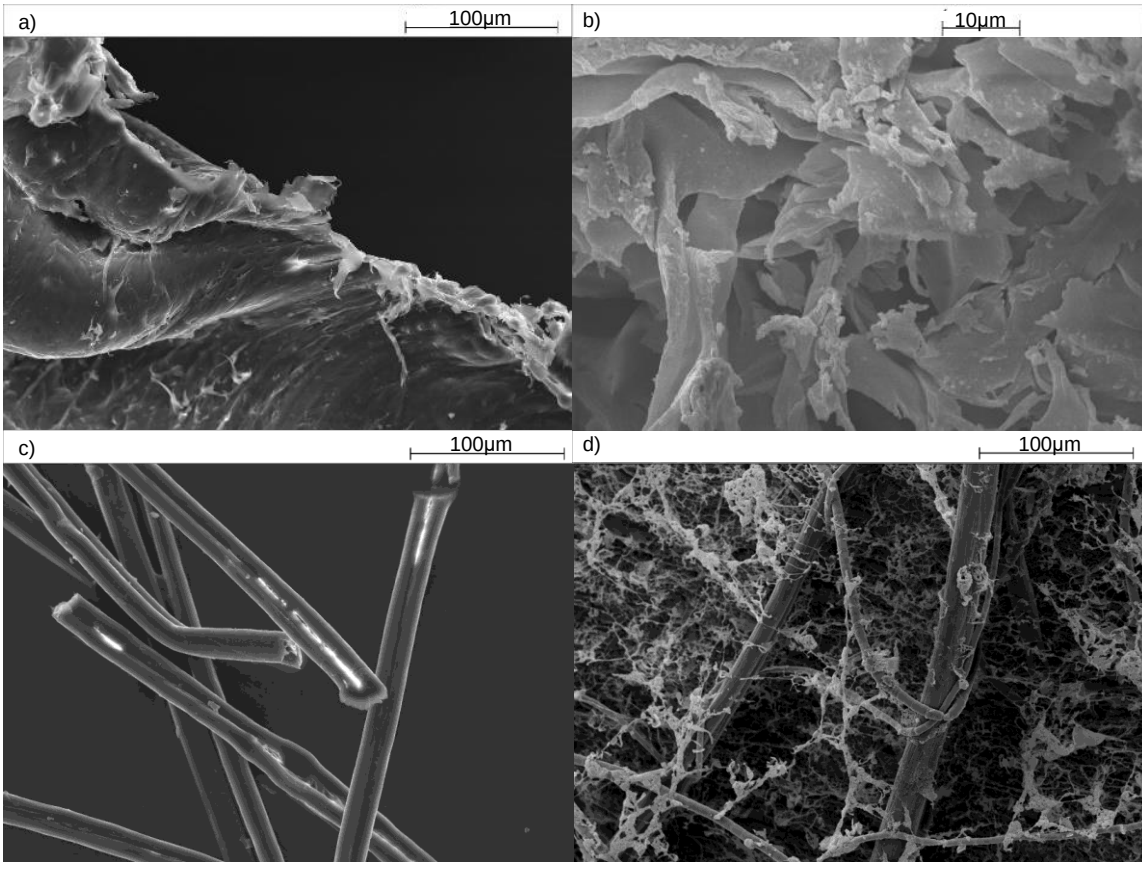


Figure 2.5: SEM images of microplastics before and after biofilm colonisation: a) clean Polyethylene terephthalate (PET) b) biofilmed PET c) clean Nylon, polyester and acrylic (NP&A) fibres and d) biofilmed NP&A fibres

Changes in salinity and suspended sediment that occur across a freshwater-marine boundary is known to affect the development of flocs and thus overall settling velocity of particles, especially as the relative density of the particle changes as it moves into denser saline water (Ivens Portela et al., 2013; Li et al., 2019; Manning and Schoellhamer, 2013; Mietta et al., 2009) . As water becomes more saline (and water density increases), particles are more likely to stay suspended within the water column, although this also depends on physical influences such as flow velocity and turbidity. Settling velocity is thus a key parameter used to predict sediment transport pathways, yet no comprehensive study has yet experimentally quantified the combination of these effects (biofilm, salinity and sediment concentration) for microplastics.

Several microplastic settling experiments have been conducted, providing important insights into microplastic transport and are summarised in Appendix A, table A.1 (Andersen et al., 2021; Bagaev et al., 2017; Ballent et al., 2012; Elagami et al., 2022; Hoellein et al., 2019; Kaiser et al., 2019, 2017; Khatmullina and Isachenko, 2017; Kowalski et al., 2016; Möhlenkamp et al., 2018; Nguyen et al., 2022; Van Melkebeke et al., 2020; Waldschläger et al., 2020a; Waldschläger and Schüttrumpf, 2019). Experiments usually comprise of a settling tube or column, which is filled with water, and microplastics are placed under the surface and released. The subsequent settling time is then either recorded with a stopwatch or determined through video analysis to calculate settling velocity. Microplastics of various polymers have been tested under a range of environments, such as biofouling and different salinities. For example, Kaiser et al., (2017) demonstrated how biofouling increases settling velocity of microplastics, even buoyant polymers: the sinking velocities of polystyrene increased by up to 81% after 6 weeks of incubation. The effects of salinity on various types of microplastic settling were investigated by Kowalski et al., (2016) whereby experiments demonstrated that sinking was not only related to particle size, polymer density and fluid density but also to the microplastic shape. This study also showed that theoretical formulas

are not accurate for calculating microplastic settling (Kowalski et al., 2016). Suspended sediment in aquatic environments must also be taken into consideration and has been investigated using settling experiments. Andersen et al., (2021) showed that fragments and fibres of polyvinylchloride (PVC) in the size range of 63-125 μm can form aggregates (flocculate) with fine-grain natural sediment. This has implications for microplastic settling in high-turbidity estuarine and coastal environments as it suggests that microplastics incorporated in aggregates may settle faster than individual particles resulting in increased microplastics in the bed (Andersen et al., 2021). The rising velocities of buoyant microplastics have also be analysed. For example, Waldschläger et al., (2020a) studied the sinking and rising velocities of weathered fluvial microplastics of various shapes from environmental samples and also highlighted how formulas for predicting microplastic transport do not account for biofouling, fragmentation and degradation and are therefore inaccurate.

Although the influence of various environmental factors of microplastic settling has been investigated through these experiments, the combination of factors that a particle will experience as it moves from a river out to the ocean has not been researched. This knowledge gap is investigated within this thesis, where various microplastic settling experiments are conducted with clean and biofouled particles of different polymers and shapes under different salinities and sediment concentrations that replicate environmental conditions.

## 2.3 Microplastics in rivers

As highlighted by settling experiments, the movement of microplastics through various environmental conditions must be considered when quantifying microplastic transport and accumulation. Furthermore, despite the widespread recognition that rivers dominate the global flux of plastics to the ocean, there is a key knowledge gap regarding the nature of that flux, the behaviour of microplastics in transport and its pathways from rivers into the ocean (Jambeck *et al.,* 2015; Lebreton *et al.,* 2017). There is growing evidence that plastic pollution can harm biota, wider ecosystems and human health in addition to societal and economic repercussions through damaging shipping, fisheries and tourism (McIlgorm *et al.,* 2011). Although many of the potential ecotoxicological consequences of plastics are well known, research has only recently begun to explore the source to sink dynamics of plastics in the environment (Carlin *et al.,* 2020; Reichert *et al.,* 2018; Sussarellu *et al.,* 2016). Microplastic research has predominantly focussed on marine systems where studies tend to sample either at the water surface or bed sediment (Hidalgo-Ruz and Thiel, 2012; Karlsson *et al.,* 2017). Yet, floating marine plastic debris represents just 2-6% of the estimated plastic flux entering aquatic systems annually, so it is likely these studies underestimate plastic loads (Eriksen et al., 2014; Jambeck et al., 2015).This prevents progress towards a holistic understanding of microplastic dynamics and leads to biases when identifying zones of high microplastic accumulation, as well as curtailing the evolution of effective mitigation and policy measures to reduce ecological, environmental and social impact. Given that rivers are the major source of plastic flux to the ocean, they are also the first order of control on how microplastics are distributed and delivered into coastal seas and the wider marine environment. Therefore, to robustly predict the transport, fate and biological interactions of microplastics in aquatic environments at a global scale, the distribution and abundance of

microplastics in the water column of riverine and delta systems must be identified and understood (Peng *et al.,* 2017; Wang *et al.,* 2016).

The majority of plastic pollution originates from land based sources through mismanaged waste, urban and storm water runoff, degradation of larger plastics into microplastics, wastewater treatments plants (WWTPs) and industry (Horton et al., 2017a; Lechner and Ramler, 2015; Ogden and Everard, 2020; Sun et al., 2019; Wang et al., 2020). Rivers often act as a substantial conveyor of plastics to the oceans and therefore fluvial transport mechanisms of microplastics must be fully understood. Microplastic transport in rivers is first influenced by the particle properties, including buoyancy, shape and size and the river hyrdodynamics, such as turbulence and velocity (Haberstroh *et al.,* 2021b; Khatmullina and Isachenko, 2017; Waldschläger and Schüttrumpf, 2019). It has been argued that microplastics can be expected to follow transport behaviour comparable to naturally occurring sediment particles of hydraulically equivalent properties (Enders *et al.,* 2019; Harris, 2020; Hoellein *et al.,* 2019; Kane and Clare, 2019). As a result, a high proportion of fluvial microplastics have been anticipated to be deposited within bed sediment (Drummond *et al.,* 2022). However, the majority of microplastics don't exist in round shapes like sediments, but as fragments, fibres, and films that have been weathered and fragmented with transport behaviour varying significantly between forms (Browne *et al.,* 2011; Harris, 2020). Settling experiments have shown that using sediment dynamics predictions are not always accurate, as microplastics tend to be weathered and fragmented (Chapter 4; Waldschläger and Schüttrumpf, 2019) . Furthermore, fate will be impacted by biofilm growth, which will be likely to increase particle density and interactions with suspended sediment and matter which may lead to aggregation (Kaiser et al., 2017). Additionally, as plastic moves from a riverine to ocean environment, it will cross a salinity boundary which further changes particle buoyancy (Kooi *et al.,* 2017; Chapter 4). Therefore, due to their relatively low densities (in comparison to sediment) the majority of microplastics are, predicted to be in

suspension rather than deposited within the bed (Harris, 2020). Despite this, most of microplastic sampling in rivers is conducted at the water surface or the riverbed.

There are several different methods for sampling microplastics with the three main strategies being i) selective sampling, ii) bulk sampling and iii) volume-reduced sampling and often depends on whether water or sediment is being collected (Razeghi et al., 2021). Selective sampling involves direct collection of larger items (1-5 mm) usually on the water surface or shore. Bulk sampling refers to when the whole volume of the sample is collected without reduction during the process of sampling. Finally, volume-reduced sampling results in the volume of the sample being reduced during collection, where only a portion of the sample is kept. This is a common method for water samples, where on-site filtering by nets or sieving results in a relatively small concentrated final sample (Razeghi et al., 2021). This normally involves trawling with manta, plankton or neuston nets deployed off of a boat and submerged and towed for a set time at low speed (Hidalgo-Ruz and Thiel, 2012). As the volume of water that has passed through the net within the sampling time can be calculated from the area of the net and either using a flow meter or calculations based on the distance travelled, the microplastic concentration can be determined (Razeghi et al., 2021). Pump sampling has also been used whereby water is pumped manually or with a motor through an inline filter. In addition, the grab sampling method involves using a bucket to collect water and then sieve in the field (Han et al., 2020). Sediment samples are frequently collected using grab samplers, corers, hand spades or stainless steel spoons (Razeghi et al., 2021).

Concentrations of microplastics in aquatic environments vary substantially worldwide as show in Fig. 2.6. Research has tended to dominant marine environments, yet recently, the amount of studies being conducted in fluvial areas has dramatically increased. Studies tend to sample the water surface or riverbed, with concentrations being highly variable. For example 14-25 microplastics $m^{-3}$ have been identified in the Thames River (UK), which drains the whole of Great London, home to 15 million people, where secondary microplastics in the form of films and fragments made up the majority of the samples (94%) (Rowley *et al.,*

2020). Napper *et al.,* (2021) sampled the Ganges River (India), one of the most important catchments of South Asia, with an average of 38 microplastics $m^{-3}$ detected in surface water and fibres being the dominate microplastic type (91%). Dris *et al.,* (2018) identified 66 microplastics $m^{-3}$ in the Marne and Seine tributaries of the Seine River (France), which drains Paris, with a population of 10 million, researching exclusively at fibres. On the other hand, 4,137 microplastics $m^{-3}$ have been identified in the Yangtze River (China), with the Yangtze estuary being one of the most important industrial areas of china and highly populated, where the most abundant type of microplastic once more being fibres (Zhao *et al.,* 2014). This highlights the importance of considering the scale of the river in addition to seasonality, hydrology and proximity to urban areas.

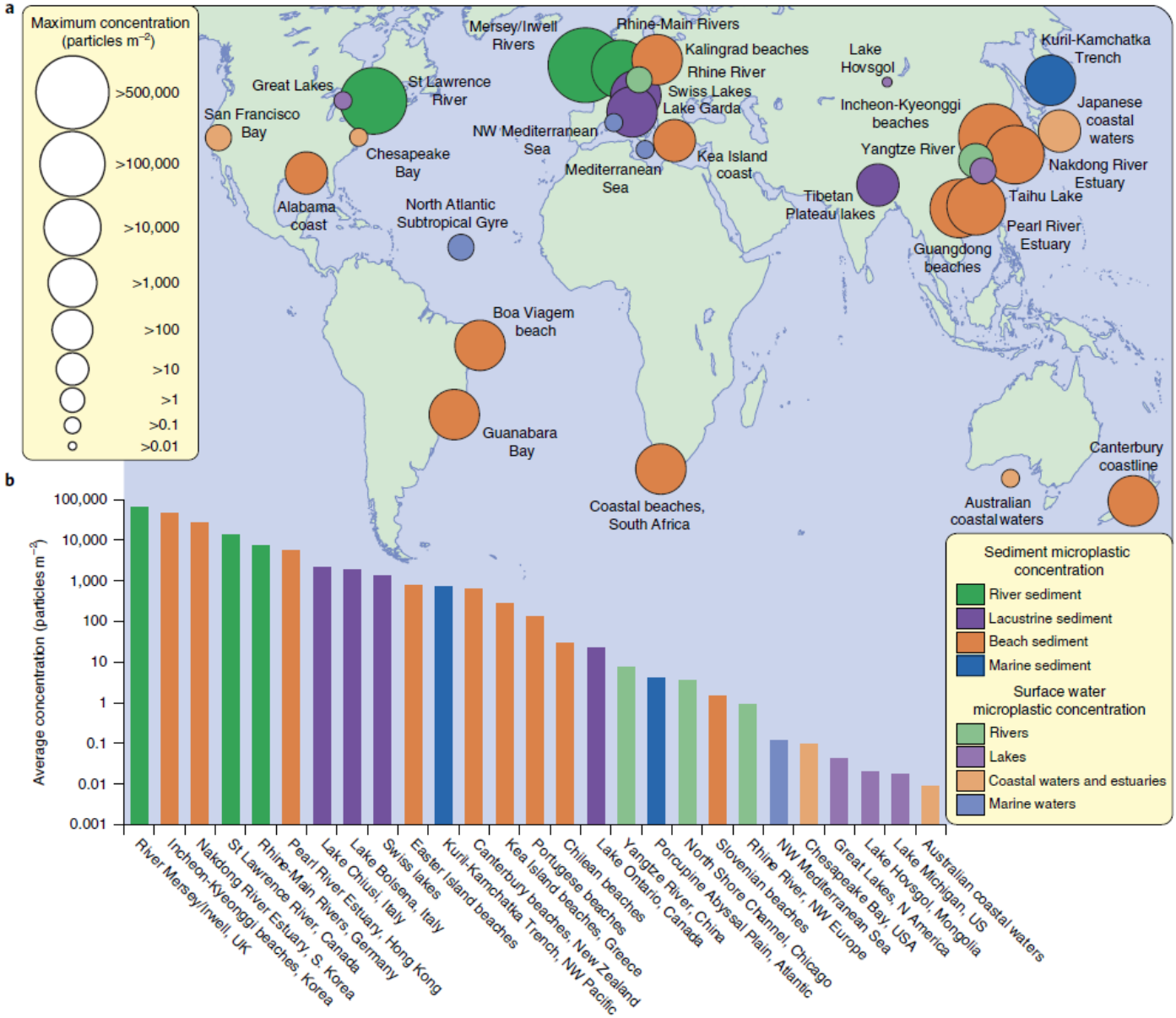


Figure 2.6: Global microplastic concentrations reported in sediment and aquatic environments, a) mapped as maximum concentrations and b) ranked by average concentration. Source: Hurley *et al.,* 2018

In addition, modelling has endeavoured to estimate the amount of microplastics being transported by rivers into the oceans. Lebreton et al. (2017) provide an estimate of global annual input of plastic pollution from rivers into the oceans of 1.15-2.41 million tonnes with 67% originating from just 20 rivers (Fig 2.7). However there are several limitations to modelling and many predictions within the literature have contradicted each other, with a more recent model estimating that over 1,000 rivers are accountable for 80% of plastic waste entering the ocean (Meijer *et al.,* 2021). This highlights the need for more research into the transport of microplastics in rivers, to not only determine the amounts of microplastic passing through these systems, but how ecological risk changes throughout the course of the river into the ocean.

The majority of microplastic studies in rivers are from China, North American or Western Europe, yet numerical models, supported by observations of floating plastics, predict the disproportional contribution of Southeast Asian rivers in plastic emissions to the ocean (Lebreton *et al.,* 2017; Schmidt *et al.,* 2017; van Emmerik *et al.,* 2019). Of the ten rivers predicted by Schmidt *et al.,* (2017) to be the top contributors to marine plastic debris, few studies have been conducted in those areas, despite frequently being referred to as the top polluters as highlighted by Figure 2.8. Furthermore, few studies have directly sampled microplastic concentrations within the water column, which may result in inaccurate concentrations being reported. This demonstrates the need for more research to be conducted in Southeast Asia, especially throughout the water column. The Mekong River of Southeast Asia has been identified as one of the top contributors to marine plastic pollution, with an estimated plastic load of up to 37,000 tonnes per year (Lebreton et al., 2017; Schmidt et al., 2017). The consequences of plastic pollution in the Mekong could be severe due to the high biodiversity of the basin and the millions of people that rely on its productivity.

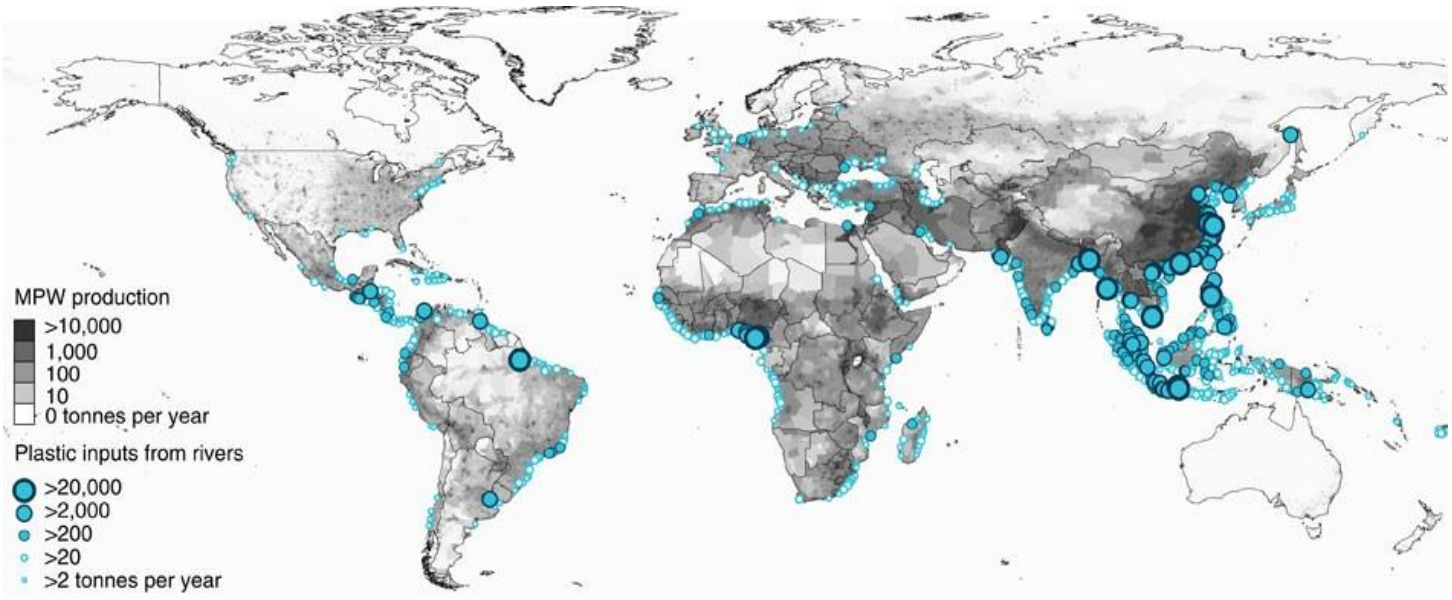


Figure 2.7: The mass of plastic from rivers flowing into the oceans in tonnes per year. Source Lebreton *et al.,* 2017

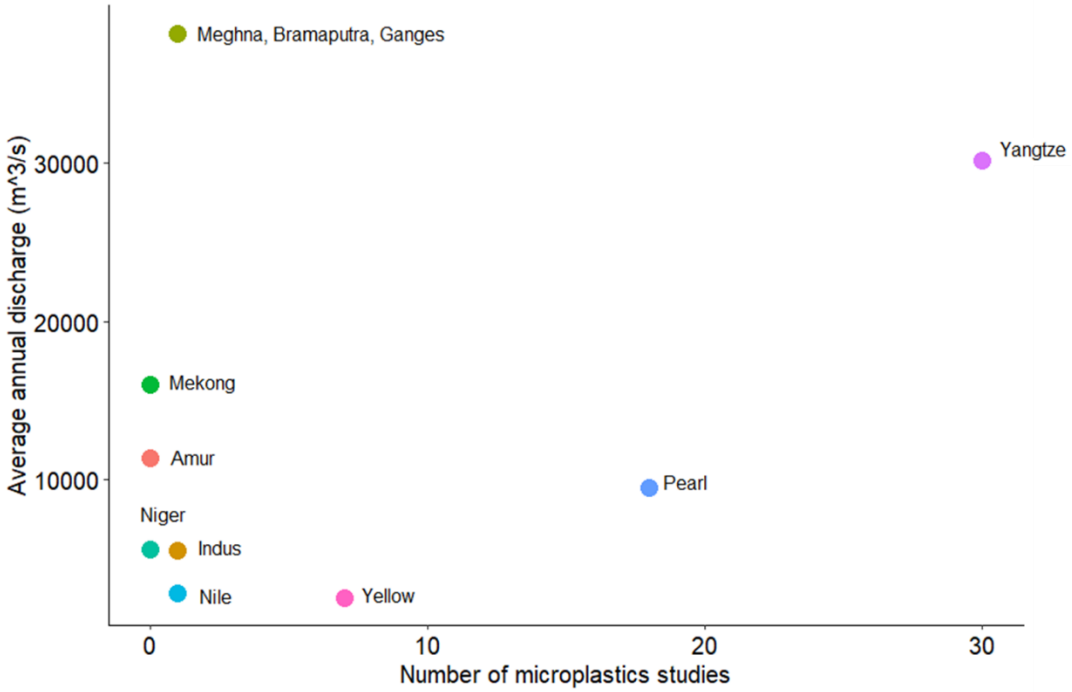


Figure 2.8: Rivers with the top predicted plastic input into the oceans from Schmidt *et al.,* 2017 by average annual discharge and the number of microplastic studies conducted. Discharge data was acquired from Khan *et al.,* 2015 and Gupta 2008. Note Schmidt *et al.,* 2017 concludes the top 10 rivers but discharge data for the Haihe River was unavailable. No microplastics studies have been conducted in that area however.

### 2.3.1 The Mekong River

The Mekong River is the longest (4,800km) river in Southeast Asia and has the 10th largest water discharge globally (Adamson *et al.,* 2009; Hoang *et al.,* 2016). The Mekong is also predicted to be one of the top contributors of plastic loads into the ocean, with an estimated plastic load of up to 37,000 tonnes per year (Lebreton *et al.,* 2017; Schmidt *et al.,* 2017). A monsoon-driven flood pulse occurs annually, with majority of the volume of water carried by the with concentrated in a single wet season (Campbell, 2009; Räsänen *et al.,* 2017). This flood pulse sustains ecological productivity by transporting huge amounts of nutrients and sediments, in addition to reaching floodplains and creating diverse habitats (Räsänen *et al.,* 2017). Furthermore, the Mekong holds a substantial amount of economic and ecological resources with a key driver for ecological productivity (Holtgrieve *et al.,* 2013). The Mekong River is one of the most biodiverse freshwater ecosystems globally, containing large and diverse fisheries with the Lower Mekong Basin supporting between 1,000-1,700 species (Ackiss *et al.,* 2019; Kingston *et al.,* 2011). The inland fisheries of the Mekong are one of the world's largest, having an estimated yield of 4.4 million tonnes per year (Adamson, 2006). The ecological productivity of the river is the basis for the livelihoods and food security of the majority of the 70 million people that live in the basin (Räsänen and Kummu, 2013). Other major water-dependent economic sectors are agriculture, and energy such as hydropower production (Hoang *et al.,* 2016). Yet the resources of the Mekong River are vulnerable to seasonal changes of sediment load, water quality and river flow (Kingston *et al.,* 2011). A more in depth description of the Mekong River, including hydrology, biodiversity, economy and environmental concerns can be found in §5.1.

To our knowledge, only one other study of microplastic concentration has been conducted in the Mekong River where Haberstroch *et al.,* (2021) sampled sites close to Phnom Penh, Cambodia, during the monsoon season. Furthermore, this is one of the few studies to sample throughout the water column (Dris *et al.,* 2018; Lenaker *et al.,* 2019).

Here, we present field measurements distributed across a much wider range of sites across the lower alluvial reaches of the Mekong River and its delta, in Cambodia and Vietnam. We provide insights into the distribution of microplastics and how this varies with depth across eight sites in the Mekong in addition to quantifying the particulate flux and assessing the implications for microplastic discharge into the South China Sea.

## 2.4 Trapping of microplastics in coral reefs

The movement and ultimate fate of microplastics in aquatic environments is generally unknown, with the “missing plastic” phenomenon still remaining. However, the trapping of microplastics in natural aquatic ecosystems has recently been published, encompassing corals, seagrasses, saltmarshes, and mangroves (Cesarini and Scalici, 2022; Cozzolino et al., 2022, 2020; Y. Huang et al., 2021; Li et al., 2018; Navarrete-Fernández et al., 2022; Ogbuagu et al., 2022; Stead et al., 2020; Unsworth et al., 2021). These habitats are the foundation of highly biodiverse and productive ecosystems that provide shelter, nursery grounds and nutrients for a huge range of species as well as numerous ecosystems services for hundreds of millions of people (Huang *et al.,* 2021). In addition, as these ecosystems are often complex structures forming canopies, which can easily trap particles and may act as a sink for microplastic pollution. Field measurements have revealed accumulation of plastics in aquatic canopies, although the knowledge of transport and depositional processes is extremely limited, along with the underlying drivers of these mechanisms. Physical experiments enable investigation of flow and particulate transport processes otherwise difficult to measure in natural settings. The infancy of this research area solicits further investigation given the foremost importance these complex aquatic canopies have on the ecological system health, function, and potential subsequent transfer of microplastic through the food web (Auta *et al.,* 2017).

The flow processes of submerged aquatic vegetation canopies have been studied more widely, with the fundamental hydrodynamics presented in a review by Nepf (2012) and is summarised in Fig.2.9. The complexity of canopy morphology, heterogeneity, and flexural rigidity introduces distinct difference in hydrodynamics between canopy type (Hamed *et al.,* 2017). As the density of a canopy increased, the velocity profile is impacted resulting in hydrodynamic changes within the canopy, which may impact particle trapping. While the hydrodynamics remain only partially quantified due to the vast natural variability, recent studies provide advanced spatiotemporal measurements within scaled seagrass canopies and corals (Houseago *et al.,* 2022; van Wiechen, 2020a). Within a canopy, flow can be accelerated or attenuated, creating various flow velocity gradients over the vertical profile, which influences turbulence and therefore modulates the transport dynamics of suspended particles such as microplastics.

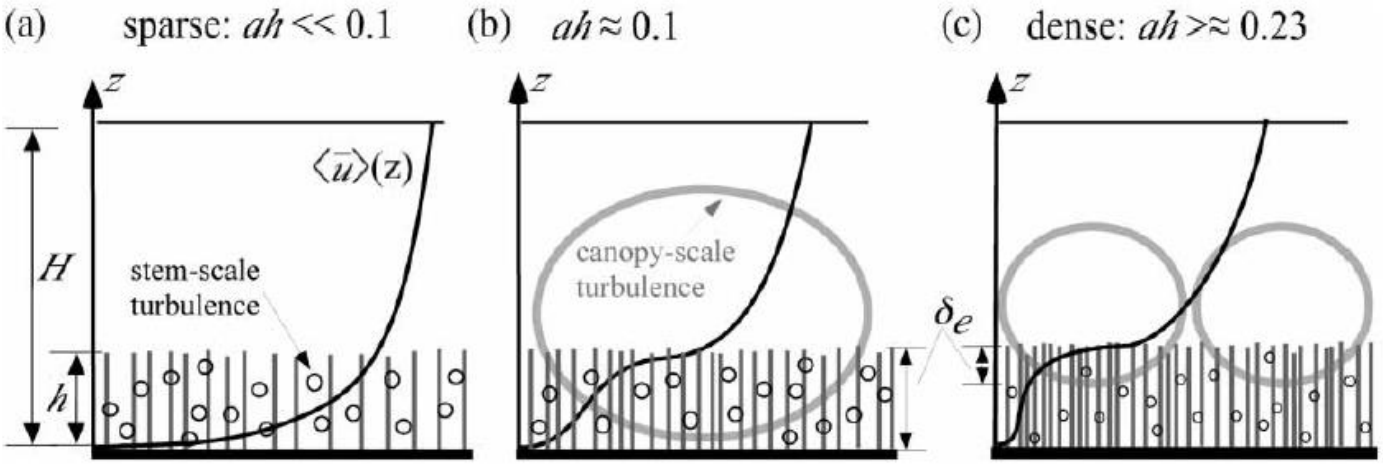


Figure 2.9: The mean velocity profiles through submerged meadows of increasing roughness density (*ah*). The meadow height is *h* and water depth is *H*. Source Nepf (2012)

Recent work has begun to investigate the drivers of plastic trapping in various canopies (Cozzolino et al., 2022; de los Santos et al., 2021b; de Smit et al., 2021; Ogbuagu et al., 2022) yet our understanding of the mechanisms and controls on microplastic trapping is limited. Seagrass seed dispersal and capture by ecosystem engineers has been tested with increase in velocity, habitat complexity, higher turbulence and erosive processes

allowing more seeds to be trapped by eelgrass and bivalves (Meysick *et al.,* 2019). These mechanisms could also apply to microplastic trapping. de los Santos et al., (2021b) investigated for the first time the amount of microplastic trapping by a marine canopy in a hydraulic flume under unidirectional flows. These experiments demonstrated how seagrass is able to retain microplastics at several flow velocities and trap denser microplastics due to erosive processes forming scour around the shoots (de los Santos *et al.,* 2021b). Floating microplastics were also retained within the canopy, due to the seagrass forming a barrier, but only at low flow velocities (de los Santos et al., 2021b). In addition, de Smit *et al.,* (2021) tested and compared individual coral, seagrass and macroalgae for their potential as microplastic sinks using a flume within the field. Corals were shown to capture the highest number of particles in their complex canopy structure, yet also resulted in a high amount of microplastics being deposited into the sediment (de Smit et al., 2021). This highlights how microplastics may be accumulating in the beds of complex ecosystems. Further experiments have also revealed how macroalgae traps microplastics, yet differences are observed within- and between-species often due to canopy densities (Cozzolino et al., 2022). This demonstrates that various species of organisms within a canopy must be considered for their microplastic trapping and accumulation potential. In addition, flume experiments revealed that saltmarsh systems can influence hydrodynamics above and within canopies, enhancing turbulence and sheer stresses and therefore impacting microplastic accumulation (Ogbuagu et al., 2022). Microplastics may also adhere to the canopy, which is dependent on surface characteristics and structural complexity (Martin *et al.,* 2019a). Furthermore, through reduction in bottom shear stress, canopies are known to hamper resuspension rates of sediment, trapping particles into the bed (Bos *et al.,* 2007; Gacia and Duarte, 2001). Therefore, these habitats may facilitate microplastic trapping, accumulation and burial in their associated sediment (de Smit *et al.,* 2021)**.**

Scleractinian coral can form very complex canopies and are one of the most biodiverse ecosystems globally, with 25% of all ocean species being found on reefs,

including 4,000 fish species (Hughes *et al.,* 2017; Richmond, 1993). Corals form the first trophic link through their algal symbiosis and offer the majority of the habitat structure for reef organisms (Richmond, 1993). Reefs form land, provide sand for tropical beaches and structures to attenuate waves that would otherwise create widespread coastal erosion (Monismith, 2007; Richmond, 1993). However reefs are at risk from many anthropogenic drivers, especially climate change and rising sea temperatures, which may be accentuated by other pollutants such as microplastics (Hughes *et al.,* 2017). Coral reefs are particularly at risk to microplastic pollution due to their coastal location and the mainly terrestrial origin of marine plastic waste (Lebreton *et al.,* 2017; Reichert *et al.,* 2018). Microplastics can accumulate in the nearshore zone due to wave and wind dynamics, with shallow reefs being especially in danger when low tides occur, resulting in microplastics being more likely to settle within the canopy (Forsberg *et al.,* 2020).

There is growing evidence that corals ingest microplastics and can cause harm such as through reducing photosynthetic capability and growth, bleaching, disturbing initiation of symbiotic relationships, blocking their normal food intake and increasing risk of disease through tissue abrasion (Corinaldesi *et al.,* 2021; Mendrik *et al.,* 2021; Okubo *et al.,* 2018; Reichert *et al.,* 2019, 2018). The long-term impacts of this could be widespread, influencing not only the numerous species that rely on reefs for survival, but also communities that depend on them for multiple ecosystem services. Entrapment of microplastics by coral reefs would not only increase the possibility of these negative impacts but also the likelihood of accidental ingestion by other aquatic organisms. A recent U.N. brief on plastics and coral reefs highlighted the need for improved quantification of the patterns, concentrations and impacts of microplastic pollution on coral ecosystems to evaluate the extent of risk (Sweet *et al.,* 2019). Understanding passive coral reef trapping mechanisms through their complex structures is vital to determine the impacts of microplastics on coral reefs and associated organisms in addition to the role reefs play as a microplastic sink. Despite the potential harm for reefs being known, the amount of microplastics being trapped within reefs and related

microplastic exposure remains understudied, in addition to the hydrodynamics within coral canopies that will influence entrapment.

Microplastic transport depends on particle size, shape, density, biofilm formation and interaction with other suspended material. Distribution is also influenced by hydrodynamical conditions and therefore a combination of bio-physical factors will determine particle fate and entrapment (de los Santos *et al.,* 2021b; Zhang, 2017). Reefs can act as physical barriers that entrap microplastics, but the coupled interaction between microplastic transport and hydrodynamics are not understood. Chapter 6 implements physical modelling to evaluate microplastic transport and trapping processes within canopies of branching coral, at two coral densities to address this knowledge gap. Experimental techniques track microplastic transport and distribution throughout the canopies. Artificial surrogates are employed to enable controlled conditions that build upon current hydrodynamic knowledge from the literature, while supporting the assessment of microplastic transport and trapping without harming corals.

[Page intentionally left blank]

# Chapter 3.

# Laboratory and field methodology

## 3.1 Introduction

This chapter provides details of the methodologies utilised in each of the research chapters to evaluate and determine the key controlling factors that influence microplastic fate in aquatic environments. A multidisciplinary approach was used that combines innovative experiments, fieldwork and physical modelling. First, a suite of settling experiments was employed to determine how settling of microplastics differs from freshwater to marine environments. The role of biofouling and suspended sediment was also analysed here. Next, abundances and fluxes of microplastics were analysed through fieldwork within a large river system, namely the Mekong River of Cambodia and Vietnam. This was coupled with hydrological data to explore how microplastics are transported within the water column across various sites. Finally, using a hydraulic flume, the role of complex coral ecosystems as a sink for microplastics was investigated under a range of flow conditions.

## 3.2 Settling experiments

### 3.2.1 The microplastic particles

The majority of observed macroplastics in riverine systems are from packaging of a range of polymer densities, as turbulence of rivers allows polymers to remain buoyant (Schwarz *et al.,* 2019). Therefore, polymer types commonly found across freshwater and ocean environments, including beaches, sediment and epipelagic areas were chosen for the settling experiments (Schwarz *et al.,* 2019). Three types of plastic polymers were selected: fragments of polyethylene terephthalate (PET) (1.39g/cm$^3$) and polyvinyl chloride (PVC)

(1.44g/cm$^3$) (Direct Plastics Limited, Sheffield, UK) were generated using a carving file. This ensured fragmentation of plastic and heterogenous shapes and sizes that replicates environmental degradation of microplastics (Rummel *et al.,* 2017). Fibres were generated from nylon, polyester and acrylic (NP&A) yarn (1.01-2.30g/cm$^3$) (The Knitting Network, Sittingbourne, UK). The properties of the polymers used in the experiments are summarised in Table 3.1. Fragments and fibres were generated to be in the typical size range of microplastics commonly found in aquatic environments (0.01-5 mm) (Hidalgo-Ruz *et al.*, 2012). In addition, irregular shapes of microplastics were chosen instead of pellets and spheres, to represent weathered and degraded plastics more typically found in the aquatic environment. This allowed an estimate of settling velocities of microplastic particles that resemble those found in aquatic environments.

Table 3.1: Summary of microplastic properties used to settling experiments. Size ranges (a-axis) were determined with a self-developed code in Matlab, see more details below.

| Polymer | Density (g/cm$^3$) | Size range (mm) |
|---|---|---|
| Polyethylene terephthalate (PET) | 1.39 | 0.02-4.20 |
| Polyvinyl chloride (PVC) | 1.44 | 0.04 -4.94 |
| Nylon, polyester and acrylic (NP&A) | 1.01-2.30 | 0.02-0.59 |

To colonise biofilms on microplastic particles, the methods of Hoellein *et al.,* (2019) were adapted. Benthic sediment and overlying water was collected from the Humber River, Hull, UK (53.7144° N, 0.4458° W). Fifty grams of benthic sediment and 200ml of river water was placed in flasks with microplastics in a shaking incubator for 10 days at 37 °C, 200 rpm. The flasks were then left at room temperature for 6 months. It should be noted that fibres are known to have significantly less bacterial abundance in biofilm colonisation compared to fragments and pellets (Hoellein *et al.,* 2019) and it was therefore expected that there would be less biofilm formation on fibre samples. Examples of plastics before and after biofilm growth are shown in figure 3.1.

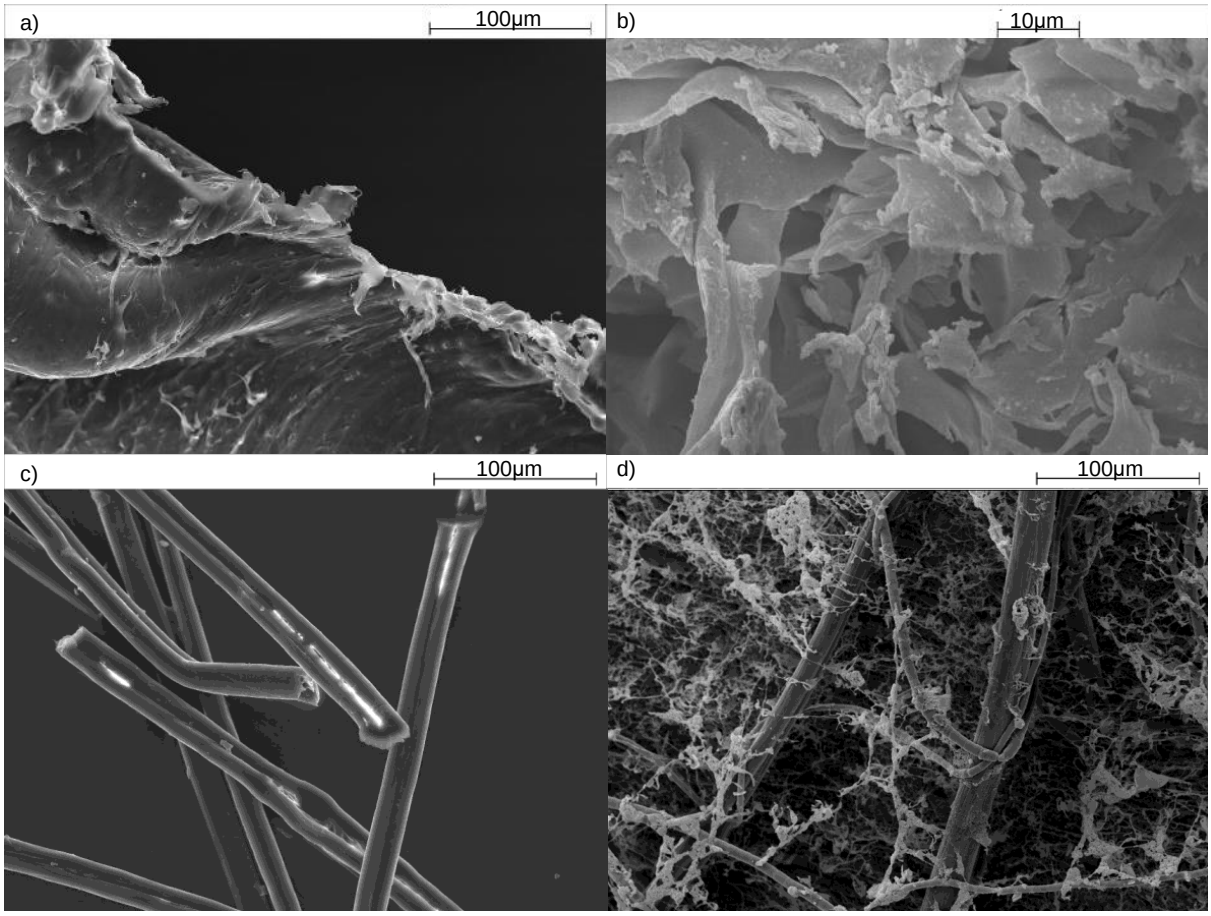


Figure 3.1 Scanning electron microscope (SEM) images of microplastics before and after biofilm colonisation: a) clean polyethylene terephthalate (PET) b) biofilmed PET c) clean nylon, polyester and acrylic (NP&A) fibres and d) biofilmed NP&A fibres

To initiate the formation of flocs (aggregated mass of material), kaolinite, a clay particle abundant in estuarine environments was chosen (100-600mg/L) and mixed with high concentrations of clean and biofilmed microplastics, with each polymer kept in separate 200ml conical flasks. This was repeated for each salinity and polymer type. The sediment range of 100-600mg/L was chosen from data collected by the Mekong River Commission (Mekong River Commission, 2021) and incorporates suspended sediment concentrations found from fluvial to delta environments of one of the top contributing rivers to marine plastic pollution. To replicate turbulent flow, the sediment-microplastic mixtures were shaken horizontally at 300rpm for 5 minutes then 150rpm for 20 minutes. To ensure any flocs formed held together, particles were extracted from the beakers with a glass pipette while they were still being shaken at 80rpm and dropped in the water column (see below).

### 3.2.2 Experimental setup

The settling velocity of the microplastic particles was determined through a series of non-intrusive sinking experiments conducted in a Laboratory Spectral Flocculation Characteristics (LabSFLOC) plexiglass column with dimensions of 12 cm x 12 cm x 33 cm (Fig. 3.2, analogous to previous settling velocity experiments (Andersen et al., 2021; Ballent et al., 2012; Elagami et al., 2022; Kaiser et al., 2017, 2019; Khatmullina and Isachenko, 2017; Manning et al., 2007; Möhlenkamp et al., 2018; Nguyen et al., 2022; Van Melkebeke et al., 2020; Waldschläger et al., 2020b; Waldschläger and Schüttrumpf, 2019), Appendix A, Table A.1 ). The LabSFLOC settling column is combined with an LED light panel and high-resolution video camera (Fig.3.2) that collects particle settling video data that is processed to understand size, shape and velocity of individual particles and flocs. This allows individual particles to be easily analysed for their settling behaviour and aggregation. It is comparable to previous microplastic settling experiments that have utilised similar water columns.

The LabSFLOC water column was filled with distilled water of salinities (n=3, ppm, SAL) ranging from SAL0-30 to represent the change in salinity from a freshwater to a fully marine environment. Distilled water was utilised to ensure no impurities were impacting microplastic transport. Water temperature and pH were recorded at least 15 minutes before each experimental run and immediately after to ensure consistency. Fifteen minutes allows the water column to settle after any disturbances caused by measuring temperature and pH (Khatmullina and Isachenko, 2017). Before each experiment, microplastics were immersed in water of the same salinity and temperature used in the experimental water column in glass petri dishes to ensure no electrostatic discharge from particles, which may prevent or alter sinking behaviour (Kaiser et al., 2017). For clean and biofilmed particles, microplastics were placed 0.01 m below the water surface of the LabSFLOC to prevent any restraint caused by surface tension and left to move freely. For microplastics that were being tested under different sediment concentrations, a glass pipette was utilised for transferring particles so not to disturb any formed flocs.

A series of images were taken of the particle movement. At least 100 particles per condition were recorded for PET and PVC experimental series. However for fibres, particles tended to clump together which made analysis of movement difficult. Therefore at least 10 particles were recorded per variable for fibre analysis. For PET total n = 1,796, PVC n = 1,015 and NP&A n = 1,111. Particles travelled at least 15cm before image recording took place to ensure microplastics had reached terminal settling velocity. This distance was chosen in accordance with measurements from other studies (Khatmullina and Isachenko, 2017; Kowalski *et al.,* 2016; Waldschläger and Schüttrumpf, 2019). For each polymer (PET, PVC and NP&A fibres), measurements were taken for clean and biofilmed particles under 3 salinities (SAL0, 18 and 30) and 3 sediment (clay) concentrations (100 mg, 400 mg and 600 mg), resulting in 54 scenarios. Finally, to assess the impact of biofilm growth on settling velocity, measurements were taken at 0,1,2,4 and 8 weeks for biofilmed PET fragments at SAL18. Images were analysed using a self-developed code in Matlab (R2020a) (MATLAB, 2020), see Appendix A. Particle detection was made using the 'imbinarize' function available in Matlab, using global thresholding (Otsu, 1979) or adaptive thresholding (Bradley and Roth, 2007) depending on image characteristics. Particle properties, including area, were obtained using the 'regionprops' function. The velocities were obtained with self-developed cross-correlation based Particle Tracking Velocimetry (PTV) routines.

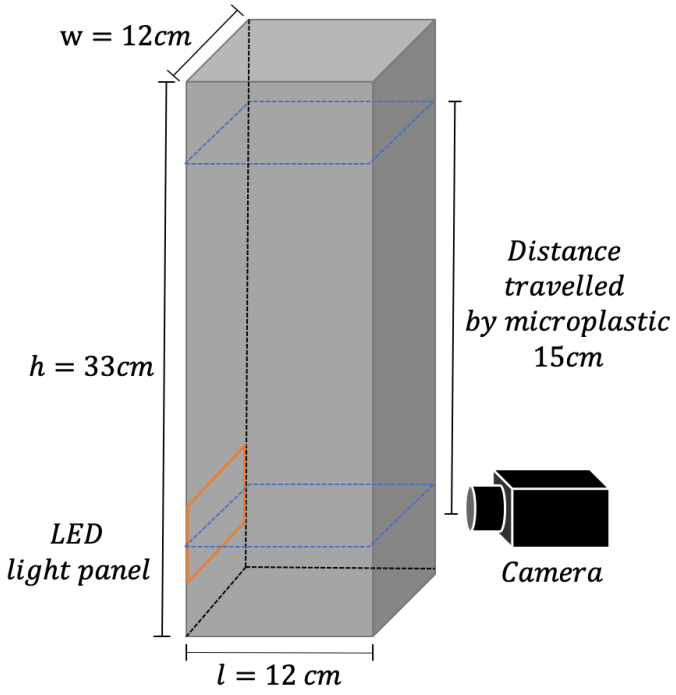


Figure 3.2: Schematic of the laboratory spectral flocculation characteristics (LabSFLOC) experimental setup: pexiglass column of height 33cm with a square cross section of 12x12cm, filled with deionised water of varying salinities.

### 3.2.3 Statistical analysis

To understand the effects of microplastic condition (clean or biofilmed), salinity and clay concentration on settling velocity of microplastics, the combined interactions of [condition and salinity] and [condition and clay concentration] were assessed using generalised least square means analysis. All statistical analysis was conducted using R Studio (R Core Team, 2013). Interactions were considered statistically significant if $p < 0.05$. Post hoc analysis was conducted using the lsmeans package, (Lenth, 2016) Tukey adjusted to understand significant differences between the least-squares means of specific variables by fitting linear models. For biofilm growth analysis from 0-8 weeks, a repeated measures ANOVA was utilised after square root transformation to ensure equal variance (verified with Levene Test) and post hoc analysis.

### 3.2.4 Comparison to settling velocity predictions and formulae

As settling of microplastics has been related to the transitional flow regime, the formula of Ferguson and Church, (2004) for smooth, varied and angular grains was chosen for comparison of measured settling velocities:

$$w = \frac{RgD^2}{C_1 v + (0.75 C_2 RgD^3)} \quad \textbf{(1)}$$

Where $w$ denoted the particle's settling velocity, $R$ its submerged specific gravity, $g$ the acceleration due to gravity, $D$ its diameter, v the kinematic viscosity of the fluid and where $C_1$ and $C_2$ are constants with changing empirical values depending on the type of particle as described by Ferguson and Church. For our comparisons shown in Fig. 4.5, the constants for angular grains were utilised where $C_1$ = 24 and $C_2$ = 1.2. The measurements from the experiments and theoretical predictions were plotted in terms of settling velocity and equivalent diameter ($D_e$):

$$D_e = 2\sqrt{\frac{A}{\pi}} \quad \textbf{(2)}$$

Where $A$ , mm$^2$ is area of the particle as the particle is assumed to be spherical. This is to determine whether settling predictions of microplastics using formula based on sediment dynamics are applicable for microplastic transport.

## 3.3 Microplastics in the Mekong River

### 3.3.1 Site Locations

Fieldwork was conducted in Cambodia and Vietnam July 2019 at eight locations as shown in Figure.3.3. The upstream extent of our sampling was the town of Kratie and the rural area of Kampi, ~250 km north of Phnom Penh. Kampi is the location of a deep pool in the Mekong channel which is a natural habitat of the Irrawaddy Dolphin (Halls et al., 2013). The next area was in the Tonlé Sap River, Mekong River, and Bassac River at Phnom Penh, the capital of Cambodia. The final area was Can Tho, Vietnam, located next to Bassac River, the largest city on a distributary of the Mekong River in Vietnam with a busy waterway, Can Tho River. Examples of the river sites are shown in Fig.3.4 and 3.5.

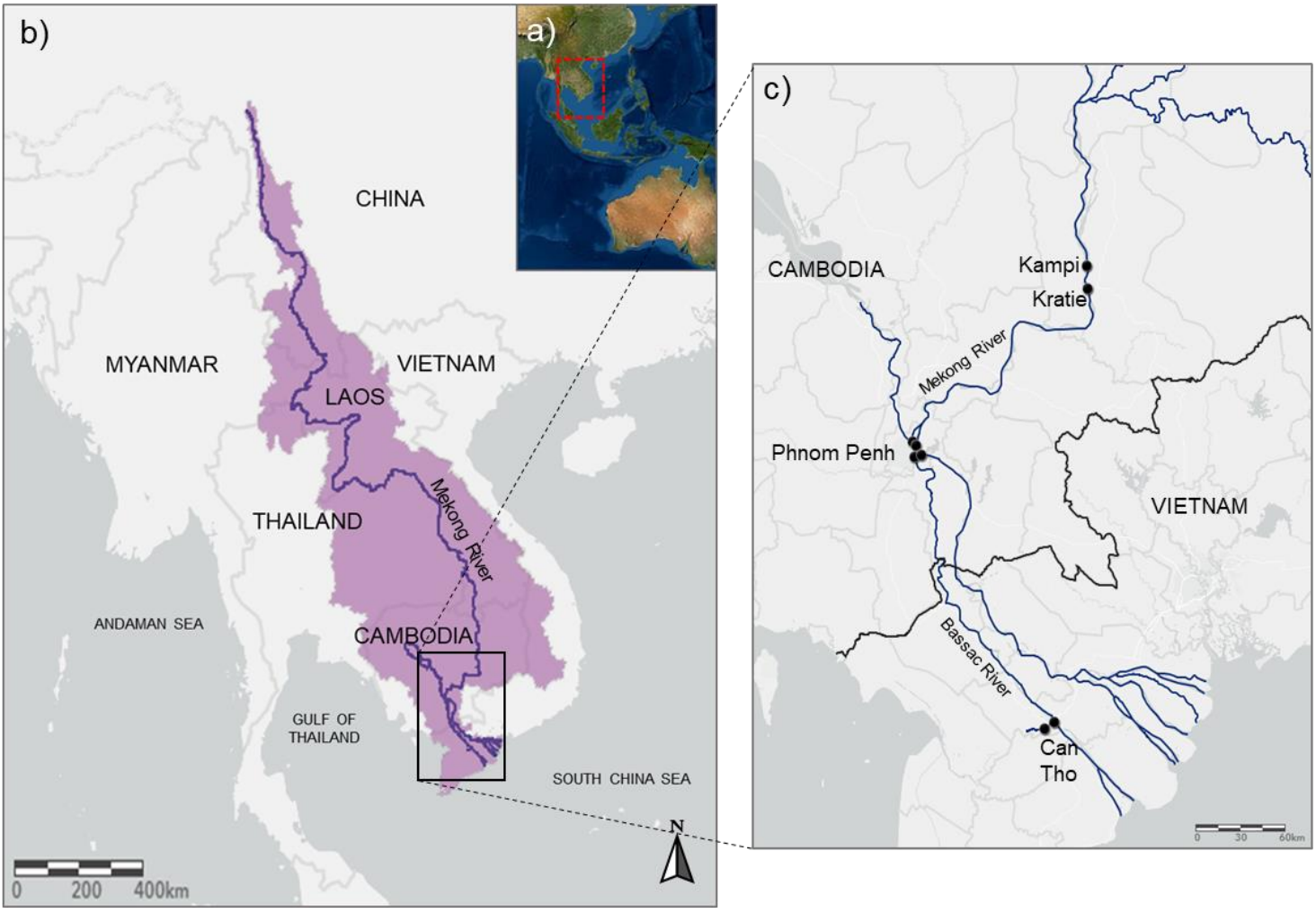


Figure 3.3: a) Overview of Mekong River location b) The Mekong River Basin area c) Sampling locations within the Mekong Basin in Cambodia (Kampi, Kratie and Phnom Penh) and Vietnam (Can Tho). Basemap for a) World Imagery49. Basemap for b) and c): Light Gray Canvas Map50, layers: GMS Major River Basin51 and Main Rivers52, Great Mekong Subregion Secretariat

Figure 3.4: The Mekong River Kratie, Cambodia.

Figure 3.5: The Mekong River at Phnom Penh, Cambodia.

### 3.3.2 Water sample collection

Five plankton nets, with a mesh size of 250 µm, were attached to a line at 4 m intervals with a weight on the end (Fig.3.6-3.8). This allowed samples to be collected at the surface and throughout the water column, with the number of depths collected dependent on the depth of the river at that location. Dive watches were attached to the rope to collect depth measurements. The nets were deployed from the back of a stationary boat for 5 minutes at each site, resulting in one collection per depth per site (n = 31). Using a water pump, each net was rinsed from the outside to ensure no contamination occurred and all material was collected in the codend. Each cod end was removed and rinsed with DI water into one glass bottle per net before being transferred to the laboratory for separation and analysis. The net was then rinsed inside and out before the next sample was collected. At the same time as the nets were deployed, an Acoustic Doppler current profiler (ADCP) was used to record and calculate the flow of the river. An example of plastic on the banks of the river and a sample collected in the codend are shown in Figure 3.9.

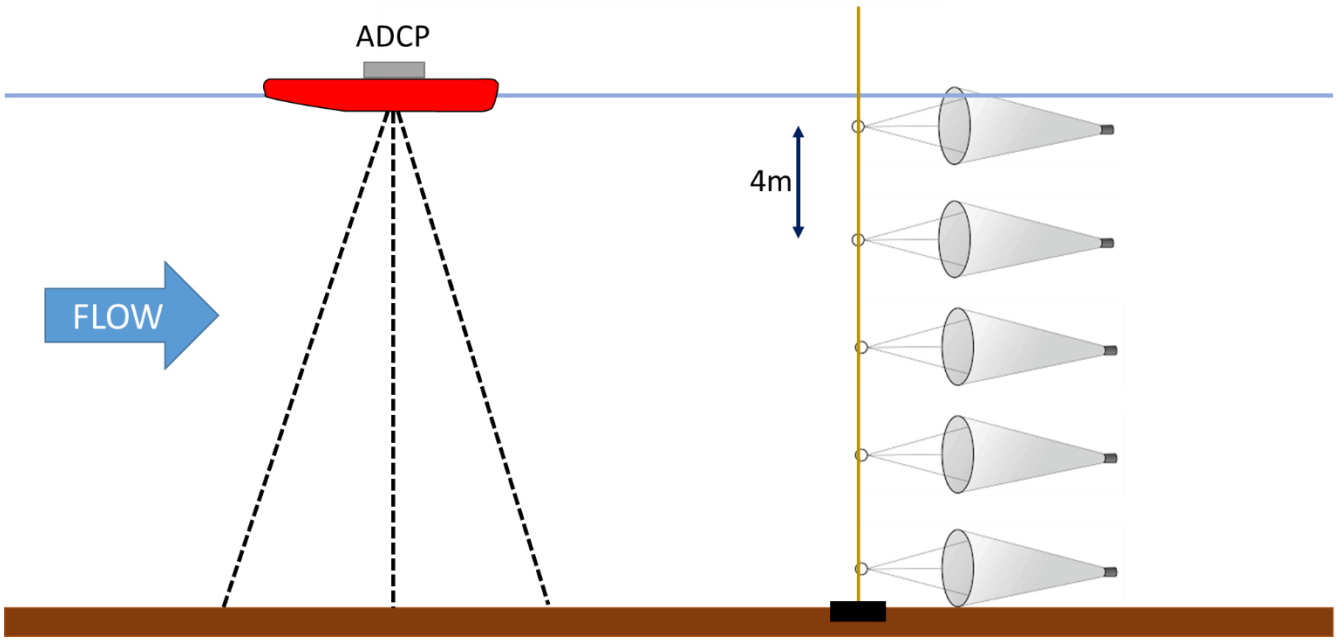


Figure 3.6: Setup of the water sample collection with five plankton nets throughout the water column and Acoustic Doppler current profiler (ADCP) used to record and calculate the flow of the river.


Figure 3.7: ADCP used to record and calculate flow of the river.

Figure 3.8: Plankton nets used for sampling microplastics in the Mekong River.

Figure 3.9: Examples of plastic on the banks and the shrubs of the Mekong River, Cambodia and microplastics collected in the plankton net codend.

### 3.3.3 Separation and filtration

Analysis of samples was conducted at the University of Hull, UK. Water samples were first vacuum filtered onto 55 µm-pore size Whatmann GF filter papers, covered and dried at room temperature. Next, each filter paper was placed in a glass flask and 30 ml of $H_2O_2$ (30%) was added. Flasks were put in a shaking incubator at 50°C, 100 rpm for 24 hours to digest any organic material. $H_2O_2$ (30%) at 50°C was chosen as it has been shown to be an efficient reagent for digesting organics while causing minimal damage to any microplastics present (Duan *et al.,* 2020; Nuelle *et al.,* 2014). Trials were also run on mock samples to test multiple digestion methods and confirmed this was the most efficient. Finally, 200 ml of deionised water was added to each sample, vacuum filtered, rinsed twice, and dried at room temperature.

### 3.3.4 Identification of microplastics

Filter papers were first analysed with an Olympus SZX10 microscope, Olympus UC30 camera, and (Olympus) CellSens software to identify and count suspected microplastics manually for each filter paper. The particles were then examined for polymer content using Fourier transform infrared (FT-IR) analysis, with a Thermo Fisher Scientific iN10 Nicolet spectrometer equipped with the OMNIC Picta software (Thermo Scientific OMNIC Series). Due to the large number of particles being identified as potential microplastics, 10% of each type of particle seen at every depth at each site was tested to gain a representation of every type observed, resulting in 719 suspected particles being verified. The spectra were recorded with 12 scans in the region of 800 – 6000 $cm^{-1}$. The spectra of a particle is recorded and compared to well-established polymer libraries in addition to contamination libraries which were identified from control samples. Examples of FT-IR spectra are shown in Appendix B, Figure B.1. Particles were determined as plastic if there was a match of at least 70%, the standard protocol for microplastic FT-IR analysis (Cai et al., 2019; Lusher et al., 2013). If more than 10% of each type of plastic at each depth and location were identified as plastic, it was assumed all particles in that subcategory were plastic. Plastics were organised as plastic-type (fibre, fragment, and film) and polymer type: polyethylene terephthalate (PET), polypropylene (PP), polyethylene (PE), Low-density polyethylene (LDPE), and “other” which includes non-typical polymers such as polyacrylonitrile (PAN).

### 3.3.5 Prevention of contamination

To prevent samples from being contaminated by airborne particles during the analysis - such as textile fibres, the following measures were taken. During collection and laboratory analysis, cotton clothing including lab coats were worn instead of synthetic materials in addition to Laboratory Latex gloves. All liquid reagents (deionised water, $H_2O_2$, and ethanol) used were passed through a filter paper (55 µm-pore size Whatmann GF) using a vacuum

pump before being used. Glass equipment was triple rinsed using filtered deionised water and stored sealed to prevent contamination. Work surfaces were cleaned with filtered 100% ethanol and all processes were performed in a fume hood to prevent airborne contamination. During each step of the analysis, a filter paper was placed on the work surface to account for contamination and procedural blanks were also run to determine contamination risks. These filter papers were examined using optical and FT-IR analysis as above. If polymers were identified, they were added to a contamination library which the environmental samples were all compared to. Out of the 719 suspected particles tested, only 3 matched the contamination library.

### 3.3.6 Calculation of microplastic concentration and flux

First, the volume of water, $m^3$, passing through the sampling net is calculated:

$$V = vAt \quad \textbf{(2)}$$

Where $v$ denotes the flow velocity, m $s^{-1}$, $A$ denotes the cross-sectional area, $m^2$, of the net, and $t$ is the length of sampling, s. Concentration of microplastics $C_{mp}$ , # per $m^3$ is calculated as follows:

$$C_{mp,number} = \frac{n_{mp}}{V} \quad \textbf{(2)}$$

Where $n_{mp}$ denotes the number of microplastics. Next flux is calculated as, where Q, $m^3/s$, is the discharge within the portion of water sampled (acquired from ADCP data):

$$Flux = QC_{mp} \quad \textbf{(3)}$$

### 3.3.7 Comparison to previous study

Haberstoch *et al.* (2021) also sampled the Tonlé Sap River, Lower and Upper Mekong River, and Bassac River at Phnom Penh in August and September of 2019. Total concentrations were compared at each site between our study (July 2019) and Haberstoch et al. (2021) to determine any trends and relationships between discharge and microplastic concentration. Haberstroch et al. (2021) sampled twice at each location, the first during August and the beginning of September, and the second in September. Average discharge data was acquired from a fully validated Mike11 model of the Phnom Penh region forced with observed discharge data from the river gauge at Kratie.

### 3.3.8 Statistical analysis

As the results were count data, Poisson regression model analysis was carried out to assess the differences between microplastic concentration/flux and location ($n = 8$). Spearman's rank test was used to determine the correlation between microplastic concentration/flux and depth at each site at a significance level of $p < 0.05$. All analysis was conducted using R Studio (R Core Team, 2013).

## 3.4. Trapping of microplastics by coral reefs

### 3.4.1 Microplastic particles

The transport and trapping of microplastics, in association with sparse and dense coral canopies are evaluated through experimental physical modelling described below.

Secondary microplastic particles in the form of fragments of recycled, ground melamine plastic, density 1.6 g/cm$^3$ (Little River Research & Design, Illinois), were chosen as the test polymer. Fragments were sieved to collect size fractions of a range of 1-5 mm. This ensured fragmentation of plastic and heterogeneous shapes and sizes that replicates the environmental degradation of microplastics (Rummel *et al.,* 2017). In addition, irregular shapes of microplastics were chosen instead of pellets and spheres to represent weathered and degraded plastics that are more typically found in the aquatic environments. Furthermore, to ensure plastics represented those found in the environment such as coastal systems, biofilmed microplastic particles were used. The properties of a polymer determine particle buoyancy, but retention and distribution of microplastics in the water column are also influenced by the colonisation of microorganisms forming a biofilm (Hoellein *et al.,* 2019; Chapter 4). Biofouling can alter the density of plastics, causing particles to sink or rise faster, which has considerable implications from a hydrodynamic perspective (Lagarde *et al.,* 2016; Rummel *et al.,* 2017). To colonise fragments with biofilms, the methods of Hoellein *et al.,* (2019) were adapted. Benthic sediment and overlying water was collected from the Humber River, Hull, UK. Fifty grams of sediment and 200 ml of river water was placed in flasks with microplastics in a shaking incubator for 10 days at 37°C, 200 rpm. The flasks were then left at room temperature for at least 2 weeks. Examples of biofouling can be seen in Chapter 4, Figure 4.1, where the same methods were utilised. Fragments were soaked overnight in water of the same salinity and temperature as the experimental environment to ensure no electrostatic discharge from particles, which may alter transport behaviour.

### 3.4.2 Surrogate canopies

Coral colonies were replicated using a scan of a staghorn coral *Acropora* genus (CULTS Copyright DSIGNRCMC 2020). Staghorn corals were chosen as they encompass approximately 160 species and around one-fifth of extant reef-building corals globally (IUCN, 2009). They are branching, stony corals that provide complex habitats for numerous reef organisms and coastal protection for thousands of people worldwide (IUCN, 2009). *Acropora* have a broad range of sizes, with branches growing from a couple of centimetres to over two metres. The models were printed in polylactic acid (PLA) with a base diameter $d_s$ = 100 mm and overall height $h_v$ = 150 mm, producing a submergence ratio ($h_v/h_w$) of 0.38 (Fig.3.10) (standing water depth $h_w$ = 400 mm), consistent within the broad range of the natural environment (Santos *et al.,* 2016). The model consisted of 11 branches of various lengths and diameters. Two coral canopies were assessed for microplastic capture: a) sparse (15 corals) and b) dense (48 corals) to encompass various reef formations, and were arranged in staggered configurations of 1.85 m long within a 2 m test section (Fig.3.11). Individual dynamically- and geometrically-scaled canopy elements of coral were populated on a baseboard (10 mm thick) in a systematic staggered geometry to produce a full canopy spanning the entire flume width (0.5 m) and length 1.85 m located in the middle of the flume, with a canopy height, $h_c$ of 0.15 m (Fig.3.11). The canopy length exceeded 10 $h_c$ to encompass a developing flow regime downstream of the leading edge (Nepf, 2012). Canopy densities represent *in situ* measurements of 15 corals/m$^2$ for the sparse and for 48 corals/m$^2$ for the dense canopy. A thin layer of fine silica sand (120 μ) was fixed to the top surface of the baseboard to increase the surface roughness to a level comparable to natural environments. This baseboard was also used as a control to represent a barebed, with all velocities tested.

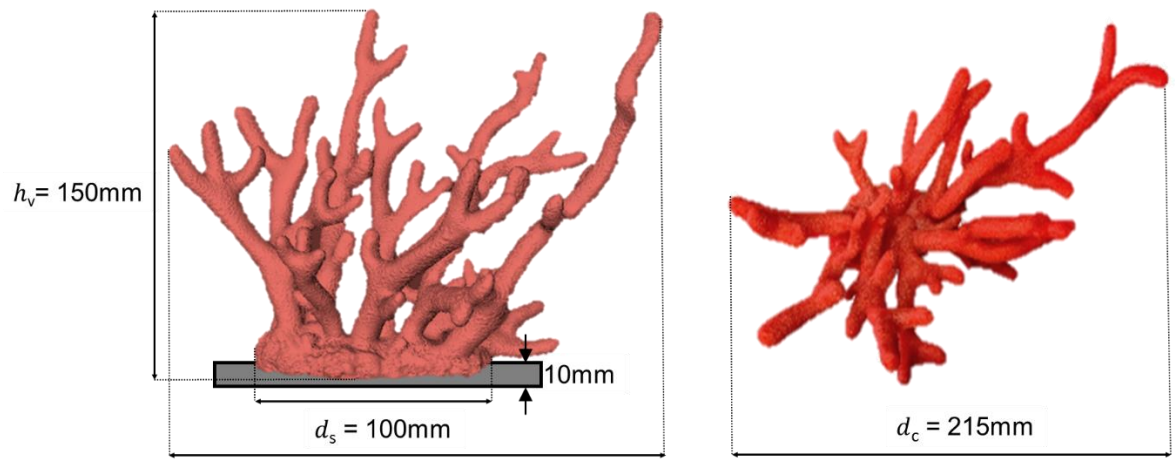


Figure 3.10: Diagram of the staghorn coral (*Acropora* genus) model attached to the baseboard

### 3.4.3 Flume setup, trials, and data acquisition

Microplastic fragment trapping by complex habitat structures was simulated in the Geomorphology and Hydrology Laboratory, University of Hull, using the combined wave-current flume of length 8 m, width 0.5 m, and height 0.5 m. Experiments were operated under unidirectional flow with a standing water depth of $(H_w)$ 0.40 m. With coordinate system $x, y, z$ whereby $x = 0$ at the upstream canopy front edge, and $y = 0$ at the baseboard top.

The retention of microplastics within each canopy was determined under four different bulk incoming velocities $U$ = 0.15, 0.2, 0.25, 0.3 m/s which have been observed in shallow coral reefs (Johansen, 2014). A set weight of fragments were tested per simulation: canopy type, and four flow velocities, resulting in 12 trials and subsequent trapping analysis in total. Before each simulation, the flume was run for 2 minutes to allow the flow to stabilise. Fragments were released with a siphon at a constant rate for 10 minutes submerged at the top of the water column under the surface. The distance of release depended on the flow speed but was tested prior to the experiments to ensure microplastics were in suspension when they entered the front of the canopy. Upon introduction of all microplastics, the flume was run for 1 hour, enabling assessment of transport rates and processes during this time. A

net was located downstream of the canopy to capture any microplastics not trapped in the canopy and preventing them from being recirculated in the system (Fig. 3.11). Examples of the dense and sparse coral canopy set-ups are shown in Fig 3.12-3.14.

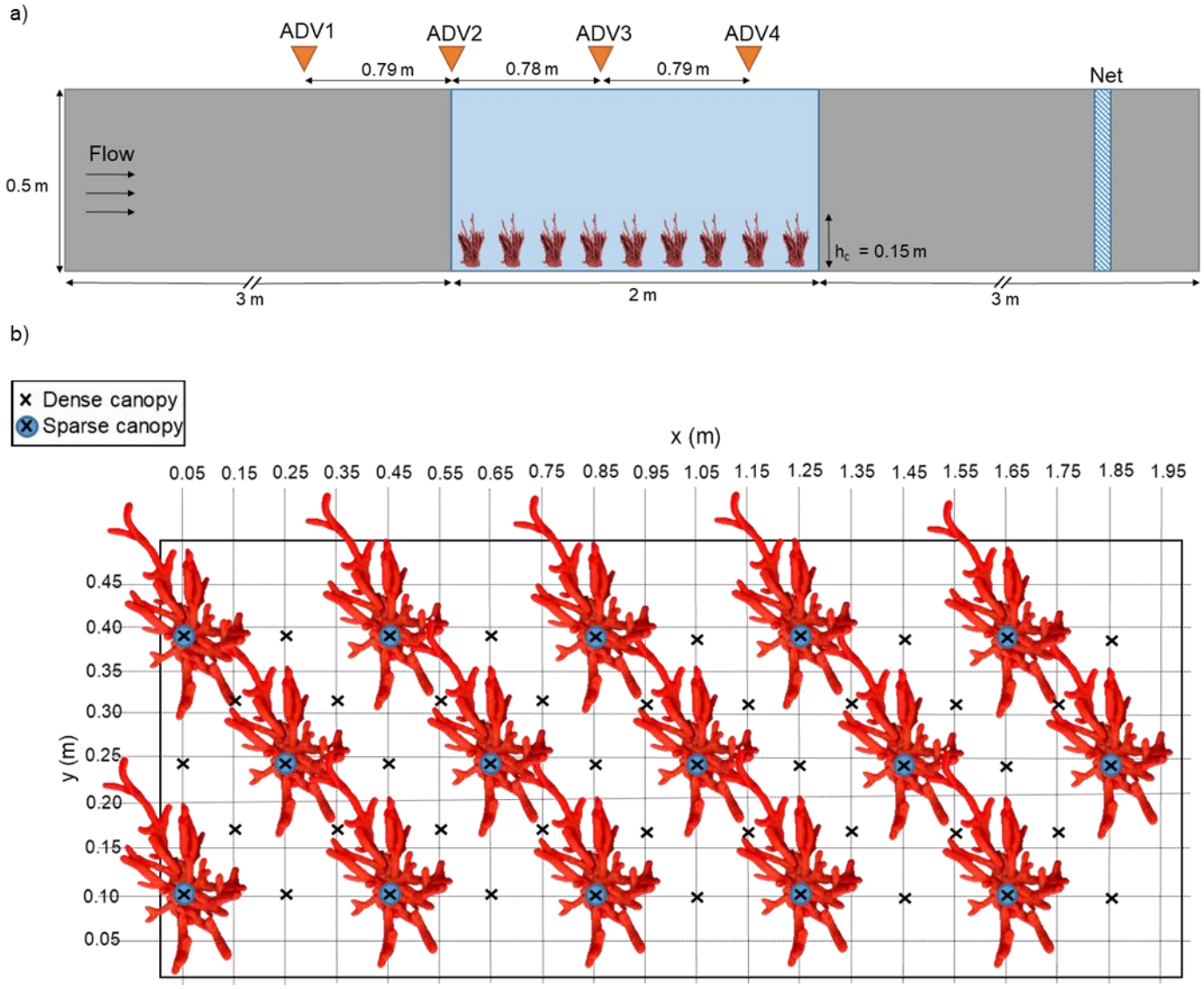


Figure 3.11: The flume setup: a) side view of the flume and test section containing the canopy. Four acoustic Doppler velocimeters (ADVs) were placed in the flume and a net to capture microplastics. b) The arrangement of sparse and dense corals within the canopy

To evaluate the distribution of microplastics under different scenarios, overhead and side images were also taken at the end of each run by overhead cameras at $x$ = 0.07 m, 0.9 m, and 1.7 m, and side cameras at $x$ = 0.12 m and 1.1 m. Flume sidewalls were lined black to increase the visual contrast of microplastics. Complementary manual measurements were

recorded to validate the optical measurements and tracking. Following each run, the microplastics at the downstream net were collected, dried, and weighed to determine the percentage of microplastics that remain within the canopy under different flow regimes and canopy densities. The microplastic particles that trapped within the test section were then collected, with the whole system cleaned before the next scenario was conducted.

To quantify the associated hydrodynamics, flow velocities were acquired using acoustic Doppler velocimeters (ADVs), (Nortek, Vectrino) using a sampling rate of 50 Hz for 5 minutes, upstream and evenly spaced throughout the test section. This was conducted separately from the microplastic data acquisition to avoid disruption to the flow field. Several branches were removed during the acquisition of velocity data in the dense canopy, as implemented in previous studies (Pujol *et al.,* 2012). It is acknowledged that this approach results in a slight modification to the flow structures but provides a primary fundamental quantification of flow properties in each canopy (Abdolahpour *et al.,* 2017). Velocity measurements were taken in front and throughout the canopy at $x$ = -0.78 m (ADV1), 0 m(ADV2), 0.79 m (ADV3), and 1.57 m (ADV4) (Fig.3.11); and at vertical positions of $z/h_c$ = 0.43, 0.57, 0.70, 0.90, 1.03, 1.17, 1.37, 1.57, 1.70, 2.03, 2.37, 2.57.

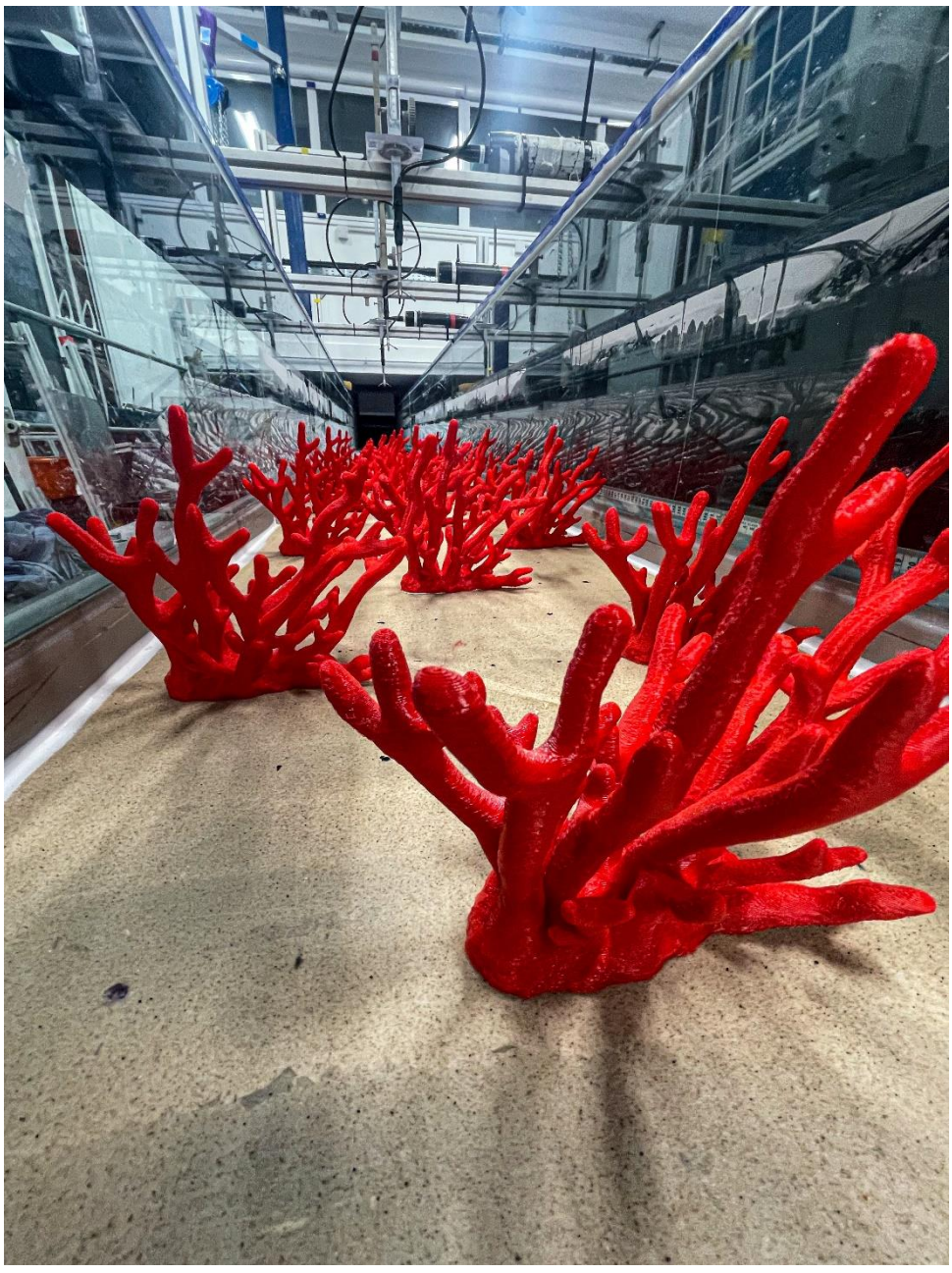

Figure 3.12: The flume setup of the sparse coral canopy

Figure 3.13: The flume setup of the dense coral canopy

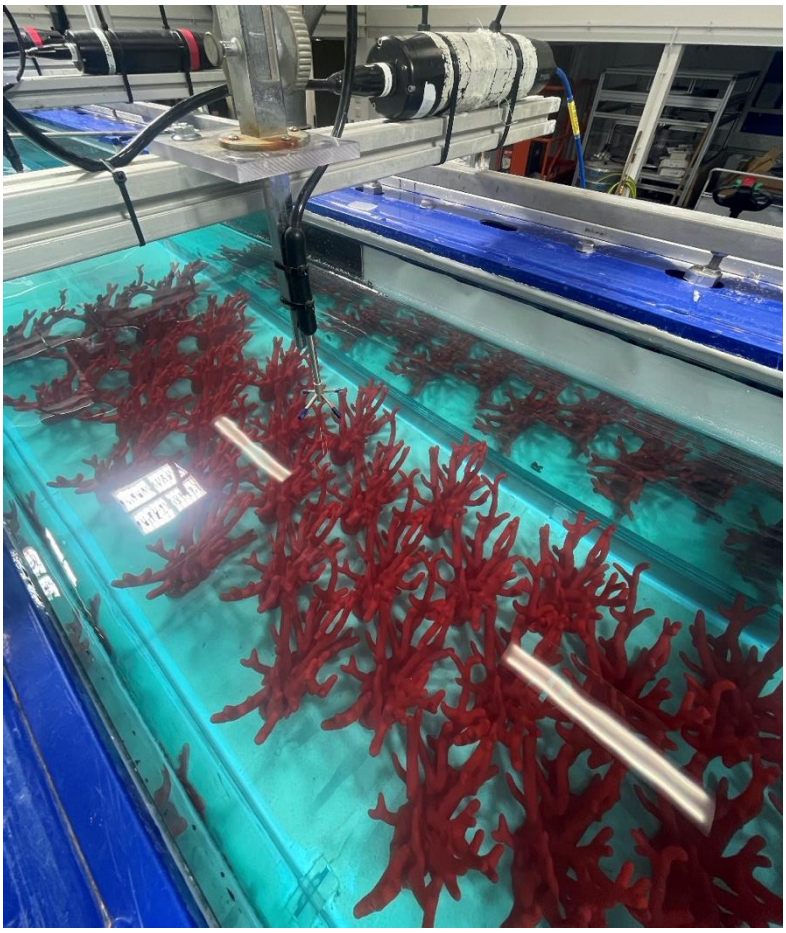

Figure 3.14: The flume setup of the dense coral canopy from above showing one of the ADCPs

[Page intentionally left blank]

# Chapter 4.

# Shifting settling regimes of aquatic microplastics

---


## Abstract

Rivers are the major conveyor of plastics to the marine environment, but the mechanisms that impact microplastic (<5 mm) transport, and thus govern fate of the material in the environment, are largely unknown. This prevents progress in understanding microplastic dynamics and identifying zones of high accumulation, as well as curtailing the development of effective mitigation and policy measures. Using a suite of novel settling experiments we show, for the first time, that microplastic settling is highly influenced by a combination of biofilm growth, water salinity and suspended clay concentrations typically seen across fluvial to marine environments. Results indicate that biofilms significantly increased settling velocity of three different polymer types of non-buoyant microplastics (fragments and fibres, size range 0.02-4.94 mm) on average by 40%, and significant increases in settling velocity were observable within hours. We also demonstrate how these impacts are both polymer and shape specific and that settling regimes also differ according to both salinity and sediment concentrations, which are typical of freshwater-marine boundaries found in estuaries. Our results demonstrate how existing transport formulae are inadequate to capture these impacts and highlight the importance of considering these processes within next generation predictive frameworks to understand and robustly predict the fate and impact of microplastic pollution within aquatic environments.


***This chapter is currently in review with Nature Communications Earth & Environment. Please see the contribution statement on page vi.***

## 4.1 Introduction

Estimates of plastic flux entering the ocean annually vary between 4.8 to 12.7 million metric tonnes, while floating marine plastic is calculated to be only 268,940 tonnes, accounting for just 2-6% of the estimated plastic entering aquatic systems every year (Eriksen et al., 2014; Jambeck et al., 2015). Land-based sources such as mismanaged waste, have resulted in rivers becoming a major pathway for plastic pollution to enter the marine environment (Jambeck *et al.,* 2015; Lebreton *et al.,* 2017). Yet, as microplastics (< 5mm), move through a river basin and transfer to the marine environment, they will undergo a range of environmental gradients and physical, biological and chemical transitions, including changes in salinity and sediment concentrations. Additionally, weathering and biofilm growth will also impact the vertical distribution of microplastics through the water column (Duan *et al.,* 2021; Hoellein *et al.,* 2019; Vroom *et al.,* 2017).

The likelihood that a given microplastic particle will settle out of suspension when entering an aquatic system varies depending on the physicochemical, hydrodynamic and biological conditions of the environment (Hoellein *et al.,* 2014; Zhang, 2017). First, microplastic distribution is dependent on the polymer properties (density, shape, size, etc.), but as subsequent growth of surficial biofilm occurs within minutes to hours of entering an aquatic system (Amaral-Zettler et al., 2020; Zettler et al., 2013a) (Fig.4.1) the particle density can change rapidly. This results in alterations to particle buoyancy and thus relative density to the ambient fluid, which has considerable implications in varying a particle's trajectory in the water column (Chubarenko *et al.,* 2016; Cooksey and Wigglesworth-Cooksey, 1995; Fazey and Ryan, 2016; Lagarde *et al.,* 2016; Rummel *et al.,* 2017). In addition, with surficial biofilms, microplastic particles can also become parts of hetero-aggregates (or flocs), which includes other naturally suspended sediment (Cunha *et al.,* 2019; Long *et al.,* 2015). The development of flocs, and further associated changes in density and particle size, is known

to affect the settling velocity of particles (Andersen et al., 2021; Manning et al., 2010a). While silts and clays that undergo flocculation are typically 0.06 mm or smaller in size, flocculation can occur at larger grain sizes, including sand (Cuthbertson et al., 2018; Manning et al., 2010b). Indeed, Besseling et al. (2017) has demonstrated the aggregation of 70nm and 1050nm polystyrene particles with clay in natural freshwaters (Besseling et al., 2017b). However, the impact of floc formation on microplastic distribution, settling and fate is currently unquantified for larger particles and within saline waters (Andersen et al., 2021; Long et al., 2015; Möhlenkamp et al., 2018).

Changes in salinity and suspended sediment concentration that occur across a freshwater-marine boundary is known to affect the development of flocs and thus overall settling velocity of particles, especially as the relative density of the particle changes as it moves into denser saline water (Ivens Portela *et al.,* 2013; Li *et al.,* 2019; Manning and Schoellhamer, 2013; Mietta *et al.,* 2009). As water becomes more saline (and water density increases), particles are more likely to stay suspended within the water column. Settling velocity is thus a key parameter used to predict sediment transport pathways, yet no comprehensive study has yet experimentally quantified the combination of these effects (biofilm, salinity and sediment concentration) for microplastics (Appendix A, table A.1) (Bagaev et al., 2017; Ballent et al., 2012; Hoellein et al., 2019; Kaiser et al., 2017; Khatmullina and Isachenko, 2017; Kowalski et al., 2016; Laursen et al., 2022; Möhlenkamp et al., 2018; Waldschläger and Schüttrumpf, 2019).

Here, we experimentally quantify how microplastic settling velocities vary through time as a function of biofilm growth and as they transition from freshwater to saline conditions in addition to experiencing various sediment concentrations typically found in estuarine environments. The various salinity and suspended sediment conditions were tested to ensure the experiments were environmentally relevant as possible, as the majority of microplastics originate from land-based source and will therefore undergo these environmental changes as they transition from fluvial to marine systems. Three non-buoyant

microplastics types were tested: Polyethylene terephthalate (PET), Polyvinyl chloride (PVC) fragments and nylon, polyester and acrylic (NP&A) fibres. It is acknowledged that there are more several common polymers frequently found in aquatic environments. However, preliminary experiments that included buoyant microplastics (polystyrene (PS), polypropylene (PP) and high-density polyethylene (HDPE)) showed that the majority of these particles remained buoyant even after biofouling. Furthermore, as floating microplastics constitute only 2-6% of the estimated plastic entering aquatic environments annually, it is vital to gain an increased understanding of how non-buoyant microplastics are transported in these systems (Eriksen et al., 2014; Jambeck et al., 2015). Therefore this study focused on non-buoyant particles. Using high-resolution measurements of particle settling velocities, we demonstrate how biofilm growth, changes in salinity and sediment concentration impact microplastic settling velocities, and show how these impacts are polymer and shape specific. Furthermore, our analysis reveals that widely applied sediment transport formulae (Engelund and Hansen, 1967; Ferguson and Church, 2004; Meyer-Peter et al., 1993; Van Rijn and Kroon, 1993) are inaccurate for predicting microplastic fate and transport; microplastic interactions with- and relative density changes due to- biofouling, as well as salinity and sediment concentration changes, are not well-constrained for microplastics in sediment transport laws.

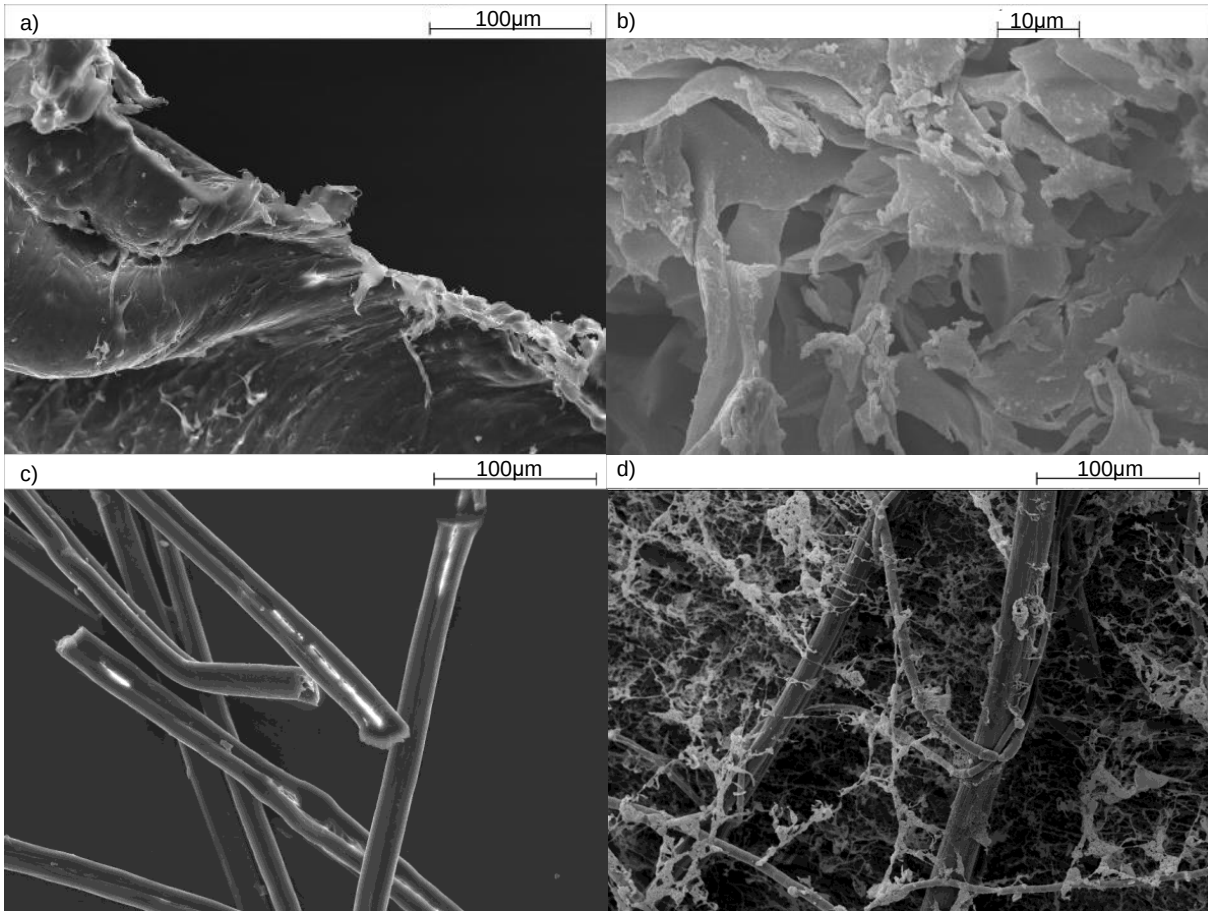


Figure 4.1 Scanning electron microscope (SEM) images of microplastics before and after biofilm colonisation: a) clean polyethylene terephthalate (PET) b) biofilmed PET c) clean nylon, polyester and acrylic (NP&A) fibres and d) biofilmed NP&A fibres

## 4.2 Methods

### 4.2.1 The microplastic particles

The majority of observed macoplastics in riverine systems are from packaging of a range of polymer densities, as turbulence of rivers allows polymers to remain buoyant (Schwarz *et al.,* 2019). Therefore, polymer types commonly found across freshwater and ocean environments, including beaches, sediment and epipelagic areas were chosen for the settling experiments (Schwarz *et al.,* 2019). Three types of plastic polymers were selected: fragments of polyethylene terephthalate (PET) (1.39 g/cm$^3$) and polyvinyl chloride (PVC) (1.44 g/cm$^3$) (Direct Plastics Limited, Sheffield, UK) were generated using a carving file. This ensured fragmentation of plastic and heterogenous shapes and sizes that replicates environmental degradation of microplastics (Rummel *et al.,* 2017). Fibres were generated

from nylon, polyester and acrylic (NP&A) yarn (1.01-2.30 g/cm$^3$) (The Knitting Network, Sittingbourne, UK). The properties of the polymers used in the experiments are summarised in Table 4.1. Fragments and fibres were generated to be in the typical size range of microplastics commonly found in aquatic environments (0.01-5 mm) (Hidalgo-Ruz *et al.*, 2012). In addition, irregular shapes of microplastics were chosen instead of pellets and spheres, to represent weathered and degraded plastics more typically found in the aquatic environment. This allowed an estimate of settling velocities of microplastic particles that resemble those found in aquatic environments.

Table 4.2: Summary of microplastic properties used to settling experiments. Size ranges (a-axis) were determined with a self-developed code in Matlab, see more details below.

| Polymer | Density (g/cm$^3$) | Size range (mm) |
|---|---|---|
| Polyethylene terephthalate (PET) | 1.39 | 0.02-4.20 |
| Polyvinyl chloride (PVC) | 1.44 | 0.04 -4.94 |
| Nylon, polyester and acrylic (NP&A) | 1.01-2.30 | 0.02-0.59 |

To colonise biofilms on microplastic particles, the methods of Hoellein *et al.,* (2019) were adapted. Benthic sediment and overlying water was collected from the Humber River, Hull, UK (53.7144° N, 0.4458° W). Fifty grams of benthic sediment and 200ml of river water was placed in flasks with microplastics in a shaking incubator for 10 days at 37 °C, 200 rpm. The flasks were then left at room temperature for 6 months. It should be noted that fibres are known to have significantly less bacterial abundance in biofilm colonisation compared to fragments and pellets (Hoellein *et al.,* 2019) and it was therefore expected that there would be less biofilm formation on fibre samples. Examples of plastics before and after biofilm growth are shown in figure 4.1.

To initiate the formation of flocs (aggregated mass of material), kaolinite, a clay particle abundant in estuarine environments was chosen (100-600 mg/L) and mixed with high concentrations of clean and biofilmed microplastics, with each polymer kept in separate 200

ml conical flasks. This was repeated for each salinity and polymer type. The sediment range of 100-600 mg/L was chosen from data collected by the Mekong River Commission (Mekong River Commission, 2021) and incorporates suspended sediment concentrations found from fluvial to delta environments of one of the top contributing rivers to marine plastic pollution. To replicate turbulent flow, the sediment-microplastic mixtures were shaken horizontally at 300 rpm for 5 minutes then 150 rpm for 20 minutes. To ensure any flocs formed held together, particles were extracted from the beakers with a glass pipette while they were still being shaken at 80rpm and dropped in the water column (see below).

### 4.2.2 Experimental setup

The settling velocity of the microplastic particles was determined through a series of non-intrusive sinking experiments conducted in a Laboratory Spectral Flocculation Characteristics (LabSFLOC) plexiglass column with dimensions of 12 cm x 12 cm x 33 cm (Fig. 4.2, analogous to previous settling velocity experiments (Andersen et al., 2021; Ballent et al., 2012; Elagami et al., 2022; Kaiser et al., 2017, 2019; Khatmullina and Isachenko, 2017; Manning et al., 2007; Möhlenkamp et al., 2018; Nguyen et al., 2022; Van Melkebeke et al., 2020; Waldschläger et al., 2020b; Waldschläger and Schüttrumpf, 2019), Appendix A, Table A.1 ). The LabSFLOC settling column is combined with an LED light panel and high-resolution video camera (Fig.4.2) that collects particle settling video data that is processed to understand size, shape and velocity of individual particles and flocs. This allows individual particles to be easily analysed for their settling behaviour and aggregation. It is comparable to previous microplastic settling experiments that have utilised similar water columns.

The LabSFLOC water column was filled with distilled water of salinities (n=3, ppm, SAL) ranging from SAL 0-30 to represent the change in salinity from a freshwater to a fully marine environment. Distilled water was utilised to ensure no impurities were impacting microplastic transport. Water temperature and pH were recorded at least 15 minutes before each experimental run and immediately after to ensure consistency. Fifteen minutes allows the water column to settle after any disturbances caused by measuring temperature and pH

(Khatmullina and Isachenko, 2017). Before each experiment, microplastics were immersed in water of the same salinity and temperature used in the experimental water column in glass petri dishes to ensure no electrostatic discharge from particles, which may prevent or alter sinking behaviour (Kaiser et al., 2017). For clean and biofilmed particles, microplastics were placed 0.01 m below the water surface of the LabSFLOC to prevent any restraint caused by surface tension and left to move freely. For microplastics that were being tested under different sediment concentrations, a glass pipette was utilised for transferring particles so not to disturb any formed flocs.

A series of images were taken of the particle movement. At least 100 particles per condition were recorded for PET and PVC experimental series. However for fibres, particles tended to clump together which made analysis of movement difficult. Therefore at least 10 particles were recorded per variable for fibre analysis. For PET total n = 1,796, PVC n = 1,015 and NP&A n = 1,111. Particles travelled at least 15cm before image recording took place to ensure microplastics had reached terminal settling velocity. This distance was chosen in accordance with measurements from other studies (Khatmullina and Isachenko, 2017; Kowalski *et al.,* 2016; Waldschläger and Schüttrumpf, 2019). For each polymer (PET, PVC and NP&A fibres), measurements were taken for clean and biofilmed particles under 3 salinities (SAL0, 18 and 30) and 3 sediment (clay) concentrations (100 mg, 400 mg and 600 mg), resulting in 54 scenarios. Finally, to assess the impact of biofilm growth on settling velocity, measurements were taken at 0,1,2,4 and 8 weeks for biofilmed PET fragments at SAL18. Images were analysed using a self-developed code in Matlab (R2020a) (MATLAB, 2020), see Appendix A. Particle detection was made using the ‘imbinarize’ function available in Matlab, using global thresholding (Otsu, 1979) or adaptive thresholding (Bradley and Roth, 2007) depending on image characteristics. Particle properties, including area, were obtained using the 'regionprops' function. The velocities were obtained with self-developed cross-correlation based Particle Tracking Velocimetry (PTV) routines.

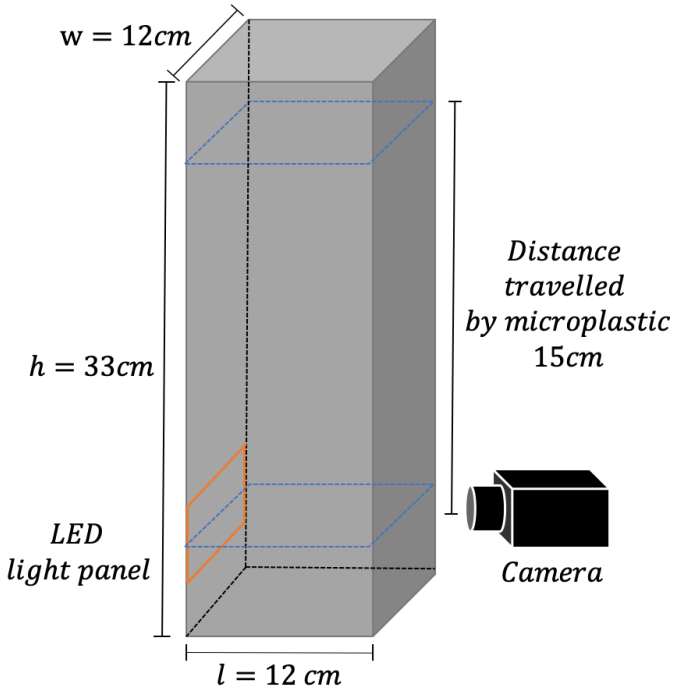


Figure 4.2: Schematic of the laboratory spectral flocculation characteristics (LabSFLOC) experimental setup: pexiglass column of height 33 cm with a square cross section of 12x12 cm, filled with deionised water of varying salinities.

### 4.2.3 Statistical analysis

To understand the effects of microplastic condition (clean or biofilmed), salinity and clay concentration on settling velocity of microplastics, the combined interactions of [condition and salinity] and [condition and clay concentration] were assessed using generalised least square means analysis. All statistical analysis was conducted using R Studio (R Core Team, 2013). Interactions were considered statistically significant if $p < 0.05$. Post hoc analysis was conducted using the lsmeans package, (Lenth, 2016) Tukey adjusted to understand significant differences between the least-squares means of specific variables by fitting linear models. For biofilm growth analysis from 0-8 weeks, a repeated measures ANOVA was utilised after square root transformation to ensure equal variance (verified with Levene Test) and post hoc analysis.

### 4.2.4 Comparison to settling velocity predictions and formulae

As settling of microplastics has been related to the transitional flow regime, the formula of Ferguson and Church, (2004) for smooth, varied and angular grains was chosen for comparison of measured settling velocities:

$$w = \frac{RgD^2}{C_1 v + (0.75 C_2 RgD^3)} \quad \textbf{(3)}$$

Where $w$ denoted the particle's settling velocity, $R$ its submerged specific gravity, $g$ the acceleration due to gravity, $D$ its diameter, v the kinematic viscosity of the fluid and where $C_1$ and $C_2$ are constants with changing empirical values depending on the type of particle as described by Ferguson and Church. For our comparisons shown in Fig. 4.5, the constants for angular grains were utilised where $C_1$ = 24 and $C_2$ = 1.2. The measurements from the experiments and theoretical predictions were plotted in terms of settling velocity and equivalent diameter ($D_e$):

$$D_e = 2\sqrt{\frac{A}{\pi}} \quad \textbf{(2)}$$

Where $A$ , mm$^2$ is area of the particle as the particle is assumed to be spherical. This is to determine whether settling predictions of microplastics using formula based on sediment dynamics are applicable for microplastic transport.

## 4.3 Results and Discussion

### 4.3.1 Biofilm and particle shape impacts

To evaluate the controlling factors that influence microplastic transport, a series of settling experiments measuring particle settling velocity were conducted; testing fragment and fibre

polymer types and shapes, the impact of biofouling, salinity, and suspended sediment concentrations on settling velocity. Comparisons were made between clean and biofilmed particles under varying salinity and clay concentrations to understand the effects of biofouling under different conditions. The impacts of salinity and clay concentrations were also evaluated for clean and biofilmed particles separately. Comparisons were considered significant when $p < 0.05$ and are summarised in Appendix A table A.2. Biofilm time trials were also conducted to understand how quickly the impacts of biofilms on settling velocities are realised. Biofilm growth had the greatest impact on microplastic settling across all salinities and clay concentrations and increased the settling velocity on average by 40%. The magnitude of this change was different between polymer types. Settling velocity increased significantly between the clean and biofilmed PET at all salinities (ppm, SAL): by 73% at SAL 0, 29% at SAL18 and 55% at SAL30, and all clay concentrations: 83% at 0 mg, 27% at 100 mg, 67% at 400 mg and 64% at 600 mg clay (Fig.4.3.a). However, for PVC fragments, the significant increase in velocity between clean and biofilmed particles was seen for fewer scenarios: 25% at SAL30, 13.5% at 0 mg and 68% at 600 mg clay (Fig 4.3.b). There was also a reduced effect of biofouling on nylon, polyester and acrylic (NP&A) fibres with a significant increase in settling velocity observed for two scenarios: 55% at SAL30 and 132% at 400 mg clay (Fig. 4.3c).

Biofilm growth causes microplastics to settle faster due to an increase in particle specific density, not area (Appendix A Fig.A.4-6), which has been observed before (Fazey and Ryan, 2016; Hoellein et al., 2019; Kaiser et al., 2017; Morét-Ferguson et al., 2010; Ye and Andrady, 1991)**.** Biofouling was expected to cause microplastics to become stickier and form flocs, leading to an observable increase in particle size (Rattanakawin and Hogg, 2001), yet this was not seen. Previous studies have shown that the growth of biofilms and consequent hetero-aggregate formation is highly dependent on microplastic polymer chemical nature (polymer type) (Lagarde *et al.,* 2016). Polypropylene (PP) fragments are more likely to form heteroaggregates with freshwater algae compared to high-density

polyethylene (HDPE), potentially due to different types of biofilm extracellular polymeric substances (EPS) being produced (Lagarde *et al.,* 2016). The chemical composition and surface texture of PET is also likely to have provided a preferred medium for microbes to grow on compared to PVC and NP&A fibres. Compared to PET and PVC fragments, NP&A fibres were far less impacted by biofilm colonisation, likely due to their shape (Hoellein *et al.,* 2019).

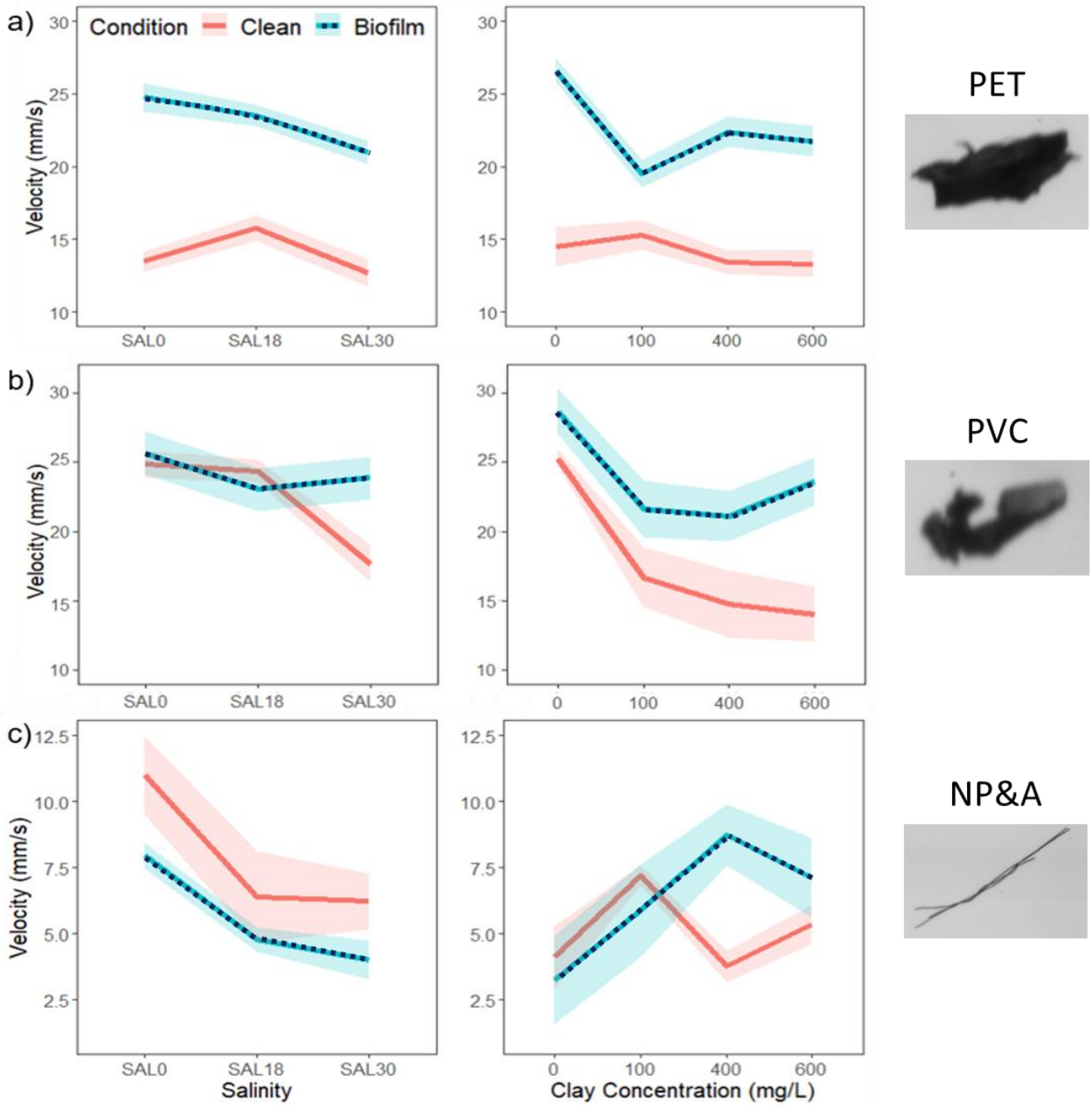


Figure 4.3: Main effects plot of condition, salinity and clay concentration on a) PET b) PVC and c) NP&A fibre microplastics. Solid lines indicate mean plots, while the shaded areas indicate confidence bands for all points. For PET n = 1,796, PVC n = 1,015 and NP&A n = 1,111. Note that for c) the scale range is smaller as settling velocity was considerably lower for NP&A fibres.

The impacts of biofilms on microplastic settling velocity occur quickly and in typically less than a week, as demonstrated by our time trials: PET fragments were biofouled and settling velocity measured over 0-8 weeks (Fig. 4.4). Settling velocity increased considerably by week 1 with average settling velocity of PET fragments being 16.85 ± 0.92 mm $s^{-1}$ (± values represent standard error) at week 0 (clean), increasing to 29.38 ± 1.16 mm $s^{-1}$ at week 1 and 36.67 ± 1.95 mm $s^{-1}$ at week 2. The settling velocity was statistically significant at the different time points ($F(3,211)=3.05$, $p<0.05$). In fact, biofilm growth significantly impacted PET settling velocity from week 0 to week 1 ($p<0.001$), week 2 ($p<0.001$), week 4 ($p<0.001$) and week 8 ($p<0.001$) and between week 1 and week 2 ($p=0.04$). This demonstrates how the dynamics of microplastics settling rates are fundamentally controlled by time; the longer a particle is exposed to biologically active aquatic environments, the more the particle properties will change.

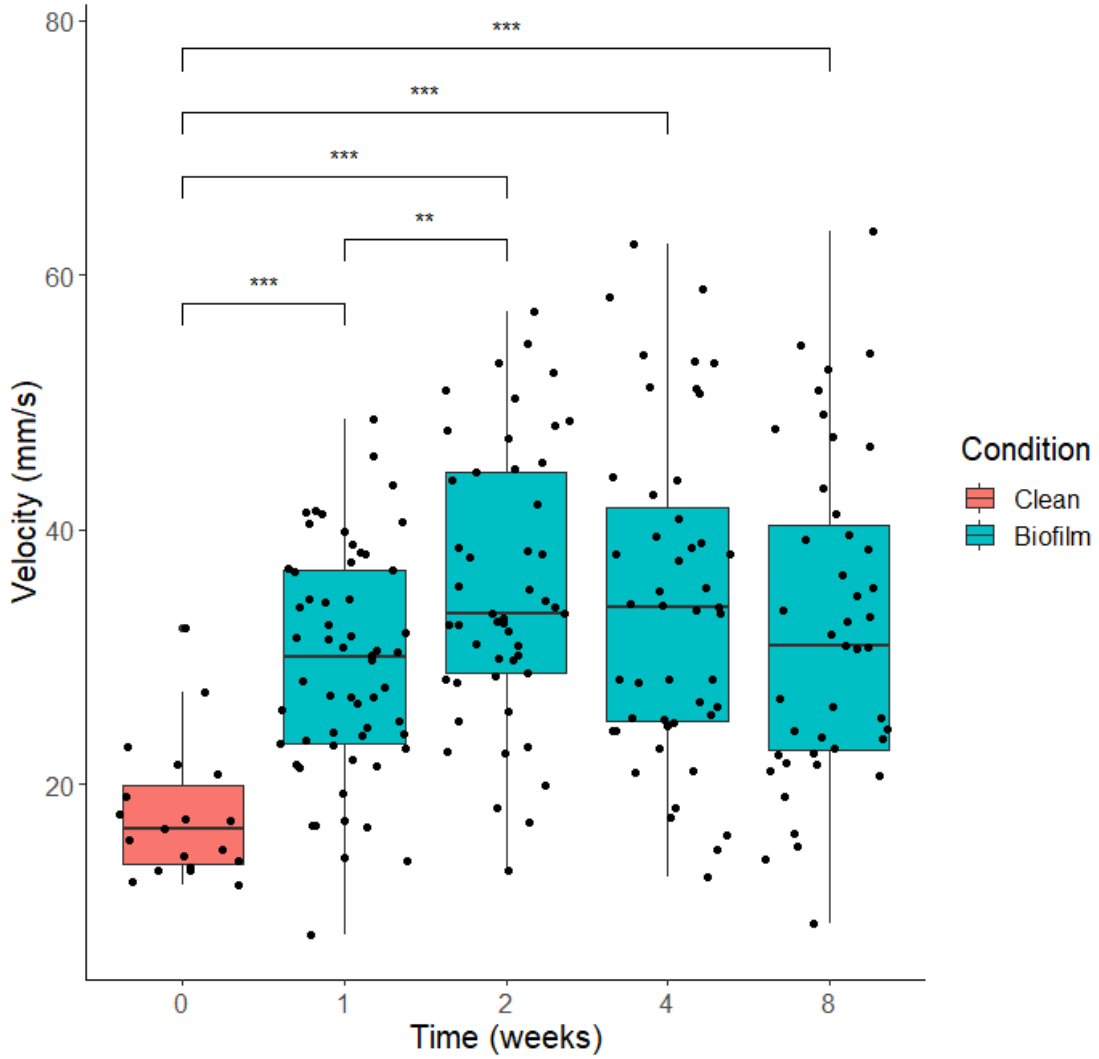


Figure 4.4: Changes in settling velocity of PET fragments over time (0-8 weeks) due to biofilm growth. Brackets demonstrate statistical significance: *** p <0.001 and ** p<0.05

### 4.3.2 Microplastic settling behaviour changes across the freshwater-marine salinity gradient

Our results reveal that microplastic settling velocity is influenced by changes in salinity and sediment concentration (Fig. 4.3) that would be experienced as microplastic particles cross the freshwater-marine boundary. It is clear that multiple environmental and biological conditions need to be considered when predicting microplastic transport. For clean PET fragments, settling velocity was significantly higher at SAL18 (15.8 mm $s^{-1}$ ± 0.54), compared

to SAL0 (13.1 mm $s^{-1}$ ± 0.40) and SAL30 (12.7 mm $s^{-1}$ ± 0.49). However, for biofouled particles, settling velocity was considerably higher at SAL0 (22.74 mm $s^{-1}$ ± 0.76) compared to SAL30 (19.68 mm $s^{-1}$ ± 0.67). The influence of salinity was much more varied for PVC fragments, with clean particles settling rates significantly lower at SAL30 (17.67 mm $s^{-1}$ ± 0.78) compared to SAL0 (24.90 mm $s^{-1}$ ± 1.10) as expected. Biofilmed PVC fragments settled significantly faster at SAL0 (25.67 mm/s +/- 0.98) compared to SAL18 (23.05 mm $s^{-1}$ ± 0.97) but a lesser effect on settling velocity was observed due to salinity under these conditions. Finally, no significant effect on settling rate due to salinity was observed for NP&A fibres. Polymer-specific salinity impacts have been shown previously, with higher salinity leading to lower settling velocities for certain polymers (Kaiser et al., 2017). Salinity lowers settling velocity for polystyrene (PS) particles, yet for higher density polymers such as PET and PVC salinity had less of an impact (Kowalski *et al.,* 2016). Conversely, Wang *et al.,* (2021) described how an increase in salinity only had minor impacts on PET but showed impacts on PVC, lowering the settling velocity. This is similar to our results; especially clean PET and PVC particles, with salinity having much more impact on clean PVC fragments compared to PET. However, our results show the much greater impact of biofilm growth on these relationships. As NP&A fibres have a lower density, a decrease in settling due to increase in salinity was expected, yet this was not seen perhaps due to the shape and surface area of fibres compared to spheres and fragments. These results indicate that the settling regimes for microplastics change as they move from a freshwater to marine environment, altering ecological risk as exposure for different species changes depending on the location of microplastics. The various settling regimes must be considered when sampling and predicting the transport and fate of microplastics within these environments.

Within the suspended sediment experiments, aggregation of microplastics and kaolinite was not observed, as particle size did not increase (see Appendix A). However, settling velocity was still impacted. For PET and PVC fragments, overall settling decreased with higher sediment concentrations but for NP&A fibres the impacts were more variable

(Fig. 4.3). Again, patterns differed between polymers and whether microplastics were biofouled or not. Settling velocity remained similar for clean PET particles across all sediment concentrations and significant changes in settling velocity only occurred for biofilmed PET fragments, with highest settling rates at 0 mg (26.60 mm $s^{-1}$ ± 1.21) and statistical significance between 0 mg and 100 mg (19.50 mm $s^{-1}$ ± 0.93) and 600 mg (21.73 mm $s^{-1}$ ± 1.25). For clean PVC, settling rates were considerably higher at 0 mg (25.28 mm $s^{-1}$ ± 0.77), compared to 400 mg (14.73 mm $s^{-1}$ ± 0.81) and 600 mg (14.04 mm $s^{-1}$ ± 1.00). For PVC, the highest settling rate was also observed at 0 mg for biofilmed PVC fragments (28.69 mm $s^{-1}$ ± 1.13) compared to 100 mg (21.66 mm $s^{-1}$ ± 1.06), 400 mg (21.12 mm $s^{-1}$ ± 1.25) and 600 mg (23.60 mm $s^{-1}$ ± 1.09). The decrease in settling velocity of PET and PVC fragments with clay mixing was unexpected**.** The surface properties of microplastics, such as charge and friction will play an important role in how they are transported (Mei *et al.,* 2020). The mixing of kaolinite and microplastics may have caused abrasion (Appendix A Fig.A.7) and also likely increased the drag of the particles, lowering their settling velocity. Also, the drag coefficient may have increased due to a small amount of clay attaching to the particles. Flocs may have also formed in the mixing procedure but as the rate of aggregation strength of flocs depends on electrical charge of particles, perhaps the forces between particles here were weak and caused flocs to break down during transfer or deposition in the settling column (Mietta *et al.,* 2009), or the electrochemical forces between clay and polymer particles are not as strong and need to be studied further. For NP&A fibres, the impact of clay concentration was very different compared to the other polymers. The highest settling occurred at 100 mg for clean NP&A fibres, (7.20 mm $s^{-1}$ ± 0.48) but was only significantly different to 400 mg (3.76 mm $s^{-1}$ ± 0.22). However, for biofilmed NP&A fibres, settling rate was highest at 400 mg (8.44 mm $s^{-1}$ ± 1.01) and lowest at 0 mg (3.25 mm $s^{-1}$ ± 0.46) with significant differences between 0 mg and 100 mg (5.90 mm $s^{-1}$ ± 0.51), 400 mg (8.73 mm $s^{-1}$ ± 1.02) and 600 mg (7.12 mm $s^{-1}$ ± 0.70). Kaolinite particles have been observed to adsorb onto the surface of polystyrene latex microspheres 1 μm in diameter which may have occurred here, increasing density and settling, yet overall particle size/area was not altered

significantly (Li *et al.,* 2020). It should be noted that some fibres did clump (Appendix A Fig.A.8) and this made calculation of settling difficult, which may have impacted the results. Fibres may clump and tangle in turbulent conditions, so this should be considered for future studies. No PET or PVC particles were observed to clump together in this way.

### 4.3.3 Comparison with empirical predictions

It has been argued that microplastics in aquatic systems will behave in a way that is comparable to natural sediment and therefore microplastic fate can be predicted using the same methods available for natural particles (Enders *et al.,* 2019; Harris, 2020; Hoellein *et al.,* 2019). To assess this we compare our results to a widely applied universal sediment transport formula that resolves Stoke's Law for fine grained sediment transport and turbulent fluid motion for larger grains to determine grain settling velocity (see methods) (Ferguson and Church, 2004). The theoretical settling velocity was calculated to be much higher compared to both clean and biofilmed experimental results for all sizes of PET (Fig.4.5.a). Any models using this formula (Francalanci *et al.,* 2021) will over-predict settling of PET microplastics resulting in a greater microplastic load in suspension than would be expected. For PVC microplastics, the formula both over and under-predicted settling velocities depending on particle size (Fig.4.5.b). Sediment equations could be used if the microplastics have hydraulically equivalent physical properties (Kane and Clare, 2019), however microplastics exist in a much wider range of shapes than natural sediment grains. The expected values were very different for observed fibre settling probably due to this reason (Appendix A). Despite Waldschläger and Schüttrumpf, (2019) developing a new formula for settling of microplastics, we were unable to make comparisons using their predictions as they rely on needing 3-axis dimensions for individual particles and do not consider the impacts of biofouling, which we have shown as a first order control. Indeed, our physical experiments highlight the need for a new generation of transport formulae that consider irregular microplastic shapes, biofouling and the high sensitivity to changes in salinity.

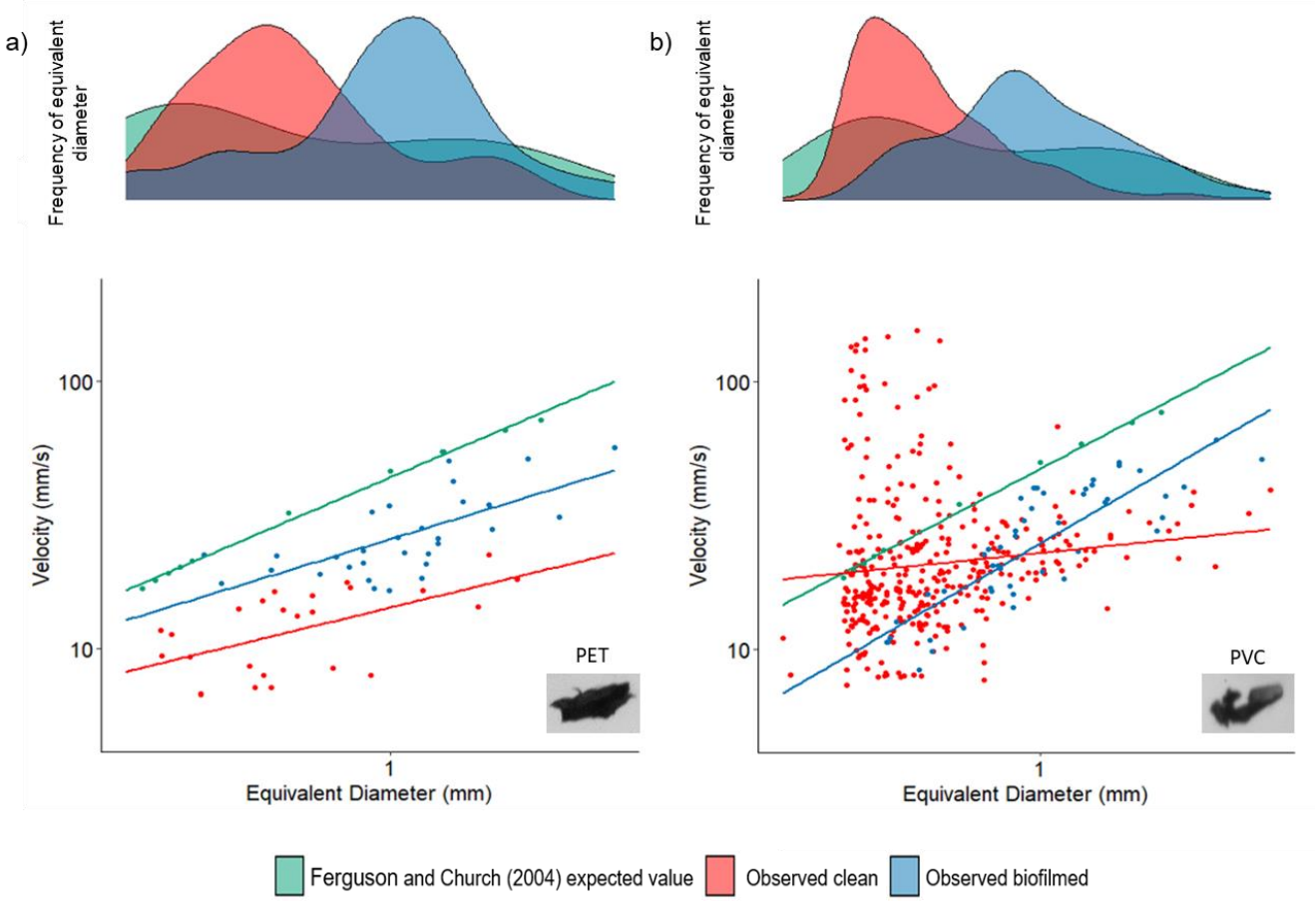


Figure 4.5: Expected settling velocity calculated using Ferguson and Church (2004) compared to our observed experimental values for clean and biofilmed microplastics of a) PET (n=38) and b) PVC (n=383). Marginal density plots indicate the distribution of velocity and equivalent diameter data. Smaller particles were analysed during the experiments, especially for PVC fragments

Currently, the factors that control microplastic transport and fate are poorly understood, which hinders our ability to manage and protect aquatic environments. Here we have demonstrated that biofouling is a first order control on the settling velocity of microplastic, with impacts observed over only a few days. The effect varies by polymer type and ambient conditions (salinity/clay concentration), and evolves in time. This highlights that the changes in microplastic settling regimes from a riverine to marine environment must be appreciated to precisely predict microplastic fate and the formation of any high concentration zones in the environment.

Although herein we only explore three types of non-buoyant microplastic, the results demonstrate a suite of novel and important insights into aquatic microplastic transport. Future work should build on the methods explored here, testing a wider range of microplastic polymers, perhaps those from environmental samples, in addition to buoyant polymers in order to gain a more comprehensive understanding of microplastic settling in aquatic environments. A range of size fractions must also be further tested, especially for their ability to aggregate with suspended siliciclastic sediments (Besseling et al., 2017b). Other types of sediment, such as sand, types of clays and carbonates, should also be investigated for their impact on microplastic transport.

Whilst available sediment transport formulae are useful for basic plastic transport predictions, we support and unequivocally show they are largely inaccurate and must be urgently updated to incorporate these key factors identified herein into new predictive frameworks, particularly biofouling, salinity impacts and time functions. This would allow more robust predictions of microplastic fallout and retention in fluvial systems and therefore more precisely forecast microplastic loads into estuaries, coastal seas and oceans along with improving projections of microplastic fate (Jambeck et al., 2015; Lebreton et al., 2017). This should be accompanied by fieldwork that sampled throughout the water column, such as in Chapter 5. In turn, this would improve monitoring and sampling campaigns and enhance future assessments of ecological impact of plastics through the freshwater-marine transition.

[Page intentionally left blank]

# Chapter 5.

# The transport and vertical distribution of microplastics in the Mekong River, Southeast Asia

---


**Abstract**

Rivers are known to be the main vector of plastic debris to the oceans, yet little is known about the sources, transport mechanisms, and fate of microplastics (<5 mm) in these systems. This impedes accurate predictions of microplastic flux to the oceans as well as our understanding of ecological risk and wider socioeconomical impacts on communities that rely on riverine environments. Here we report on microplastic concentrations, for the first time, within the Mekong River of Cambodia and Vietnam, with 24 microplastics $m^{-3}$ detected on average. Samples were taken throughout the water column at various sites of the river, one of the top polluting rivers globally, and its tributaries in Cambodia and Vietnam. We demonstrate that on average 86% of microplastic transport occurs within the water column below the water surface. Concentration was highly varied between sites, with the maximum found at Can Tho, Vietnam (64 microplastics $m^{-3}$) and the minimum at Kampi, Cambodia (2 microplastics $m^{-3}$). The majority of microplastics were identified as fibres, with expected sources from textiles and wastewater treatment plants (WWTPs). We compare our results to a previous study in the Mekong River, Cambodia, and demonstrate that microplastic abundance does not follow simple suspended sediment transport laws, with concentration decreasing during higher flows perhaps due to dilution and flooding. Furthermore, we highlight the need for sampling to include the characterisation of microplastic depth profiles and sampling throughout the year to accurately predict and monitor riverine microplastic fluxes. This research provides a greater understanding of microplastic concentrations in a

major river, which can improve predictive models and help inform effective waste management strategies due to insights into sources.

## 5.1. Introduction

Despite the widespread recognition that rivers dominate the global flux of plastics to the ocean, there is a key knowledge gap regarding the nature of that flux, the behaviour of microplastics (<5 mm) in transport, and the pathways from rivers into the ocean (Jambeck *et al.,* 2015; Lebreton *et al.,* 2017). There is growing evidence that plastic pollution can harm biota, wider ecosystems, and human health in addition to having societal and economic repercussions through damaging shipping, fisheries, and tourism (McIlgorm *et al.,* 2011). Although many of the potential ecotoxicological consequences of plastics are well known, research has only recently begun to explore the source to sink dynamics of plastics in the environment (Carlin et al., 2020; Hurley et al., 2018; Reichert et al., 2018; Sussarellu et al., 2016; Woodward et al., 2021). Microplastic research has predominantly focussed on marine systems where studies tend to sample either at the water surface or bed sediment (Hidalgo-Ruz and Thiel, 2012; Karlsson *et al.,* 2017). Yet, floating marine plastic debris represents just 2-6% of the estimated plastic flux entering aquatic systems annually, so it is likely these studies underestimate plastic loads (Eriksen et al., 2014; Jambeck et al., 2015). This prevents progress towards a holistic understanding of microplastic dynamics and leads to biases when identifying zones of high microplastic accumulation, as well as curtailing the evolution of effective mitigation and policy measures to reduce ecological, environmental, and social impact. Given that rivers are the major source of plastic flux to the ocean, they are also the first order of control on how microplastics are distributed and delivered into coastal seas and the wider marine environment. Therefore, to robustly predict the transport, fate and biological interactions of microplastics in aquatic environments at a global scale, the distribution and abundance of microplastics in the water column of riverine and delta systems must be identified and understood (Peng *et al.,* 2017; Wang *et al.,* 2016).

The majority of plastic pollution originates from land-based sources through mismanaged waste, urban and stormwater runoff, degradation of larger plastics into microplastics, wastewater treatments plants (WWTPs), and industry (Horton et al., 2017a; Lechner and Ramler, 2015; Ogden and Everard, 2020; Sun et al., 2019; Wang et al., 2020). Rivers often act as a substantial conveyor of plastics to the oceans and therefore fluvial transport mechanisms of microplastics must be fully understood. Microplastic transport in rivers is first influenced by the particle properties, including buoyancy, shape and size, and the river hydrodynamics, such as turbulence and velocity (Haberstroh *et al.,* 2021b; Khatmullina and Isachenko, 2017; Waldschläger and Schüttrumpf, 2019). It has been argued that microplastics can be expected to follow transport behaviour comparable to naturally occurring sediment particles of hydraulically equivalent properties (Enders *et al.,* 2019; Harris, 2020; Hoellein *et al.,* 2019; Kane and Clare, 2019). As a result, a high proportion of fluvial microplastics have been anticipated to be deposited within bed sediment (Drummond *et al.,* 2022). However, the majority of microplastics don't exist in round shapes like sediments, but as fragments, fibres, and films that have been weathered and fragmented with transport behaviour varying significantly between forms (Browne *et al.,* 2011; Harris, 2020). Settling experiments have shown that using sediment dynamics predictions are not always accurate, as microplastics tend to be weathered and fragmented (Chapter 4; Waldschläger and Schüttrumpf, 2019). Furthermore, fate will be impacted by biofilm growth, which will be likely to increase particle density and interactions with suspended sediment and matter which may lead to aggregation (Kaiser et al., 2017). Additionally, as plastic moves from a riverine to an ocean environment, it will cross a salinity boundary which further changes particle buoyancy (Kooi *et al.,* 2017; Chapter 4). Therefore, due to their relatively low densities (in comparison to sediment), the majority of microplastics are, predicted to be in suspension rather than deposited within the bed (Harris, 2020).

Lebreton et al. (2017) provide an estimate of the global annual input of plastic pollution from rivers into the oceans of 1.15-2.41 million tonnes with 67% originating from

just 20 rivers. However there are several limitations to modelling and many predictions within the literature have contradicted each other, with a more recent model estimating that over 1,000 rivers are accountable for 80% of plastic waste entering the ocean (Meijer *et al.,* 2021). This highlights the need for more research into the transport of microplastics in rivers, to not only determine the amounts of microplastic passing through these systems but how ecological risk changes throughout the course of the river into the ocean. Studies tend to sample the water surface or riverbed, with concentrations being highly variable: for example 14-25 microplastics $m^{-3}$ in the Thames River (UK) (Rowley *et al.,* 2020), 38 microplastics $m^{-3}$ in the Ganges River (India) (Napper *et al.,* 2021), 66 microplastics $m^{-3}$ in the Marne and Seine rivers (France) (Dris *et al.,* 2018), and 4,137 microplastics $m^{-3}$ in the Yangze River (China) (Zhao *et al.,* 2014). The majority of microplastic studies in rivers are from China, North America, or Western Europe, yet numerical models, supported by observations of floating plastics, predict the disproportional contribution of Southeast Asian rivers in plastic emissions to the ocean (Lebreton *et al.,* 2017; Schmidt *et al.,* 2017; van Emmerik *et al.,* 2019). Of the ten rivers predicted by Schmidt *et al.,* (2017) to be the top contributors to marine plastic debris, few studies have been conducted in those areas, despite frequently being referred to as the top polluters as highlighted by Figure 5.1. Furthermore, few studies have directly sampled microplastic concentrations within the water column, which may result in inaccurate concentrations being reported. This demonstrates the need for more research to be conducted in Southeast Asia, especially throughout the water column. The Mekong River of Southeast Asia has been identified as one of the top contributors to marine plastic pollution, with an estimated plastic load of up to 37,000 tonnes per year (Lebreton et al., 2017; Schmidt et al., 2017). The consequences of plastic pollution in the Mekong could be severe due to the high biodiversity of the basin and the millions of people that rely on its productivity. A detailed introduction to the Mekong River is discussed in the next sections (§5.1.1-5.1.4).

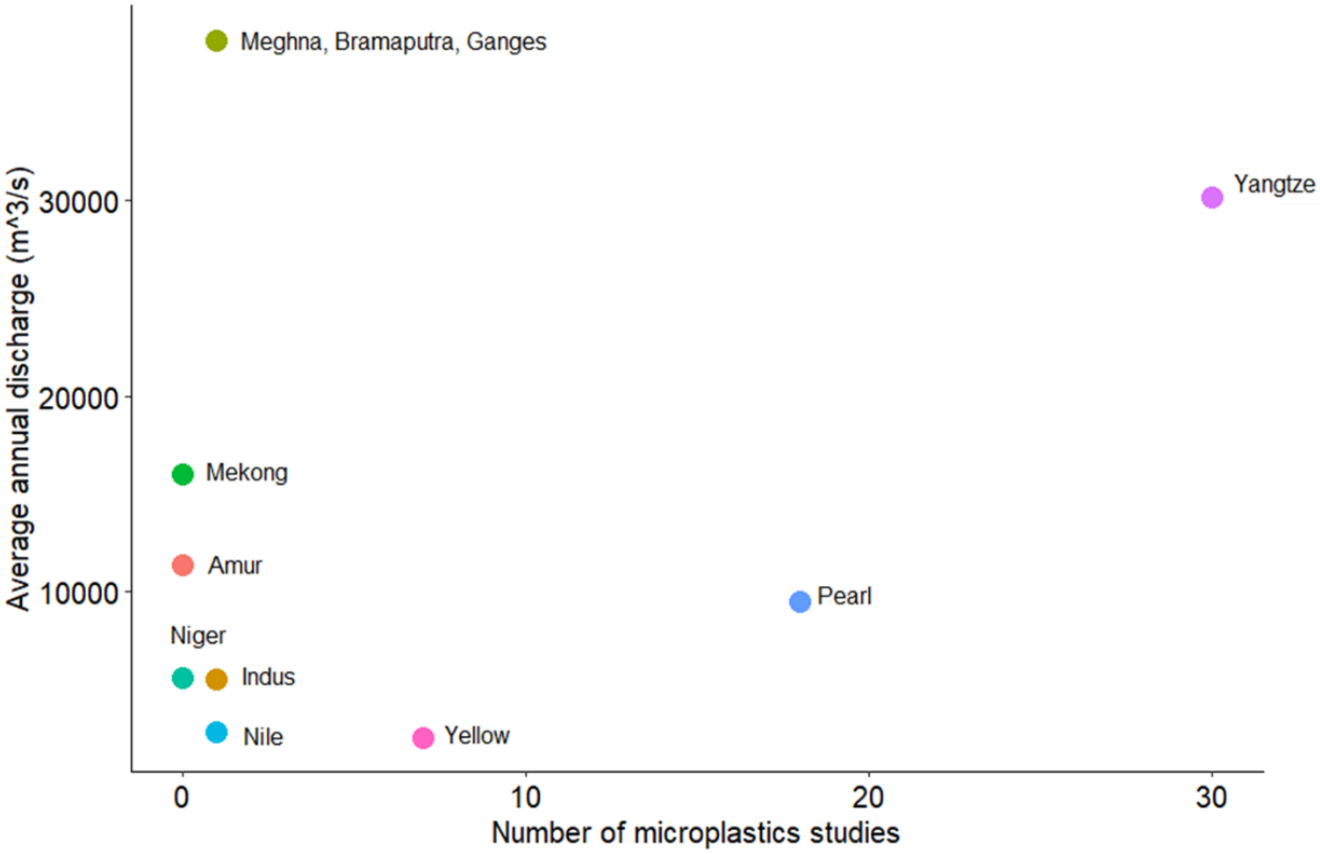


Figure 5.1: Rivers with the top predicted plastic input into the oceans from Schmidt *et al.,* 2017 by average annual discharge and the number of microplastic studies conducted to highlight lack of studies in top riverine plastic polluters. Discharge data were acquired from Khan *et al.,* 2015 and (Gupta, 2008). Note Schmidt *et al.,* 2017 concludes the top 10 rivers but discharge data for the Haihe River was unavailable and therefore not included. No microplastics studies have been conducted in that area however.

### 5.1.1 The Mekong River

The Mekong River is the longest river in Southeast Asia at 4,800km long, flowing northwest-Southeast with the 10$^{th}$ largest water discharge globally that drains into the South China Sea (Fig. 5.2) (Adamson et al., 2009; Gupta, 2022; Hoang et al., 2016). Originating in the Tibetan Highlands over 5100 m above sea level, the Mekong River flows through China's Yunnan Province into Myanmar, Lao People's Democratic Republic (PDR), Thailand, and Cambodia before discharging via numerous distributaries within its delta that is

predominantly in Vietnam (Fig. 5.2) (Campbell, 2009; Gupta, 2022). Most catchments have a dendritic form, where the width of the catchment decreases downstream forming a characteristic tear-drop shape (Campbell, 2009). However, the Mekong catchment progressively widens down the valley, forming a pan-shape, with its widest area being immediately upstream of the delta, as a result of the upper parts of the river being confined within the complex geological folds at the edge of the Himalayas (Campbell, 2009). Geographically, the Mekong is distinguished by two zones: the Upper and the Lower Mekong Basin, with complex geomorphology and seasonal changes highly influencing the flow dynamics (Gupta, 2009). Furthermore, the Mekong is highly biodiverse and ranked second globally after the Amazon River (Ziv et al., 2012). The geology, hydrology, biodiversity, economic importance, and environmental concerns will be described in more detail below. A summary of the characteristics of the Mekong River is shown in Table 5.1 with Figure 5.3 displaying the river profile.

Table 5.1 Summary of dimensions of the Mekong River with world rankings. Source Gupta (2022)

| Characteristics | Measurement | World rank |
|---|---|---|
| Basin area | 795000 $km^2$ | 21 |
| Channel length | 4880 km | 12 |
| Volume of mean annual discharge at mouth | 475 x $10^9$ $m^3$ | 9 |
| Mean discharge | 15000 $m^3s^{-1}$ | 8 |
| Average annual suspended sediment discharge | 160 x $10^6$ t | 10 |

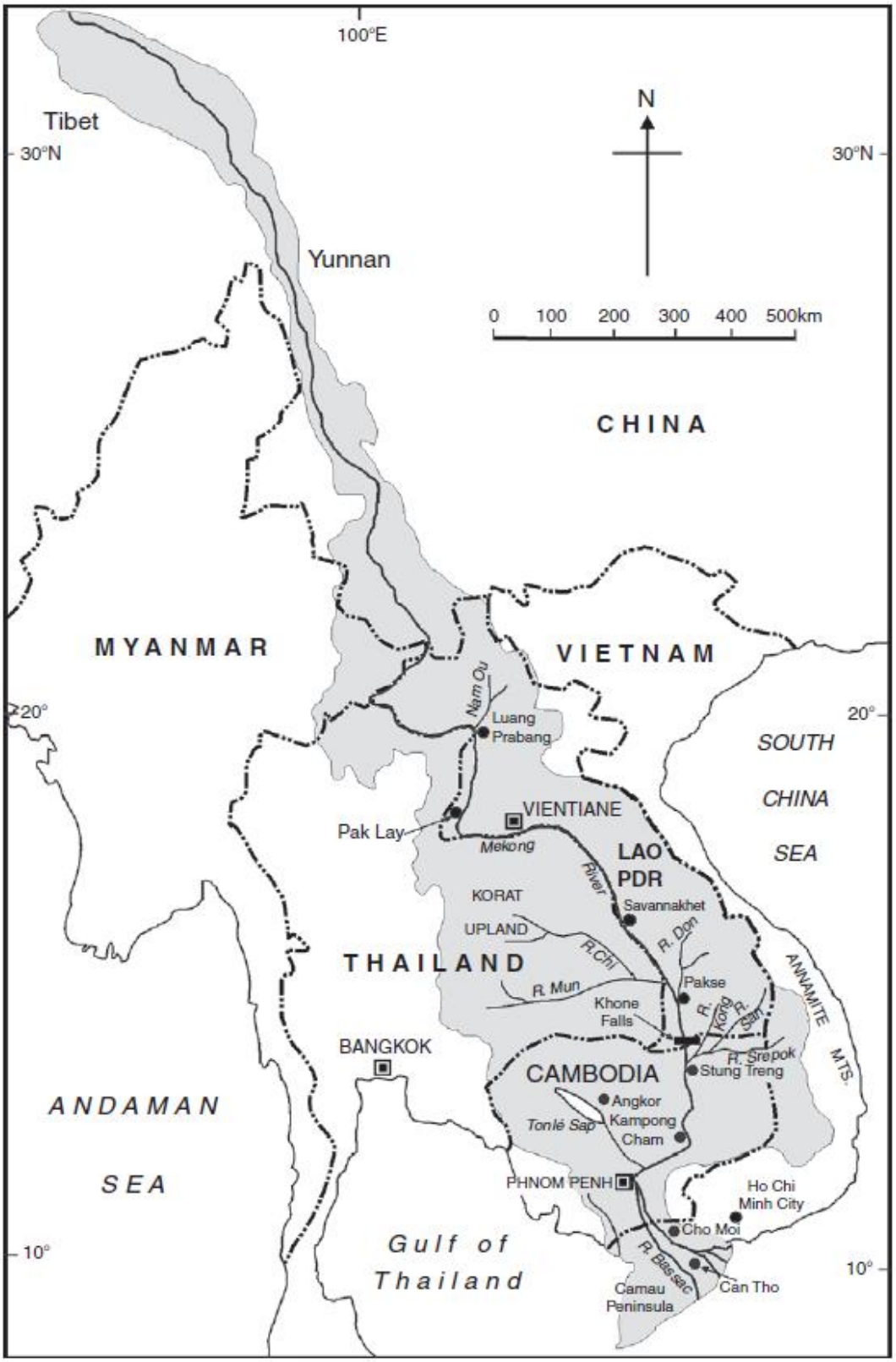


Figure 5.2: The Mekong Basin location map. Source Gupta (2022)

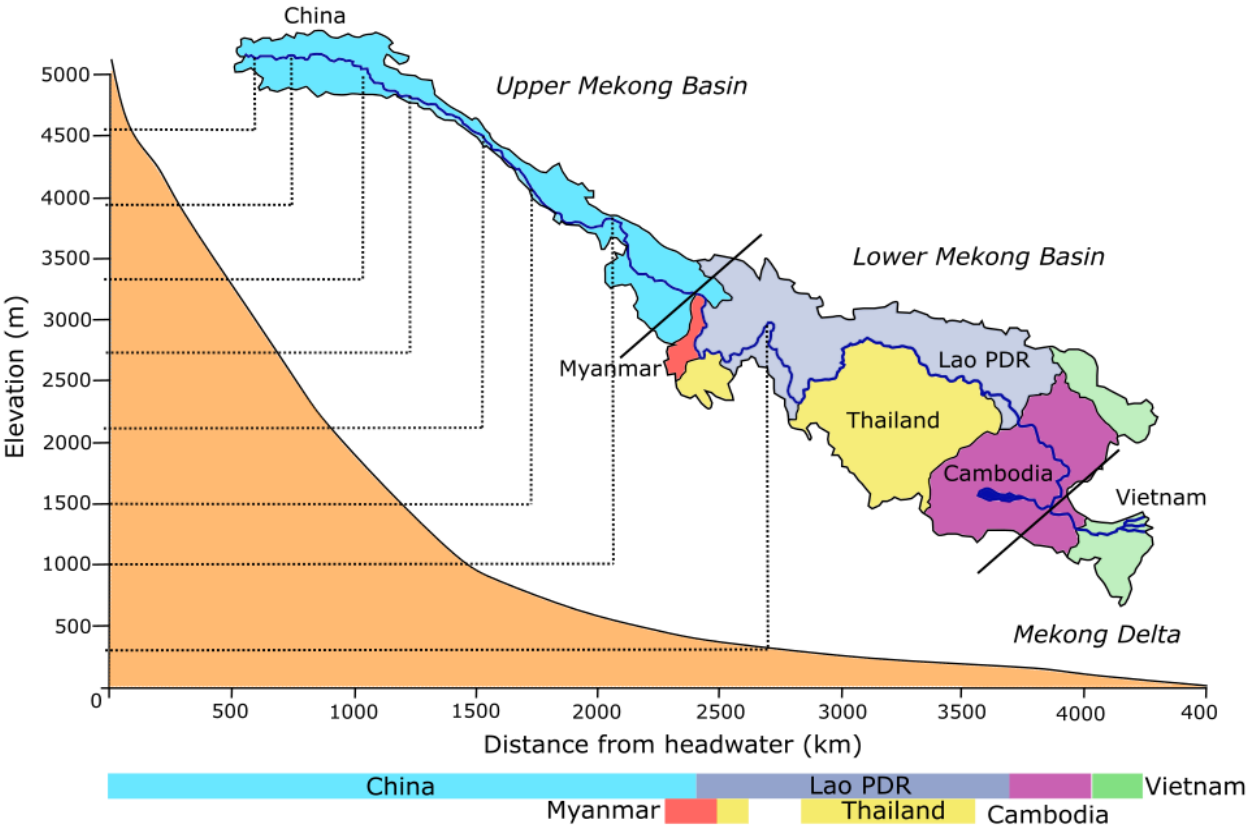


Figure 5.3: The river profile of the Mekong River. Adapted from Mekong River Commission (2001)

For approximately 3000 km, the Mekong River flows on rock through constricted valleys within mountainous regions (Gupta, 2022). The steep mountain slopes continue for the next 1000 km but the basin widens in Lao PDR and Thailand, where the river runs on both rock and alluvium (Gupta, 2022, 2009). The Mekong widens after 4000 km from its source and flows across alluvial lowland of Cambodia before the delta reaches Vietnam (Fig. 5.3) (Gupta, 2009). The Mekong Basin is split into three parts: 1) The Upper Basin, which is in Tibet and China 2) The Lower Mekong Basin, from Yunnan in China to Cambodia, including the Tonlé Sap Lake and within the Lower Basin 3) The Mekong Delta, beginning at Phnom Penh extending to the coast of Vietnam. This chapter concerns the Lower Mekong Basin, from Kratie, Cambodia, downstream through the Mekong Delta, Vietnam. Gupta and Liew (2007) divided the Mekong from the Chinese border to the South China Sea into eight units as shown in Figure 5.4. Specifically, the work in this chapter was undertaken in units 5/6-8 of the Mekong River, with further geological details of each unit section described in Table 5.2.

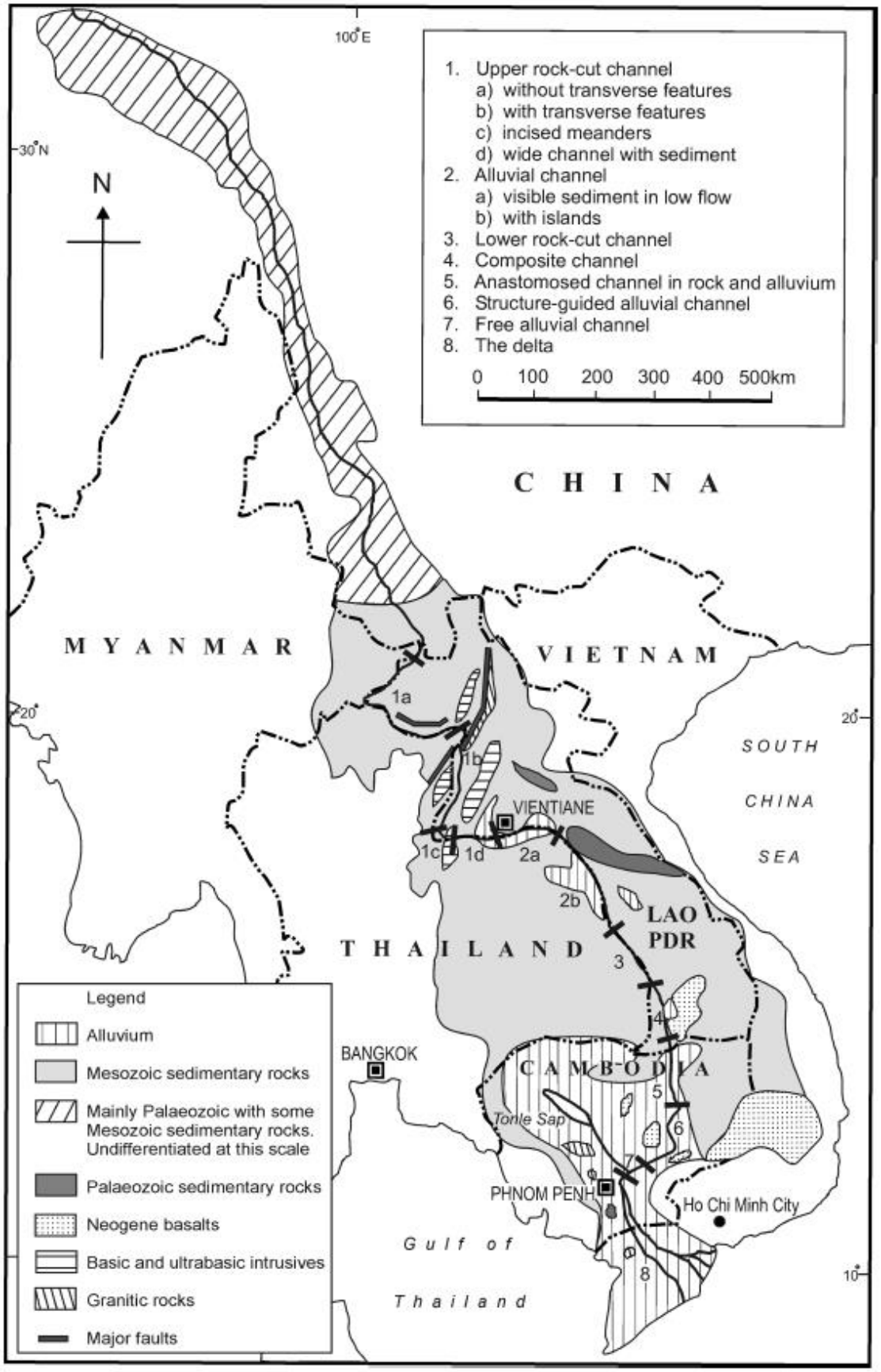


Figure 5.4: Map of the generalised basin geology and river units (1-8) of the Mekong River. Source Gupta (2022)

Table 5.2: Characteristics of the Mekong River south of the China border. Note that all measurements are approximate. “Variable” is due to difficulty in averaging because of too many scour holes. The width for unit 7 is several kilometres and increasing while unit 8 consists of several deltaic distributes and is tidal. In addition, the seasonal stage change is difficult to measure for unit 7 and 8.

| Unit | Length (km) | Width (km) | Bed material | Bank material | Average Slope | Low flow depth (m) | Seasonal stage change |
|---|---|---|---|---|---|---|---|
| 1a | 500 | 200-700 | rock | rock | 0.0003 | ~5 | 10 |
| 1b | 250 | 200-2000 | rock | alluvium on rock | 0.0003 | ±10 | 15-20 |
| 1c | 30 | 500-600 | rock | alluvium on rock | 0.0003 | 7 | 15 |
| 1d | 130 | 200-1400 | rock | alluvium on rock | 0.0003 | <5 | 10-12 |
| 2a | 100 | 800-1300 | alluvium | alluvium | 0.0001 | ~3 | 13 |
| 2b | 400 | 2000 | alluvium | alluvium | 0.00006 | ≤5 | 12-14 |
| 3 | 200 | 400-2000 | rock | alluvium on rock | 0.0002 | variable | 20 |
| 4 | 150 | 750-5000 | rock | alluvium | 0.00006 | variable | ~15 |
| 5 | 200 | 15000 | rock | alluvium on rock | 0.0005 | 8 | 9 |
| 6 | 225 | 3000 | alluvium | alluvium | 0.00005 | ~5 | 14-18 |
| 7 | 50 | | alluvium | alluvium | 0.000005 | | |
| 8 | 330 | | alluvium | alluvium | 0.000005 | | |

### 5.1.2 The hydrology of the Mekong River

The precipitation of the Mekong Basin is highly seasonal and associated with the Asian Monsoon Climate system which contains two monsoonal systems, the Southwest Asian Monsoon and the Southeast Asia Monsoon (Delgado et al., 2012; Gupta, 2022). The wet season usually lasts from mid-May to October and accounts for more than 90% of annual precipitation in many areas, with floods occurring typically later in the wet season, while the dry season is from November to April (Fig. 5.5) (Gupta, 2022; Räsänen and Kummu, 2013). The discharge of the Mekong is reflected in the seasonality of rainfall. Following the summer snowmelt from the Tibetan Plateau, the discharge increases slightly in May. (Campbell, 2009; Gupta, 2022). Between June and November, the majority of the annual discharge (80%) is seen during the Mekong’s flood pulse, concentrated in a single wet season peak (Fig.5.5) (Campbell, 2009; Räsänen et al., 2017). Within the Lower Mekong Basin, heavy rainfall results in extensive inundation of the lower floodplains. This results in key eco-hydrologic interactions such as the recycling of nutrients that drive fish migration and life

cycles such as spawning and contributes to the vast fish abundance and production of the inland fisheries (§ 5.1.3) (Baran et al., 2012). A unique feature of the Mekong's flood pulse is the flow reversal that occurs from Tonlé Sap Lake, Cambodia, the largest lake in Southeast Asia. During the wet season, Tonlé Sap Lake receives water from the mainstream Mekong via the Tonlé Sap River, with its mean surface area changing from 3500 $km^2$ in the dry season to a maximum of 14500 $km^2$ in the wet season (Adamson et al., 2009). The water then flows back to the Mekong during the dry season. An example of a large flood is shown in, Figure 5.6. This flood pulse sustains ecological productivity by transporting large amounts of nutrients and sediments, in addition to reaching floodplains and creating diverse habitats (Räsänen et al., 2017). The floods that occur in the wet season are some of the largest produced by any river, regarding runoff per unit catchment area, and are created by steep catchments and strong tropical storms (Campbell, 2009). The arrival time of the floods changes further downstream; in Thailand and Lao PDR, this tends to be in August, in Cambodia the flood peaks are typically in September while it is in October for the delta in Vietnam (Gupta, 2022). As a result of a dynamic flood-pulse, the Mekong River system and Tonlé Sap Lake forms a very important ecosystem.

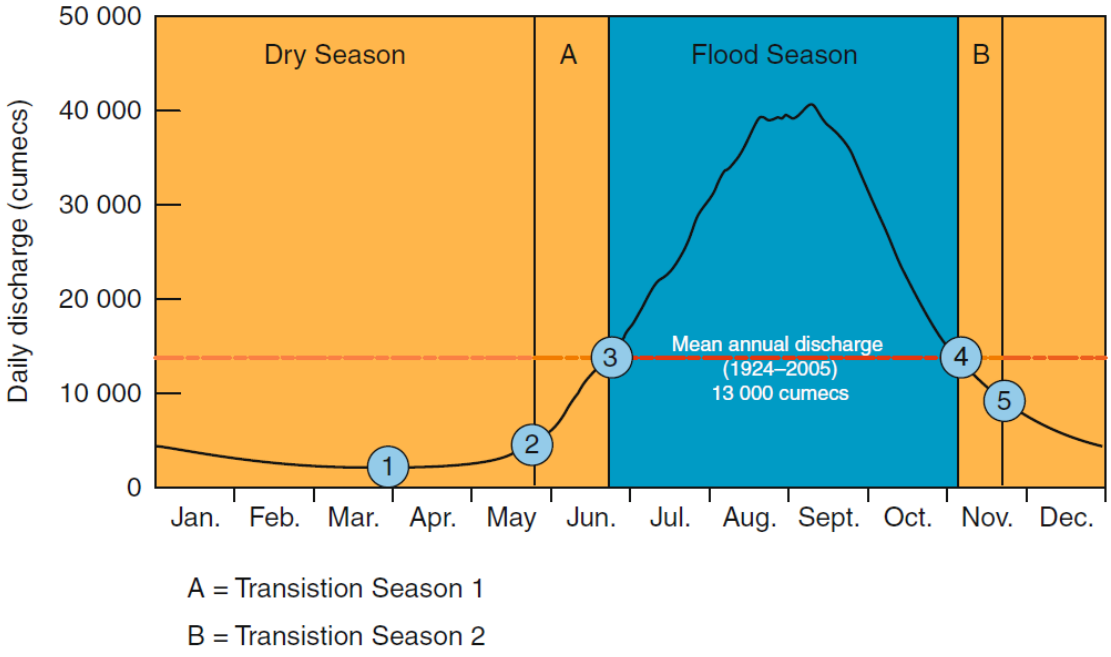


Figure 5.5: The daily discharge variation of the Mekong River throughout its four hydrological seasons. Source Adamson 2006.

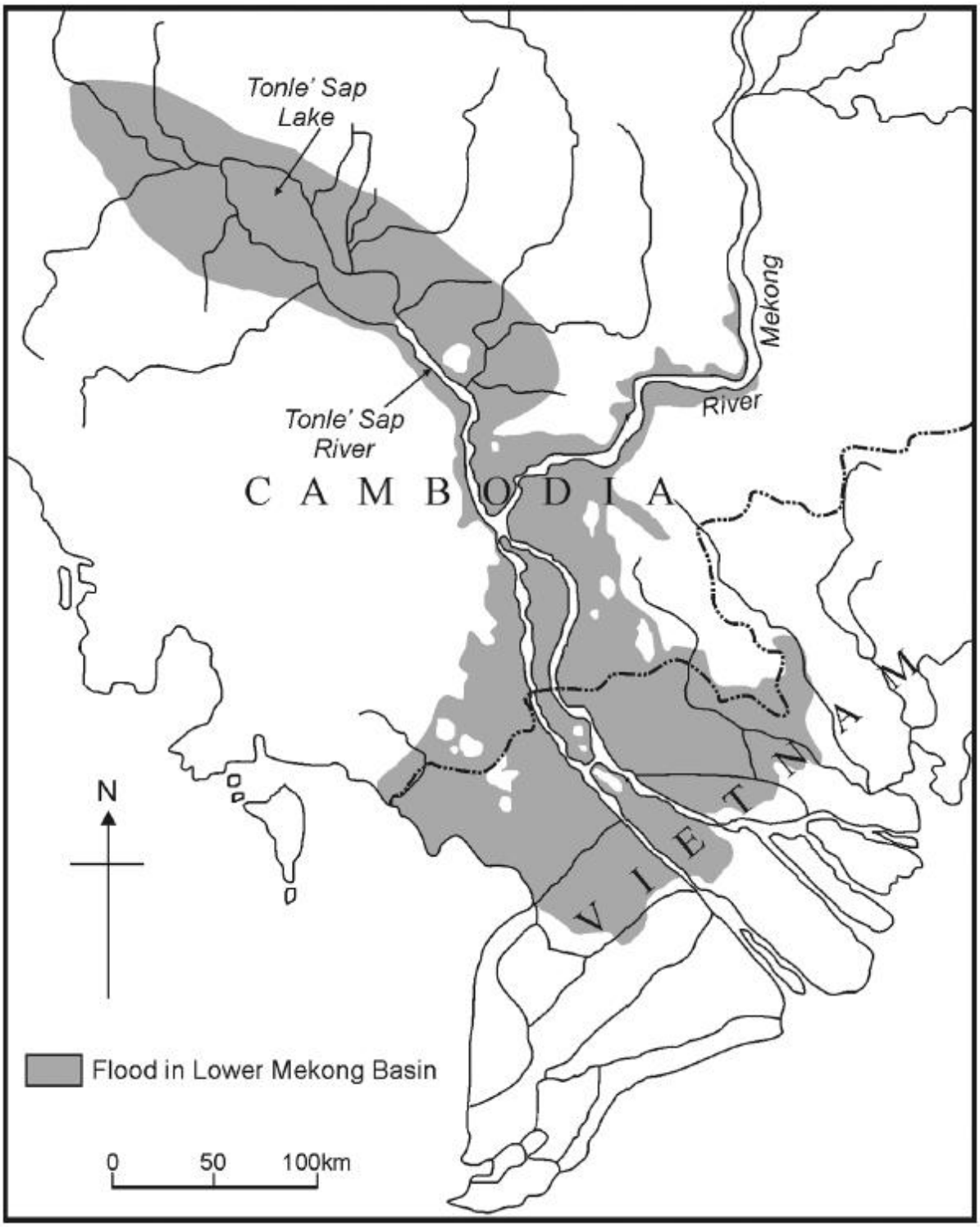


Figure 5.6: The historical flood of the Mekong, 2000. Source Gupta (2022) Map prepared from SPOT imagery by Centre for Remote Imaging, Sensing and Processing, Singapore.

### 5.1.3 The biodiversity and economic importance of the Mekong River

The Mekong River carries a substantial amount of economic and ecological resources with a key driver for ecological productivity being the annual flood pulse due to the seasonal monsoon climate (Holtgrieve et al., 2013). Indeed, the Mekong River is one of the most biodiverse freshwater ecosystems globally, containing large and diverse fisheries with the Lower Mekong Basin supporting between 1,000-1,700 species (Ackiss et al., 2019; Kingston et al., 2011). The Mekong Fish Database reports 924 species of fish in the Mekong River with Rainboth, (1996) estimating that there are 500 fish species in Cambodia alone (Valbo-Jørgensen, 2002). At least 50% of the Mekong fish species are known to migrate within the basin, with fish species grouped into different migratory guilds depending on the distance of seasonal migration and the different habitats explored for feeding, shelter and spawning (Valbo-Jørgensen et al., 2009). The species groups are blackfishes (local movements), greyfishes (medium longitudinal and lateral migrations), and whitefishes (long-distance longitudinal and lateral migrations) (Baran, 2010). The grouping system also recognises the importance of the flood regime in driving the habitats available, the lifecycle and the behaviour of the fishes (Valbo-Jørgensen et al., 2009). For example, during the start of the wet season when the mainstream river waters rise, grey and whitefishes undergo upstream/downstream migrations and lateral migrations to inundated spawning grounds such as floodplains (Baran et al., 2012). An example of the relation of fish spawning to the hydrology of the Mekong Delta is shown in Figure 5.7 (Vu et al., 2021).

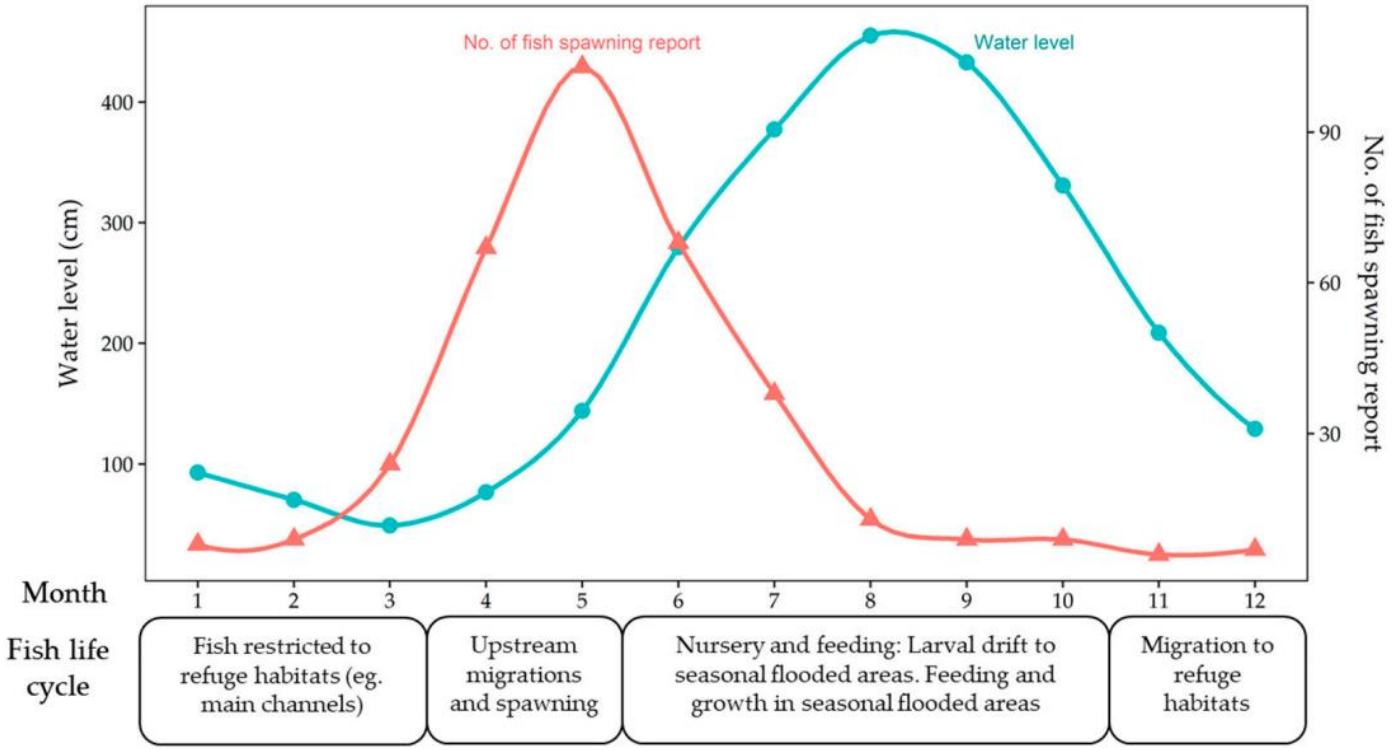


Figure 5.7: Fish spawning in relation to flooding regimes in the Mekong Delta. Sources Vu et al., 2021

Furthermore, the complex geomorphology and diversity of habitats of the Mekong river had resulting in three migratory systems being identified (Lower, Middle, and Upper Mekong migration system) causing differences in fish population and production (Dugan et al., 2010). As this chapter concerns the Lower Mekong Basin and Mekong Delta, only the Lower Mekong migration system will be described. This system is characterised by productive lowland floodplains and the delta and displays the highest production of fish in the Mekong River with approximately 670 species that contain fresh, brackish, and marine species (Dugan et al., 2010). The Lower system contains no waterfalls and the migratory corridors from the delta to the deep pools in Cambodia remain accessible year-round due to the minimum flood level being maintained, allowing fish dispersion (Valbo-Jørgensen et al., 2009). This high ecological productivity is the basis for the livelihoods and food security of the majority of the 70 million people that live in the basin, producing 50-80% of the annual protein for communities (Ackiss et al., 2019; Räsänen and Kummu, 2013). 60 million people

live in the Lower Basin countries, with 85% of the population living in rural areas. This is due to the majority of people being dependent on fisheries which are linked to river activities (Baran et al., 2007). Other major water-dependent economic sectors are agriculture, and energy such as hydropower production (Hoang et al., 2016).

Throughout the basin, food security and malnutrition are major risks, resulting in fish becoming a major source of protein intake. In Cambodia and Vietnam, the annual average fish protein consumption is 52.4 and 49.5 kg capita $^{-1}$ year $^{-1}$ respectively, while the global average fish consumption is 20.2 kg capita $^{-1}$ year $^{-1}$ (Food and Agriculture Organisation of the United Nations (FAO), 2018; Hortle, 2009). This highlights the importance of the Mekong fish to the local communities and the highly productive area that is the Mekong Basin. The inland fisheries of the Mekong are one of the world's most productive, having an estimated yield of 4.4 million tonnes per year with 47-80% of the catch comprising of migratory fish species (Adamson, 2006). Furthermore, the Mekong River Commission has estimated that the value of wild fish caught annually is approximately 1 billion US dollars (Gupta, 2022). The *dai* fishery of Cambodia is important for more than 1.2 million people who live in the floating villages and riparian areas surrounding Tonlé Sap Lake, where it is the primary economic activity and protein source and responsible for approximately 70% of Cambodia's total annual catch (Salmivaara et al., 2016). This fishery is also highly dependent on the seasonal flood dynamics of Tonlé Sap Lake with the inundated floodplain habitats increasing food availability, shelter, and spawning grounds resulting in increased fish production (Kummu and Sarkkula, 2008). In addition, the Mekong delta provides over 60% of the total fish and other aquatic products production in Vietnam (Baran, 2010). Yet the resources of the Mekong River are vulnerable to seasonal changes in sediment load, water quality, and river flow (Kingston et al., 2011).

### 5.1.4 Environmental concerns of the Mekong River

The Mekong River is threatened by several factors including proposed and constructed dams, increased erosion on basin slopes, and degradation of aquatic life

(Gupta, 2022). Degradation of the environment is expected to arise from pollution from fertilizers and urban discharges, excessive sedimentation, and engineering control further upstream, allowing saline water to move higher up the system (Gupta, 2022). These environmental changes are expected to have already affected some of the 1200 species identified in the Mekong River, especially the endangered species such as the giant freshwater catfish (*Pangasianodon gigas*) and the Irrawaddy dolphin (*Orcaella brevirostris)* (Gupta, 2022). In addition, the area is under threat from the projected magnitude of climate change including sea level rise, increasing temperatures, and unpredictable rainfall causing flooding in some areas and drought in others (Kingston et al., 2011). The dry season discharge from the Tibetan Plateau may also be reduced along with the southwest monsoon strength increasing (Campbell, 2009). This will alter the size and duration of baseflows, and the timing of the onset and end of the wet season (Campbell, 2009). The pressures on the Mekong River will likely be exacerbated by the ever-increasingly population growth of the communities relying on the Mekong River which is expected to reach 100 million by 2050 (Varis et al., 2012). Demands on natural resources for urbanisation, irrigated agriculture, electricity, and food production are already apparent (Adamson, 2006). Despite the rapid regional economic growth, many people live in impoverished conditions often with a lack of access to clean water and sanitation.

Furthermore, the Mekong is also predicted to be one of the top contributors of plastics into the ocean, with an estimated plastic load of up to 37,000 tonnes per year (Lebreton et al., 2017; Schmidt et al., 2017). As plastic production and populations surrounding the Mekong River continue to rise, it is likely that the amount of plastic waste in the Mekong will increase further. The consequences of increasing plastic pollution in the Mekong are currently unknown but due to the growing evidence of the potential ecotoxicological consequences of plastics in the aquatic environment, the biodiversity of the Mekong and therefore the wider economy that relies on the resources are likely to be at risk (Roman et al., 2022). To our knowledge, only one other study for microplastic discharge has

been conducted on the Mekong River, despite it being identified as one of the top polluting rivers worldwide (Schmidt et al., 2017). Haberstroch *et al.,* (2021) sampled sites close to Phnom Penh, Cambodia, during the monsoon season. Furthermore, this is one of the few studies to sample vertically throughout the water column (Dris et al., 2018; Lenaker et al., 2019). Here, we present field measurements distributed across a much wider range of sites across the lower alluvial reaches of the Mekong River and the Delta, in Cambodia and Vietnam. We provide insights into the distribution of microplastics in the Mekong River across eight sites at various depths, in addition to quantifying the particulate flux and assessing the implications for discharge into the South China Sea. This provides valuable insights into the extent to which the Mekong River is being polluted by plastic pollution. The wider potential ecological consequences this may have within the Mekong are also discussed.

## 5.2. Methods

### 5.2.1 Site Locations

Fieldwork was conducted in Cambodia and Vietnam July 2019 at eight locations as shown in Figure.5.8. The upstream extent of our sampling was the town of Kratie and the rural area of Kampi, ~250 km north of Phnom Penh. Kampi is the location of a deep pool in the Mekong channel which is a natural habitat of the Irrawaddy Dolphin (Halls et al., 2013). The next area was in the Tonlé Sap River, Mekong River, and Bassac River at Phnom Penh, the capital of Cambodia. The final area was Can Tho, Vietnam, located next to Bassac River, the largest city on a distributary of the Mekong River in Vietnam with a busy waterway, Can Tho River. Examples of the river sites are shown in Fig.5.9 and 5.10.

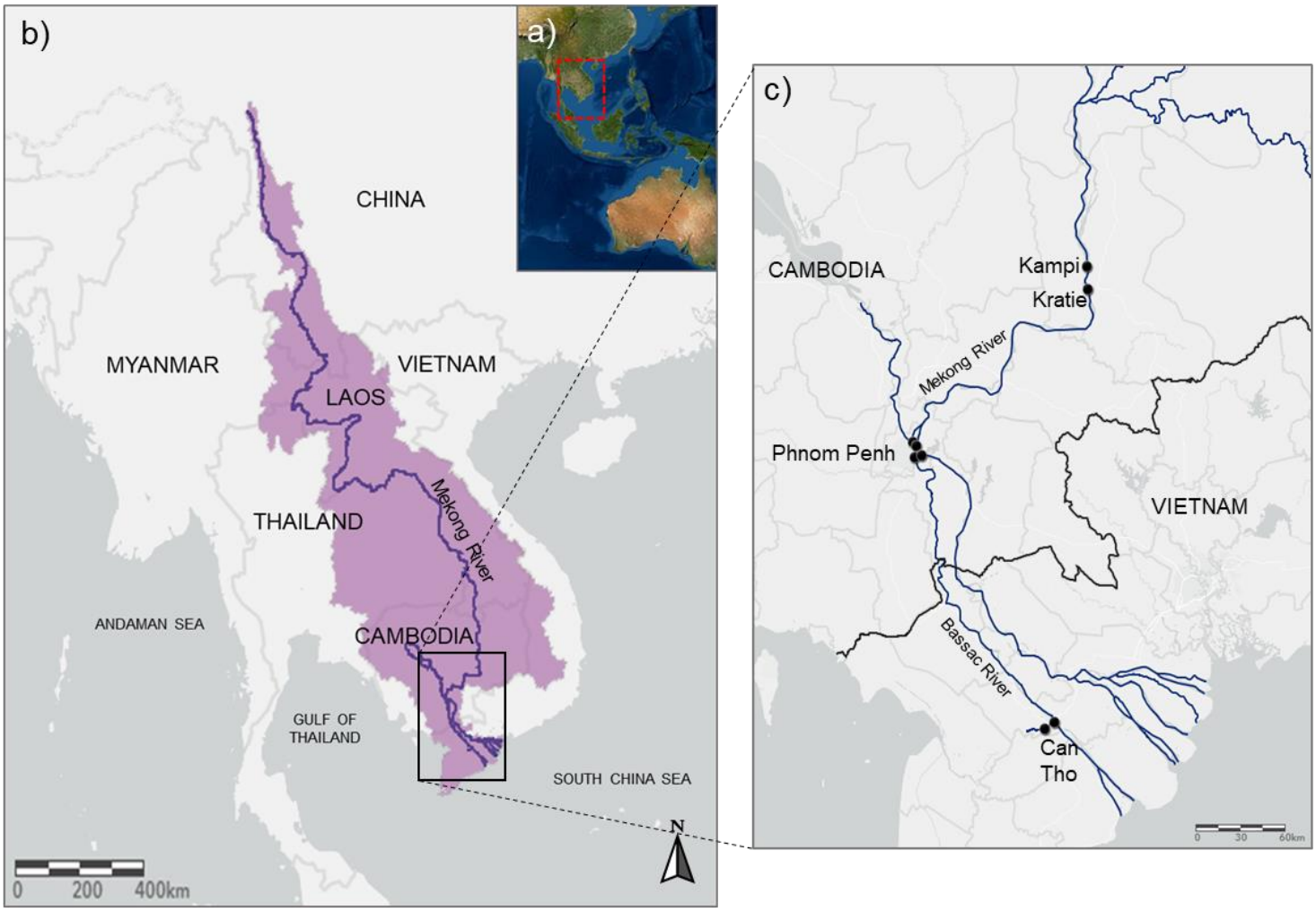


Figure 5.8: a) Overview of Mekong River location b) The Mekong River Basin area c) Sampling locations within the Mekong Basin in Cambodia (Kampi, Kratie and Phnom Penh) and Vietnam (Can Tho). Basemap for a) World Imagery49. Basemap for b) and c): Light Gray Canvas Map50, layers: GMS Major River Basin51 and Main Rivers52, Great Mekong Subregion Secretariat

Figure 5.9: The Mekong River Kratie, Cambodia.

Figure 5.10: The Mekong River at Phnom Penh, Cambodia.

### 5.2.2 Water sample collection

Five plankton nets, with a mesh size of 250 µm, were attached to a line at 4 m intervals with a weight on the end (Fig.5.11-5.13). This allowed samples to be collected at the surface and throughout the water column, with the number of depths collected dependent on the depth of the river at that location. Dive watches were attached to the rope to collect depth measurements. The nets were deployed from the back of a stationary boat for 5 minutes at each site, resulting in one collection per depth per site (n = 31). Using a water pump, each net was rinsed from the outside to ensure no contamination occurred and all material was collected in the codend. Each cod end was removed and rinsed with DI water into one glass bottle per net before being transferred to the laboratory for separation and analysis. The net was then rinsed inside and out before the next sample was collected. At the same time as the nets were deployed, an Acoustic Doppler current profiler (ADCP) was used to record and calculate the flow of the river. An example of plastic on the banks of the river and a sample collected in the codend are shown in Figure 5.14.

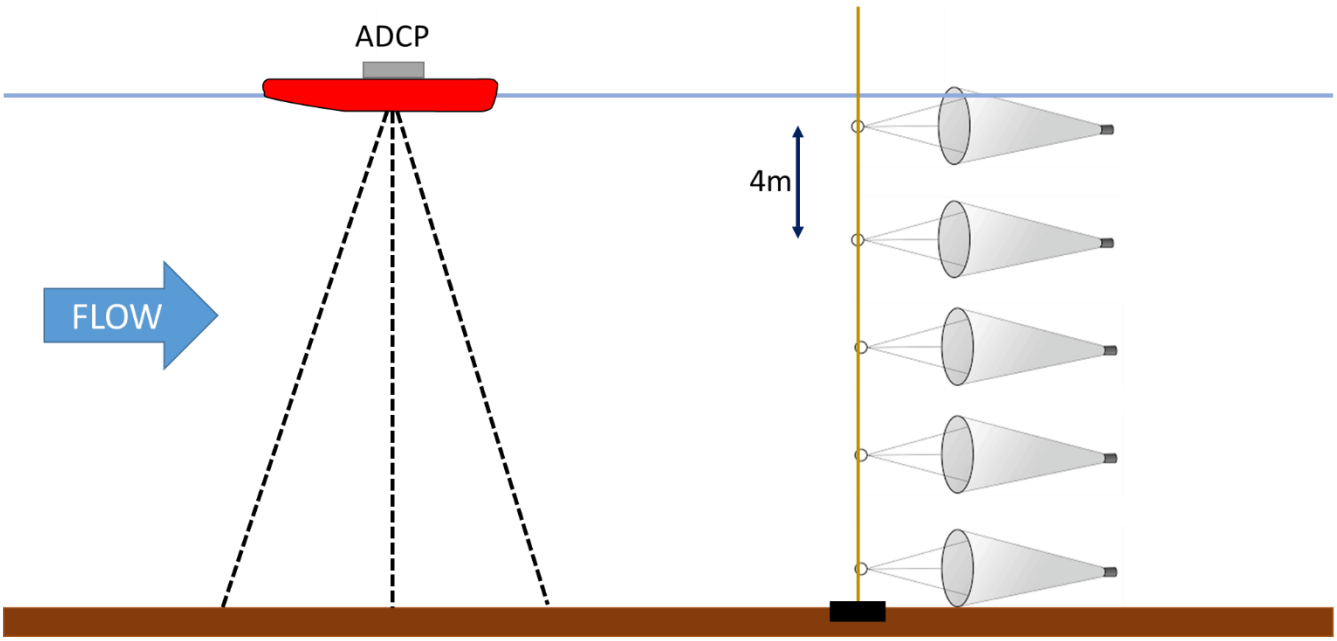


Figure 5.11: Setup of the water sample collection with five plankton nets throughout the water column and Acoustic Doppler current profiler (ADCP) used to record and calculate the flow of the river.


Figure 5.12 ADCP used to record and calculate flow of the river.

Figure 5.13 Plankton nets used for sampling microplastics in the Mekong River.

Figure 5.14: Examples of plastic on the banks and the shrubs of the Mekong River, Cambodia and microplastics collected in the plankton net codend.

### 5.2.3 Separation and filtration

Analysis of samples was conducted at the University of Hull, UK. Water samples were first vacuum filtered onto 55 µm-pore size Whatmann GF filter papers, covered and dried at room temperature. Next, each filter paper was placed in a glass flask and 30 ml of $H_2O_2$ (30%) was added. Flasks were put in a shaking incubator at 50°C, 100 rpm for 24 hours to digest any organic material. $H_2O_2$ (30%) at 50°C was chosen as it has been shown to be an efficient reagent for digesting organics while causing minimal damage to any microplastics present (Duan *et al.,* 2020; Nuelle *et al.,* 2014). Trials were also run on mock samples to test multiple digestion methods and confirmed this was the most efficient. Finally, 200 ml of deionised water was added to each sample, vacuum filtered, rinsed twice, and dried at room temperature.

### 5.2.4 Identification of microplastics

Filter papers were first analysed with an Olympus SZX10 microscope, Olympus UC30 camera, and (Olympus) CellSens software to identify and count suspected microplastics manually for each filter paper. The particles were then examined for polymer content using Fourier transform infrared (FT-IR) analysis, with a Thermo Fisher Scientific iN10 Nicolet spectrometer equipped with the OMNIC Picta software (Thermo Scientific OMNIC Series). Due to the large number of particles being identified as potential microplastics, 10% of each type of particle seen at every depth at each site was tested to gain a representation of every type observed, resulting in 719 suspected particles being verified. The spectra were recorded with 12 scans in the region of 800 - 6000$cm^{-1}$. The spectra of a particle is recorded and compared to well-established polymer libraries in addition to contamination libraries which were identified from control samples. Examples of FT-IR spectra are shown in Appendix B, Figure B.1. Particles were determined as plastic if there was a match of at least 70%, the standard protocol for microplastic FT-IR analysis (Cai et al., 2019; Lusher et al., 2013). If more than 10% of each type of plastic at each depth and location were identified as plastic, it was assumed all particles in that subcategory were plastic. Plastics were organised as plastic-type (fibre, fragment, and film) and polymer type: polyethylene terephthalate (PET), polypropylene (PP), polyethylene (PE), Low-density polyethylene (LDPE), and “other” which includes non-typical polymers such as polyacrylonitrile (PAN).

### 5.2.5 Prevention of contamination

To prevent samples from being contaminated by airborne particles during the analysis - such as textile fibres, the following measures were taken. During collection and laboratory analysis, cotton clothing including lab coats were worn instead of synthetic materials in addition to Laboratory Latex gloves. All liquid reagents (deionised water, $H_2O_2$, and ethanol) used were passed through a filter paper (55 µm-pore size Whatmann GF) using a vacuum

pump before being used. Glass equipment was triple rinsed using filtered deionised water and stored sealed to prevent contamination. Work surfaces were cleaned with filtered 100% ethanol and all processes were performed in a fume hood to prevent airborne contamination. During each step of the analysis, a filter paper was placed on the work surface to account for contamination and procedural blanks were also run to determine contamination risks. These filter papers were examined using optical and FT-IR analysis as above. If polymers were identified, they were added to a contamination library which the environmental samples were all compared to. Out of the 719 suspected particles tested, only 3 matched the contamination library.

### 5.2.6 Calculation of microplastic concentration and flux

First, the volume of water, $m^3$, passing through the sampling net is calculated:

$$V = vAt \quad \textbf{(4)}$$

Where $v$ denotes the flow velocity, $m\ s^{-1}$, $A$ denotes the cross-sectional area, $m^2$, of the net, and $t$ is the length of sampling, s. Concentration of microplastics $C_{mp}$ , # per $m^3$ is calculated as follows:

$$C_{mp,number} = \frac{n_{mp}}{V} \quad \textbf{(2)}$$

Where $n_{mp}$ denotes the number of microplastics. Next flux is calculated as, where Q, $m^3/s$, is the discharge within the portion of water sampled (acquired from ADCP data):

$$Flux = QC_{mp} \quad \textbf{(3)}$$

### 5.2.7 Comparison to previous study

Haberstoch *et al.* (2021) also sampled the Tonlé Sap River, Lower and Upper Mekong River, and Bassac River at Phnom Penh in August and September of 2019. Total concentrations

were compared at each site between our study (July 2019) and Haberstoch et al. (2021) to determine any trends and relationships between discharge and microplastic concentration. Haberstroch et al. (2021) sampled twice at each location, the first during August and the beginning of September, and the second in September. Average discharge data was acquired from a fully validated Mike11 model of the Phnom Penh region forced with observed discharge data from the river gauge at Kratie.

### 5.2.8 Statistical analysis

As the results were count data, Poisson regression model analysis was carried out to assess the differences between microplastic concentration/flux and location (n = 8). Spearman's rank test was used to determine the correlation between microplastic concentration/flux and depth at each site at a significance level of $p < 0.05$. All analysis was conducted using R Studio (R Core Team, 2013).

## 5.3. Results

All samples taken were found to contain microplastics. 1,444 particles were identified as plastic, with counts varying with location and depth, with a greater amount of microplastics observed downstream. There were significant differences in total microplastic concentration between sites: Kampi (2 microplastics $m^{-3}$, GLM, $p<0.01$) and Kratie (3 microplastics $m^{-3}$, GLM, $p<0.05$) had considerably lower microplastic concentrations while Lower Mekong Phnom Penh (40 microplastics $m^{-3}$, GLM, $p<0.05$) and Can Tho (64 microplastics $m^{-3}$, GLM, $p<0.01$) had considerably higher microplastic concentrations (Fig.5.15). The patterns were similar for microplastic flux between locations, with Kampi ($1.7 \times 10^{-6}$ microplastics $s^{-1}$,GLM, $p<0.01$), Kratie ($2.5 \times 10^{-6}$, microplastics $s^{-1}$, GLM , $p<0.01$), Tonlé Sap River ($9 \times 10^{-6}$, microplastics $s^{-1}$, GLM, $p<0.01$) and Bassac River Phnom Penh ($19 \times 10^{-6}$ microplastics $s^{-1}$, GLM, $p<0.01$) having significantly lower microplastic fluxes while Can Tho ($67 \times 10^{-6}$ microplastics $s^{-1}$,GLM, $p<0.05$) had considerably higher microplastic concentrations (Fig.5.15).

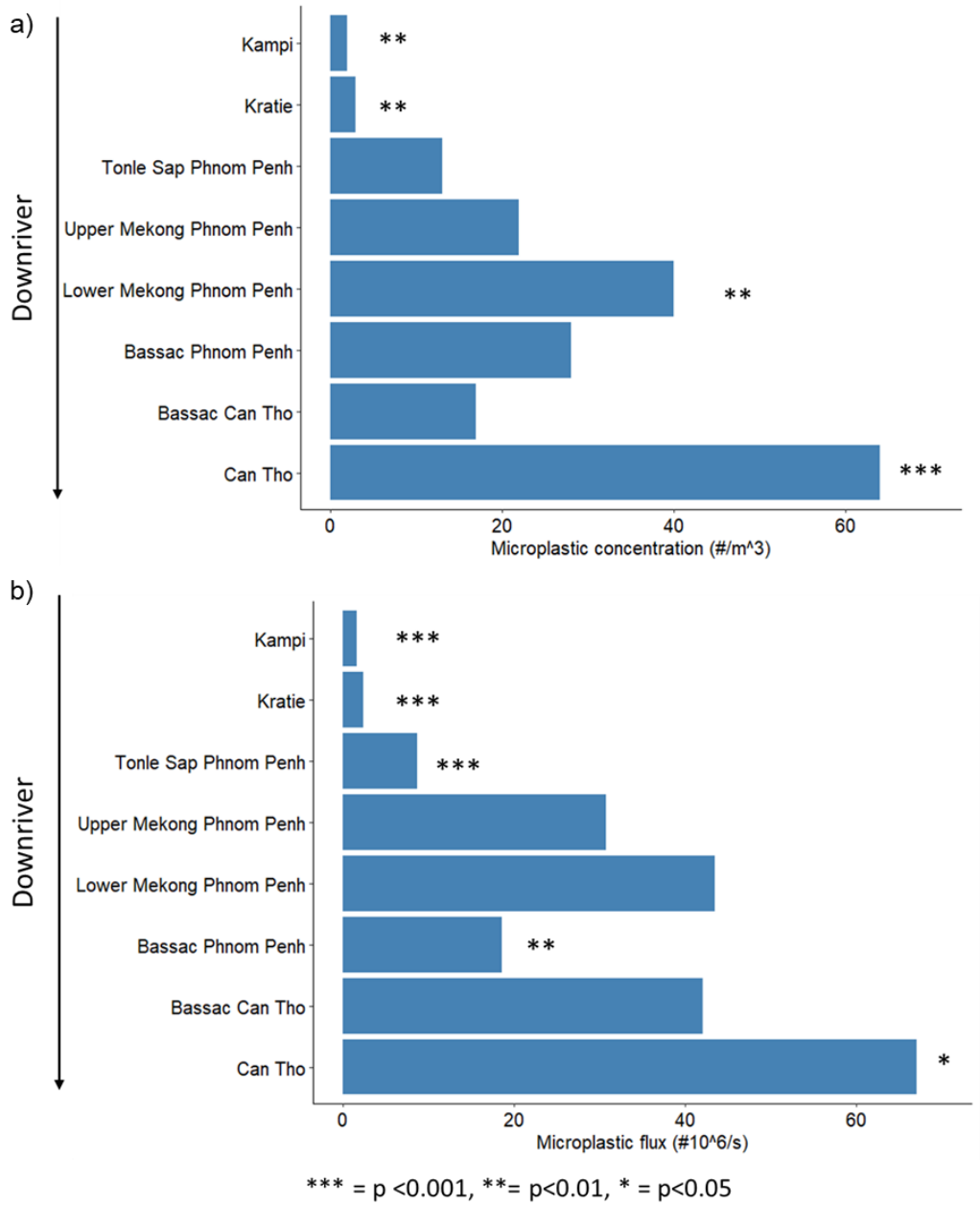


Figure 5.15: a) Total microplastic concentration and b) total microplastic flux between sites at Kampi, Kratie, Phnom Penh (Tonlé Sap River, Upper and Lower Mekong River and Bassac River) and Can Tho (Bassac River and Can Tho River

When looking at how microplastic concentration and flux varied with depth at each location, patterns are very varied (Fig.5.16 and Fig. 5.17). On average, 86% of microplastics (concentration) were observed within the water column, below the water surface: 67% at Kratie, 83% at Tonlé Sap, 98% at Lower Mekong Phnom Penh, 93% at Bassac Phnom Penh, 94% at Bassac Can Tho and 83% at Can Tho (Kampi and Upper Mekong Phnom Penh had no surface sampling). Spearman's rank correlation was conducted to determine if there is a relationship between microplastic concentration and depth. No correlation was observed apart from a positive correlation for Bassac Can Tho ($p<0.05$) where at the surface the concentration was 1 microplastic $m^{-3}$ increasing to 3 microplastics $m^{-3}$ at 3.3 m and 5.4 m to 5 microplastics $m^{-3}$ at 7.5 m and 11.5 m. When looking at microplastic flux with depth, patterns change slightly (Fig.5.17). Again no correlation was observed at any site apart from Bassac Can Tho ($p<0.05$) with a positive correlation.

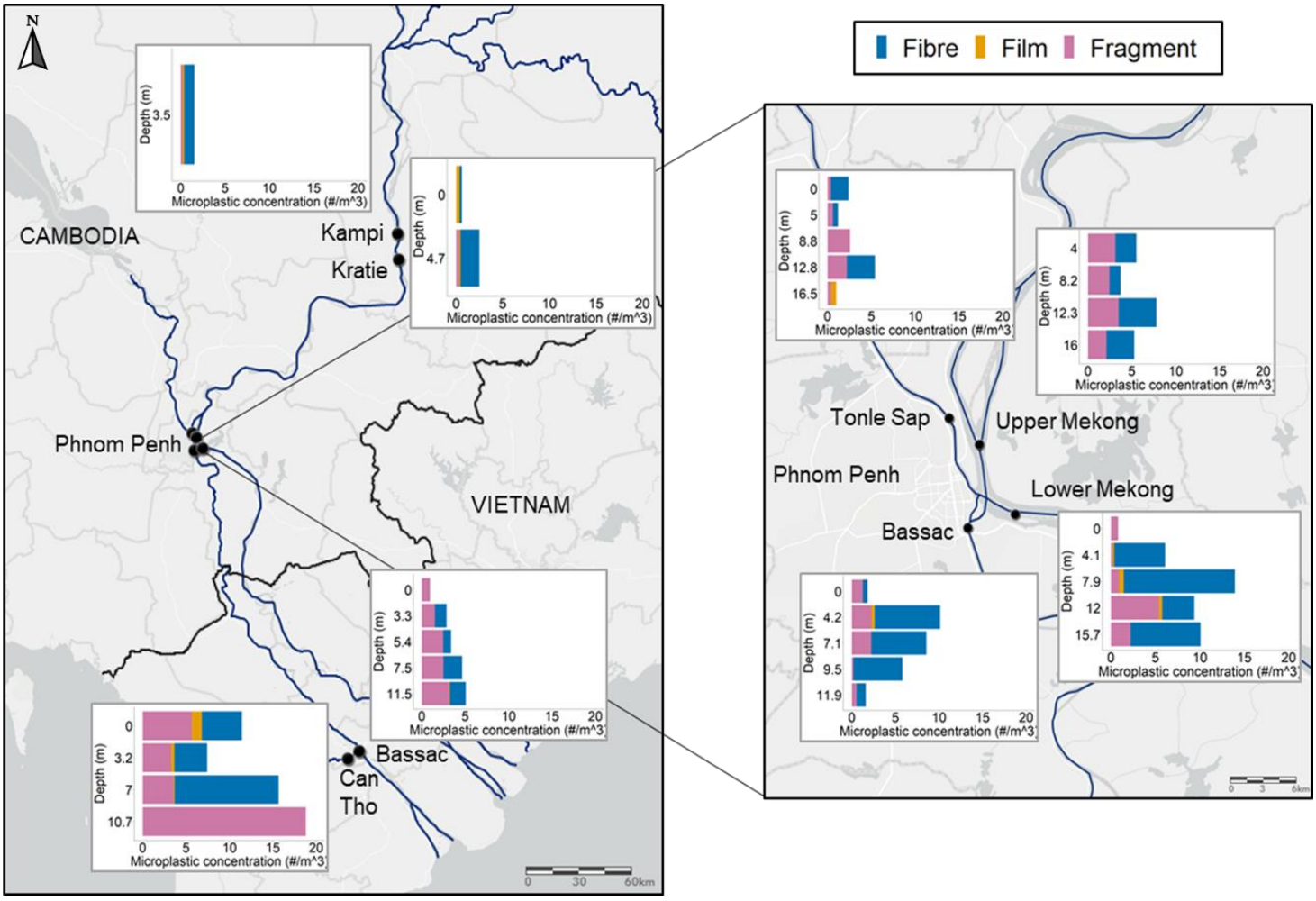


Figure 5.16: Microplastic concentration at each location with depth at Kampi, Kratie, Phnom Penh (Tonlé Sap River, Upper and Lower Mekong River and Bassac River) and Can Tho (Bassac River and Can Tho River)

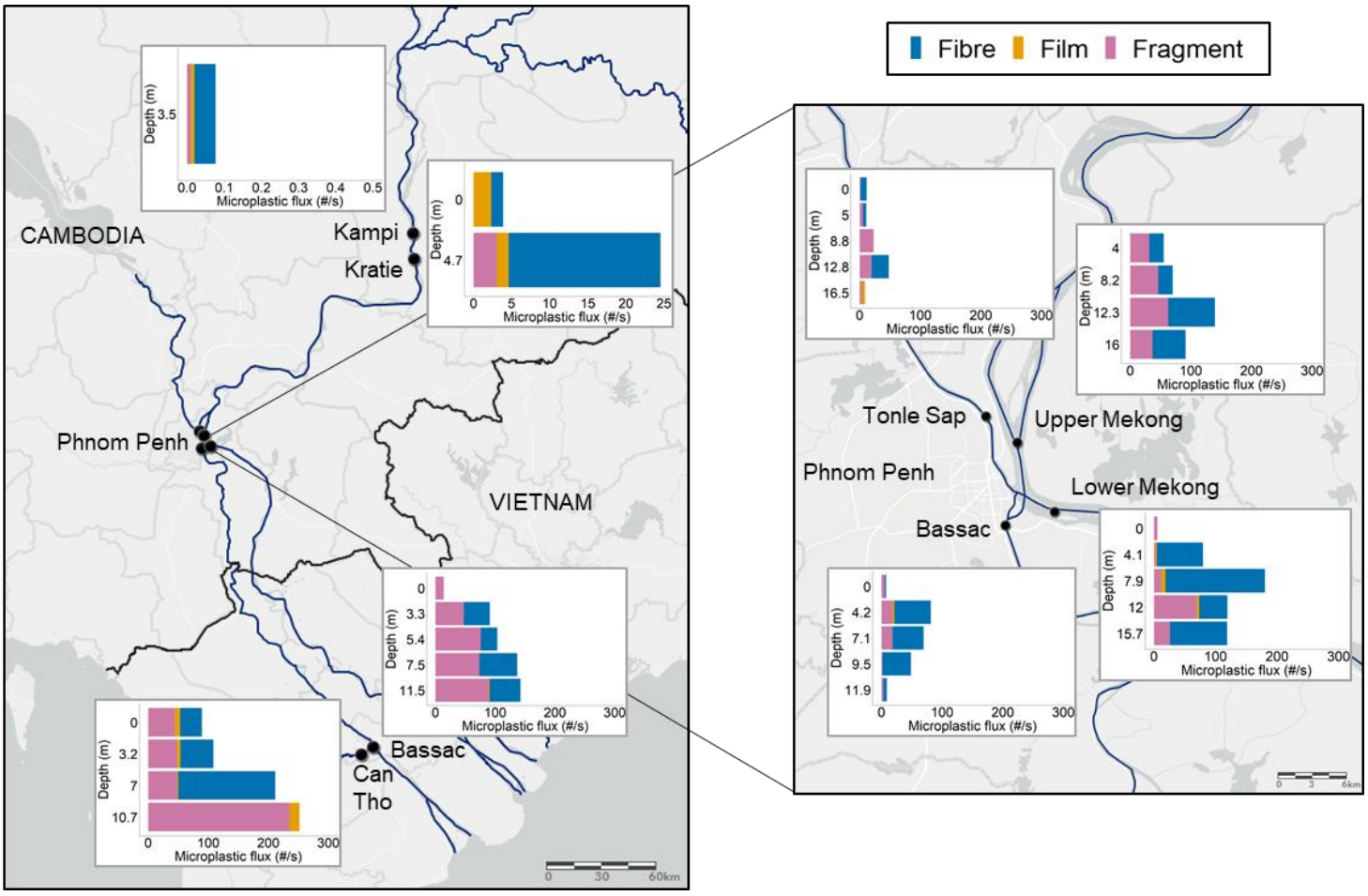


Figure 5.17: Microplastic flux at each location with depth at Kampi, Kratie, Phnom Penh (Tonlé Sap River, Upper and Lower Mekong River and Bassac River) and Can Tho (Bassac River and Can Tho River).

Of the total microplastics found, 53% (766) were fibres, 44% (623) were fragments and 3% (42) were films (Fig.5.18 and 5.19). No plastic pellets or spheres were observed. The majority of the total amount of microplastics were classified as PET and “other” with 35% (501) being PET, 34% (493) “other”, 22% (313) PP, 5% (79) LDPE, and 4% (60) PE (Fig.5.19). The size distribution of microplastics was mostly in 1 mm-3 mm range (35%) with only 5% being <0.1 mm and 7% being 3-4 mm (Fig.5.19). Examples of microplastics and their associated FT-IR spectra are shown in Appendix B, Figure B.1.

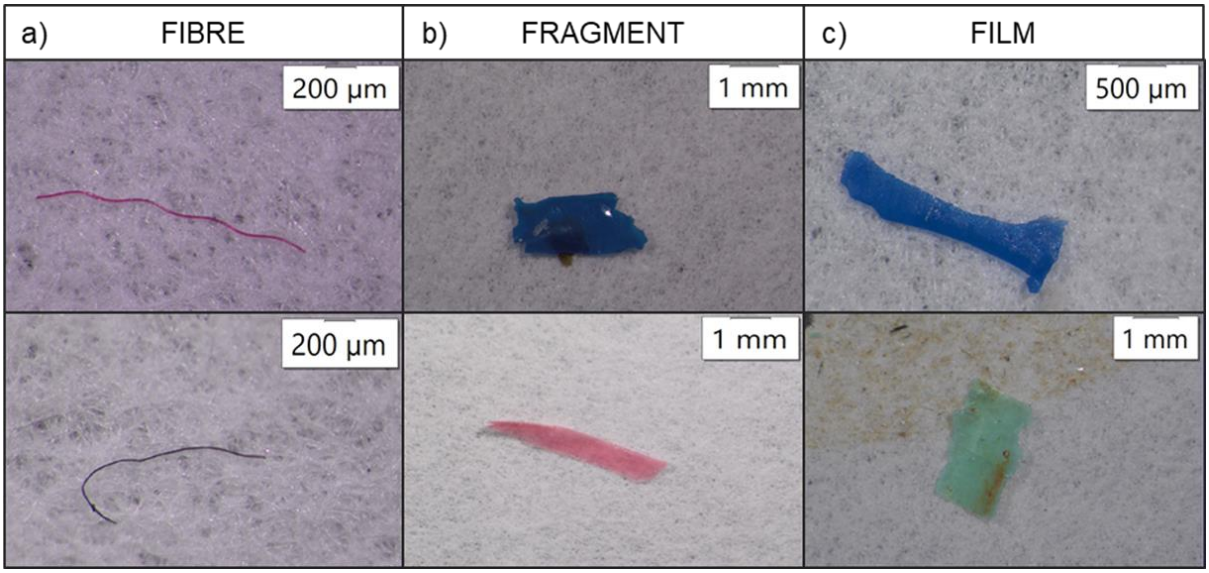


*Figure 5.18: Examples of microplastic types found in the Mekong River a) fibres b) fragments and c) films. Photographed with an Olympus SZX10 microscope, Olympus UC30 camera, and (Olympus) CellSens software*

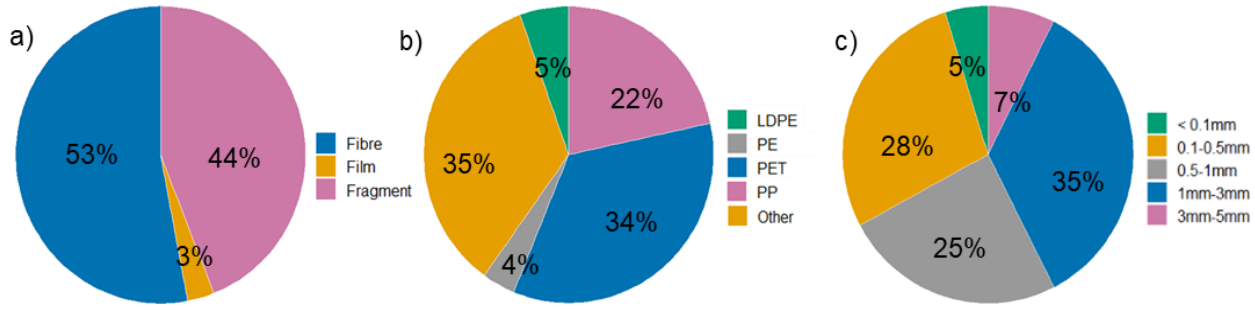


*Figure 5.19: Characteristics of the total microplastics found across all samples: a) percentage of each type of plastic: fibre, film, or fragment; b) percentage of each polymer type: low-density polyethylene (LDPE), polyethylene (PE), polyethylene terephthalate (PET), polypropylene (PP), and “other” which includes non-typical and c) the size range of microplastics: <0.1 mm, 0.1-0.5 mm, 0.5-1 mm, 1-3 mm and 3-5 mm.*

This study (July 2019) reported considerably higher microplastic concentrations at the Upper Mekong, Lower Mekong, and Bassac Rivers of Phnom Penh compared to August and September 2019 as described by Haberstroch *et al.,* (Fig. 5.20). Total microplastic concentration decreased from July to September at those locations. For example, the total concentration for the Lower Mekong was 40 microplastics $m^{-3}$ in July, decreasing to 9 microplastics $m^{-3}$ in Haberstoch *et al.,* (2021) first sampling to 8 microplastics $m^{-3}$ in their second sampling. However, concentrations were similar for each month at Tonlé Sap River.

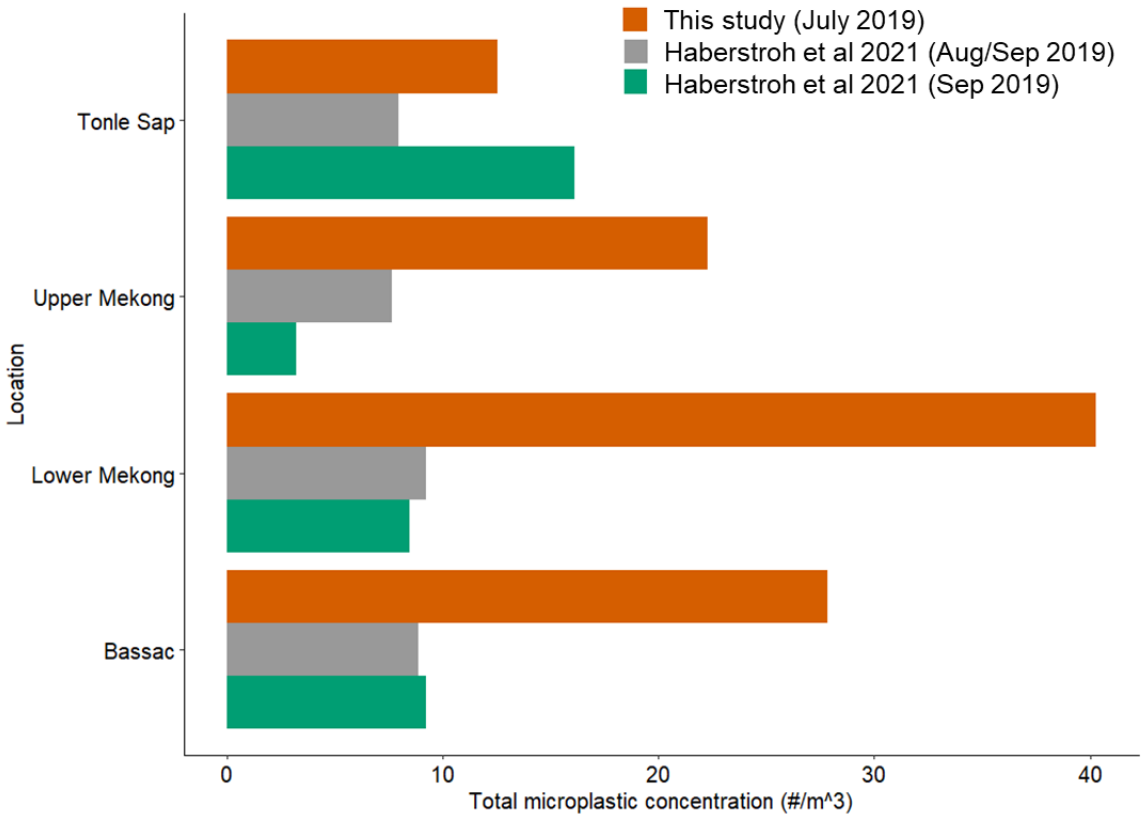


*Figure 5.20: A comparison of the total microplastic concentration at the Upper Mekong River, Tonlé Sap River, Bassac River, and Lower Mekong River of Phnom Penh, Cambodia. Microplastic concentration data from July 2019 (orange) is from this study while data from August and September 2019 (grey/green) are from Haberstroch et al., (2021).*

To fully understand the changes in microplastic concentration, the discharge of the river must be considered and is shown in Figure 5.21. Negative correlations are observed for the Upper Mekong River, Bassac River, and Lower Mekong River whereby the concentration

of microplastics decreases with an increase in river discharge. For the Tonlé Sap River, no clear relationship is observed.

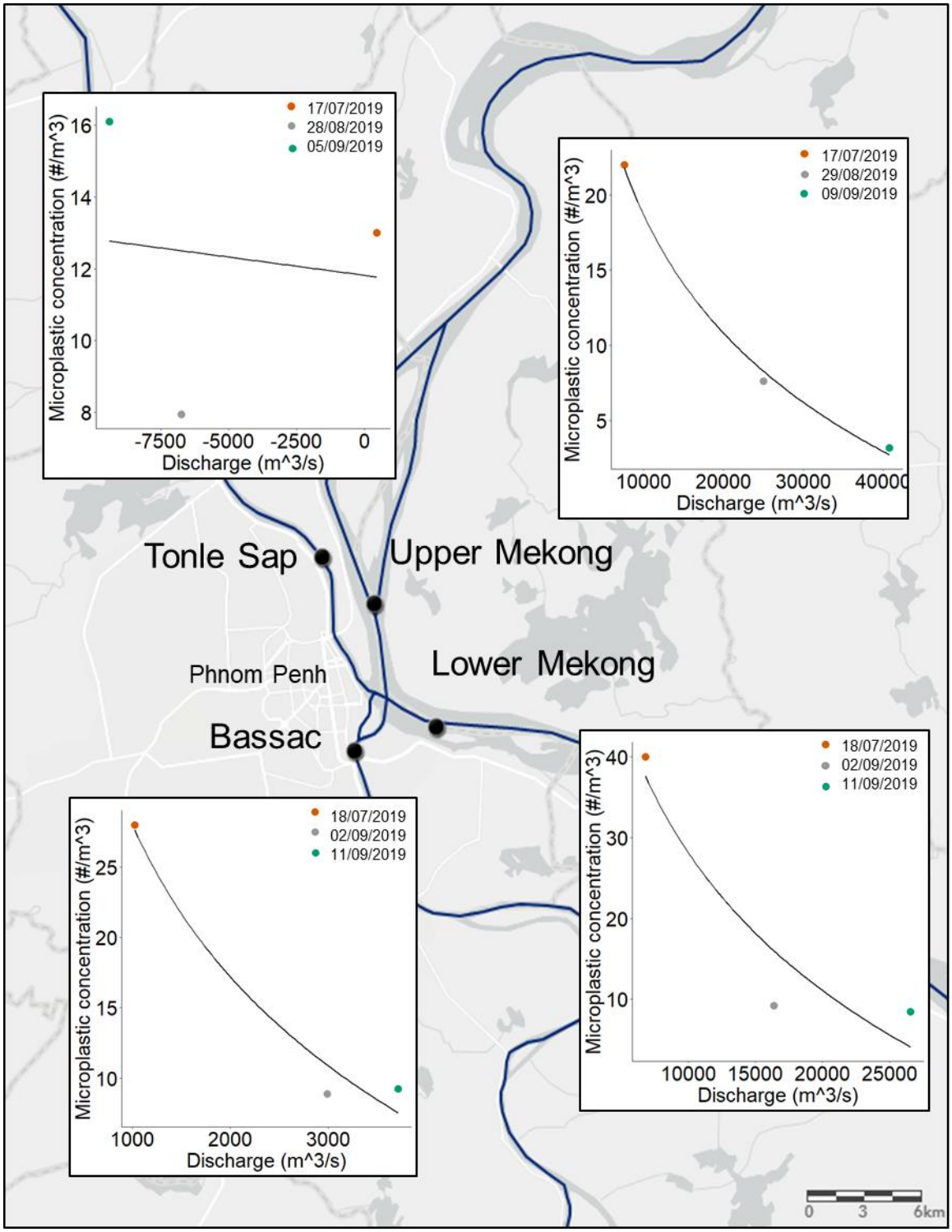


*Figure 5.21: Microplastic concentration in relation to river discharge at the Upper Mekong River, Tonlé Sap River, Bassac River, and Lower Mekong River of Phnom Penh, Cambodia. Microplastic concentration data from July 2019 (orange) is from this study while data from August and September 2019 (grey/green) are from Haberstroch et al., 2021. Discharge data from a fully validated Mike11 model of the Phnom Penh region forces with observed discharge data from the river gauge at Kratie.*

*Note the negative discharge at Tonlé Sap is negative during August and September, driven by the flow reversal during the wet season*

## 5.4. Discussion

A wider understanding of the abundance, transport mechanisms, and fate of microplastics is necessary to accurately predict riverine microplastic loads into the oceans and understand associated ecological and human risks (Chen *et al.,* 2021). The Mekong River is commonly reported to be one of the top polluting rivers globally, discharging plastic waste into the South China Sea (Lebreton *et al.,* 2017; Meijer *et al.,* 2021). Despite this, there is limited research on major rivers in Southeast Asia. Current approaches to modelling and monitoring fluvial microplastic transport mostly rely on surface sampling and assumptions to estimate depth concentrations, with vertical distribution at varying flows being essentially unknown (Cowger et al., 2021; Lenaker et al., 2019; Waldschläger et al., 2020b). Accurately predicting and monitoring microplastic fluxes in riverine systems must include sampling and characterisation of microplastic concentration depth profiles (Cowger *et al.,* 2021). Furthermore, the ecological and socioeconomic impacts of fluvial plastic pollution should be quantified, especially in areas such as the Lower Mekong Basin where communities are highly dependent on the health of the river which also faces a number of other challenges such as sand mining, climate change impacts and habitat degradation (Hackney *et al.,* 2020; Varis *et al.,* 2012; Xue *et al.,* 2011).

### 5.4.1 Abundance of microplastics in the Mekong River

In our study, an average of 24 microplastics $m^{-3}$ was detected in the Mekong River, yet this was highly variable between sites and increased downstream. The most rural locations, Kampi and Kratie (Cambodia) had, perhaps unsurprisingly, the lowest concentrations at 2 and 3 microplastics $m^{-3}$ respectively (Fig.5.17). Abundance increased dramatically within the Lower Mekong Phnom Pehn as population density increases, such that Cambodia's capital displays a total concentration of 40 microplastics $m^{-3}$. However, there was a decrease in

abundance between the two Bassac River sites, with concentration decreasing from 28 microplastics $m^{-3}$ at Phnom Pehn to 17 microplastics $m^{-3}$ at Can Tho, Vietnam. The largest concentration was observed at Can Tho River with 64 microplastics $m^{-3}$. This suggests a large amount of microplastics transported by the Bassac river from Cambodia settle in bed sediments or are distributed onto the floodplain through flooding or irrigation practices, before reaching the delta, whilst plastic discharge associated with the city of Can Tho is predominantly routed into the Can Tho River rather than passing downstream of Can Tho in the Bassac River. The high abundance at Can Tho was expected as it is the largest city on the Mekong delta. The rural-urban transition and downstream increase has been observed in other studies due to changes in population density, with densely populated urban environments identified as important sources of microplastics (Chen et al., 2021; Dikareva and Simon, 2019; Dris et al., 2015; Horton et al., 2017b; Kataoka et al., 2019; Yan et al., 2019; L. Zhang et al., 2020).

The abundance with depth at each location also needs to be considered and indicates that relying on surface water concentrations may significantly underestimate microplastic quantities (Lenaker *et al.,* 2019). The distribution of microplastics in the water column varied by location, but on average, 86% of microplastics were found below the surface sample. It is difficult to predict how much of the water column should be sampled to gain a full representation of microplastic concentration as distribution varied widely with depth between sites (Fig.5.16 and 5.17). However, by calculating which depth would equate to the average microplastic concentration across all depths at each site, the optimum sampling depth can be calculated. For the Mekong, this was calculated to be 59% of the total depth and therefore this depth can be used for efficient monitoring that is representative. This highlights that the common practice of sampling only the water surface can cause substantial bias in predicting microplastic concentrations (Lenaker *et al.,* 2019).

The settling, storage, and entrainment dynamics of fine material within rivers is complex due to the inputs from multiple sources throughout watercourses and their relation

to fluvial dynamics (Chen *et al.,* 2021). Dispersal in the water column is impacted by stream velocities, channel depth, particle type, and polymer density (Lenaker *et al.,* 2019). Microplastic settling experiments have shown the need to consider the biological influence on particle density which increases settling (Hoellein et al., 2019; Kaiser et al., 2017; Chapter 4). To date, few studies have investigated the vertical distribution of microplastics in riverine environments (Haberstroh *et al.,* 2021a; Lenaker *et al.,* 2019; Liu *et al.,* 2021).

One other study on microplastics has been conducted in the Mekong River, and reported the majority of microplastics at the surface and declining with depth overall at Phnom Pehn (Haberstroh *et al.,* 2021). Haberstroch et al. (2021) sampled in August and September 2019 while our study was in July. Our study reported considerably higher total microplastic concentrations at all sites at Phnom Penh, apart from Tonlé Sap River where abundances were similar compared to those reported in August and September values (Fig.5.20). This may be due to several reasons. First, peak monsoon was during August and September when discharge levels would have been considerably higher compared to July and several flood events occurred, causing dilution. Figure 5.21 highlights how lower microplastic concentrations occurred during high flow. Dilution of microplastic concentration due to high flow has been reported elsewhere and may have occurred in Phnom Penh (Chen *et al.,* 2021; Watkins *et al.,* 2019). Significantly higher macroplastic (>5 mm) distribution at the riverbed was reported during low flow periods in shallow waters of the Mekong, Vietnam, compared to flooding periods (Karpova *et al.,* 2022). The impacts of increasing discharge are location specific due to factors that influence runoff such as land cover and use and amount of rainfall, where tropical rivers tend to have higher runoff and sediment yield per unit area compared to other climates (Chen *et al.,* 2021; Chong *et al.,* 2021). Empirical and modelling studies highlight the importance of hydrological regimes in controlling the fate of microplastics, with those carried downstream in suspension expected to be deposited in low-flow periods where they accumulate on the riverbed until high flow causes entrainment (Nizzetto *et al.,* 2016b; Hurley *et al.,* 2018; Frei *et al.,* 2019;

Waldschläger and Schüttrumpf, 2019; Chen *et al.,* 2021; Chapter 4). Furthermore, flooding flushes resuspended microplastics downstream or overbank to be deposited onto floodplains while also delivering plastics from terrestrial sources into the river flow (Drummond *et al.,* 2022; Hurley *et al.,* 2018). Post-flooding events have shown significant decreases in microplastics compared to pre-flood as microplastics are flushed out and therefore flooding may be the main supplier of microplastics to the oceans within river systems (Hurley *et al.,* 2018). Results from the Ganges River report higher numbers of microplastics found pre-monsoon compared to post-monsoon, highlighting the need for sampling across all seasons (Napper *et al.,* 2021). However high flow events also have the potential to drive microplastics in sediment further into the riverbed to less-mobile regions resulting in long-term burial due to hyporheic exchange flow (Drummond et al., 2022, 2015).

### 5.4.2 Comparison to suspended sediment transport and fluxes

It is widely thought that research on natural sediments can provide insights into understanding microplastic transport and fate in aquatic environments (Waldschläger *et al.,* 2022). In particular, finer grain size fractions have been related to microplastics, suggesting that their distribution is governed by similar mechanisms (Enders *et al.,* 2019). The basic relationship between suspended sediment and discharge is well known with increasing discharge typically resulting in increasing suspended sediment (Rivera *et al.,* 2019). As our results highlighted differences in microplastic concentrations at various discharges between studies, the relationship was analysed to determine if it follows similar patterns to sediment transport. Figure 5.21 demonstrates that microplastic concentration follows the opposite pattern to suspended sediment where an increase in discharge is associated with a decrease in microplastic concentration at all sites around Phnom Penh apart from Tonlé Sap River which may be explained by the annual flow reversal during the monsoon. As discussed previously (§5.4.1), dilution of microplastic loads appears to have occurred at increased discharge. Furthermore, these results suggest that microplastic concentrations could be supply limited rather than capacity limited in rivers as concentrations do not increase with

discharge**.** This highlights the need to sample throughout the year to fully understand and predict changes in microplastic levels in rivers and indicates that we should not rely on sediment dynamics to explain microplastic transport dynamics.

Although predicting microplastic transport and fate based on sedimentary laws provides basic insights into potential distribution, it does not take into consideration the complex behaviour of microplastics (Waldschläger *et al.,* 2022). For example, microplastics are present in a range of densities, approximately 0.5-2.65 g/$m^{-3}$, while sediment is often assumed to be 2.65 g/$cm^{-3}$ (quartz sand). Furthermore, the density of microplastics may change over time due to aggregation, flocculation, and fragmentation, yet exact levels of change are yet to be quantified (Skalska *et al.,* 2020). Settling experiments have revealed that theoretical approaches from conventional sediment transport theory are inaccurate for predicting microplastic fate (Chapter 4; Waldschläger and Schüttrumpf, 2019). Shape has also been highlighted as more significant in determining fate than for natural sediments as microplastics tend to have more variation in type and form (Waldschläger and Schüttrumpf, 2019; Van Melkebeke *et al.,* 2020).

These results provide several implications for predicting microplastic loads in major rivers. Spatial and temporal variations in microplastic concentrations must be assessed (Chen *et al.,* 2021). Concentrations and fluxes of microplastic will change depending on seasonal discharge, with sampling campaigns needing to be conducted throughout the year to form accurate predictions on microplastic loads from rivers into oceans. This includes sampling at low flow where it is expected that microplastic concentration will be higher, due to decreasing discharge and constant microplastic input. This is opposite to what is expected of suspended sediment, to which microplastic transport is often related. However, the scale of the river must be considered: As the Mekong is a major river, future studies must be conducted within rivers of various scales and locations to determine if patterns of discharge and microplastic concentration are the same as concluded here (Woodward et al., 2021).

### 5.4.3 Characteristics of microplastics

The majority of microplastics were classified as fibres (53%), followed by fragments (44%) with only a small amount being films (3%) and no pellets or spheres. Fibres are typically the most common type of plastic found in rivers (Chen et al., 2021; Dris et al., 2018; Eo et al., n.d.; Feng et al., 2021; Lin et al., 2018; Zhao et al., 2014). In addition, most were determined to be PET (35%) or “other” (34%) which included polyacrylonitrile (PAN), or polyacrylates. PET is typically used in packaging for food and drinks but PET fibres, or polyester, have several applications such as in clothing and textiles. PAN is also used heavily in the clothing industry. Polyacrylates are primarily used in paints and may be found in fragment forms but are also used in textiles. The source of fibres in waterways has been associated with WWTP effluent, stormwater inputs, and agricultural drainage (Frei *et al.,* 2019; Hoellein and Rochman, 2021; McCormick *et al.,* 2016; Woodward *et al.,* 2021). Domestic wastewater often contains large amounts of synthetic fibres due to the release from textile washing (Alam *et al.,* 2019; Jiang *et al.,* 2019). Even when water is treated before being discharged into rivers, only a limited number of WWTPs have the ability to filter microplastics (Frei et al., 2019).

Whether or not a microplastic particle will settle in a fluvial system varies depending on the hydrodynamic, physicochemical, and biological conditions (Hoellein et al., 2014; Woodward et al., 2021; Zhang, 2017). Due to several microplastic settling experiments detailing the change in settling regimes due to polymer density, it was expected that patterns of polymers with depth would be observed, with higher density ones such as PET closer to the riverbed (Khatmullina and Isachenko, 2017; Chapter 4; Waldschläger and Schüttrumpf, 2019). Previous studies sampling with depth has reported low-density particles (such as PP) decreasing with depth, while higher-density particles increased with depth, as expected (Lenaker *et al.,* 2019). On the other hand, it has also been reported that microplastic composition does not change with depth due to turbulent flow creating a homogenous

mixture of microplastics within the water column (Dris *et al.,* 2018). No patterns of plastic or polymer type with depth were seen in this study, which is likely a result of turbulent mixing.

Experiments have also highlighted that particle density shifts induced by biofilm growth can cause a substantial change in settling rates for microplastics (Kaiser *et al.,* 2017; Chapter 4). A biofilm can grow on a microplastic rapidly (minutes to hours) when in riverine environments and significant impacts on microplastic settling can occur over a number of days (Zettler *et al.,* 2013a; Chapter 4). Therefore, less dense polymers such as PE may sink faster than previously predicted, even if they have only been in suspension for a short period of time. In addition, the variation in microplastic type and polymer distribution with depth over different studies highlights the difficulty in modelling microplastic transport accurately without considering hydrodynamics and biological interactions.

### 5.4.4 Ecological risk

The presence of microplastics in fluvial systems poses a significant threat to biodiversity and entire riverine ecosystems. Within the highly biodiverse Mekong Basin, fish and other organisms such as decapods and molluscs form one of the largest inland fisheries worldwide providing substantial sources of food and income to millions of people (Karpova *et al.,* 2022). However, in recent years the productivity of these fishing areas has decreased, theoretically as a result of various types of habitat degradation and pollution such as fertilisers, pesticides and untreated wastewater (Food and Agriculture Organisation of the United Nations (FAO), 2018, 2016). As the majority of microplastics were found throughout the water column, rather than the surface, the ecological risk may be higher than previously thought and already impacting these species. The risk of microplastic pollution to ecologically and socioeconomically important species must be determined and include an assessment of microplastic distribution.

Potential toxicity to biota has been extensively studied, especially in fishes (Enyoh *et al.,* 2020). Due to their size, microplastics are easily ingested by fish, with river studies showing various sizes accumulating in digestive tracts and gills, and larger fish containing

more microplastics than smaller ones (European Environment Agency, 2016; Horton *et al.,* 2018; Jabeen *et al.,* 2017; Khan *et al.,* 2020; McNeish *et al.,* 2018; Pegado *et al.,* 2018; Sanchez *et al.,* 2014; Sembiring *et al.,* 2020; Slootmaekers *et al.,* 2019; Su *et al.,* 2019; Zhang *et al.,* 2021). As microplastics age and fragment, chemicals can leach out into the environment and have detrimental impacts on organisms. Exposure studies have demonstrated that ingested microplastics can cause several repercussions to fish health including reduced food intake, altered feeding behaviour, lower immunity, reproduction, metabolism, and endocrine function (Horton *et al.,* 2018; Kumar *et al.,* 2021). Organisms that are adapted to feed on particulate matter such as filter-feeding bivalves can also accidentally ingest microplastics. Microplastics can change filtration ability, reduce food uptake, growth, and impair immunity and reproductive health (Avio *et al.,* 2015; Zhang *et al.,* 2020). Bivalves play important roles in ecosystem functioning such as removing suspended particles and increasing water clarity which promotes primary production. Therefore any impacts on bivalves may have repercussions throughout the food web (Castorani *et al.,* 2015). Microplastics have been observed in bivalves such as mussels, clams, and oysters from China, Korea, France, Germany, Canada the US, especially fibres (Cho *et al.,* 2019; Davidson and Dudas, 2016; Li *et al.,* 2015; Qu *et al.,* 2018; Rochman *et al.,* 2015; Van Cauwenberghe and Janssen, 2014).

Fibres are often reported to be the most common type of microplastic ingested causing blockage of digestive tracts and hindering food intake (Bellas *et al.,* 2016; Nadal *et al.,* 2016; Neves *et al.,* 2015; Wright *et al.,* 2013). These results show concentrations of microplastics throughout the water column at several locations along the Mekong River. It is therefore highly likely that biota such as fish, molluscs and invertebrates of the Mekong River will be exposed to microplastic pollution, especially as fibres were the predominant type observed. It is uncertain whether feeding guild determines the uptake of microplastic in biota, with some authors stating that accidental ingestion can occur at the same rate throughout

the water column, while others conclude certain feeding strategies such as filter or detritivorous feeding will be more at risk (Windsor *et al.,* 2019).

Bioaccumulation in the food web can also occur, with microplastics being transferred from lower trophic levels such as small fish, to higher trophic levels including larger fish, fish-eating birds, and eventually to humans (Collard *et al.,* 2019; Kasamesiri and Thaimuangpho, 2020; Silva-Cavalcanti *et al.,* 2017; Winkler *et al.,* 2020). Although the implications for human health are currently unknown, there is growing evidence of microplastics in humans which may originate from eating seafood, especially molluscs and small fish that tend to be eaten whole (Ding *et al.,* 2022; Smith *et al.,* 2018). This may be occurring in the Mekong River, impacting a wide range of species and ecosystems and also the fate of microplastics. However, despite a large body of evidence showing the uptake and impact of microplastics on aquatic organisms, there remains little consensus on ecotoxicological implications, especially at environmental applicable concentrations. Our results demonstrate that a variety of species throughout the water column will be exposed to microplastics, yet more extensive research is necessary on microplastic exposure and ecological risk. Precaution must be taken to ensure the biodiversity of the Mekong is protected, as well as the livelihoods, food security, and economy of millions of people in the surrounding area.

## 5.5. Conclusion

This study has investigated microplastic abundance throughout the water column at numerous sites within the Mekong River, one of the top contributors to marine plastic waste, and its tributaries of Cambodia and Vietnam. We show that microplastic abundance in fluvial systems is highly dependent on hydrodynamical and seasonal flows and that microplastic concentration does not follow suspended sediment transport laws. It appears that flooding flushes microplastics toward the ocean, with higher microplastic concentrations seen before peak flow. We expect that higher concentrations will be seen at low discharge, but seasonal sampling is needed, as hysteresis may occur, delaying microplastic flow.

There still remains a large gap in our current knowledge of potential sources, transport, accumulation, and fate of microplastics in major rivers as well as identifying associated impacts. Bedload microplastic transport must also be considered where turbidity currents may fragment, distribute or bury microplastics (Waldschläger *et al.,* 2022). However, FT-IR analysis may cause lower levels of microplastic concentrations to be predicted, as many particles identified as plastic but as they were weathered or degraded, did not meet the threshold match to the polymer libraries.

Furthermore, this study highlights the importance of sampling throughout the water column, with an average of 86% of microplastics seen below the water surface. This demonstrates that previous predictions for riverine microplastic fluxes may be greatly underestimating discharge into the ocean as concluded by Hurley et al., (2018). This study demonstrated that sampling must take place below the water column to be representative of the total riverine microplastic load, with an optimum sampling depth calculated to allow efficient monitoring of microplastics. Microplastics have several ecological and socioeconomical implications for the Mekong River, such as detrimental impacts on a variety of species and associated fisheries. Remediation of microplastics at the relevant sources is an effective way to avoid contamination and was identified mainly to be fibres from textiles (Woodward et al., 2021) .

Filtering and capture of microplastic fibres can be achieved at WWTPs and stricter waste management policies are vital to protect the natural environment (Woodward et al., 2021). This study provides greater insight into the concentration of microplastic in the Mekong River which will support improvements of models and the formation of more effective waste management strategies.

[Page intentionally left blank]

# Chapter 6.
# Transport and trapping of microplastics in coral reefs: a physical experimental investigation

---

**Abstract**

The “missing plastic” phenomenon, whereby the transport and ultimate fate of microplastics (<5mm) in aquatic environments is largely unknown. Complex and biodiverse coastal ecosystems are vulnerable to microplastic pollution as they are often situated near riverine and shoreline sources of plastic pollution, which are input into the ocean. The broader ecological impact is likely considerable with a suite of largely unquantified repercussions for associated ecosystem services for hundreds of millions of people. Ecosystems may contain an aquatic canopy covering the bed, such as those formed by seagrass meadows, or more structurally complex coral reefs that can trap particles. Despite the potential consequences and recent field measurements that have revealed the accumulation of plastic debris in a variety of aquatic canopies (such as those formed by coral reefs), the transport and dispositional processes that drive microplastic trapping is barely understood. Here, we investigate for the first time the prevalence of microplastic retention by branching coral canopies in a hydraulic flume under several controlled unidirectional flow conditions. Trapping efficiency by coral canopies was found to be dependent on bulk velocity and canopy density, with up to 99% of microplastics retained across the duration of the experiments. Surprisingly, sparse reefs may be as vulnerable to microplastic trapping and contamination that denser canopies, with the latter found to retain only up to 18% more microplastics than in sparser conditions. Flow velocity profiles were also acquired to understand the relationships between canopy hydrodynamics and microplastic trapping and distribution. Our results provide a new understanding of microplastic transport dynamics and entrapment mechanisms within coral canopies and provide insights into the role of reefs as a

microplastic sink. The broader ecological implications of our findings are outlined and discussed.

## 6.1 Introduction

The movement and ultimate fate of microplastics in aquatic environments is generally unknown, with the “missing plastic” phenomenon still remaining. However, the trapping of microplastics (particles <5 mm in diameter) in natural aquatic ecosystems has recently been published, encompassing corals, seagrasses, saltmarshes, and mangroves (Cesarini and Scalici, 2022; Cozzolino et al., 2022, 2020; Y. Huang et al., 2021; Li et al., 2018; Navarrete-Fernández et al., 2022; Ogbuagu et al., 2022; Stead et al., 2020; Unsworth et al., 2021). These habitats are the foundation of highly biodiverse and productive ecosystems that provide shelter, nursery grounds, and nutrients for a huge range of species as well as numerous ecosystem services for hundreds of millions of people (Huang *et al.,* 2021). In addition, as these canopies are often complex structures, they can easily trap particles and may act as a sink for microplastic pollution. Field measurements have revealed the accumulation of plastics in aquatic canopies, although the knowledge of transport and depositional processes is extremely limited, along with the underlying drivers of these mechanisms. Physical experiments enable the investigation of flow and particulate transport processes otherwise difficult to measure in natural settings. The infancy of this research area warrants further investigation given the foremost importance these complex aquatic canopies have on the ecological system health, function, and potential subsequent transfer of microplastic through the food web (Auta *et al.,* 2017).

Scleractinian coral can form very complex canopies and is one of the most biodiverse ecosystems globally, with 25% of all ocean species being found on reefs, including 4,000 fish species (Hughes *et al.,* 2017; Richmond, 1993). Corals form the first trophic link through their algal symbiosis and offer the majority of the habitat structure for reef organisms (Richmond, 1993). Reefs form land, and provide sand for tropical beaches and structures to

attenuate waves that would otherwise create widespread coastal erosion (Monismith, 2007; Richmond, 1993). However, reefs are at risk from many anthropogenic drivers, especially climate change and rising sea temperatures, which may be accentuated by other pollutants such as microplastics (Hughes *et al.,* 2017). Coral reefs are particularly at risk of microplastic pollution due to their coastal location and the mainly terrestrial origin of marine plastic waste (Lebreton *et al.,* 2017; Reichert *et al.,* 2018). Microplastics can accumulate in the nearshore zone due to wave and wind dynamics, with shallow reefs being especially in danger when low tides occur, resulting in microplastics being more likely to settle within the canopy (Forsberg *et al.,* 2020).

There is growing evidence that corals ingest microplastics and can cause harm such as by reducing photosynthetic capability and growth, bleaching, disturbing initiation of symbiotic relationships, blocking normal food intake, and increasing the risk of disease through tissue abrasion (Corinaldesi *et al.,* 2021; Mendrik *et al.,* 2021; Okubo *et al.,* 2018; Reichert *et al.,* 2019, 2018). The long-term impacts of this could be widespread, influencing not only the numerous species that rely on reefs for survival but also communities that depend on them for multiple ecosystem services. Entrapment of microplastics by coral reefs would not only increase the possibility of these negative impacts but also the likelihood of accidental ingestion by other aquatic organisms. A recent U.N. brief on plastics and coral reefs highlighted the need for improved quantification of the patterns, concentrations, and impacts of microplastic pollution on coral ecosystems to evaluate the extent of risk (Sweet *et al.,* 2019). Understanding passive coral reef trapping mechanisms through their complex structures is vital to determine the impacts of microplastics on coral reefs and associated organisms in addition to the role reefs play as a microplastic sink. Despite the potential harm to reefs being known, the amount of microplastics being trapped within reefs and related microplastic exposure remains understudied, in addition to the hydrodynamics within coral canopies that will influence entrapment.

Recent work has begun to investigate the drivers of plastic trapping in various canopies (Cozzolino et al., 2022; de los Santos et al., 2021b; de Smit et al., 2021, 2020) yet our understanding of the mechanisms and controls on microplastic trapping is limited. Seagrass seed dispersal and capture by ecosystem engineers has been tested with an increase in velocity, habitat complexity, higher turbulence, and erosive processes allowing more seeds to be trapped by eelgrass and bivalves (Meysick *et al.,* 2019). These mechanisms could also apply to microplastic trapping. Furthermore, flume experiments show how seagrass can retain floating plastic at several flow velocities and trap denser microplastics due to erosive processes forming scour around the shoots (de los Santos *et al.,* 2021b). Experiments have also revealed how macroalgae traps microplastics, yet differences are observed within- and between-species often due to canopy densities (Cozzolino et al., 2022). In addition, saltmarsh systems have been observed to influence hydrodynamics above and within canopies, impacting microplastic accumulation (Ogbuagu et al., 2022). Individual coral and macroalgae have also been tested for their potential as microplastic sinks using a flume within the field, with corals capturing the highest number of particles in their canopy structure (de Smit *et al.,* 2021). Microplastics may also adhere to the canopy, which is dependent on surface characteristics and structural complexity (Martin *et al.,* 2019a). Furthermore, through reduction in bottom shear stress, canopies are known to hamper resuspension rates of sediment, trapping particles into the bed (Bos *et al.,* 2007; Gacia and Duarte, 2001). Therefore, these habitats may facilitate microplastic trapping, accumulation, and burial in their associated sediment (de Smit *et al.,* 2021)**.**

Microplastic transport depends on particle size, shape, density, biofilm formation, and interaction with other suspended materials (Chapter 4). Distribution is also influenced by hydrodynamical conditions and therefore a combination of bio-physical factors will determine particle fate and entrapment (de los Santos *et al.,* 2021b; Zhang, 2017). The flow processes of submerged aquatic vegetation canopies have been studied more widely, with the fundamental hydrodynamics presented in a review by Nepf (2012). The complexity of

canopy morphology, heterogeneity, and flexural rigidity introduces a distinct differences in hydrodynamics between canopy types (Hamed *et al.,* 2017). While the hydrodynamics remain only partially quantified due to the vast natural variability, recent studies have provided advanced spatiotemporal measurements within scaled seagrass canopies and corals (Houseago *et al.,* 2022; van Wiechen, 2020a). Within a canopy, flow can be accelerated or attenuated, creating various flow velocity gradients over the vertical profile, which impact turbulence and therefore modulate the transport dynamics of suspended particles such as microplastics.

Reefs can act as physical barriers that entrap microplastics, but the coupled interactions between microplastic transport and hydrodynamics is not understood. This study implements physical modelling to evaluate microplastic transport and trapping processes within canopies of branching coral, at two coral densities. Experimental techniques track microplastic transport and distribution throughout the canopies. Artificial surrogates are employed to enable controlled conditions that build upon current hydrodynamic knowledge from the literature while supporting the assessment of microplastic transport and trapping without harming corals.

The overall aim of this study is to investigate the role of complex coral habitat structures on the transport, trapping, and fate of microplastics. Different canopy densities are evaluated in addition to exploring the relationships between the canopy hydrodynamics and microplastic transport and distribution.

## 6.2. Materials and methods

### 6.2.1 Microplastic particles

The transport and trapping of microplastics, defined as <5 mm in diameter, in association with sparse and dense coral canopies are evaluated through experimental physical modelling described below.

Secondary microplastic particles in the form of fragments of recycled, ground melamine plastic, density 1.6 g/cm³ (Little River Research & Design, Illinois), were chosen as the test polymer. Fragments were sieved to collect size fractions of a range of 1-5 mm. This ensured fragmentation of plastic and heterogeneous shapes and sizes that replicates the environmental degradation of microplastics (Rummel *et al.,* 2017). In addition, irregular shapes of microplastics were chosen instead of pellets and spheres to represent weathered and degraded plastics that are more typically found in the aquatic environments. Furthermore, to ensure plastics represented those found in the environment such as coastal systems, biofilmed microplastic particles were used. The properties of a polymer determine particle buoyancy, but retention and distribution of microplastics in the water column are also influenced by the colonisation of microorganisms forming a biofilm (Hoellein *et al.,* 2019; Chapter 4). Biofouling can alter the density of plastics, causing particles to sink or rise faster, which has considerable implications from a hydrodynamic perspective (Lagarde *et al.,* 2016; Rummel *et al.,* 2017). To colonise fragments with biofilms, the methods of Hoellein *et al.,* (2019) were adapted. Benthic sediment and overlying water was collected from the Humber River, Hull, UK. Fifty grams of sediment and 200 ml of river water was placed in flasks with microplastics in a shaking incubator for 10 days at 37°C, 200 rpm. The flasks were then left at room temperature for at least 2 weeks. Examples of biofouling can be seen in Chapter 4, Figure 4.1, where the same methods were utilised. Fragments were soaked overnight in water of the same salinity and temperature as the experimental environment to ensure no electrostatic discharge from particles, which may alter transport behaviour.

### 6.2.2 Surrogate canopies

Coral colonies were replicated using a scan of a staghorn coral *Acropora* genus (CULTS Copyright DSIGNRCMC 2020). Staghorn corals were chosen as they encompass approximately 160 species and around one-fifth of extant reef-building corals globally (IUCN, 2009). They are branching, stony corals that provide complex habitats for numerous reef

organisms and coastal protection for thousands of people worldwide (IUCN, 2009). *Acropora* have a broad range of sizes, with branches growing from a couple of centimetres to over two metres. The models were printed in polylactic acid (PLA) with a base diameter $d_s$ = 100 mm and overall height $h_v$ = 150 mm, producing a submergence ratio ($h_v/h_w$) of 0.38 (Fig.6.1) (standing water depth $h_w$ = 400 mm), consistent within the broad range of the natural environment (Santos *et al.,* 2016). The model consisted of 11 branches of various lengths and diameters. Two coral canopies were assessed for microplastic capture: a) sparse (15 corals) and b) dense (48 corals) to encompass various reef formations, and were arranged in staggered configurations of 1.85 m long within a 2 m test section (Fig.6.2). Individual dynamically- and geometrically-scaled canopy elements of coral were populated on a baseboard (10 mm thick) in a systematic staggered geometry to produce a full canopy spanning the entire flume width (0.5 m) and length 1.85 m located in the middle of the flume, with a canopy height, $h_c$ of 0.15 m (Fig.6.2). The canopy length exceeded 10 $h_c$ to encompass a developing flow regime downstream of the leading edge (Nepf, 2012). Canopy densities represent *in situ* measurements of 15 corals/m$^2$ for the sparse and for 48 corals/m$^2$ for the dense canopy. A thin layer of fine silica sand (120 µ) was fixed to the top surface of the baseboard to increase the surface roughness to a level comparable to natural environments. This baseboard was also used as a control to represent a barebed, with all velocities tested.

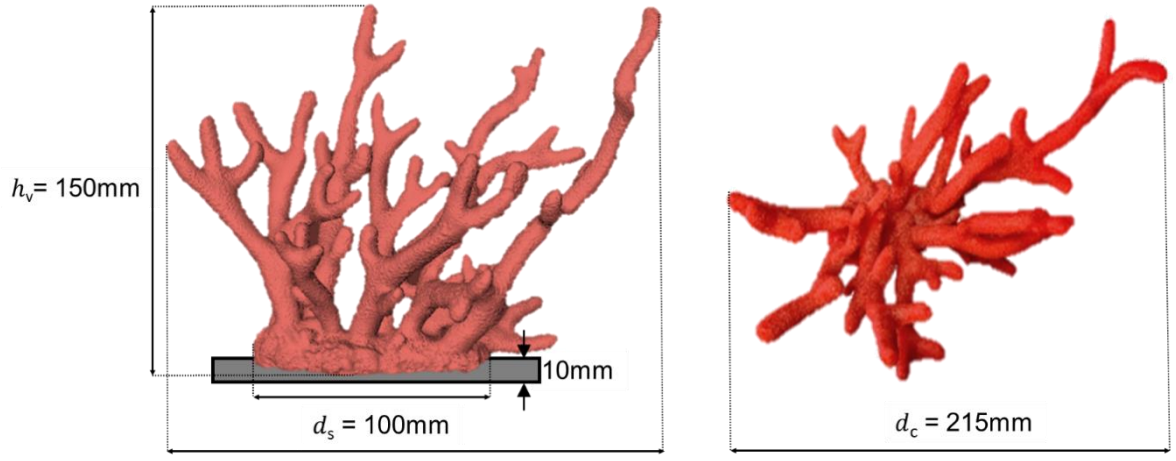


Figure 6.1: Diagram of the staghorn coral (*Acropora* genus) model attached to the baseboard

### 6.2.3 Flume setup, trials, and data acquisition

Microplastic fragment trapping by complex habitat structures was simulated in the Geomorphology and Hydrology Laboratory, University of Hull, using the combined wave-current flume of length 8 m, width 0.5 m, and height 0.5 m. Experiments were operated under unidirectional flow with a standing water depth of $(H_w)$ 0.40 m. With coordinate system $x, y, z$ whereby $x = 0$ at the upstream canopy front edge, and $y = 0$ at the baseboard top.

The retention of microplastics within each canopy was determined under four different bulk incoming velocities $U$ = 0.15, 0.2, 0.25, 0.3 m/s which have been observed in shallow coral reefs (Johansen, 2014). A set weight of fragments were tested per simulation: canopy type, and four flow velocities, resulting in 12 trials and subsequent trapping analysis in total. Before each simulation, the flume was run for 2 minutes to allow the flow to stabilise. Fragments were released with a siphon at a constant rate for 10 minutes submerged at the top of the water column under the surface. The distance of release depended on the flow speed but was tested prior to the experiments to ensure microplastics were in suspension when they entered the front of the canopy. Upon introduction of all microplastics, the flume was run for 1 hour, enabling assessment of transport rates and processes during this time. A net was located downstream of the canopy to capture any microplastics not trapped in the canopy and preventing them from being recirculated in the system (Fig. 6.2). Examples of the dense and sparse coral canopy set-ups are shown in Fig 6.3-6.5.

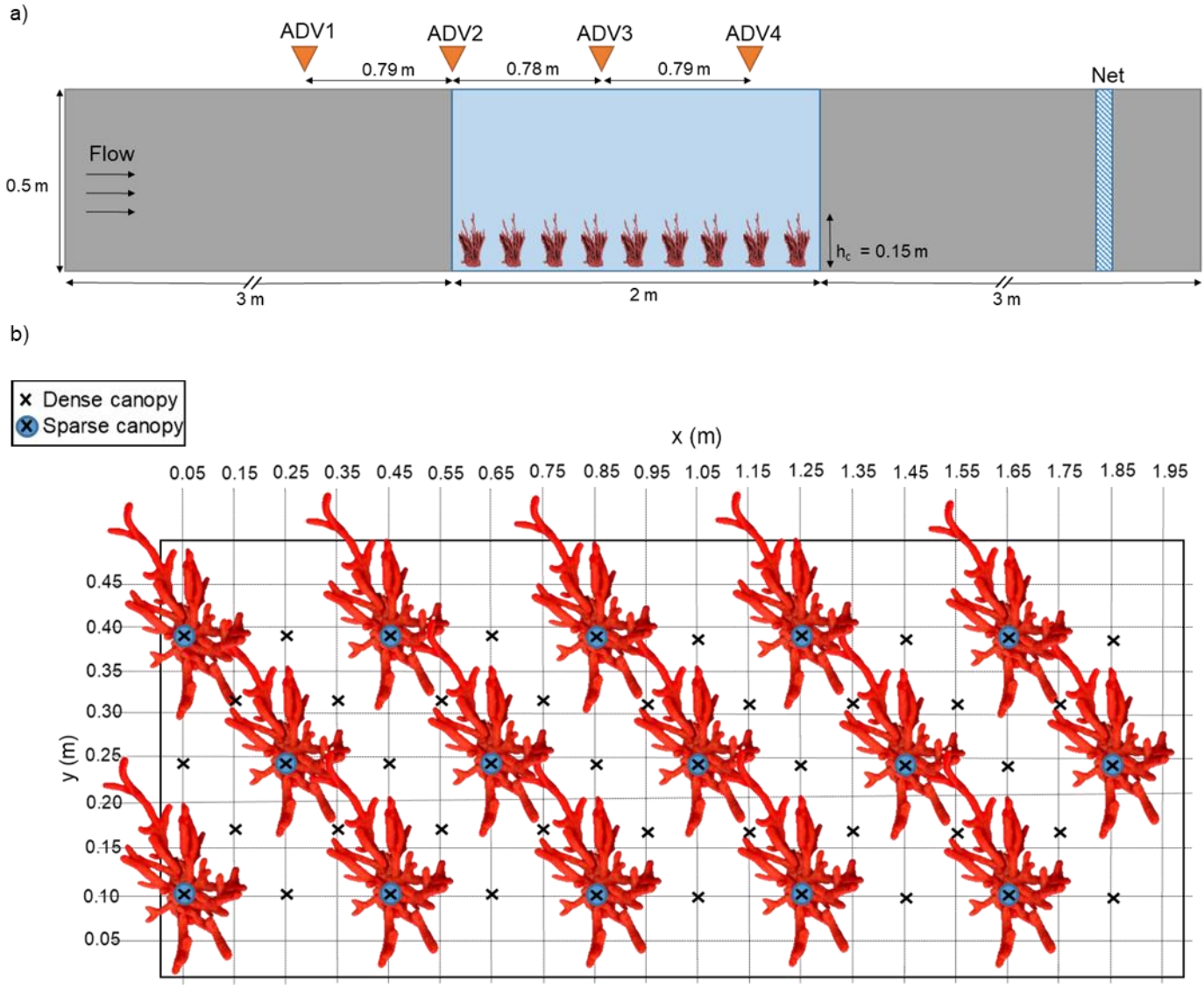


Figure 6.2: The flume setup: a) side view of the flume and test section containing the canopy. Four acoustic Doppler velocimeters (ADVs) were placed in the flume and a net to capture microplastics. b) The arrangement of sparse and dense corals within the canopy

To evaluate the distribution of microplastics under different scenarios, overhead and side images were also taken at the end of each run by overhead cameras at $x$ = 0.07 m, 0.9 m, and 1.7 m, and side cameras at $x$ = 0.12 m and 1.1 m. Flume sidewalls were lined black to increase the visual contrast of microplastics. Complementary manual measurements were recorded to validate the optical measurements and tracking. Following each run, the microplastics at the downstream net were collected, dried, and weighed to determine the percentage of microplastics that remain within the canopy under different flow regimes and

canopy densities. The microplastic particles that trapped within the test section were then collected, with the whole system cleaned before the next scenario was conducted.

To quantify the associated hydrodynamics, flow velocities were acquired using acoustic Doppler velocimeters (ADVs), (Nortek, Vectrino) using a sampling rate of 50 Hz for 5 minutes, upstream and evenly spaced throughout the test section. This was conducted separately from the microplastic data acquisition to avoid disruption to the flow field. Several branches were removed during the acquisition of velocity data in the dense canopy, as implemented in previous studies (Pujol *et al.,* 2012). It is acknowledged that this approach results in a slight modification to the flow structures but provides a primary fundamental quantification of flow properties in each canopy (Abdolahpour *et al.,* 2017). Velocity measurements were taken in front and throughout the canopy at $x$ = -0.78 m (ADV1), 0 m(ADV2), 0.79 m (ADV3), and 1.57 m (ADV4) (Fig.4.2); and at vertical positions of $z/h_c$ = 0.43, 0.57, 0.70, 0.90, 1.03, 1.17, 1.37, 1.57, 1.70, 2.03, 2.37, 2.57.

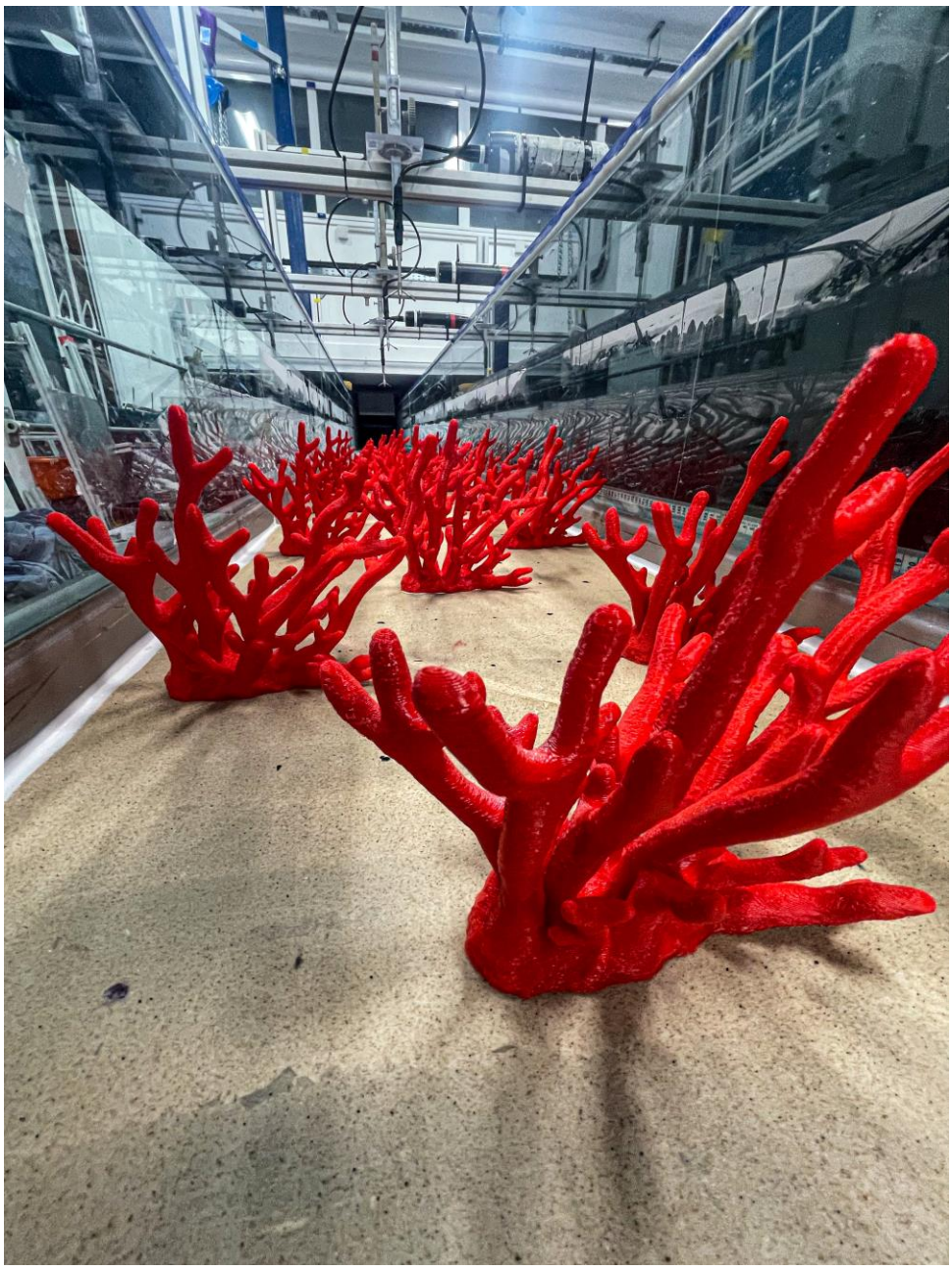

Figure 6.3: The flume setup of the sparse coral canopy

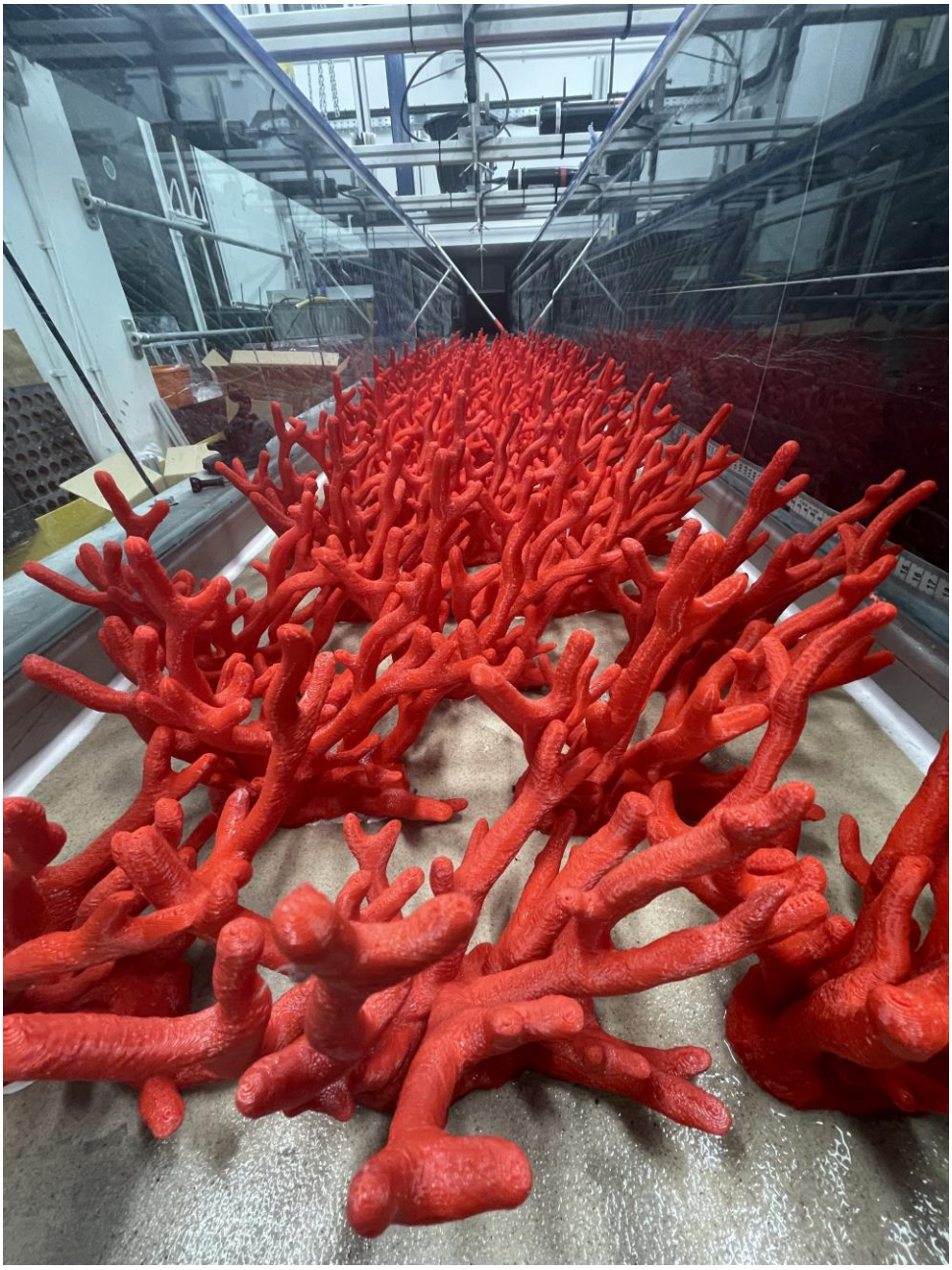

Figure 6.4: The flume setup of the dense coral canopy

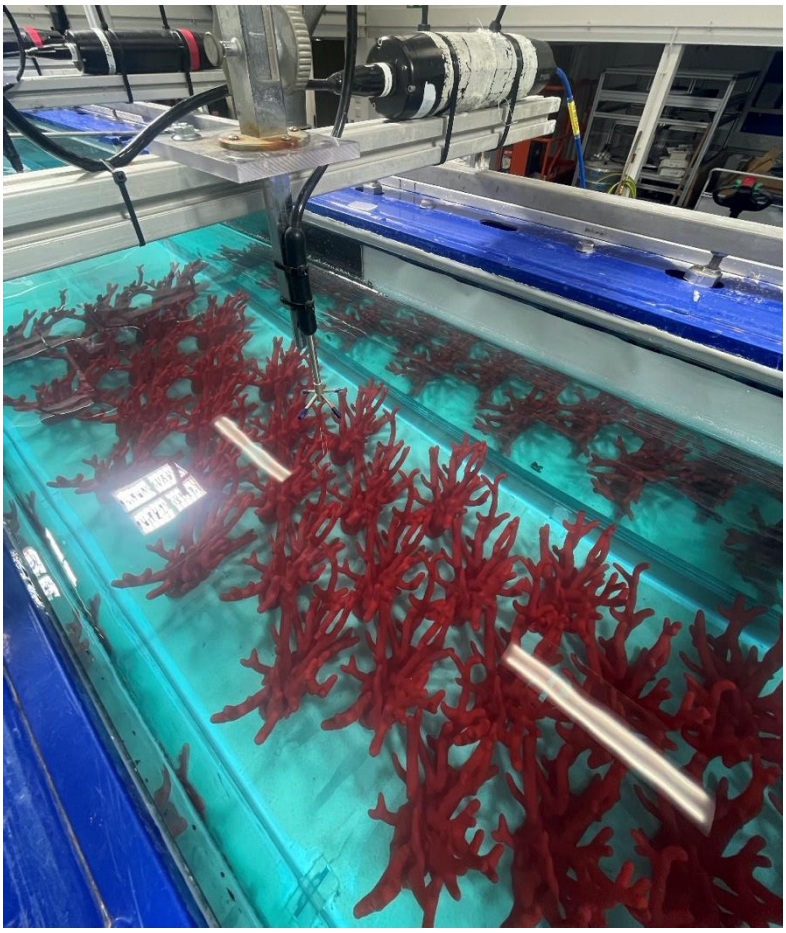

Figure 6.5: The flume setup of the dense coral canopy from above showing one of the ADCPs

## 6.3. Results

### 6.3.1 Microplastic trapping efficiency

When evaluating the results, the measurement of 1 hour must be considered when interpreting the percentage trapped within the canopy. The percentage trapped results allow comparison between the trapping efficiencies of each scenario tested but it must be noted that although microplastics appeared “trapped” within the canopy, particles might eventually move through after the 1 hour period. The amount of microplastics retained within the canopy after the 1-hour experimental duration varied depending on the canopy density and flow velocity (Fig.6.6). For the bare bed conditions, the majority of microplastics (99.2%) were trapped at 0.15 m/s, followed by 81.7% at 0.20 m/s. Trapping efficiency was similar at

0.25 m/s and 0.30 m/s at 13.0% and 10.4% respectively (Fig.6.6.a). For the sparse and dense coral canopies, the proportions of microplastic retained were comparative across velocities. At 0.15 m/s and 0.20 m/s trapping efficiency was very similar and substantial, with approximately 99% (ranging from 99.3-99.9%) for both sparse and dense canopies (Fig.6.6.b and c). At 0.15 m/s and 0.20 m/s, the dense canopy only retained 0.1% and 0.5% respectively more than the sparse canopy respectively**.** Trapping efficiency decreased slightly at 0.25 m/s with 92.3% of microplastics being captured for the sparse canopy and 97.7% for dense, with dense corals retaining 6.3% more than sparse. At 0.30 m/s the captured amount decreased again, with 79.3% of microplastics retained within the sparse corals while 94.4% within the dense. Dense canopies captured 18% more than sparse canopies at 0.30 m/s.

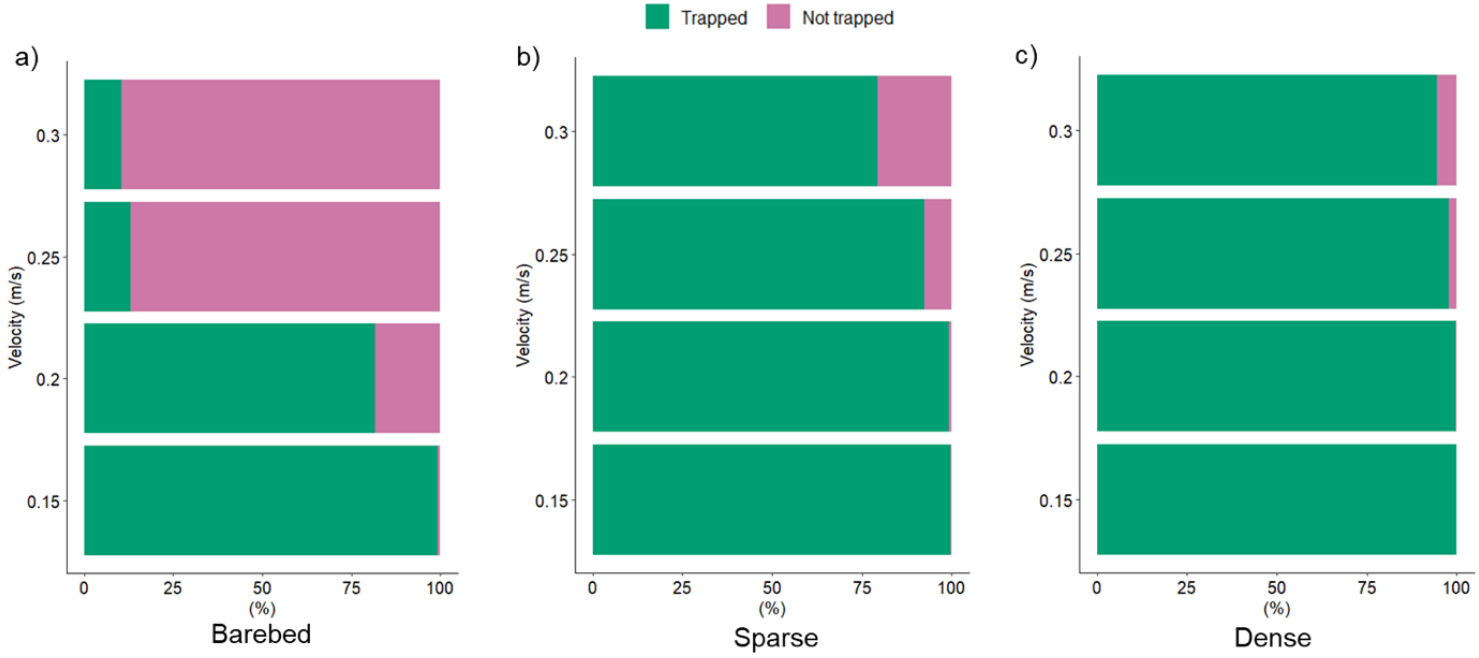


Figure 4.6: The amount of microplastic (%) trapped within each canopy: a) barebed b) sparse coral and c) dense coral and varying velocities from 0.15 to 0.30 m/s within the 1 hour test period

Yet, when looking at the distribution of microplastics within the canopies, patterns vary between sparse and dense. Figure 6.7 shows the distribution of microplastics for both coral canopies at the end of each experiment, with hashed areas representing high accumulation and smaller dots representing lighter deposition. For the sparse canopy, at 0.15 m/s the majority of microplastics are deposited within the first metre, with a large proportion collecting in the centre (Fig.6.7a). As velocity increases, the distribution gradually moves into the second meter. A large amount collects in the centre for both 0.20 and 0.25 m/s, whereas microplastics are more dispersed across the entire width of the canopy for 0.30 m/s. Microplastics also tended to collect behind the coral structures and occasionally on branches or within the coral structure itself, for example for 0.15 m/s at $x$ = 0.35 m (Fig.6.8a)

For the dense canopy, the majority of microplastics stayed within the first metre of the canopy despite an increase in velocity (Fig.6.7b). At velocities 0.15, 0.20, and 0.25 m/s, a large amount was retained within 0-0.75 m, whereas for 0.30 m/s the majority was dispersed within 0.5-0.25 m. Smaller amounts were distributed throughout the rest of the canopy at all velocities. A considerable amount of microplastics were observed to be collecting on the branches and within the coral structures (Fig.6.10a and b) and behind the corals for example at $x$ = 0.20 m (Fig.6.10c).

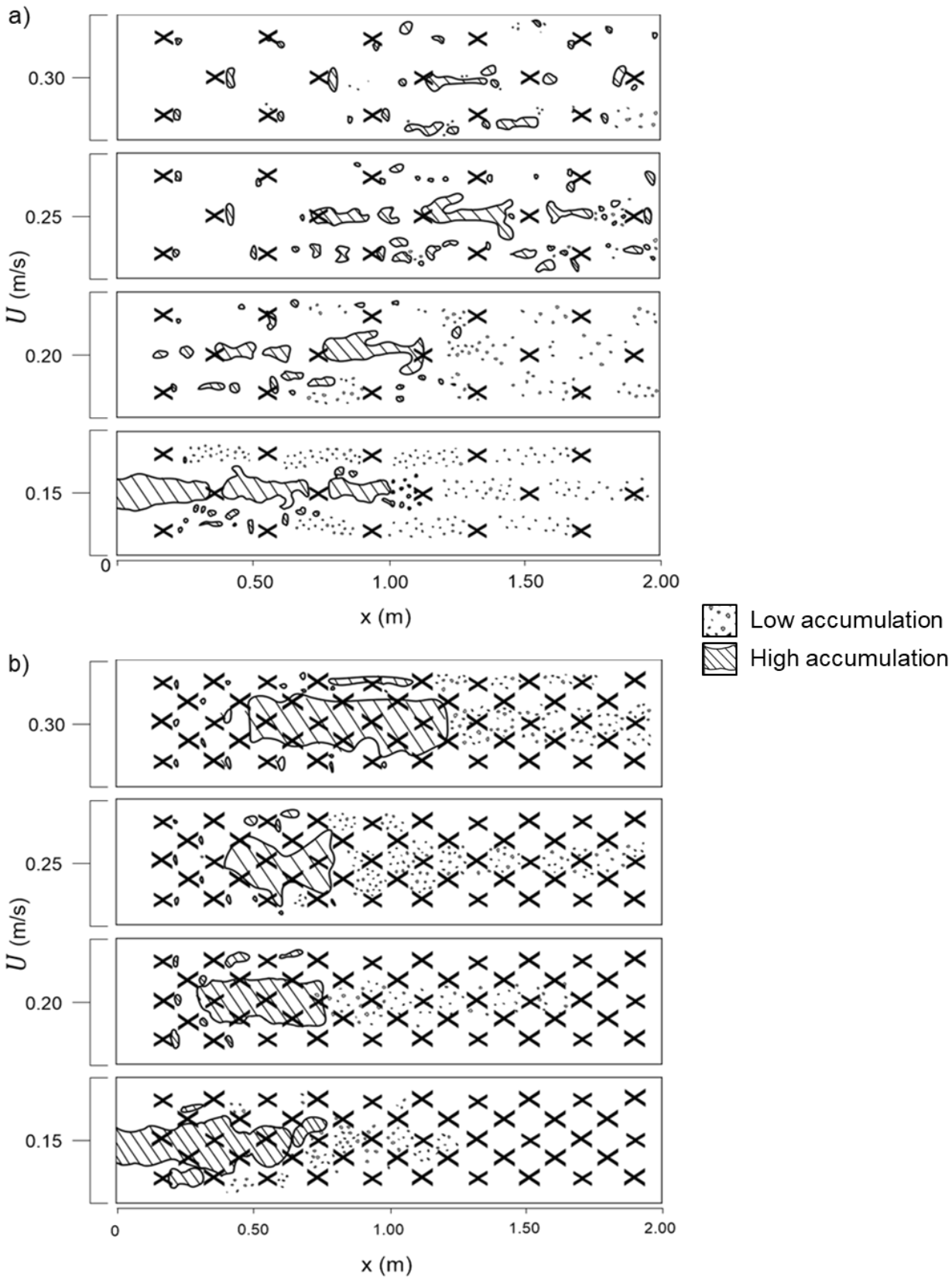


Figure 6.7: The distribution of microplastics within a) sparse and b) dense coral canopies at varying velocities. Each coral is represented by a cross. Produced from overhead photos taken at the end of each experimental run.

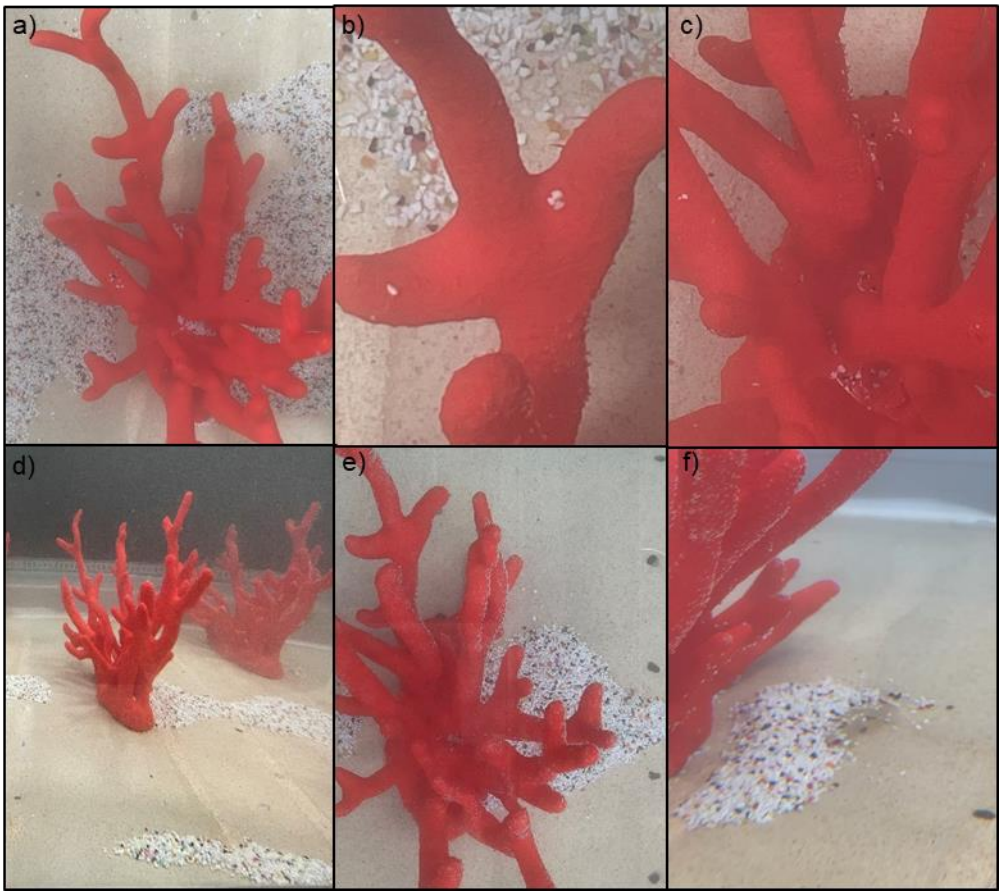


Figure 6.8: Examples of distribution of microplastics in the sparse canopy at a), b) and c) 0.15 m/s d) 0.20 m/s, e) 0.25 m/s and f) 0.30 m/s

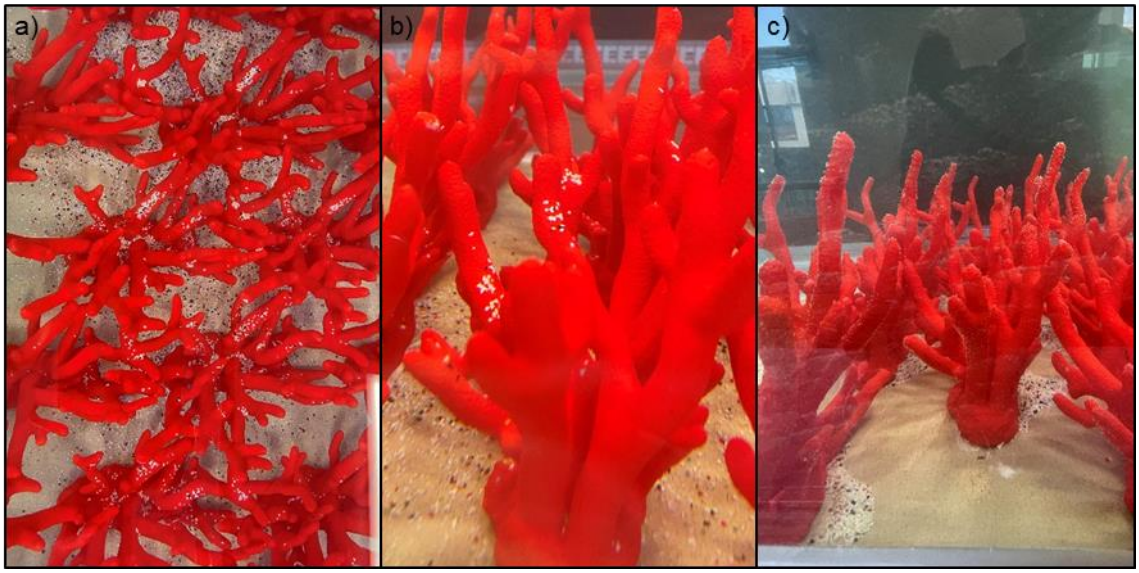


Figure 6.9: Examples of distribution of microplastics in the dense canopy at a) and b) 0.15 m/s and c) 0.20 m/s

### 6.3.2 Hydrodynamics

The relationships between the different canopies and flow hydrodynamics were quantified and explored by the acquisition of velocity profiles throughout the flume. This study forms part of a wider project on coral hydrodynamics and for the purposes of this research, only the streamwise velocities ($U$) are present, not the turbulence dynamics. Figure 6.10 presents the streamwise velocity profiles along the canopy, whereby before the canopy (ADV1, $x$ = -0.78 m) all velocity profiles for bare bed, sparse and dense canopies were very similar. Moving into the canopy, (ADV2, $x$ = 0 m) all profiles follow a logarithmic profile, with bare bed and sparse being very similar magnitudes while the velocity for the dense canopy is slightly slower towards the bed. Within the canopy, at ADV3 ($x$ = 0.79 m) the velocity profile for both coral canopies deviates considerably from the bare bed with a notable decrease in velocity within the canopy. Fig.6.11 shows profiles at 0.30 m/s for all canopies whereby the bare bed scenario was compared to the sparse and dense canopies at $x$ = 0.79 m. Sparse and dense canopy velocity profiles do differ from one another, with the sparse canopy velocity decreasing to negative values close to the bed. A similar pattern is seen for ADV4 at $x$ = 1.57 m, where sparse and dense velocity profiles deviated considerably from the barebed, but no negative velocity values are observed.

Figure 6.12 presents the mean streamwise velocity profiles for the sparse coral canopy, for each incoming bulk flow velocity tested. A free stream layer is present for all conditions at $z$ > 0.2, while the flow is reduced within the canopies, reaching near zero close to the bed ( z < 0.03), with slightly negative values in all cases. The flow velocity over the canopy is higher than the incoming bulk velocity in all scenarios with the increase being more pronounced at higher incoming bulk velocities, resulting in stronger velocity gradients.

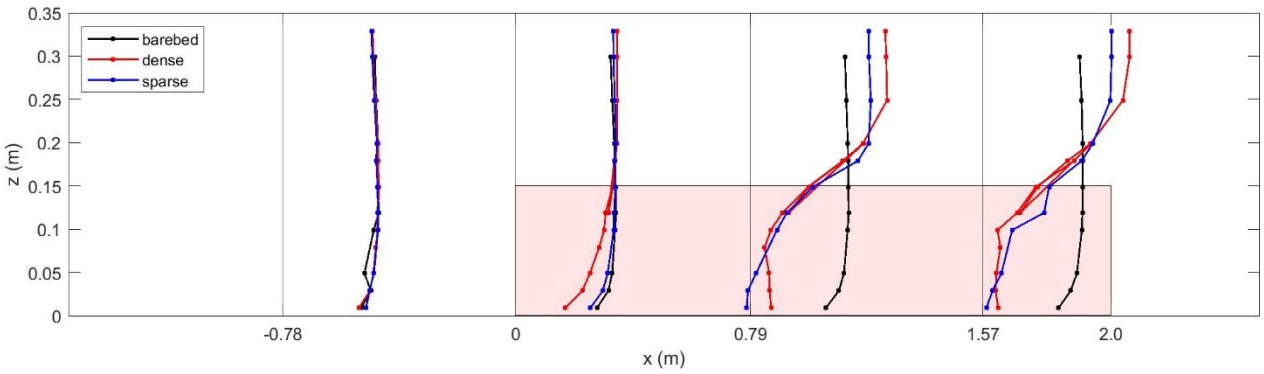


Figure 6.10: Velocity profiles at 0.30 m/s for barebed (black), sparse (blue), and dense (red) canopies throughout the flume. The red box indicates the canopy with 0m denoting the start of the canopy and flow moving from left to right. ADV1 x = -0.78 m, ADV2 x = 0 m (start of canopy), ADV3 x = 0.79 m and ADV4 x =1.57 m.

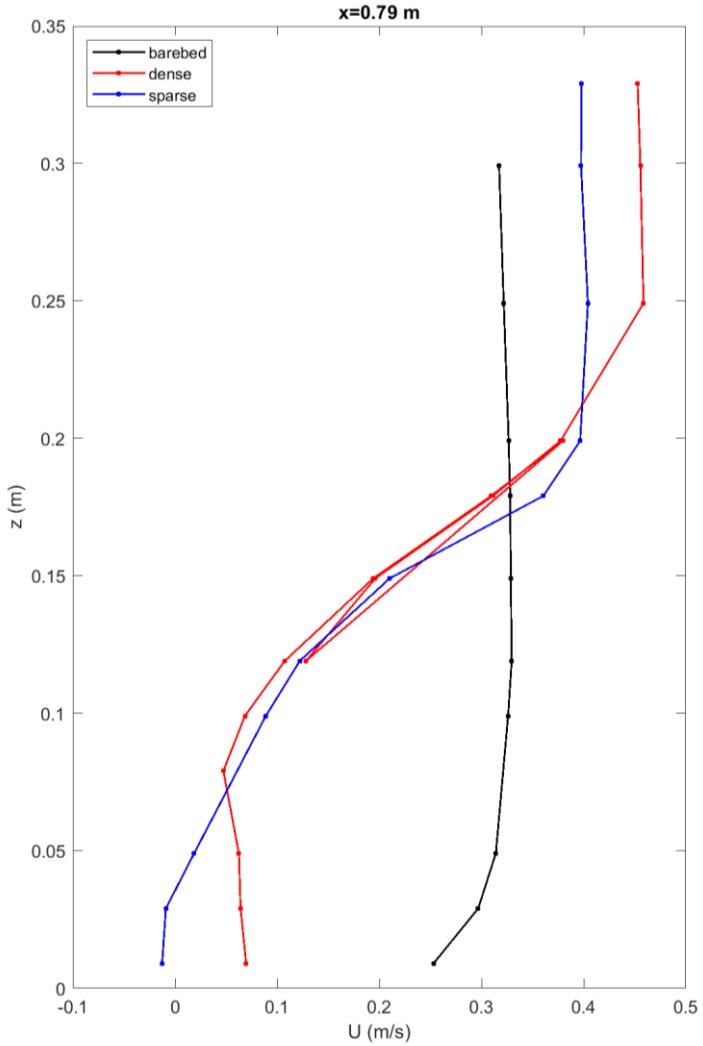


Figure 6.11: Velocity profiles of barebed (black), sparse (blue), and dense (red) canopies at x = 0.79 m (ADV3) for 0.3m/s.

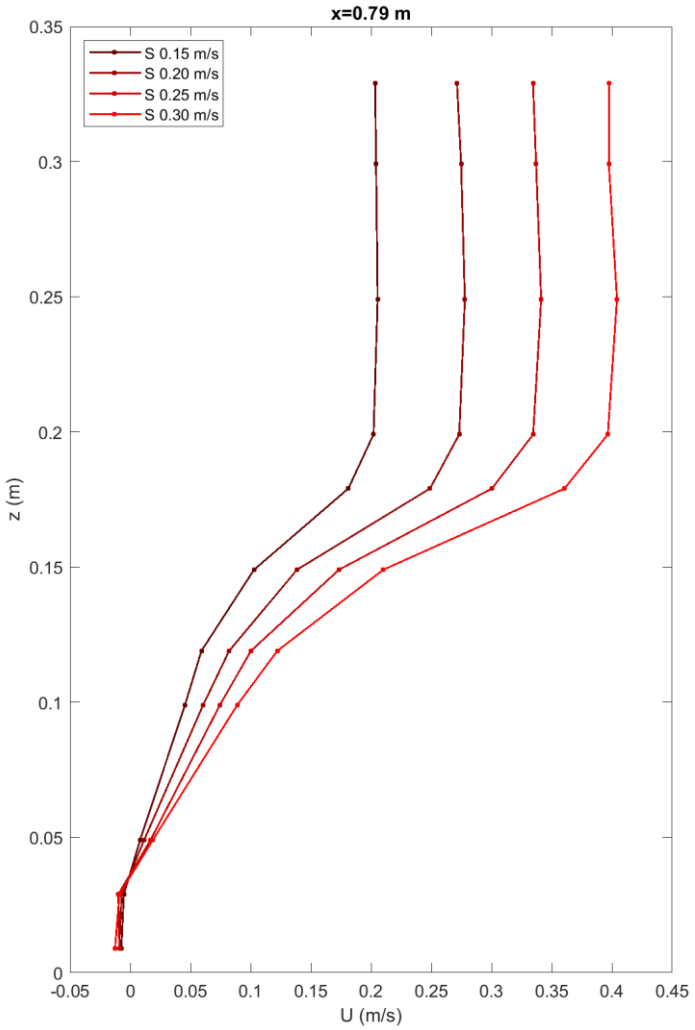


Figure 6.12: Velocity profiles of the sparse canopy at ADV3, x = 0.79 m within the canopy for the various bulk incoming velocities tested from 0.15-0.3 m/s.

## 6.4. Discussion

The monitoring of microplastic concentrations has been well documented, but fundamental knowledge gaps remain on the mechanisms that govern microplastic transport, accumulation, trapping, and fate within marine ecosystems (Reichert *et al.,* 2021; Zhang, 2017). Due to the hydrodynamics of the nearshore zone and biofilm growth altering particle density, microplastics from rivers and the coast (where most marine plastic originates) can be trapped and deposited within ecosystems such as coral reefs, making them a potential microplastic sink (Forsberg *et al.,* 2020; Jambeck *et al.,* 2015; Chapter 4). Coral reefs cover

approximately 250,000 $km^2$ worldwide and therefore may be acting as a major area of accumulation for microplastics (Burke *et al.,* 2011; Reichert *et al.,* 2021). We investigated for the first time the trapping mechanisms of microplastics by coral canopies under experimental conditions with a range of unidirectional flows. A staghorn coral was used as a model to represent variation in reef arrangements with sparse and dense canopies. Our experiments demonstrated how corals can act as a sink for microplastic pollution under a range of conditions. The hydrodynamics that drives these trapping mechanisms were also investigated, highlighting the energy-dissipative effects of reefs. However, even sparse canopies can trap a considerable amount of microplastics, which has implications for wider reef ecosystems, and ecological risk must be assessed within the context of these results.

### 6.4.1 Microplastic trapping mechanisms

In our study, up to 99% of microplastics were captured by both sparse and dense coral canopies after 1 hour, but this did vary with flow velocity and canopy density (Fig.6.6). The dense canopy was able to capture 18% more than sparse canopy at 0.30 m/s but only 0.1% more at 0.15 m/s. Furthermore, the distribution within the canopies differed with coral density and velocity (Fig.6.7). Several trapping mechanisms were identified in coral structures and include; a) particles interception with the coral and settling to the bed, with the coral acting as a barrier; b) microplastics settling on to the branches of the coral or becoming trapped within the coral structure itself and c) accumulation in the downstream region of individual corals. A reef may therefore increase the residence time or trapping efficiency of a microplastic rather than fully capturing it and stopping its trajectory. From our experiments, we conclude that the trapping efficiency is larger at slower velocities and denser coral arrangements. This supports previous work where seagrass canopies were shown to have a greater probability of trapping microplastics at lower velocities and higher shoot density (de los Santos *et al.,* 2021b). Sparse seagrass meadows were able to retain microplastics too, with trapping increasing with canopy density but not linearly which is supportive of our

findings here, as particle retention did not increase in direct proportion to an increase in flow velocity (de los Santos *et al.,* 2021b). However, the retention and trapping of microplastics was dependent on polymer type, with less dense particles such as polystyrene more likely to escape the canopy at higher velocities compared to more dense polymers (de los Santos *et al.,* 2021b). This emphasises the need to consider multiple types of polymers in experimental studies.

Corals have previously been shown to trap considerably more microplastics due to their structural complexity and rough surface compared to other habitats such as macroalgae and seagrass (de Smit *et al.,* 2021; Jeyasanta *et al.,* 2020). Other important benthic habitats including saltmarshes and mangroves that provide invaluable ecosystem services have also been identified as having a high capacity for accumulating microplastics (Cozzolino *et al.,* 2020; de Smit *et al.,* 2021; Garcés-Ordóñez *et al.,* 2019; Huang *et al.,* 2020; Martin *et al.,* 2019b; Zhou *et al.,* 2020). The results presented herein demonstrate that the trapping efficiency of both sparse and dense corals is considerable. Furthermore, as microplastics were observed to settle on the branches and within coral (Fig 6.8 and 6.9), it can be assumed that the coral organism will interact with microplastics. Therefore, the behaviour of live coral in response to microplastics must also be considered when determining trapping efficiency. For example, the role of adhesion to biogenic habitats such as seagrass leaves has been identified as an important capture mechanism (Agawin and Duarte, 2002; Goss *et al.,* 2018). This has also been observed for corals, where adhesion aided in removing microplastics from the water column, capturing up to 40 times more particles than suspension feeding by corals (Corona *et al.,* 2020; Martin *et al.,* 2019b). Other studies support passive removal as the primary mechanism for trapping, which was observed here, but emphasise that increased deposition is the main retention process, causing bed sediment to become a major microplastic sink (Corona *et al.,* 2020; de Smit *et al.,* 2021; Utami *et al.,* 2021). This has been confirmed by field studies, with sediments adjacent to reefs identified as major accumulation sites of microplastics, due to the mixing

and bioturbation of organisms such as bivalves (Jeyasanta *et al.,* 2020; Näkki *et al.,* 2017; Utami *et al.,* 2021). However, adhesion may also encourage deposition whereby mucus production on the coral surface traps and carries particles to the reef sediments (Utami *et al.,* 2021; Wild *et al.,* 2004). Where cleaning mechanisms have proven ineffective, corals have been observed to overgrow microplastics (Reichert *et al.,* 2018). Therefore, passive processes, especially deposition, provide higher trapping efficiencies compared to active ingestion alone (Martin *et al.,* 2019b). This is supported by our study, which demonstrates that the majority of microplastics were deposited due to corals acting as a barrier. However, the combination of passive and active trapping mechanisms must be considered, and require more investigation which is discussed below, especially as corals screen large volumes of water through suspension feeding (Reidenbach *et al.,* 2006). Our results may therefore underestimate the trapping efficiency of corals, as other capture mechanisms will be present for live organisms, although this will be dependent on environmental conditions.

The impacts of varying densities of canopies must also be considered. Previous studies have observed no difference in microplastic retention between seagrass and unvegetated areas, while other observations have seen a larger accumulation in meadows compared to bare bed conditions, which may be explained by differences in canopy density and flow dynamics (Cozzolino *et al.,* 2020; Huang *et al.,* 2020). Our study supports the latter, with high microplastics trapping efficiency in sparse and dense canopies compared to the bare bed. This highlights the importance of considering the patchiness of canopy density *in situ* which will alter trapping efficiency and could be tested in future studies.

### 6.4.2 Canopy hydrodynamics

Aquatic vegetation is known to alter the hydrodynamics of coastal environments, influencing turbulence and mixing processes and therefore must be considered here as will influence the trajectory of microplastics (Nepf, 2012; Waycott *et al.,* 2009). Hydrodynamics has been identified as a key driver to determine the accumulation of microplastics in various vegetated

coastal ecosystems (de los Santos *et al.,* 2021). The velocity profiles presented here are part of a wider project that will investigate the influence of hydrodynamics on microplastic distribution in more detail. For the purpose of this study, we offer insights into the influence of hydrodynamics on trapping efficiency such as changes in streamwise velocity within the canopy, but more detailed analysis is needed. While one bulk incoming velocities had been shown here, comparable patterns are seen across all the incoming velocities tested (for example Fig.6.12).

Based on Lowe et al. (2005) flow velocity is attenuated within a canopy and as corals form very complex three-dimensional structures, they reduce water turbulence (Moberg and Folke, 1999; Lowe *et al.,* 2005). Before the canopy section (ADV1), the incoming flow was comparable for all scenarios (Fig. 6.10)**.** However, it was expected that the higher-density canopies would result in lower in-canopy streamwise velocities compared to sparse corals. This was observed at the front of the dense canopy (ADV2) and can be associated with the greater drag imposed by the larger frontal area (Nepf, 2012). The subsequent slower velocities near the dense canopy front provide a reasonable explanation for the bulk of microplastics being deposited in the first meter of the canopy (Fig.6.7b). However, it must be noted that this is a temporal process and that this study only ran scenarios for 1 hour. Therefore, microplastics may eventually move through the canopy and this should be taken into account.

Further into the canopy (ADV3), flow adjustment was observed due to both canopies, where the streamwise velocities of both sparse and dense decreased (Fig 6.10 and 6.11). The streamwise velocity profiles for both canopies differed notably from the barebed, characterised by lower velocities within the canopy and higher velocities above the canopy. Sufficient drag can be imposed by the canopy to force the incoming flow over the canopy (Houseago, 2021; van Wiechen, 2020b). The decrease in streamwise velocity within the canopies can be explained by a developing shear layer above the canopy which contains large-scale vortices and causes an increase in turbulent kinetic energy (TKE) (Lefebvre *et*

*al.,* 2010). This in turn can cause flow instability and the formation of a mixing layer and is indicated by the presence of the inflection point in the velocity profiles (Ghisalberti, 2002). Within the canopy, velocities are reduced and the dissipation of energy results in the production of TKE determined by the canopy properties (Nepf, 1999). These processes have previously been identified to be fundamental to sediment mobility and could be applied to microplastics (Lefebvre *et al.,* 2010; Tinoco and Coco, 2016). As microplastics had already begun to settle when they entered the canopy, they were likely to have avoided the developing mixing layer and instead be slowed down by the overall reduction in flow velocity caused by the presence of the canopy.

Areas of accumulation occurred within both canopies but varied depending on density and velocity. For the sparse canopy, microplastics tended to accumulate on the lee side of individual corals, especially in the centre (Fig. 6.7a). Negative velocities are recorded for the sparse canopy (ADV3), (Fig 6.10 and 6.8) which supports the retention of microplastics in the middle of the canopy and behind the corals (Fig 6.7a). This may be explained by the development of a horseshoe vortex around the base of corals preventing the movement further downstream (Link *et al.,* 2012)**.** On the other hand, for the denser arrangement, although particles still accumulated downstream of the individual corals, microplastics were more dispersed within the canopy, with a higher abundance of particles collecting on the branches and within the coral structures. This further highlights the need to consider the arrangement of corals within a canopy as it appeared that for the sparse canopy, individual corals were impacting the settling of microplastics independently whereas for the dense canopy the impacts were due to interactions of multiple corals as they were closer together. At the end of the canopy (ADV4), the flow seems to have stabilised which can be explained by the increase in distance from the canopy front, which causes streamwise velocity impacts.

Furthermore, microplastic trapping recorded in corals presented may differ from some natural environments as the bi-directional effects of waves were not tested, which are

known to produce different near-bed turbulence dynamics. Waves may prevent sedimentation and increase the chances of resuspension which would either cause more particles to become trapped in a coral structure from the seabed, or result in a reduction of microplastic capture as particles move into the water column (de Smit *et al.,* 2020). There is a strong need to conduct comparable experiments under wave-driven flows. In addition, other complex variables that exist *in situ* on coral reefs must be assessed such as the influence of tides and the ecological interaction with reef organisms.

### 6.4.3 Ecological risk

Coral reefs support a large amount of biodiversity, the livelihoods of more than 500 million people worldwide, and provide invaluable ecosystem services such as coastal protection (Corona *et al.,* 2020; Fisher *et al.,* 2015; Hughes *et al.,* 2017). Exposure of reefs to microplastics can occur in several ways, especially at low tide, and therefore of increasing concern (Hall *et al.,* 2015). Our experiments demonstrate how the structure of a coral reef can retain a considerable amount of microplastics through passive microplastic uptake due to their structural complexity, especially at slower flow velocities and high coral density. This trapping of microplastics will make particles more bioavailable to reef organisms. Structural complexity and rigidness is also an important feature for coastal protection, meaning these valuable ecosystems and their services are threatened by accumulating microplastics and their associated risks (Bouma *et al.,* 2005; Graham and Nash, 2013; Heck Jr. *et al.,* 2003; Lefcheck *et al.,* 2019). However, the active uptake of microplastics (ingestion) by corals and reef organisms may also be contributing to the role of reef ecosystems as long-term microplastic sinks. The ecological implications of this must be considered in terms of threats to the reef and associated organisms' health.

Microplastics have been identified *in situ* in the water of reefs throughout the tropics including the South China Sea, the Maldives, the Great Barrier Reef, and the coast of India (Ding *et al.,* 2019; Hall *et al.,* 2015; Y. Huang *et al.,* 2021; Saliu *et al.,* 2018; Tan *et al.,* 2020;

Vidyasakar *et al.,* 2018; Zhang *et al.,* 2019). As shown by our experiments, microplastics in the water column of a reef are shown to come into physical contact with the corals. A considerable amount of microplastics were observed on the branches and within the coral structure, especially for the dense canopy and lower velocities. Corals are unselective suspension feeders which tend to ingest particles in the range of 0.2-1,000 µm and therefore can accidentally ingest plastic particles (Anthony, 1999; Hall *et al.,* 2015). Indeed there is growing evidence that corals do ingest microplastics which can result in several damaging impacts including reduced photosynthetic ability, feeding, growth, and survival (Allen *et al.,* 2017; Chapron *et al.,* 2018; Hall *et al.,* 2015; Mendrik *et al.,* 2021; Reichert *et al.,* 2019, 2018). However ingestion/egestion rates differ between species and long-term exposure impacts are mostly unknown (Martin *et al.,* 2019b; Utami *et al.,* 2021). In addition, ingested microplastic can get stuck within gastrovascular cavities, with particles being found within coral skeletons and tissues due to translocation during growth, resulting in permanent accumulation (Hierl *et al.,* 2021; Krishnakumar *et al.,* 2021; Reichert *et al.,* 2018; Rotjan *et al.,* 2019). Furthermore, overgrowth and encrustation of adhered microplastic can occur (Hierl *et al.,* 2021; Reichert *et al.,* 2018)**.** As such, there is a high indication from the results presented that coral reefs will be exposed to and may accumulate microplastics, and therefore associated uptake and impacts could occur. This shows how the active uptake of microplastics is also an important factor to consider in long-term microplastic sinks, yet ecological implications may be considerable.

The decrease in coral health due to microplastic exposure will not only affect corals but may potentially influence the entire reef ecosystem. The structural complexity of a coral reef supports abundant and diverse fauna, facilitating survival, especially reef fish, by providing refuge spaces and nursery grounds (Baalkhuyur *et al.,* 2018; Graham and Nash, 2013). As we concluded that denser reefs will be more likely to trap microplastics and retain a larger quantity, these areas with higher biodiversity will be more at risk. Further environmental consequences include accidental ingestion by reef organisms and the spread

of disease, especially if waves continue to cause resuspension (de los Santos *et al.,* 2021b; Lamb *et al.,* 2018). Microplastics have been observed in several reef fish which may have occurred through grazing on the epilithic algal matrix covering corals that had captured particles (Baalkhuyur *et al.,* 2018; Wilson *et al.,* 2021). Our observations demonstrate that microplastics can settle onto coral branches and therefore incorporation into the algal matrix is likely to occur. Bioaccumulation of microplastics can also arise through the food web (Murray and Cowie, 2011).

However, it appears more microplastics have been found within reef sediments than in the water, supporting our results that corals increase particle settling (Jeyasanta *et al.,* 2020). Although this may reduce exposure to certain reef species, benthic fauna such as deposit and detritus-feeding organisms may be more at risk and must be investigated (Wright *et al.,* 2013). Sea cucumbers, gastropods, and sea urchins have been observed to accumulate environmental microplastics but the full repercussions to the entire reef system are unknown and require further work (Sayogo *et al.,* 2020; Sweet *et al.,* 2019; Tahir *et al.,* 2020). This highlights how due to the high trapping efficiency of coral reefs, a complete environmental assessment of the impacts of microplastics on these ecosystems is needed.

## 6.5 Conclusion

This study has examined the trapping efficiency of coral canopies, one of the most important biodiverse ecosystems globally, in relation to coral density, hydrodynamics, and potential ecological risk. Here, it was demonstrated that the trapping efficiency of coral canopies varies due to bulk velocity and canopy density. However, even sparse arrangements of corals can retain a considerable amount of microplastics. Trapping mechanisms by coral canopies were identified and include: a) interception of particles with the coral acting as a barrier and microplastics and settling to the bed; b) settling of microplastics on the branches or within the structure of the coral and becoming trapped, and c) accumulation in the downstream region of individual corals. Spatial variation of microplastic distribution occurred

due to different scenarios. For example, the majority of microplastics settled within the first meter of the test section for dense canopy while microplastic distribution was more varied within the sparse canopy. Furthermore, we provide evidence that trapping efficiency is driven by the dissipative effects of complex coral structures, yet the arrangement of corals within the canopy is expected to play a large role in microplastic fate as structures may cause cumulative impacts of flow dynamics.

Due to these findings, it can be speculated that coral reefs may form a sink for microplastic pollution through their observed high trapping efficiency of microplastics that may otherwise have been transported greater distances in the water column. However, as denser reefs with more structural complexity are linked to both higher biodiversity and microplastic trapping efficiency, the implications for entire reef systems and the associated ecosystem services and communities that rely on reefs worldwide must be assessed in future research. This study provides insights into how coral reefs can act as a considerable area of accumulation for microplastics and therefore their role in the “missing” plastic problem.

Although this study provides the first insight into the trapping mechanisms of corals, there remain several knowledge gaps. The arrangement of corals *in situ* will include greater spatial heterogeneity and patchiness in addition to containing a wide variety of different species with various morphologies. This will alter the structural impact on flow dynamics and therefore the deposition of microplastics. The influence of waves and tides must also be considered. Future work should test a wider range of polymer types with different densities and various shapes such as fibres and films as this will influence the eventual fate in reef environments. Furthermore, the trapping efficiency should be tested over longer periods of time to fully assess the role of coral reefs as microplastic sinks.

[Page intentionally left blank]

# Chapter 7.

# Synthesis and Conclusions

## 7.1 Introduction

The research presented above sought to understand and determine the key controlling factors that influence microplastic fate in aquatic environments. In this section, each of the substantive elements of the research are revisited with the key findings reaffirmed before the outcomes are thematically synthesised in a holistic manner.

Initially, novel settling experiments were performed to demonstrate the density-driven influence of biofouling and salinity on microplastics (Chapter 4). The transport dynamics of microplastics in the Mekong River were then analysed with fieldwork and in relation to fluvial hydrodynamics and vertical distributions of plastic flux in full-scale riverine flows (Chapter 5). Finally, the trapping efficiency of coral reefs was assessed to highlight the influence of aquatic canopies on trapping and settling in regard to microplastic fate (Chapter 6). This chapter forms links between these three substantive studies presented in Chapters 4, 5 and 6. The research advances are synthesised into main components: 1) the transport dynamics of aquatic microplastics (§7.2), 2) the relation to sediment transport (§7.3) and 3) the ecological risk (§7.4). The implications of these advances in scientific knowledge are referred to throughout. Future research directions are discussed in §7.5 and finally, an overall thesis summary centred on the initial research aim and questions is detailed in §7.6.

## 7.2 Transport dynamics of aquatic microplastics

Currently, the global load of plastics floating on the ocean surface is much lower than expected (Cózar et al., 2014; Eriksen et al., 2014). It is widely recognised that land-based sources, including mismanaged waste, have resulted in rivers becoming a major conveyor of

plastic pollution to the marine environment (Jambeck *et al.,* 2015; Lebreton *et al.,* 2017). As microplastics move from a riverine to a marine environment, they will undergo a series of biological, physical and chemical transitions such as changes in salinity gradients, suspended sediment concentrations and fluctuations in turbulence. Settling of microplastics is initially governed by the properties of the particle including size, shape and density but once a plastic particle enters an aquatic system, a biofilm will begin to form within minutes to hours (Zettler *et al.,* 2013b; Amaral-Zettler, *et al.,* 2020). Interactions with physical structures formed by aquatic ecosystems must also be considered which could intercept the particle trajectory and cause accumulation.

Previous work has evaluated the settling behaviour of microplastics, yet experiments often use particles that are not representative of plastics released and present in the environment, i.e. clean and of regular shapes (Khatmullina and Isachenko, 2017; Kowalski *et al.,* 2016; Möhlenkamp *et al.,* 2018; Waldschläger and Schüttrumpf, 2019). In regards to the general movement of microplastics from source to sink, although the frequency of riverine studies has increased, fieldwork continues to dominate in the marine environment with sampling mostly occurring at the surface of the water column or bed sediment. This fails to quantify microplastics that do not float or completely settle and therefore underestimations of microplastic concentrations are expected. Furthermore, the role of complex coastal ecosystems such as coral reefs in the trapping and eventual sinking of microplastics that are moving from rivers to the ocean has been overlooked. To understand these processes, this thesis used experiments (Chapters 4 and 6) and fieldwork (Chapter 5) to assess the transport dynamics of aquatic microplastics, which are summarised in Figure 7.1.

First, using novel settling experiments, it was shown that multiple environmental and biological conditions influence microplastic transport dynamics (Chapter 4). Here, it was demonstrated that biofilm growth is the main factor influencing microplastic settling (average 40% increase in settling rate) across a range of salinities that would occur as a particle moves from fluvial to marine systems (SAL0-30) (Fig.7.1). In addition, the impacts of

biofouling were shown to take effect typically within a week (§4.3.2, Fig.4.4). The influence of biofouling was due to an increase in particle density rather than encouraging aggregation and increase in particle size. Although the impacts of biofilm growth on microplastic settling have been observed before (Hoellein et al., 2019; Kaiser et al., 2017; Morét-Ferguson et al., 2010), it has not previously been shown to play a dominant role in influencing microplastic settling across the freshwater-marine transition. Settling dynamics did differ across the range of salinities, with the rate of settling depending on microplastic polymer and shape; for example, the impacts of biofouling on microplastic settling are not as extreme for fibres and may be due to their shape. The impacts of varying suspended sediment concentrations were also tested, as it was expected that aggregation of particles would occur as concentrations increased. Although no flocs were observed, increasing sediment concentrations did result in a decrease in settling for some polymers perhaps through abrasion. This emphasises the need to consider a range of conditions that will influence microplastic transport dynamics in specific situations and management practices.

These experiments further highlighted the need to consider the entire water column when predicting microplastic transport dynamics, as settling regimes vary for different particles under various conditions. As a result, different particles are expected to be found in different portions of the water column. As rivers have consistently been identified as important conveyors of plastic to the ocean, the transport dynamics of microplastics within them must be fully understood (Jambeck *et al.,* 2015; Lebreton *et al.,* 2017; Schmidt *et al.,* 2017). Therefore, to understand the transport of microplastics within a major river, field sampling was conducted aimed at capturing particle distribution throughout the water column and across a range of urban and rural locations (Chapter 5). It was found that higher microplastic concentrations did occur in more urbanised areas, but the majority of microplastics (on average 86%) were located below the water surface (>2 m depth). Results from the settling experiments (Chapter 4) suggest that clear patterns of microplastic dispersion due to polymer types, such as a higher abundance of denser polymers with

increased depth would be expected. However, this was not observed and can be explained by the turbulent structures within the flow causing resuspension and mixing. The importance of hydrological regimes was also highlighted. When this study was compared to Haberstroch *at al.,* (2021) in the same region, it is clear that microplastic concentration decreased with increasing discharge (Fig.7.1). This demonstrates that transport dynamics are influenced by a complex range of mechanisms and that sampling should not just occur at the water surface or during high flow as this can vastly under-predict microplastic abundance. This has been shown for studies of microplastics on channel beds and the water column at the same locations where abundances differ greatly (Woodward et al., 2021).

Finally, when microplastics are discharged from river systems into the marine environment, they may pass through a number of aquatic ecosystems that form complex structures such as seagrasses, mangroves and coral reefs. The influence of vegetation and canopies on microplastic transport dynamics must be considered, especially in coastal areas where the majority of the influx of plastic pollution is passing. Few studies have been conducted that quantify microplastic trapping in seagrasses or by single structures of macroalgae and corals (de los Santos *et al.,* 2021a; de Smit *et al.,* 2021). Experiments to determine the role of coral reefs on microplastic transport dynamics and trapping were therefore conducted (Chapter 6). Sparse (15 corals) and dense (45 corals) canopies were able to retain high quantities of microplastics (up to 99% over 1-hour Fig.6.3). Trapping efficiency was dependent on flow velocity and canopy density, with slower velocities and denser coral arrangements retaining more microplastics. Surprisingly, the difference between sparse and dense trapping efficiency was not large, with the dense canopy capturing 18% more microplastics than the sparse canopy at 0.30 m/s but only 0.1% more at 0.15 m/s. The trapping efficiency was assessed in relation to the influence of the canopies on hydrodynamics, which could explain the trapping mechanisms observed. Overall, lower streamwise velocities were seen within the canopies and were associated with the greater drag caused by the larger frontal area (Nepf, 2012). This demonstrated the influence of

corals on the transport dynamics of microplastics and the high trapping potential of reefs (Fig. 7.1). It is therefore expected that corals may be acting as a substantial, previously unquantified, area of accumulation and sink for microplastic pollution.

In summary, this research presents new insights into several of the transport dynamics of microplastics that must be considered when predicting microplastic fate in aquatic environments (Fig.7.1). The combination of these mechanisms allows a greater understanding of the transport of microplastics from riverine to marine environments in a holistic manner.

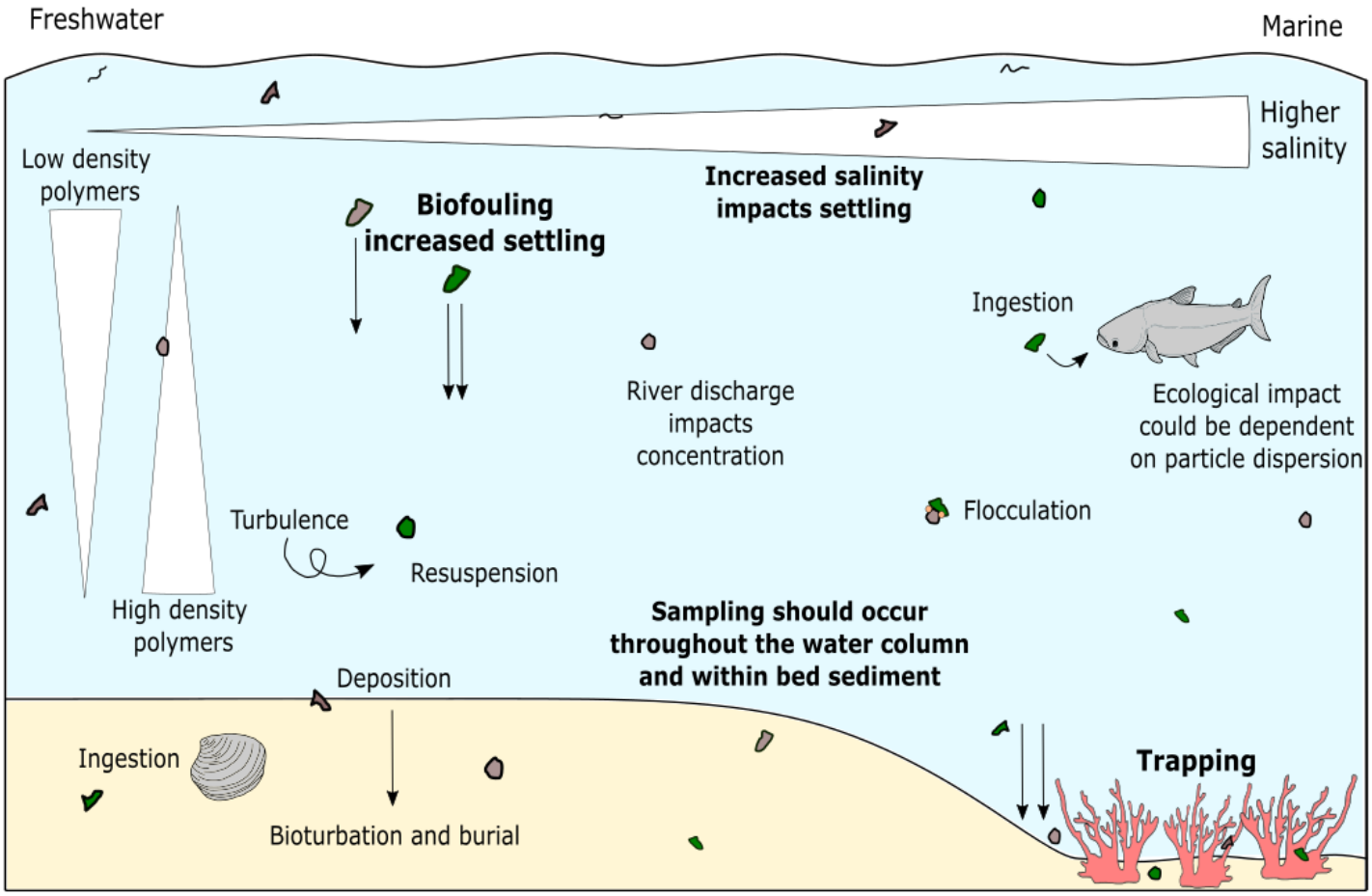


Figure 7.1: The multiple transport mechanisms of microplastics in aquatic environments that were investigated in this thesis. Mechanisms include particle density, biofouling, biological interaction (ingestion), turbulence, salinity, river discharge and trapping in aquatic canopies. This highlights the need to sample throughout the water column and within sediment to fully understand microplastic concentrations, in addition to ecological impact, adapted from Waldschläger *et al.,* (2022).

## 7.3 Relation to sediment transport

It has often been argued that microplastics in aquatic environments will behave in a similar way to natural sediments and therefore fundamental knowledge about sediment transport can be transferred to microplastic fate (Enders *et al.,* 2019; Waldschläger *et al.,* 2022). This has resulted in theoretical foundations on natural sediments being utilised to form predictions of the transport of aquatic microplastics (Horton and Dixon, 2018). However, it has been identified that although sediment dynamics can help in the basic understanding of microplastic transport, more knowledge specific to microplastics is necessary to improve predictive capacity (Waldschläger *et al.,* 2022). Many aspects of this research support this statement and are discussed briefly below.

First, within the settling experiments (Chapter 4), the settling rates of microplastics were compared to a universal sediment transport formula that resolves Stokes' Law for fine-grained sediment transport (Ferguson and Church, 2004). The results showed that sediment transport formulae can over and under-predict microplastic settling depending on the polymer type. The theoretical settling velocity for polyethylene terephthalate (PET) microplastics predicted by the Ferguson and Church (2004) model was shown to be considerably higher than observed and therefore any models using this formula will over-predict the settling of PET. This would result in higher amounts of microplastics being transported in suspension than expected. However, for polyvinyl chloride (PVC) particles, settling velocity was both over and under-predicted by Ferguson and Church (2004) depending on whether the particles were biofouled or not. It is noted that sediment equations may be utilised if microplastics have hydraulically equivalent physical properties to grains, yet microplastics exist in a much wider range of shapes and sizes than natural sediment. Therefore, these experiments demonstrated the clear need for a new generation of transport formula specifically for microplastics that considers irregular shapes, biofouling and changes over time and salinity.

To test the comparison between sediment transport and microplastics further, the relationship between microplastic concentrations and riverine discharge was assessed. The basic mechanisms for the wider transport of suspended sediment in rivers are well known with rising discharge typically resulting in an increase in suspended sediment (Rivera *et al.,* 2019). Microplastic concentrations from the Mekong River were compared Haberstroh *et al.,* 2021 who sampled in the same area and year (Chapter 5). The concentration of microplastics is observed to decrease with rising discharge, which is the opposite trend to siliciclastic sediment transport (Fig. 5.18). This suggests that microplastic concentrations are supply limited rather than capacity limited in rivers as microplastic abundance does not increase with discharge. This further highlights that assumptions on microplastic transport based on sediment dynamics are not always robust and the relationships require further assessment.

However, when it comes to the interaction of particles within aquatic canopies, known sediment dynamics do appear to be able to give some insight into the trapping patterns of microplastics. Indeed, such ecosystems are known for their ability to promote the deposition of suspended sediment and reduce resuspension (Gacia and Duarte, 2001). A considerable amount (up to 99%) of microplastics were retained within coral canopies presented in Chapter 6. Changes to the flow dynamics resulting from the interaction between the coral canopies and the flow profile will have caused this high microplastic trapping efficiency including a decrease in streamwise velocity and the development of horseshoe vortex structures within the canopy. Such processes have also been identified as fundamental to sediment mobility (Lefebvre *et al.,* 2010). Therefore, in some locations comparisons between microplastics and sediment transport are valid and as such research on natural sediments can guide our understanding of microplastic transport. However, whether or not similar amounts of microplastics and siliclastic sediments would be deposited and retained into the bed of canopies is unknown and differences may arise due to wider variation is particle densities for microplastics. Furthermore, due to the results presented in Chapters 4 and 5

the amount of microplastics interacting with coral canopies should not be based on sediment transport laws. As previously discussed, it was shown that formulae for sediment dynamics can over or under-predict microplastic settling, and that the amount of microplastics being transported in rivers may not be currently accurately predicted due to sampling and modelling methods that do not consider the entire water column or hydrological changes throughout the year. Therefore, the results presented in this thesis highlight that although much of our understanding of microplastic transport can be guided by sediment dynamics, it should not be relied upon and new theories must be developed specifically for microplastics.

## 7.4 Ecological risk

The size of microplastics means they are often accidentally ingested by organisms, with the ecological harm due to microplastic exposure now being well documented (Eerkes-Medrano *et al.,* 2015; Wright *et al.,* 2013). Ecological risk must be taken into account when assessing microplastic levels in aquatic environments and results from this research have important implications for the exposure of aquatic organisms and ecosystems to microplastic pollution which are discussed briefly below.

Fundamentally, the distribution of microplastics in the water column will alter the bioavailability of microplastics to organisms. It has been demonstrated that settling and therefore transport and deposition of microplastics throughout the water column is influenced by biofouling, salinity and sediment (Chapter 4), in addition to seasonal variations in riverine discharge (Chapter 5) and aquatic canopies (Chapter 6). Biofouling was found to increase microplastic settling through impacts on specific density and therefore can cause particles to settle faster. In addition, biofilm growth has been reported to cause buoyant microplastics to settle (Fazey and Ryan, 2016). This will influence the bioavailability of plastic particles at depth to different types of organisms. Furthermore, it has been shown that biofouled microplastics are more likely to be ingested than clean microplastics perhaps due to the

biofilm creating olfactory cues that resemble normal prey items for certain organisms (Vroom *et al.,* 2017) increasing the ecological risk bottom-dwelling species are exposed to.

Chapter 5 demonstrated how microplastics within the water column represent the majority of microplastics moving in the water of a fluvial system. Previous research had tended to only sample at the water surface and therefore total microplastic concentration is likely to have been underpredicted. Therefore, the ecological risk may be higher in these areas than previously expected, as organisms throughout the water column that encompass a range of feeding guilds will be exposed to microplastics. Resuspension of microplastics due to turbulence may also result in the continuous re-exposure to organisms. Thus, for a riverine ecosystem, fishes and benthic organisms are highly likely to be exposed to microplastics which could lead to multiple impacts on health, such as lower immunity and altered feeding behaviour as observed by exposure studies (Horton *et al.,* 2018; Kumar *et al.,* 2021). This has implications for entire ecosystems and highlights the need to consider the ecological risk of microplastics throughout the water column, not only at the water surface.

Finally, the ecological risk of microplastic trapping by aquatic canopies must be considered. Chapter 6 demonstrated the high trapping efficiency of both sparse and dense coral canopies. The accumulation of microplastics in these highly biodiverse habitats could have repercussions for the ecology of the reef system. First, exposure of corals to microplastics can cause numerous negative impacts on coral health and functioning, such as reduced photosynthetic ability and tissue necrosis (Hall *et al.,* 2015; Mendrik *et al.,* 2021; Reichert *et al.,* 2018). This may eventually cause bleaching and decline of the reef, which could affect the numerous organisms that rely on corals for protection and nursery grounds (Reichert *et al.,* 2018). In addition, the accumulation of microplastics in coral canopies may lead to higher bioavailability of microplastics to a range of biota within the reef system including fish, sea cucumbers and gastropods. As this was the first study to determine the high microplastic trapping efficiencies of coral canopies, the potential exposure of

microplastics to reefs and associated organisms may not have been fully considered before. The implications of the findings in this thesis require further work which is discussed in §7.4.

## 7.5 Recommendations for future research

### A. Development of a framework that includes the drivers of microplastic transport and fate

The research and results presented here have demonstrated the complex transport mechanisms of aquatic microplastics across a variety of scenarios. It has been highlighted in several ways that although sediment dynamics can provide a basic understanding of microplastics transport, it should not be relied upon to make accurate predictions of microplastic loads and fate. The main factors that influence microplastic settling, such as biofouling. suspended sediment and weathering should be further assessed with laboratory studies (detailed below) to understand how impacts change over time and depending on a wider range of polymers. This would allow sediment formulae such as Ferguson and Church (2004), and attempts at microplastic transport formulas such as Waldschläger and Schüttrumpf (2019), to be updated with microplastic-specific settling regime drivers and the development of an accurate framework for microplastic transport.

### B. Standardisation of field sampling methodologies

Widespread monitoring campaigns in rivers would be highly beneficial to understand the amount of microplastics being transported within rivers and out into the ocean. However, standardisation of field sampling methodologies is needed to allow for comparison between sites and robust data acquisition globally. This should include:

i) *Sampling throughout the water column.* This research highlighted how the majority of microplastics were found below the surface of the water column in a major river. Therefore, if sampling is only conducted at the surface, the abundance of microplastics will be underpredicted. Sampling must be representative of the entire water column. This may be achieved by sampling at an optimum depth that represents the average microplastic

concentration of the water column. For the Mekong river this was calculated at 59% of the total depth, yet this must be tested within different rivers of various scales and location.

ii) *Seasonal sampling*. Many riverine studies tend to sample during high flow as it is expected this will be when the highest amount of microplastics will be transported. However, it was shown here that microplastic concentration varies with discharge in the opposite way to suspended sediment. Traditional sediment rating curves show that as the water level rises, a greater sediment supply is observed resulting in increased sediment concentration. However, lower microplastic concentrations were observed at higher discharge levels. This suggests that the input of microplastics from land to rivers remains fairly constant throughout the year, therefore the rise in discharge dilutes microplastics concentrations. Therefore to fully understand the amount of microplastics being transported by a river, field campaigns must be conducted throughout the year. This will allow annual microplastic discharge to be more accurately calculated.

*iii) Sediment sampling*. To fully comprehend microplastic abundance in a river, the amount being deposited in sediment must also be quantified. This would include sampling within the bed sediment and the banks of the river. This will show in what areas microplastics stop being transported in suspension and will further increase the accuracy of microplastic loads travelling to marine environments.

## C. Ecological risk assessment

Microplastics are contaminating highly biodiverse areas globally, yet there is a lack of ecological risk assessments being conducted to completely understand the risk to biota. Although ecological risk was discussed above, a more comprehensive understanding of the impacts of microplastics on biota in rivers and marine ecosystems is needed. First, the biota that are likely to be exposed to microplastics must be determined, in addition to concentration levels of exposure. Sampling throughout the water column in all aquatic environments is needed, including rivers and coral reefs. Collection and dissection of biota from a variety of feeding guilds and habitats should be conducted to determine exposure

levels. Next, the relationship between exposure levels and possible adverse effects on the organisms can then be assessed by reviewing laboratory exposure experiments. This would allow a greater understanding of potential ecological risks and areas to be identified that are in need of protection. Furthermore, this will also help understand the risk to associated communities that rely on these ecosystems for their livelihood and food security and push for the formation of robust policies and mitigation measures.

### D. Further laboratory-based data acquisition

A suite of further experiments could be undertaken to better quantify controls on microplastic transport:

*i) Further application of LabSFLOC settling experiments.* This research used the LabSFLOC methodology for the first time in regard to microplastic settling and demonstrated how it is a useful tool to assess plastic particle settling accurately (Chapter 4). However, the scope of these experiments can be expanded. A wider range of polymers should be tested such as polystyrene (PS), high-density polyethylene (HDPE) and fibres which represent the vast amount of plastic types found in aquatic environments. The biofouling-specific influence on microplastic settling has already been quantified, but the impacts due to salinity and suspended sediment need further assessment for a wider range of polymer types. Furthermore, the impacts of suspended sediment within the LabSFLOC water column should be assessed to understand the environmental impacts of fluvial systems on microplastic settling in more detail. In addition, the role of turbulence and waves on microplastic settling should be explored that replicates environmental conditions. The LabSFLOC set-up can be modified to test this by using a larger tank with a paddle system.

*ii) Increase in complexity of canopy experiments.* Within this research, the impacts of coral canopies on microplastic settling were examined. While this provided preliminary research into the role of complex canopies on microplastic settling, the scope of this research can be greatly expanded. First, it would be insightful to test a range of different canopies under various conditions. Corals exist in a range of morphologies and therefore it is expected the

trapping efficiency will differ depending on the species. The arrangements of corals within a reef are also highly variable. Canopies of different coral types should therefore be investigated but canopies containing a mixture of coral species can also be evaluated, in addition to different arrangements of corals. Moreover, other complex ecosystem structures must be evaluated for their microplastic trapping efficiency, including seagrass and mangroves, which can be compared to coral reefs. Future work may include a variety of canopy lengths and submergence ratios. Different types of microplastics that represent the range of polymers and shapes seen in aquatic environments must also be tested within these experiments. Furthermore, it is noted that only unidirectional flows were evaluated in this research. The influence of waves on microplastic deposition in coral reefs must be quantified. Experimental results can be further validation through fieldwork *in situ.*

*iii) Longer duration of data acquisition*. To ensure a fuller evaluation of the impacts of biofouling on settling and the trapping of microplastics by aquatic canopies, longer measurement durations of experiments are needed. In addition, experiments with microplastics on the surface of the water should be conducted to determine the amount of time particles will take to enter the water column when they originate from non-aquatic sources.

*iv) Introduction of live corals to flume experiments.* It was identified in this research that the passive removal of microplastics by coral canopies will result in large trapping efficiencies. However, to gain a greater understanding of the trapping of microplastics by corals through active and passive removal, live corals should be utilised. This would be a significant challenge to insure that the corals remain healthy throughout the experimental period, but would allow exact measurements of the amount of microplastics trapped due to coral structures, ingestion and stuck on the branches or within the structure itself. The introduction of mobile bed sediment should also be used to test the amount of microplastics deposited into the bed via canopy trapping.

## 7.6 Thesis Summary

This thesis is concluded by reviewing the initial research aim and questions, which are subsequently supported by a summary of how they were accomplished throughout the corresponding chapters. The following overarching research aim formed the basis of this thesis:

*Evaluate and determine the key controlling factors that influence microplastic fate in aquatic environments*

Following a review of previous research, it was determined that the current knowledge of microplastic transport mechanisms was limited and that a multidisciplinary approach was necessary to fully understand the fate of microplastics in aquatic systems. As the majority of marine plastic pollution originates from inland, the influence of changing conditions from rivers to the ocean must be quantified and understood. First, the biological and environmental impacts on microplastic settling velocity were tested under a range of conditions to replicate the change in environment from freshwater to marine systems. This was achieved through a variety of settling experiments conducted in Chapter 4. The assessment of microplastic distribution in the water column of a major river under different seasonal conditions was then determined in Chapter 5, demonstrating the influence of fluvial dynamics. Finally, the role of aquatic canopies, namely corals, which will be exposed to microplastics as they move out of a river into the marine environment, on microplastic retention was evaluated in Chapter 6. The outputs of this thesis have provided novel and improved approaches to expand the understanding of microplastic transport in aquatic environments. The scientific results deliver advancements in understanding the biological influence on microplastic settling over a range of environmental conditions, the distribution of microplastic concentrations in a major river and the role of coral reefs in the eventual fate of microplastics.

**Research question 1:** How does polymer type and biofilm formation affect the transport of microplastics through influences on density?

**Research question 2:** How do changes in water conditions (such as freshwater to marine salinity gradients) and suspended sediment alter how microplastics settle?

The use of novel settling experiments was implemented for Chapter 4 to determine the principle mechanisms that influence microplastic settling from freshwater to marine environments and answer research questions 1 and 2. Notably, biofouling was identified as the main influence on the settling of several types of microplastics through changes in particle-specific density. Settling regimes were also influenced by polymer type due to density and salinity concentrations. However, no aggregation of particles was observed, with the impacts of suspended sediment not as considerable as expected.

**Research question 3:** How are microplastics distributed throughout major rivers and how does this influence ecological risk?

A field campaign detailed in Chapter 5 allowed the distribution of microplastics throughout the water column of a major river, The Mekong, to be assessed and answer research question 3. The majority of microplastics were identified to be within the water column rather than at the surface at all locations sampled in Vietnam and Cambodia. This highlighted the need for updated field techniques as previous fieldwork that only samples at the water surface could be underpredicting microplastics concentrations. It was also shown that microplastic concentration and distribution differed depending on seasonal river discharge. Furthermore, as the majority of microplastics were found within the water column, the ecological risk may be higher than previously predicted and affect a wider range of aquatic organisms.

**Research question 4:** How do structurally complex ecosystems such as coral reefs control the transport, fate and sinking dynamics of microplastics from a riverine environment?

Coral canopies were evaluated for their microplastic trapping efficiency in a hydraulic flume under several flow conditions detailed in Chapter 6 to answer research question 4. As coral reefs are often found in coastal environments, they are highly likely to be exposed to microplastic pollution that is moving out of a river and into the ocean. Trapping efficiency was dependent on canopy density and bulk velocity, yet both sparse and dense canopies were observed to retain a considerable amount of microplastics. Canopies were recorded to decrease streamwise velocities resulting in the accumulation of microplastics throughout the canopy. This highlights for the first time the role of coral reefs as an area of accumulation and a sink for microplastic pollution with experimental evidence.

[Page intentionally left blank]

# References


Abdolahpour, M., Hambleton, M., Ghisalberti, M., 2017. The wave-driven current in coastal canopies. J. Geophys. Res. Ocean. 122, 3660–3674. https://doi.org/10.1002/2016JC012446

Ackiss, A.S., Dang, B.T., Bird, C.E., Biesack, E.E., Chheng, P., Phounvisouk, L., Vu, Q.H.D., Uy, S., Carpenter, K.E., 2019. Cryptic Lineages and a Population Dammed to Incipient Extinction? Insights into the Genetic Structure of a Mekong River Catfish. J. Hered. https://doi.org/10.1093/jhered/esz016

Adamson, P., 2006. An evaluation of landuse and climate change on the recent historical regime of the Mekong, Report produced for Mekong River Commission mekonginfo.org.

Adamson, P., Rutherfurd, I., Peel, M., Conlan, I., 2009. Chapter 4 - The hydrology of the Mekong River, in: The Mekong, Biophysical Environment of an International River Basin. Academic Press, pp. 53–76.

Agawin, N.S.R., Duarte, C.M., 2002. Evidence of direct particle trapping by a tropical seagrass meadow. Estuaries 25, 1205–1209. https://doi.org/10.1007/BF02692217

Alam, F.C., Sembiring, E., Muntalif, B.S., Suendo, V., 2019. Microplastic distribution in surface water and sediment river around slum and industrial area (case study: Ciwalengke River, Majalaya district, Indonesia). Chemosphere 224, 637–645. https://doi.org/10.1016/j.chemosphere.2019.02.188

Allen, A.S., Seymour, A.C., Rittschof, D., 2017. Chemoreception drives plastic consumption in a hard coral. Mar. Pollut. Bull. 124, 198–205. https://doi.org/10.1016/j.marpolbul.2017.07.030

Amaral-Zettler, L.A., Zettler, E.R., Mincer, T.J., 2020. Ecology of the plastisphere. Nat. Rev. Microbiol. https://doi.org/10.1038/s41579-019-0308-0

Andersen, T.J., Rominikan, S., Olsen, I.S., Skinnebach, K.H., Fruergaard, M., 2021. Flocculation of PVC microplastic and fine-grained cohesive sediment at environmentally realistic concentrations. Biol. Bull. 240, 42–51. https://doi.org/10.1086/712929

Andrady, A., 2011. Microplastics in the marine environment. Mar. Pollut. Bull. 62, 1596–1605.

Anthony, K.R.N., 1999. Coral suspension feeding on fine particulate matter. J. Exp. Mar. Bio. Ecol. 232, 85–106. https://doi.org/10.1016/S0022-0981(98)00099-9

Auta, Helen Shnada, Emenike, C., Fauziah, Shahul Hamid, Auta, H S, Emenike, C.U., Fauziah, S H, 2017. Distribution and importance of microplastics in the marine environment: A review of the sources, fate, effects, and potential solutions Microplastic Pollution-Remediation studies View project Remediation of Polycyclic Aromatic Hydrocarbons in Environment View project Distribution and importance of microplastics in the marine environment: A review of the sources, fate, effects, and potential solutions. https://doi.org/10.1016/j.envint.2017.02.013

Avio, C.G., Gorbi, S., Lilan, M., Benedetti, M., Fattorini, D., D'Errico, G., Pauletto, M., Bargelloni, L., Regoli, F., 2015. Pollutants bioavailability and toxicological risk from microplastics to marine mussels. Environ. Pollut. 198, 211–222. https://doi.org/10.1016/j.envpol.2014.12.021

Avio, C.G., Gorbi, S., Regoli, F., 2017. Plastics and microplastics in the oceans: From emerging pollutants to emerged threat. Mar. Environ. Res. 128, 2–11. https://doi.org/10.1016/j.marenvres.2016.05.012

Axworthy, J.B., Padilla-Gamiño, J.L., 2019. Microplastics ingestion and heterotrophy in thermally stressed corals. Sci. Rep. 9, 18193. https://doi.org/10.1038/s41598-019-54698-7

Baalkhuyur, F.M., Bin Dohaish, E.J.A., Elhalwagy, M.E.A., Alikunhi, N.M., AlSuwailem, A.M., Røstad, A., Coker, D.J., Berumen, M.L., Duarte, C.M., 2018. Microplastic in the gastrointestinal tract of fishes along the Saudi Arabian Red Sea coast. Mar. Pollut. Bull. 131, 407–415. https://doi.org/10.1016/j.marpolbul.2018.04.040

Bagaev, A., Mizyuk, A., Khatmullina, L., Isachenko, I., Chubarenko, I., 2017. Anthropogenic fibres in the Baltic Sea water column: Field data, laboratory and numerical testing of their motion. Sci. Total Environ. 599–600, 560–571. https://doi.org/10.1016/j.scitotenv.2017.04.185

Ballent, A., de Jesus Mendes, P., Pando, S., Thomsen, L., Purser, A., 2012. Physical transport properties of marine microplastic pollution. Biogeosciences Discuss. 9, 18755–18798. https://doi.org/10.5194/bgd-9-18755-2012

Baran, E., 2010. Mekong fisheries and mainstream dams, Fisheries sections in: ICEM.

Baran, E., Chum, N., Fukushima, M., Hand, T., Hortle, K.G., Jutagate, T., Kang, B., 2012. Fish Biodiversity Research in the Mekong Basin. Springer, Tokyo, pp. 149–164. https://doi.org/10.1007/978-4-431-54032-8_11

Baran, E., Jantunen, T., Chong, C.K., 2007. Values of inland fisheries in the Mekong River Basin. WorldFish.

Barnes, D.K.A., 2002. Invasions by marine life on plastic debris. Nature 416, 808–809. https://doi.org/10.1038/416808a

Barnes, D.K.A., Galgani, F., Thompson, R.C., Barlaz, M., 2009. Accumulation and fragmentation of plastic debris in global environments. Philos. Trans. R. Soc. Lond. B. Biol. Sci. 364, 1985–1998. https://doi.org/10.1098/rstb.2008.0205

Bellas, J., Martínez-Armental, J., Martínez-Cámara, A., Besada, V., Martínez-Gómez, C., 2016. Ingestion of microplastics by demersal fish from the Spanish Atlantic and Mediterranean coasts. Mar. Pollut. Bull. 109, 55–60. https://doi.org/10.1016/j.marpolbul.2016.06.026

Besseling, E., Quik, J.T.K., Sun, M., Koelmans, A.A., 2017a. Fate of nano- and microplastic in freshwater systems: A modeling study. Environ. Pollut. 220, 540–548. https://doi.org/10.1016/j.envpol.2016.10.001

Besseling, E., Quik, J.T.K., Sun, M., Koelmans, A.A., 2017b. Fate of nano- and microplastic in freshwater systems: A modeling study. Environ. Pollut. 220, 540–548. https://doi.org/10.1016/j.envpol.2016.10.001

Bos, A.R., Bouma, T.J., de Kort, G.L.J., van Katwijk, M.M., 2007. Ecosystem engineering by annual intertidal seagrass beds: Sediment accretion and modification. Estuar. Coast. Shelf Sci. 74, 344–348. https://doi.org/10.1016/J.ECSS.2007.04.006

Bouma, T.J., De Vries, M.B., Low, E., Peralta, G., Tánczos, I.C., Van De Koppel, J., Herman, P.M.J., 2005. Trade-offs related to ecosystem engineering: A case study on stiffness of emerging macrophytes. Ecology 86, 2187–2199. https://doi.org/10.1890/04-1588

Bradley, D., Roth, G., 2007. Adaptive Thresholding using the Integral Image. J. Graph. Tools 12, 13–21. https://doi.org/10.1080/2151237x.2007.10129236

Browne, M.A., Crump, P., Niven, S.J., Teuten, E., Tonkin, A., Galloway, T., Thompson, R., 2011. Accumulation of Microplastic on Shorelines Woldwide: Sources and Sinks. Environ. Sci. Technol. 45, 9175–9179. https://doi.org/10.1021/es201811s

Burke, L., Reytar, K., Spalding, M., Perry, A., 2011. Reefs at risk revisited, World Resources Institute.

Cai, H., Du, F., Li, L., Li, B., Li, J., Shi, H., 2019. A practical approach based on FT-IR spectroscopy for identification of semi-synthetic and natural celluloses in microplastic investigation. Sci. Total Environ. 669, 692–701. https://doi.org/10.1016/j.scitotenv.2019.03.124

Campbell, I., 2009. The Mekong: Biophysical environment of an international river basin.

Carlin, J., Craig, C., Little, S., Donnelly, M., Fox, D., Zhai, L., Walters, L., 2020. Microplastic accumulation in the gastrointestinal tracts in birds of prey in central Florida, USA. Environ. Pollut. 264, 114633. https://doi.org/10.1016/J.ENVPOL.2020.114633

Carpenter, E.J., Anderson, S.J., Harvey, G.R., Miklas, H.P., Peck, B.B., 1972. Polystyrene Spherules in Coastal Waters. Science (80-. ). 178, 749–750. https://doi.org/10.1126/science.178.4062.749

Castorani, M.C.N., Glud, R.N., Hasler-Sheetal, H., Holmer, M., 2015. Light indirectly mediates bivalve habitat modification and impacts on seagrass. J. Exp. Mar. Bio. Ecol. 472, 41–53. https://doi.org/10.1016/j.jembe.2015.07.001

Cesarini, G., Scalici, M., 2022. Riparian vegetation as a trap for plastic litter. Environ. Pollut. 292, 118410. https://doi.org/10.1016/j.envpol.2021.118410

Chapron, L., Peru, E., Engler, A., Ghiglione, J.F., Meistertzheim, A.L., Pruski, A.M., Purser, A., Vétion, G., Galand, P.E., Lartaud, F., 2018. Macro- and microplastics affect cold-water corals growth, feeding and behaviour. Sci. Rep. 8, 15299. https://doi.org/10.1038/s41598-018-33683-6

Chen, H.L., Gibbins, C.N., Selvam, S.B., Ting, K.N., 2021. Spatio-temporal variation of microplastic along a rural to urban transition in a tropical river. Environ. Pollut. 289, 117895. https://doi.org/10.1016/J.ENVPOL.2021.117895

Chiba, S., Saito, H., Fletcher, R., Yogi, T., Kayo, M., Miyagi, S., Ogido, M., Fujikura, K., 2018. Human footprint in the abyss: 30 year records of deep-sea plastic debris. Mar. Policy. https://doi.org/10.1016/j.marpol.2018.03.022

Cho, Y., Shim, W.J., Jang, M., Han, G.M., Hong, S.H., 2019. Abundance and characteristics of microplastics in market bivalves from South Korea. Environ. Pollut. 245, 1107–1116. https://doi.org/10.1016/j.envpol.2018.11.091

Chong, X.Y., Gibbins, C.N., Vericat, D., Batalla, R.J., Teo, F.Y., Lee, K.S.P., 2021. A framework for Hydrological characterisation to support Functional Flows (HyFFlow): Application to a tropical river. J. Hydrol. Reg. Stud. 36. https://doi.org/10.1016/j.ejrh.2021.100838

Chubarenko, I., Bagaev, A., Zobkov, M., Esiukova, E., 2016. On some physical and dynamical properties of microplastic particles in marine environment. Mar. Pollut. Bull. 108, 105–112. https://doi.org/10.1016/j.marpolbul.2016.04.048

Cincinelli, A., Scopetani, C., Chelazzi, D., Lombardini, E., Martellini, T., Katsoyiannis, A., Fossi, M.C., Corsolini, S., 2017. Microplastic in the surface waters of the Ross Sea (Antarctica): Occurrence, distribution and characterization by FTIR. Chemosphere 175, 391–400. https://doi.org/10.1016/j.chemosphere.2017.02.024

Cole, M., Lindeque, P., Halsband, C., Galloway, T.S., 2011. Microplastics as contaminants in the marine environment: A review. Mar. Pollut. Bull. https://doi.org/10.1016/j.marpolbul.2011.09.025

Collard, F., Gasperi, J., Gabrielsen, G.W., Tassin, B., 2019. Plastic Particle Ingestion by Wild Freshwater Fish: A Critical Review. Environ. Sci. Technol. https://doi.org/10.1021/acs.est.9b03083

Cooksey, K.E., Wigglesworth-Cooksey, B., 1995. Adhesion of bacteria and diatoms to surfaces in the sea: A review. Aquat. Microb. Ecol. https://doi.org/10.3354/ame009087

Corinaldesi, C., Canensi, S., Dell'Anno, A., Tangherlini, M., Di Capua, I., Varrella, S., Willis, T.J., Cerrano, C., Danovaro, R., 2021. Multiple impacts of microplastics can threaten marine habitat-forming species. Commun. Biol. 4, 1–13. https://doi.org/10.1038/s42003-021-01961-1

Corona, E., Martin, C., Marasco, R., Duarte, C.M., 2020. Passive and Active Removal of Marine Microplastics by a Mushroom Coral (Danafungia scruposa). Front. Mar. Sci. 7, 128. https://doi.org/10.3389/FMARS.2020.00128/BIBTEX

Cowger, W., Gray, A.B., Guilinger, J.J., Fong, B., Waldschläger, K., 2021. Concentration Depth Profiles of Microplastic Particles in River Flow and Implications for Surface Sampling. Environ. Sci. Technol. 55, 6032–6041. https://doi.org/10.1021/acs.est.1c01768

Cózar, A., Echevarría, F., González-Gordillo, J.I., Irigoien, X., Ubeda, B., Hernández-León, S., Palma, A.T., Navarro, S., García-de-Lomas, J., Ruiz, A., Fernández-de-Puelles, M.L., Duarte, C.M., 2014. Plastic debris in the open ocean. Proc. Natl. Acad. Sci. U. S. A. 111, 10239–44. https://doi.org/10.1073/pnas.1314705111

Cozzolino, L., Nicastro, K.R., Seuront, L., McQuaid, C.D., Zardi, G.I., 2022. The relative effects of interspecific and intraspecific diversity on microplastic trapping in coastal biogenic habitats. Sci. Total Environ. 848, 157771. https://doi.org/10.1016/j.scitotenv.2022.157771

Cozzolino, L., Nicastro, K.R., Zardi, G.I., de los Santos, C.B., 2020. Species-specific plastic accumulation in the sediment and canopy of coastal vegetated habitats. Sci. Total Environ. 723. https://doi.org/10.1016/j.scitotenv.2020.138018

Cunha, C., Faria, M., Nogueira, N., Ferreira, A., Cordeiro, N., 2019. Marine vs freshwater microalgae exopolymers as biosolutions to microplastics pollution. Environ. Pollut. 249, 372–380. https://doi.org/10.1016/j.envpol.2019.03.046

Cuthbertson, A.J.S., Samsami, F., Dong, P., 2018. Model studies for flocculation of sand-clay mixtures. Coast. Eng. 132, 13–32. https://doi.org/10.1016/j.coastaleng.2017.11.006

Davidson, K., Dudas, S.E., 2016. Microplastic Ingestion by Wild and Cultured Manila Clams (Venerupis philippinarum) from Baynes Sound, British Columbia. Arch. Environ. Contam. Toxicol. 71, 147–156. https://doi.org/10.1007/s00244-016-0286-4

de los Santos, C.B., Krång, A.S., Infantes, E., 2021a. Microplastic retention by marine vegetated canopies: Simulations with seagrass meadows in a hydraulic flume. Environ. Pollut. 269. https://doi.org/10.1016/j.envpol.2020.116050

de los Santos, C.B., Krång, A.S., Infantes, E., 2021b. Microplastic retention by marine vegetated canopies: Simulations with seagrass meadows in a hydraulic flume. Environ. Pollut. 269. https://doi.org/10.1016/j.envpol.2020.116050

de Smit, J.C., Anton, A., Martin, C., Rossbach, S., Bouma, T.J., Duarte, C.M., 2021. Habitat-forming species trap microplastics into coastal sediment sinks. Sci. Total Environ. 772. https://doi.org/10.1016/j.scitotenv.2021.145520

de Smit, J.C., Kleinhans, M.G., Gerkema, T., Timmermans, K.R., Bouma, T.J., 2020. Introducing the TiDyWAVE field flume: A method to quantify natural ecosystem resilience against future storm waves. Limnol. Oceanogr. Methods 18, 585–598. https://doi.org/10.1002/lom3.10386

Delgado, J.M., Merz, B., Apel, H., 2012. Monsoon Variability and the Mekong Flood Regime 233–244. https://doi.org/10.1007/978-94-007-3962-8_9

Derraik, J.G.., 2002. The pollution of the marine environment by plastic debris: A review. Mar. Pollut. Bull. https://doi.org/10.1016/S0025-326X(02)00220-5

Dikareva, N., Simon, K.S., 2019. Microplastic pollution in streams spanning an urbanisation gradient. Environ. Pollut. 250, 292–299. https://doi.org/10.1016/j.envpol.2019.03.105

Ding, J., Jiang, F., Li, J., Wang, Zongxing, Sun, C., Wang, Zhangyi, Fu, L., Ding, N.X., He, C., 2019. Microplastics in the Coral Reef Systems from Xisha Islands of South China Sea. Environ. Sci. Technol. 53, 8036–8046. https://doi.org/10.1021/acs.est.9b01452

Ding, J., Sun, Y., He, C., Li, J., Li, F., 2022. Towards Risk Assessments of Microplastics in Bivalve Mollusks Globally. J. Mar. Sci. Eng. https://doi.org/10.3390/jmse10020288

do Sul, J.A.I., Costa, M.F., 2007. Marine debris review for Latin America and the Wider Caribbean Region: From the 1970s until now, and where do we go from here? Mar. Pollut. Bull. 54, 1087–1104. https://doi.org/10.1016/j.marpolbul.2007.05.004

Dris, R., Gasperi, J., Rocher, V., Tassin, B., 2018. Synthetic and non-synthetic anthropogenic fibers in a river under the impact of Paris Megacity: Sampling methodological aspects and flux estimations. Sci. Total Environ. 618, 157–164. https://doi.org/10.1016/j.scitotenv.2017.11.009

Dris, R., Imhof, H., Sanchez, W., Gasperi, J., Galgani, F., Tassin, B., Laforsch, C., 2015. Beyond the ocean: contamination of freshwater ecosystems with (micro-)plastic particles. Environ. Chem. 12, 539. https://doi.org/10.1071/EN14172

Drummond, J.D., Davies-Colley, R.J., Stott, R., Sukias, J.P., Nagels, J.W., Sharp, A., Packman, A.I., 2015. Microbial Transport, Retention, and Inactivation in Streams: A Combined Experimental and Stochastic Modeling Approach. Environ. Sci. Technol. 49, 7825–7833. https://doi.org/10.1021/acs.est.5b01414

Drummond, J.D., Schneidewind, U., Li, A., Hoellein, T.J., Krause, S., Packman, A.I., 2022. Microplastic accumulation in riverbed sediment via hyporheic exchange from headwaters to mainstems. Sci. Adv. 8. https://doi.org/10.1126/sciadv.abi9305

Duan, J., Bolan, N., Li, Y., Ding, S., Atugoda, T., Vithanage, M., Sarkar, B., Tsang, D.C.W., Kirkham, M.B., 2021. Weathering of microplastics and interaction with other coexisting constituents in terrestrial and aquatic environments. Water Res. https://doi.org/10.1016/j.watres.2021.117011

Duan, J., Han, J., Zhou, H., Lau, Y.L., An, W., Wei, P., Cheung, S.G., Yang, Y., Tam, N.F., 2020. Development of a digestion method for determining microplastic pollution in vegetal-rich clayey mangrove sediments. Sci. Total Environ. 707, 136030. https://doi.org/10.1016/J.SCITOTENV.2019.136030

Dugan, P.J., Barlow, C., Agostinho, A.A., Baran, E., Cada, G.F., Chen, D., Cowx, I.G., Ferguson, J.W., Jutagate, T., Mallen-Cooper, M., Marmulla, G., Nestler, J., Petrere, M., Welcomme, R.L., Winemiller, K.O., 2010. Fish migration, dams, and loss of ecosystem services in the mekong basin. Ambio 39, 344–348. https://doi.org/10.1007/s13280-010-0036-1

Eerkes-Medrano, D., Thompson, R.C., Aldridge, D.C., 2015. Microplastics in freshwater systems: A review of the emerging threats, identification of knowledge gaps and prioritisation of research needs. Water Res. https://doi.org/10.1016/j.watres.2015.02.012

Elagami, H., Ahmadi, P., Fleckenstein, J.H., Frei, S., Obst, M., Agarwal, S., Gilfedder, B.S., 2022. Measurement of microplastic settling velocities and implications for residence times in thermally stratified lakes. Limnol. Oceanogr. 67, 934–945. https://doi.org/10.1002/lno.12046

Enders, K., Käppler, A., Biniasch, O., Feldens, P., Stollberg, N., Lange, X., Fischer, D.,

Eichhorn, K.J., Pollehne, F., Oberbeckmann, S., Labrenz, M., 2019. Tracing microplastics in aquatic environments based on sediment analogies. Sci. Rep. 9. https://doi.org/10.1038/s41598-019-50508-2

Engelund, F., Hansen, E., 1967. A monograph on sediment transport in alluvial streams. Monografia 65.

Enyoh, C.E., Shafea, L., Verla, A.W., Verla, E.N., Qingyue, W., Chowdhury, T., Paredes, M., 2020. Microplastics Exposure Routes and Toxicity Studies to Ecosystems: An Overview. Environ. Anal. Heal. Toxicol. 35. https://doi.org/10.5620/EAHT.E2020004

Eo, S., Hong, S., Song, Y., Han, G., research, W.S.-W., 2019, undefined, n.d. Spatiotemporal distribution and annual load of microplastics in the Nakdong River, South Korea. Elsevier.

Eriksen, M., Lebreton, L.C.M., Carson, H.S., Thiel, M., Moore, C.J., Borerro, J.C., Galgani, F., Ryan, P.G., Reisser, J., 2014. Plastic Pollution in the World's Oceans: More than 5 Trillion Plastic Pieces Weighing over 250,000 Tons Afloat at Sea. PLoS One 9, e111913. https://doi.org/10.1371/journal.pone.0111913

European Environment Agency, 2016. Case Study 2: Sweden [WWW Document]. URL https://www.eea.europa.eu/publications/92-9167-052-9-sum/page005.html (accessed 11.24.17).

Fazey, F.M.C., Ryan, P.G., 2016. Biofouling on buoyant marine plastics: An experimental study into the effect of size on surface longevity. Environ. Pollut. 210, 354–360. https://doi.org/10.1016/j.envpol.2016.01.026

Feng, S., Lu, H., Yao, T., 2021. Microplastics Footprints in a High-Altitude Basin of the Tibetan Plateau, China. Water 2021, Vol. 13, Page 2805 13, 2805. https://doi.org/10.3390/W13202805

Ferguson, R.I., Church, M., 2004. A simple universal equation for grain settling velocity. J. Sediment. Res. 74, 933–937. https://doi.org/10.1306/051204740933

Fergusson, W.C., 1974. Summary. J.J.P. Staudinger (Ed.), Plast. Environ. Hutchinson Co, London 2.

Fisher, R., O'Leary, R.A., Low-Choy, S., Mengersen, K., Knowlton, N., Brainard, R.E., Caley, M.J., 2015. Species richness on coral reefs and the pursuit of convergent global estimates. Curr. Biol. 25, 500–505. https://doi.org/10.1016/j.cub.2014.12.022

Food and Agriculture Organisation of the United Nations (FAO), 2018. The State of World Fisheries and Aquaculture 2018 – Meeting the Sustainable Development Goals.

Food and Agriculture Organisation of the United Nations (FAO), 2016. The State of World Fisheries and Aquaculture 2016.

Forsberg, P.L., Sous, D., Stocchino, A., Chemin, R., 2020. Behaviour of plastic litter in nearshore waters: First insights from wind and wave laboratory experiments. Mar. Pollut. Bull. 153, 111023. https://doi.org/10.1016/j.marpolbul.2020.111023

Fossi, M.C., Panti, C., Guerranti, C., Coppola, D., Giannetti, M., Marsili, L., Minutoli, R., 2012. Are baleen whales exposed to the threat of microplastics? A case study of the Mediterranean fin whale (Balaenoptera physalus). Mar. Pollut. Bull. 64, 2374–2379. https://doi.org/10.1016/j.marpolbul.2012.08.013

Francalanci, S., Paris, E., Solari, L., 2021. On the prediction of settling velocity for plastic particles of different shapes. Environ. Pollut. 290, 118068. https://doi.org/10.1016/J.ENVPOL.2021.118068

Frei, S., Piehl, S., Gilfedder, B.S., Löder, M.G.J., Krutzke, J., Wilhelm, L., Laforsch, C., 2019. Occurence of microplastics in the hyporheic zone of rivers. Sci. Reports 2019 91 9, 1–

11. https://doi.org/10.1038/s41598-019-51741-5

Gacia, E., Duarte, C.M., 2001. Sediment retention by a Mediterranean Posidonia oceanica meadow: The balance between deposition and resuspension. Estuar. Coast. Shelf Sci. 52, 505–514. https://doi.org/10.1006/ecss.2000.0753

Galloway, T.S., Cole, M., Lewis, C., 2017. Interactions of microplastic debris throughout the marine ecosystem. Nat. Ecol. Evol. https://doi.org/10.1038/s41559-017-0116

Garcés-Ordóñez, O., Castillo-Olaya, V.A., Granados-Briceño, A.F., Blandón García, L.M., Espinosa Díaz, L.F., 2019. Marine litter and microplastic pollution on mangrove soils of the Ciénaga Grande de Santa Marta, Colombian Caribbean. Mar. Pollut. Bull. 145, 455–462. https://doi.org/10.1016/j.marpolbul.2019.06.058

Ghisalberti, M., 2002. Mixing layers and coherent structures in vegetated aquatic flows. J. Geophys. Res. 107. https://doi.org/10.1029/2001jc000871

Goss, H., Jaskiel, J., Rotjan, R., 2018. Thalassia testudinum as a potential vector for incorporating microplastics into benthic marine food webs. Mar. Pollut. Bull. 135, 1085–1089. https://doi.org/10.1016/j.marpolbul.2018.08.024

Graham, N.A.J., Nash, K.L., 2013. The importance of structural complexity in coral reef ecosystems. Coral Reefs 32, 315–326. https://doi.org/10.1007/s00338-012-0984-y

Gupta, A., 2022. Chapter 22 The Mekong River : Morphology , Evolution , Management, in: Large Rivers: Geomorphology and Management, Second Edition, Second Edition. pp. 661–686.

Gupta, A., 2009. Chapter 3: Geology and landforms of the Mekong Basin, in: The Mekong. pp. 29–51.

Gupta, A. (Ed. ., 2008. Large rivers: geomorphology and management. John Wiley & Sons.

Gupta, A., Liew, S.C., 2007. The Mekong from satellite imagery: A quick look at a large river. Geomorphology 85, 259–274. https://doi.org/10.1016/j.geomorph.2006.03.036

Haberstroh, C.J., Arias, M.E., Yin, Z., Sok, T., Wang, M.C., 2021a. Plastic transport in a complex confluence of the Mekong River in Cambodia. Environ. Res. Lett. 16. https://doi.org/10.1088/1748-9326/ac2198

Haberstroh, C.J., Arias, M.E., Yin, Z., Wang, M.C., 2021b. Effects of hydrodynamics on the cross-sectional distribution and transport of plastic in an urban coastal river. Water Environ. Res. 93, 186–200. https://doi.org/10.1002/WER.1386

Hackney, C.R., Darby, S.E., Parsons, D.R., Leyland, J., Best, J.L., Aalto, R., Nicholas, A.P., Houseago, R.C., 2020. River bank instability from unsustainable sand mining in the lower Mekong River. Nat. Sustain. 3, 217–225.

Hall, N.M., Berry, K.L.E., Rintoul, L., Hoogenboom, M.O., 2015. Microplastic ingestion by scleractinian corals. Mar. Biol. 162, 725–732. https://doi.org/10.1007/s00227-015-2619-7

Halls, A.., Conlan, I., Wisesjindawat, W., Phouthavongs, K., Viravong, S., Chan, S., Vu, V.., 2013. Atlas of deep pools of the lower Mekong River. Mekong River Commision Tech. Pap. 31, 69.

Hamed, A.M., Sadowski, M.J., Nepf, H.M., Chamorro, L.P., 2017. Impact of height heterogeneity on canopy turbulence. J. Fluid Mech. 813, 1176–1196. https://doi.org/10.1017/jfm.2017.22

Han, M., Niu, X., Tang, M., Zhang, B.T., Wang, G., Yue, W., Kong, X., Zhu, J., 2020. Distribution of microplastics in surface water of the lower Yellow River near estuary. Sci. Total Environ. 707, 135601. https://doi.org/10.1016/j.scitotenv.2019.135601

Harris, P.T., 2020. The fate of microplastic in marine sedimentary environments: A review and synthesis. Mar. Pollut. Bull. https://doi.org/10.1016/j.marpolbul.2020.111398

Heck Jr., K.L., Hays, G., Orth, R.J., 2003. Crital evaluation of the nursary role hypothsis for seagrass medows. Mar. Ecol. Prog. Ser. 253, 123–136.

Hidalgo-Ruz, V., Thiel, M., 2012. Microplastics in the Marine Environment: A Review of the Methods Used for Identification and Quantification Cellular Effects of microplastics-uptake, fate and pathologies View project. https://doi.org/10.1021/es2031505

Hierl, F., Wu, H.C., Westphal, H., 2021. Scleractinian corals incorporate microplastic particles: identification from a laboratory study. Environ. Sci. Pollut. Res. 2021 2828 28, 37882–37893. https://doi.org/10.1007/S11356-021-13240-X

Hoang, L.P., Lauri, H., Kummu, M., Koponen, J., Van Vliet, M.T.H., Supit, I., Leemans, R., Kabat, P., Ludwig, F., 2016. Mekong River flow and hydrological extremes under climate change. Hydrol. Earth Syst. Sci 20, 3027–3041. https://doi.org/10.5194/hess-20-3027-2016

Hoellein, T., Rojas, M., Pink, A., Gasior, J., Kelly, J., 2014. Anthropogenic litter in urban freshwater ecosystems: Distribution and microbial interactions. PLoS One 9, e98485. https://doi.org/10.1371/journal.pone.0098485

Hoellein, T.J., Rochman, C.M., 2021. The “plastic cycle”a watershed-scale model of plastic pools and fluxes. Front. Ecol. Environ. 19, 176–183.

Hoellein, T.J., Shogren, A.J., Tank, J.L., Risteca, P., Kelly, J.J., 2019. Microplastic deposition velocity in streams follows patterns for naturally occurring allochthonous particles. Sci. Rep. 9. https://doi.org/10.1038/s41598-019-40126-3

Holtgrieve, G.W., Arias, M.E., Irvine, K.N., Lamberts, D., Ward, E.J., Kummu, M., Koponen, J., Sarkkula, J., Richey, J.E., 2013. Patterns of Ecosystem Metabolism in the Tonle Sap Lake, Cambodia with Links to Capture Fisheries. PLoS One 8, e71395. https://doi.org/10.1371/journal.pone.0071395

Hortle, K.G., 2009. Chater 9: Fisheries of the Mekong river basin, in: The Mekong. pp. 197–249.

Horton, A.A., Dixon, S.J., 2018. Microplastics: An introduction to environmental transport processes. WIREs Water 5. https://doi.org/10.1002/wat2.1268

Horton, A.A., Jürgens, M.D., Lahive, E., van Bodegom, P.M., Vijver, M.G., 2018. The influence of exposure and physiology on microplastic ingestion by the freshwater fish Rutilus rutilus (roach) in the River Thames, UK. Environ. Pollut. 236, 188–194. https://doi.org/10.1016/j.envpol.2018.01.044

Horton, A.A., Svendsen, C., Williams, R.J., Spurgeon, D.J., Lahive, E., 2017a. Large microplastic particles in sediments of tributaries of the River Thames, UK – Abundance, sources and methods for effective quantification. Mar. Pollut. Bull. 114, 218–226. https://doi.org/10.1016/j.marpolbul.2016.09.004

Horton, A.A., Svendsen, C., Williams, R.J., Spurgeon, D.J., Lahive, E., 2017b. Large microplastic particles in sediments of tributaries of the River Thames, UK – Abundance, sources and methods for effective quantification. Mar. Pollut. Bull. https://doi.org/10.1016/j.marpolbul.2016.09.004

Horton, A.A., Walton, A., Spurgeon, D.J., Lahive, E., Svendsen, C., 2017c. Microplastics in freshwater and terrestrial environments: Evaluating the current understanding to identify the knowledge gaps and future research priorities. Sci. Total Environ. 586, 127–141. https://doi.org/10.1016/j.scitotenv.2017.01.190

Houseago, R.C., 2021. On the hydrodynamics if flexible vegetation canopies. University of Hull.

Houseago, R.C., Hong, L., Cheng, S., Best, J.L., Parsons, D.R., Chamorro, L.P., 2022. On the turbulence dynamics induced by a surrogate seagrass canopy. J. Fluid Mech. 934, 1–23. https://doi.org/10.1017/jfm.2021.1142

Huang, W., Chen, M., Song, B., Deng, J., Shen, M., Chen, Q., Zeng, G., Liang, J., 2021. Microplastics in the coral reefs and their potential impacts on corals: A mini-review. Sci. Total Environ. 762, 143112. https://doi.org/10.1016/j.scitotenv.2020.143112

Huang, Y., Xiao, X., Effiong, K., Xu, C., Su, Z., Hu, J., Jiao, S., Holmer, M., 2021. New Insights into the Microplastic Enrichment in the Blue Carbon Ecosystem: Evidence from Seagrass Meadows and Mangrove Forests in Coastal South China Sea. Environ. Sci. Technol. 55, 4804–4812. https://doi.org/10.1021/ACS.EST.0C07289

Huang, Y., Xiao, X., Xu, C., Perianen, Y.D., Hu, J., Holmer, M., 2020. Seagrass beds acting as a trap of microplastics - Emerging hotspot in the coastal region? Environ. Pollut. 257. https://doi.org/10.1016/j.envpol.2019.113450

Hughes, T.P., Barnes, M.L., Bellwood, D.R., Cinner, J.E., Cumming, G.S., Jackson, J.B.C., Kleypas, J., Van De Leemput, I.A., Lough, J.M., Morrison, T.H., Palumbi, S.R., Van Nes, E.H., Scheffer, M., 2017. Coral reefs in the Anthropocene. Nature 546, 82–90. https://doi.org/10.1038/nature22901

Hurley, R., Woodward, J., Rothwell, J.J., 2018. Microplastic contamination of river beds significantly reduced by catchment-wide flooding. Nat. Geosci. 11, 251–257. https://doi.org/10.1038/s41561-018-0080-1

IUCN, 2009. Staghorn Corals and Climate Change.

Ivens Portela, L., Ramos, S., Trigo Teixeira, A., 2013. Effect of salinity on the settling velocity of fine sediments of a harbour basin. J. Coast. Res. 165, 1188–1193. https://doi.org/10.2112/SI65-201.1

Jabeen, K., Su, L., Li, J., Yang, D., Tong, C., Mu, J., Shi, H., 2017. Microplastics and mesoplastics in fish from coastal and fresh waters of China. Environ. Pollut. 221, 141–149. https://doi.org/10.1016/j.envpol.2016.11.055

Jambeck, J.R., Geyer, R., Wilcox, C., Siegler, T.R., Perryman, M., Andrady, A., Narayan, R., Law, K.L., 2015. Plastic waste inputs from land into the ocean. Science (80-. ). 347, 768–771. https://doi.org/10.1126/science.1260352

Jeyasanta, K.I., Patterson, J., Grimsditch, G., Edward, J.K.P., 2020. Occurrence and characteristics of microplastics in the coral reef, sea grass and near shore habitats of Rameswaram Island, India. Mar. Pollut. Bull. 160. https://doi.org/10.1016/j.marpolbul.2020.111674

Jiang, C., Yin, L., Li, Z., Wen, X., Luo, X., Hu, S., Yang, H., Long, Y., Deng, B., Huang, L., Liu, Y., 2019. Microplastic pollution in the rivers of the Tibet Plateau. Environ. Pollut. 249, 91–98. https://doi.org/10.1016/j.envpol.2019.03.022

Johansen, J.L., 2014. Quantifying water flow within aquatic ecosystems using load cell sensors: A profile of currents experienced by coral reef organisms around Lizard Island, Great Barrier Reef, Australia. PLoS One 9. https://doi.org/10.1371/journal.pone.0083240

Kaiser, D., Estelmann, A., Kowalski, N., Glockzin, M., Waniek, J.J., 2019. Sinking velocity of sub-millimeter microplastic. Mar. Pollut. Bull. 139, 214–220. https://doi.org/10.1016/J.MARPOLBUL.2018.12.035

Kaiser, D., Kowalski, N., Waniek, J.J., 2017. Effects of biofouling on the sinking behavior of microplastics. Environ. Res. Lett. 12. https://doi.org/10.1088/1748-9326/aa8e8b

Kane, I.A., Clare, M.A., 2019. Dispersion, Accumulation, and the Ultimate Fate of Microplastics in Deep-Marine Environments: A Review and Future Directions. Front.

Earth Sci. 7. https://doi.org/10.3389/feart.2019.00080

Karlsson, T.M., Vethaak, A.D., Almroth, B.C., Ariese, F., van Velzen, M., Hassellöv, M., Leslie, H.A., 2017. Screening for microplastics in sediment, water, marine invertebrates and fish: Method development and microplastic accumulation. Mar. Pollut. Bull. 122, 403–408. https://doi.org/10.1016/J.MARPOLBUL.2017.06.081

Karpova, E., Abliazov, E., Statkevich, S., Dinh, C.N., 2022. Features of the accumulation of macroplastic on the river bottom in the Mekong delta and the impact on fish and decapods. Environ. Pollut. 297, 118747. https://doi.org/10.1016/J.ENVPOL.2021.118747

Kasamesiri, P., Thaimuangpho, W., 2020. Microplastics ingestion by freshwater fish in the Chi River, Thailand. Int. J. GEOMATE 18, 114–119. https://doi.org/10.21660/2020.67.9110

Kataoka, T., Nihei, Y., Kudou, K., Hinata, H., 2019. Assessment of the sources and inflow processes of microplastics in the river environments of Japan. Environ. Pollut. 244, 958–965. https://doi.org/10.1016/j.envpol.2018.10.111

Khan, F.R., Shashoua, Y., Crawford, A., Drury, A., Sheppard, K., Stewart, K., Sculthorp, T., 2020. “The plastic nile”: First evidence of microplastic contamination in fish from the nile river (Cairo, Egypt). Toxics 8. https://doi.org/10.3390/TOXICS8020022

Khatmullina, L., Isachenko, I., 2017. Settling velocity of microplastic particles of regular shapes. Mar. Pollut. Bull. 114, 871–880. https://doi.org/10.1016/j.marpolbul.2016.11.024

Kingston, D.G., Thompson, J.R., Kite, G., 2011. Uncertainty in climate change projections of discharge for the Mekong River Basin. Hydrol. Earth Syst. Sci. 15, 1459–1471. https://doi.org/10.5194/hess-15-1459-2011

Kooi, M., Van Nes, E.H., Scheffer, M., Koelmans, A.A., 2017. Ups and Downs in the Ocean: Effects of Biofouling on Vertical Transport of Microplastics. Environ. Sci. Technol. 51, 7963–7971. https://doi.org/10.1021/acs.est.6b04702

Kowalski, N., Reichardt, A.M., Waniek, J.J., 2016. Sinking rates of microplastics and potential implications of their alteration by physical, biological, and chemical factors. Mar. Pollut. Bull. 109, 310–319. https://doi.org/10.1016/j.marpolbul.2016.05.064

Krishnakumar, S., Anbalagan, S., Hussain, S.M., Bharani, R., Godson, P.S., Srinivasalu, S., 2021. Coral annual growth band impregnated microplastics (Porites sp.): a first investigation report. Wetl. Ecol. Manag. 29, 677–687. https://doi.org/10.1007/s11273-021-09786-9

Kumar, R., Sharma, P., Manna, C., Jain, M., 2021. Abundance, interaction, ingestion, ecological concerns, and mitigation policies of microplastic pollution in riverine ecosystem: A review. Sci. Total Environ. 782, 146695. https://doi.org/10.1016/j.scitotenv.2021.146695

Kummu, M., Sarkkula, J., 2008. Impact of the Mekong River flow alteration on the Tonle Sap flood pulse. Ambio 37, 185–92. https://doi.org/10.2307/25547881

Lagarde, F., Olivier, O., Zanella, M., Daniel, P., Hiard, S., Caruso, A., 2016. Microplastic interactions with freshwater microalgae: Hetero-aggregation and changes in plastic density appear strongly dependent on polymer type. Environ. Pollut. 215, 331–339. https://doi.org/10.1016/J.ENVPOL.2016.05.006

Lamb, J.B., Willis, B.L., Fiorenza, E.A., Couch, C.S., Howard, R., Rader, D.N., True, J.D., Kelly, L.A., Ahmad, A., Jompa, J., Harvell, C.D., 2018. Plastic waste associated with disease on coral reefs. Science 359, 460–462. https://doi.org/10.1126/science.aar3320

Laursen, S.N., Fruergaard, M., Andersen, T.J., 2022. Rapid flocculation and settling of

positively buoyant microplastic and fine-grained sediment in natural seawater. Mar. Pollut. Bull. 178, 113619. https://doi.org/10.1016/j.marpolbul.2022.113619

Lebreton, L.C.M., Van Der Zwet, J., Damsteeg, J.W., Slat, B., Andrady, A., Reisser, J., 2017. River plastic emissions to the world's oceans. Nat. Commun. 8, 15611. https://doi.org/10.1038/ncomms15611

Lechner, A., Ramler, D., 2015. The discharge of certain amounts of industrial microplastic from a production plant into the River Danube is permitted by the Austrian legislation. Environ. Pollut. https://doi.org/10.1016/j.envpol.2015.02.019

Lefcheck, J.S., Hughes, B.B., Johnson, A.J., Pfirrmann, B.W., Rasher, D.B., Smyth, A.R., Williams, B.L., Beck, M.W., Orth, R.J., 2019. Are coastal habitats important nurseries? A meta-analysis. Conserv. Lett. 12. https://doi.org/10.1111/conl.12645

Lefebvre, A., Thompson, C.E.L., Amos, C.L., 2010. Influence of Zostera marina canopies on unidirectional flow, hydraulic roughness and sediment movement. Cont. Shelf Res. 30, 1783–1794. https://doi.org/10.1016/j.csr.2010.08.006

Lenaker, P.L., Baldwin, A.K., Corsi, S.R., Mason, S.A., Reneau, P.C., Scott, J.W., 2019. Vertical Distribution of Microplastics in the Water Column and Surficial Sediment from the Milwaukee River Basin to Lake Michigan. Environ. Sci. Technol. 53, 12227–12237. https://doi.org/10.1021/ACS.EST.9B03850/SUPPL_FILE/ES9B03850_SI_001.PDF

Lenth, R. V., 2016. Least-Squares Means: The R Package lsmeans. J. Stat. Softw. 69, 1–33. https://doi.org/10.18637/JSS.V069.I01

Lewis, S.L., Maslin, M.A., 2015. Defining the Anthropocene. Nature. https://doi.org/10.1038/nature14258

Li, J., Yang, D., Li, L., Jabeen, K., Shi, H., 2015. Microplastics in commercial bivalves from China. Environ. Pollut. 207, 190–195. https://doi.org/10.1016/j.envpol.2015.09.018

Li, J., Zhang, H., Zhang, K., Yang, R., Li, R., Li, Y., 2018. Characterization, source, and retention of microplastic in sandy beaches and mangrove wetlands of the Qinzhou Bay, China. Mar. Pollut. Bull. 136, 401–406. https://doi.org/10.1016/j.marpolbul.2018.09.025

Li, M., He, L., Zhang, X., Rong, H., Tong, M., 2020. Different surface charged plastic particles have different cotransport behaviors with kaolinite ☆particles in porous media. Environ. Pollut. 267, 115534. https://doi.org/10.1016/j.envpol.2020.115534

Li, X., Liu, J.P., Saito, Y., Nguyen, V.L., 2017. Recent evolution of the Mekong Delta and the impacts of dams. Earth-Science Rev. https://doi.org/10.1016/j.earscirev.2017.10.008

Li, Y., Wang, X., Fu, W., Xia, X., Liu, C., Min, J., Zhang, W., Crittenden, J.C., 2019. Interactions between nano/micro plastics and suspended sediment in water: Implications on aggregation and settling. Water Res. 161, 486–495. https://doi.org/10.1016/j.watres.2019.06.018

Lin, L., Zuo, L.Z., Peng, J.P., Cai, L.Q., Fok, L., Yan, Y., Li, H.X., Xu, X.R., 2018. Occurrence and distribution of microplastics in an urban river: A case study in the Pearl River along Guangzhou City, China. Sci. Total Environ. 644, 375–381. https://doi.org/10.1016/j.scitotenv.2018.06.327

Link, O., González, C., Maldonado, M., Escauriaza, C., 2012. Coherent structure dynamics and sediment particle motion around a cylindrical pier in developing scour holes. Acta Geophys. 60, 1689–1719. https://doi.org/10.2478/s11600-012-0068-y

Liu, Y., You, J.A., Li, Y.J., Zhang, J. Di, He, Y., Breider, F., Tao, S., Liu, W.X., 2021. Insights into the horizontal and vertical profiles of microplastics in a river emptying into the sea affected by intensive anthropogenic activities in Northern China. Sci. Total Environ. 779, 146589. https://doi.org/10.1016/J.SCITOTENV.2021.146589

Lobelle, D., Cunliffe, M., 2011. Early microbial biofilm formation on marine plastic debris.pdf. Mar. Pollut. Bull. 62, 197–200.

Long, M., Moriceau, B., Gallinari, M., Lambert, C., Huvet, A., Raffray, J., Soudant, P., 2015. Interactions between microplastics and phytoplankton aggregates: Impact on their respective fates. Mar. Chem. 175, 39–46. https://doi.org/10.1016/j.marchem.2015.04.003

Lowe, R.J., Koseff, J.R., Monismith, S.G., 2005. Oscillatory flow through submerged canopies: 1. Velocity structure. J. Geophys. Res. C Ocean. 110, 1–17. https://doi.org/10.1029/2004JC002788

Lusher, A.L., McHugh, M., Thompson, R.C., 2013. Occurrence of microplastics in the gastrointestinal tract of pelagic and demersal fish from the English Channel. Mar. Pollut. Bull. 67, 94–99. https://doi.org/10.1016/J.MARPOLBUL.2012.11.028

Lusher, A.L., Tirelli, V., O'Connor, I., Officer, R., 2015. Microplastics in Arctic polar waters: The first reported values of particles in surface and sub-surface samples. Sci. Rep. 5, 1–9. https://doi.org/10.1038/srep14947

Manning, A.J., Baugh, J. V., Spearman, J.R., Whitehouse, R.J.S., 2010a. Flocculation settling Characteristics of mud: Sand mixtures. Ocean Dyn. 60, 237–253. https://doi.org/10.1007/s10236-009-0251-0

Manning, A.J., Friend, P.L., Prowse, N., Amos, C.L., 2007. Estuarine mud flocculation properties determined using an annular mini-flume and the LabSFLOC system. Cont. Shelf Res. 27, 1080–1095. https://doi.org/10.1016/j.csr.2006.04.011

Manning, A.J., Langston, W.J., Jonas, P.J.C., 2010b. A review of sediment dynamics in the Severn Estuary: Influence of flocculation. Mar. Pollut. Bull. 61, 37–51. https://doi.org/10.1016/j.marpolbul.2009.12.012

Manning, A.J., Schoellhamer, D.H., 2013. Factors controlling floc settling velocity along a longitudinal estuarine transect. Mar. Geol. 345, 266–280. https://doi.org/10.1016/j.margeo.2013.06.018

Martin, C., Corona, E., Mahadik, G.A., Duarte, C.M., 2019a. Adhesion to coral surface as a potential sink for marine microplastics. Environ. Pollut. 255. https://doi.org/10.1016/j.envpol.2019.113281

Martin, C., Corona, E., Mahadik, G.A., Duarte, C.M., 2019b. Adhesion to coral surface as a potential sink for marine microplastics. Environ. Pollut. 255, 113281. https://doi.org/10.1016/j.envpol.2019.113281

MATLAB, 2020. MATLAB.

McCormick, A.R., Hoellein, T.J., London, M.G., Hittie, J., Scott, J.W., Kelly, J.J., 2016. Microplastic in surface waters of urban rivers: Concentration, sources, and associated bacterial assemblages. Ecosphere 7. https://doi.org/10.1002/ecs2.1556

McIlgorm, A., Campbell, H.F., Rule, M.J., 2011. The economic cost and control of marine debris damage in the Asia-Pacific region. Ocean Coast. Manag. 54, 643–651. https://doi.org/10.1016/j.ocecoaman.2011.05.007

McNeish, R.E., Kim, L.H., Barrett, H.A., Mason, S.A., Kelly, J.J., Hoellein, T.J., 2018. Microplastic in riverine fish is connected to species traits. Sci. Rep. 8. https://doi.org/10.1038/s41598-018-29980-9

Mei, W., Chen, G., Bao, J., Song, M., Li, Y., Luo, C., 2020. Interactions between microplastics and organic compounds in aquatic environments: A mini review. Sci. Total Environ. https://doi.org/10.1016/j.scitotenv.2020.139472

Meijer, L.J.J., van Emmerik, T., van der Ent, R., Schmidt, C., Lebreton, L., 2021. More than

1000 rivers account for 80% of global riverine plastic emissions into the ocean. Sci. Adv. 7. https://doi.org/10.1126/sciadv.aaz5803

Mekong River Commission, 2021. Measured.Total Suspended Solids@Can Tho [WWW Document]. Mekong River Comm. Data Portal. URL https://portal.mrcmekong.org/time-series/chart?ts=444f7943518144e28be23e10943151bb&sd=2000-01-01&ed=2021-12-14

Mendoza, R.L.M., Balcer, M., 2018. Microplastics in freshwater environments: A review of quantification assessment. TrAC Trends Anal. Chem. https://doi.org/10.1016/J.TRAC.2018.10.020

Mendrik, F., Fernández, R., Waller, C., Hackney, C., Parsons, D., 2022. Shifting settling regimes of aquatic microplastics. Res. Sq. Prepr.

Mendrik, F.M., Henry, T.B., Burdett, H., Hackney, C.R., Waller, C., Parsons, D.R., Hennige, S.J., 2021. Species-specific impact of microplastics on coral physiology. Environ. Pollut. 269, 116238. https://doi.org/https://doi.org/10.1016/j.envpol.2020.116238

Meyer-Peter, E., Meeting, R.M.-I. 2nd, Stockholm, U., 1948, U., 1993. Formulas for bed-load transport. Coast. Eng. 2613–2628.

Meysick, L., Infantes, E., Boström, C., 2019. The influence of hydrodynamics and ecosystem engineers on eelgrass seed trapping. PLoS One 14. https://doi.org/10.1371/JOURNAL.PONE.0222020

Mietta, F., Chassagne, C., Manning, A.J., Winterwerp, J.C., 2009. Influence of shear rate, organic matter content, pH and salinity on mud flocculation. Ocean Dyn. 59, 751–763. https://doi.org/10.1007/S10236-009-0231-4

Moberg, F., Folke, C., 1999. Ecological goods and services of coral reef ecosystems. Ecol. Econ. 29, 215–233. https://doi.org/10.1016/S0921-8009(99)00009-9

Möhlenkamp, P., Purser, A., Thomsen, L., 2018. Plastic microbeads from cosmetic products: An experimental study of their hydrodynamic behaviour, vertical transport and resuspension in phytoplankton and sediment aggregates. Elementa 6. https://doi.org/10.1525/elementa.317

Monismith, S.G., 2007. Hydrodynamics of coral reefs. Annu. Rev. Fluid Mech. 39, 37–55. https://doi.org/10.1146/annurev.fluid.38.050304.092125

Morét-Ferguson, S., Law, K.L., Proskurowski, G., Murphy, E.K., Peacock, E.E., Reddy, C.M., 2010. The size, mass, and composition of plastic debris in the western North Atlantic Ocean. Mar. Pollut. Bull. 60, 1873–1878. https://doi.org/10.1016/j.marpolbul.2010.07.020

Mouchi, V., Chapron, L., Peru, E., Pruski, A.M., Meistertzheim, A.-L., Vétion, G., Galand, P.E., Lartaud, F., 2019. Long-term aquaria study suggests species-specific responses of two cold-water corals to macro-and microplastics exposure. Environ. Pollut. 253, 322–329. https://doi.org/10.1016/J.ENVPOL.2019.07.024

Munari, C., Infantini, V., Scoponi, M., Rastelli, E., Corinaldesi, C., Mistri, M., 2017. Microplastics in the sediments of Terra Nova Bay (Ross Sea, Antarctica). Mar. Pollut. Bull. 122, 161–165. https://doi.org/10.1016/j.marpolbul.2017.06.039

Murray, F., Cowie, P.R., 2011. Plastic contamination in the decapod crustacean Nephrops norvegicus (Linnaeus, 1758). Mar. Pollut. Bull. 62, 1207–1217. https://doi.org/10.1016/J.MARPOLBUL.2011.03.032

Nadal, M.A., Alomar, C., Deudero, S., 2016. High levels of microplastic ingestion by the semipelagic fish bogue Boops boops (L.) around the Balearic Islands. Environ. Pollut. 214, 517–523. https://doi.org/10.1016/J.ENVPOL.2016.04.054

Näkki, P., Setälä, O., Lehtiniemi, M., 2017. Bioturbation transports secondary microplastics to deeper layers in soft marine sediments of the northern Baltic Sea. Mar. Pollut. Bull. 119, 255–261. https://doi.org/10.1016/j.marpolbul.2017.03.065

Napper, I.E., Baroth, A., Barrett, A.C., Bhola, S., Chowdhury, G.W., Davies, B.F.R., Duncan, E.M., Kumar, S., Nelms, S.E., Hasan Niloy, M.N., Nishat, B., Maddalene, T., Thompson, R.C., Koldewey, H., 2021. The abundance and characteristics of microplastics in surface water in the transboundary Ganges River. Environ. Pollut. 274, 116348. https://doi.org/10.1016/J.ENVPOL.2020.116348

Napper, I.E., Thompson, R.C., 2016. Release of synthetic microplastic plastic fibres from domestic washing machines: Effects of fabric type and washing conditions. Mar. Pollut. Bull. 112, 39–45. https://doi.org/10.1016/j.marpolbul.2016.09.025

Navarrete-Fernández, T., Bermejo, R., Hernández, I., Deidun, A., Andreu-Cazenave, M., Cózar, A., 2022. The role of seagrass meadows in the coastal trapping of litter. Mar. Pollut. Bull. 174, 113299. https://doi.org/10.1016/j.marpolbul.2021.113299

Nepf, H.M., 2012. Flow and transport in regions with aquatic vegetation. Annu. Rev. Fluid Mech. 44, 123–142. https://doi.org/10.1146/annurev-fluid-120710-101048

Nepf, H.M., 1999. Drag, turbulence, and diffusion in flow through emergent vegetation. Water Resour. Res. 35, 479–489. https://doi.org/10.1029/1998WR900069

Neves, D., Sobral, P., Ferreira, J.L., Pereira, T., 2015. Ingestion of MPs by commercial fish off the Portuguese coast. Mar. Pollut. Bull. 101, 119–126.

Newman, S., 2015. The economics of marine litter, Marine anthropogenic litter. Springer, Cham. https://doi.org/10.1021/acs.est.9b01360

Nguyen, T.H., Kieu-Le, T.C., Tang, F.H.M., Maggi, F., 2022. Controlling factors of microplastic fibre settling through a water column. Sci. Total Environ. 838, 156011. https://doi.org/10.1016/j.scitotenv.2022.156011

Nizzetto, L., Bussi, G., Futter, M.N., Butterfield, D., Whitehead, P.G., 2016a. A theoretical assessment of microplastic transport in river catchments and their retention by soils and river sediments. Environ. Sci. Process. Impacts 18, 1050–1059. https://doi.org/10.1039/C6EM00206D

Nizzetto, L., Bussi, G., Futter, M.N., Butterfield, D., Whitehead, P.G., 2016b. A theoretical assessment of microplastic transport in river catchments and their retention by soils and river sediments. Environ. Sci. Process. Impacts 18, 1050–1059. https://doi.org/10.1039/C6EM00206D

Nuelle, M.T., Dekiff, J.H., Remy, D., Fries, E., 2014. A new analytical approach for monitoring microplastics in marine sediments. Environ. Pollut. 184, 161–169. https://doi.org/10.1016/j.envpol.2013.07.027

Oehlmann, J., Oetken, M., Schulte-Oehlmann, U., 2008. A critical evaluation of the environmental risk assessment for plasticizers in the freshwater environment in Europe, with special emphasis on bisphenol A and endocrine disruption. Environ. Res. 108, 140–149. https://doi.org/10.1016/j.envres.2008.07.016

Ogbuagu, C.C., Kassem, H., Udiba, U.U., Stead, J.L., Cundy, A.B., 2022. Role of saltmarsh systems in estuarine trapping of microplastics. Sci. Rep. 12, 1–14. https://doi.org/10.1038/s41598-022-18881-7

Ogden, W., Everard, M., 2020. Rapid 'fingerprinting' of potential sources of plastics in river systems: an example from the River Wye, UK. https://doi.org/10.1080/15715124.2020.1830783. https://doi.org/10.1080/15715124.2020.1830783

Okubo, N., Takahashi, S., Nakano, Y., 2018. Microplastics disturb the anthozoan-algae

symbiotic relationship. Mar. Pollut. Bull. 135, 83–89. https://doi.org/10.1016/j.marpolbul.2018.07.016

Otsu, N., 1979. A Threshold Selection Method from Gray-Level Histograms. IEEE Trans Syst Man Cybern SMC-9, 62–66. https://doi.org/10.1109/tsmc.1979.4310076

Pegado, T. de S. e. S., Schmid, K., Winemiller, K.O., Chelazzi, D., Cincinelli, A., Dei, L., Giarrizzo, T., 2018. First evidence of microplastic ingestion by fishes from the Amazon River estuary. Mar. Pollut. Bull. 133, 814–821. https://doi.org/10.1016/j.marpolbul.2018.06.035

Peng, G., Bai, M., Zhu, B., Li, D., Xu, P., 2017. Microplastics in freshwater river sediments in Shanghai, China: A case study of risk assessment in mega-cities. Environ. Pollut. 234, 448–456. https://doi.org/10.1016/j.envpol.2017.11.034

Pierce, K.E., Harris, R.J., Larned, L.S., Pokras, M.A., 2004. Obstruction and starvation associated with plastic ingestion in a Northern Gannet Morus bassanus and a Greater Shearwater Puffinus gravis. Mar. Ornithol. 32, 187–189.

PlasticsEurope, 2021. Plastics - the Facts 2021. An analysis of European plastics production, demand and waste data.

Prata, J.C., da Costa, J.P., Duarte, A.C., Rocha-Santos, T., 2019. Methods for sampling and detection of microplastics in water and sediment: A critical review. TrAC Trends Anal. Chem. 110, 150–159. https://doi.org/10.1016/j.trac.2018.10.029

Provencher, J.F., Bond, A.L., Mallory, M.L., 2014. Marine birds and plastic debris in Canada: a national synthesis and a way forward. Environ. Rev. 23, 1–13. https://doi.org/10.1139/er-2014-0039

Pujol, D., Colomer, J., Serra, T., Casamitjana, X., 2012. A model for the effect of submerged aquatic vegetation on turbulence induced by an oscillating grid. Estuar. Coast. Shelf Sci. 114, 23–30. https://doi.org/10.1016/j.ecss.2011.08.020

Qu, X., Su, L., Li, H., Liang, M., Shi, H., 2018. Assessing the relationship between the abundance and properties of microplastics in water and in mussels. Sci. Total Environ. 621, 679–686. https://doi.org/10.1016/j.scitotenv.2017.11.284

R Core Team, 2013. R: A language and environment for statistical computing. R Found. Stat. Comput. Vienna, Austria.

Rainboth, W.J., 1996. Fishes of the cambodian mekong. Food & Agriculture Org.

Räsänen, T., Kummu, M., 2013. Spatiotemporal influences of ENSO on precipitation and flood pulse in the Mekong River Basin. J. Hydrol. 476, 254–168.

Räsänen, T.A., Someth, P., Lauri, H., Koponen, J., Sarkkula, J., Kummu, M., 2017. Observed river discharge changes due to hydropower operations in the Upper Mekong Basin. J. Hydrol. 545, 28–41. https://doi.org/10.1016/j.jhydrol.2016.12.023

Rattanakawin, C., Hogg, R., 2001. Aggregate size distributions in flocculation. Colloids Surfaces A Physicochem. Eng. Asp. 177, 87–98. https://doi.org/10.1016/S0927-7757(00)00662-2

Razeghi, N., Hamidian, A.H., Wu, C., Zhang, Y., Yang, M., 2021. Microplastic sampling techniques in freshwaters and sediments: a review. Environ. Chem. Lett. 19, 4225–4252.

Reichert, J., Arnold, A.L., Hammer, N., Miller, I.B., Rades, M., Schubert, P., Ziegler, M., Wilke, T., 2021. Reef-building corals act as long-term sink for microplastic. Glob. Chang. Biol. 00, 1–13. https://doi.org/10.1111/GCB.15920

Reichert, J., Arnold, A.L., Hoogenboom, M.O., Schubert, P., Wilke, T., 2019. Impacts of microplastics on growth and health of hermatypic corals are species-specific. Environ.

Pollut. 254, 113074. https://doi.org/10.1016/J.ENVPOL.2019.113074

Reichert, J., Schellenberg, J., Schubert, P., Wilke, T., 2018. Responses of reef building corals to microplastic exposure. Environ. Pollut. 237, 955–960. https://doi.org/10.1016/j.envpol.2017.11.006

Reidenbach, M.A., Monismith, S.G., Koseff, J.R., Yahel, G., Genin, A., 2006. Boundary layer turbulence and flow structure over a fringing coral reef. Limnol. Oceanogr. 51, 1956–1968. https://doi.org/10.4319/lo.2006.51.5.1956

Richmond, R.H., 1993. Coral reefs: preent problems and future concerns resulting from anthropogenic disturbance. Am. Zool. 33, 524–536. https://doi.org/10.1093/icb/33.6.524

Rivera, I.A., Poduje, A.C.C., Molina-Carpio, J., Ayala, J.M., Cardenas, E.A., Espinoza-Villar, R., Espinoza, J.C., Gutierrez-Cori, O., Filizola, N., 2019. On the Relationship between Suspended Sediment Concentration, Rainfall Variability and Groundwater: An Empirical and Probabilistic Analysis for the Andean Beni River, Bolivia (2003–2016). Water 11, 16.

Rochman, C.M., Tahir, A., Williams, S.L., Baxa, D. V., Lam, R., Miller, J.T., Teh, F.-C., Werorilangi, S., Teh, S.J., 2015. Anthropogenic debris in seafood: Plastic debris and fibers from textiles in fish and bivalves sold for human consumption. Sci. Rep. 5, 14340. https://doi.org/10.1038/srep14340

Roman, L., Hardesty, B.D., Schuyler, Q., 2022. A systematic review and risk matrix of plastic litter impacts on aquatic wildlife: A case study of the Mekong and Ganges River Basins. Sci. Total Environ. 843, 156858. https://doi.org/10.1016/J.SCITOTENV.2022.156858

Rotjan, R.D., Sharp, K.H., Gauthier, A.E., Yelton, R., Baron Lopez, E.M., Carilli, J., Kagan, J.C., Urban-Rich, J., 2019. Patterns, dynamics and consequences of microplastic ingestion by the temperate coral, Astrangia poculata. Proc. R. Soc. B Biol. Sci. 286, 20190726. https://doi.org/10.1098/rspb.2019.0726

Rowley, K.H., Cucknell, A.C., Smith, B.D., Clark, P.F., Morritt, D., 2020. London's river of plastic: High levels of microplastics in the Thames water column. Sci. Total Environ. 740, 140018. https://doi.org/10.1016/J.SCITOTENV.2020.140018

Rummel, C.D., Jahnke, A., Gorokhova, E., Kühnel, D., Schmitt-Jansen, M., 2017. Impacts of Biofilm Formation on the Fate and Potential Effects of Microplastic in the Aquatic Environment. Environ. Sci. Technol. Lett. 4, 258–267. https://doi.org/10.1021/acs.estlett.7b00164

Ryan, P.G., Moore, C.J., van Franeker, J.A., Moloney, C.L., 2009. Monitoring the abundance of plastic debris in the marine environment. Philos. Trans. R. Soc. B Biol. Sci. 364, 1999–2012. https://doi.org/10.1098/rstb.2008.0207

Saliu, F., Montano, S., Garavaglia, M.G., Lasagni, M., Seveso, D., Galli, P., 2018. Microplastic and charred microplastic in the Faafu Atoll, Maldives. Mar. Pollut. Bull. 136, 464–471. https://doi.org/10.1016/J.MARPOLBUL.2018.09.023

Salmivaara, A., Kummu, M., Varis, O., Keskinen, M., 2016. Socio-Economic Changes in Cambodia's Unique Tonle Sap Lake Area: A Spatial Approach. Appl. Spat. Anal. Policy 9, 413–432. https://doi.org/10.1007/s12061-015-9157-z

Sanchez, W., Bender, C., Porcher, J.M., 2014. Wild gudgeons (Gobio gobio) from French rivers are contaminated by microplastics: Preliminary study and first evidence. Environ. Res. 128, 98–100. https://doi.org/10.1016/j.envres.2013.11.004

Santos, C.B. de los, Onoda, Y., Vergara, J.J., Pérez-Lloréns, J.L., Bouma, T.J., Nafie, Y.A. La, Cambridge, M.L., Brun, F.G., 2016. A comprehensive analysis of mechanical and morphological traits in temperate and tropical seagrass species. Mar. Ecol. Prog. Ser. 551, 81–94. https://doi.org/10.3354/MEPS11717

Sayogo, B.H., Patria, M.P., Takarina, N.D., 2020. The density of microplastic in sea cucumber (Holothuria sp.) and sediment at Tidung Besar and Bira Besar island, Jakarta. J. Phys. Conf. Ser. 1524. https://doi.org/10.1088/1742-6596/1524/1/012064

Schmidt, C., Krauth, T., Wagner, S., 2017. Export of Plastic Debris by Rivers into the Sea. Environ. Sci. Technol. 51, 12246–12253. https://doi.org/10.1021/acs.est.7b02368

Schwarz, A.E., Ligthart, T.N., Boukris, E., van Harmelen, T., 2019. Sources, transport, and accumulation of different types of plastic litter in aquatic environments: A review study. Mar. Pollut. Bull. 143, 92–100. https://doi.org/10.1016/j.marpolbul.2019.04.029

Sembiring, E., Fareza, A.A., Suendo, V., Reza, M., 2020. The Presence of Microplastics in Water, Sediment, and Milkfish (Chanos chanos) at the Downstream Area of Citarum River, Indonesia. Water. Air. Soil Pollut. 231. https://doi.org/10.1007/s11270-020-04710-y

Setälä, O., Fleming-Lehtinen, V., Lehtiniemi, M., 2014. Ingestion and transfer of microplastics in the planktonic food web. Environ. Pollut. 185, 77–83. https://doi.org/10.1016/j.envpol.2013.10.013

Silva-Cavalcanti, J.S., Silva, J.D.B., França, E.J. de, Araújo, M.C.B. de, Gusmão, F., 2017. Microplastics ingestion by a common tropical freshwater fishing resource. Environ. Pollut. 221, 218–226. https://doi.org/10.1016/j.envpol.2016.11.068

Skalska, K., Ockelford, A., Ebdon, J.E., Cundy, A.B., 2020. Riverine microplastics: Behaviour, spatio-temporal variability, and recommendations for standardised sampling and monitoring. J. Water Process Eng. 38. https://doi.org/10.1016/j.jwpe.2020.101600

Slootmaekers, B., Catarci Carteny, C., Belpaire, C., Saverwyns, S., Fremout, W., Blust, R., Bervoets, L., 2019. Microplastic contamination in gudgeons (Gobio gobio) from Flemish rivers (Belgium). Environ. Pollut. 244, 675–684. https://doi.org/10.1016/j.envpol.2018.09.136

Smith, M., Love, D.C., Rochman, C.M., Neff, R.A., 2018. Microplastics in Seafood and the Implications for Human Health. Curr. Environ. Heal. reports 5, 375–386. https://doi.org/10.1007/s40572-018-0206-z

Stead, J.L., Cundy, A.B., Hudson, M.D., Thompson, C.E.L., Williams, I.D., Russell, A.E., Pabortsava, K., 2020. Identification of tidal trapping of microplastics in a temperate salt marsh system using sea surface microlayer sampling. Sci. Rep. 10, 1–10. https://doi.org/10.1038/s41598-020-70306-5

Stock, F., Kochleus, C., Bänsch-Baltruschat, B., Brennholt, N., Reifferscheid, G., 2019. Sampling techniques and preparation methods for microplastic analyses in the aquatic environment – A review. TrAC Trends Anal. Chem. 113, 84–92. https://doi.org/10.1016/j.trac.2019.01.014

Su, L., Deng, H., Li, B., Chen, Q., Pettigrove, V., Wu, C., Shi, H., 2019. The occurrence of microplastic in specific organs in commercially caught fishes from coast and estuary area of east China. J. Hazard. Mater. 365, 716–724. https://doi.org/10.1016/j.jhazmat.2018.11.024

Sun, J., Dai, X., Wang, Q., van Loosdrecht, M.C.M., Ni, B.J., 2019. Microplastics in wastewater treatment plants: Detection, occurrence and removal. Water Res. 152, 21–37. https://doi.org/10.1016/j.watres.2018.12.050

Sussarellu, R., Suquet, M., Thomas, Y., Lambert, C., Fabioux, C., Pernet, M.E.J., Le Goïc, N., Quillien, V., Mingant, C., Epelboin, Y., Corporeau, C., Guyomarch, J., Robbens, J., Paul-Pont, I., Soudant, P., Huvet, A., 2016. Oyster reproduction is affected by exposure to polystyrene microplastics. Proc. Natl. Acad. Sci. U. S. A. 113, 2430–5. https://doi.org/10.1073/pnas.1519019113

Sweet, M., Martin, S., Joleah, L., 2019. Plastics and Shallow water coral reefs. https://doi.org/10.13140/RG.2.2.29699.14880.

Tahir, A., Soeprapto, D.A., Sari, K., Wicaksono, E.A., Werorilangi, S., 2020. Microplastic assessment in Seagrass ecosystem at Kodingareng Lompo Island of Makassar City. IOP Conf. Ser. Earth Environ. Sci. 564. https://doi.org/10.1088/1755-1315/564/1/012032

Tan, F., Yang, H., Xu, X., Fang, Z., Xu, H., Shi, Q., Zhang, X., Wang, G., Lin, L., Zhou, S., Huang, L., Li, H., 2020. Microplastic pollution around remote uninhabited coral reefs of Nansha Islands, South China Sea. Sci. Total Environ. 725, 138383. https://doi.org/10.1016/j.scitotenv.2020.138383

Thompson, R.C., Olson, Y., Mitchell, R.P., Davis, A., Rowland, S.J., John, A.W.G., McGonigle, D., Russell, A.E., 2004. Lost at Sea: Where Is All the Plastic? Science (80-. ). 304, 838. https://doi.org/10.1126/science.1094559

Tinoco, R.O., Coco, G., 2016. A laboratory study on sediment resuspension within arrays of rigid cylinders. Adv. Water Resour. 92, 1–9. https://doi.org/10.1016/j.advwatres.2016.04.003

Uhm, Y., 2020. Plastic Waste Trade in Southeast Asia after China's Import Ban: Implications of the New Basel Convention Amendment and Recommendations for the Future. Cal. WL Rev. 57.

UNEP, U.N.E.P., 2014. Valuing Plastics: The Business Case for Measuring, Managing and Disclosing Plastic Use in the Consumer Goods Industry.

Unsworth, R.K.F., Higgs, A., Walter, B., Cullen-Unsworth, L.C., Inman, I., Jones, B.L., 2021. Canopy Accumulation: Are Seagrass Meadows a Sink of Microplastics? Ocean. 2021, Vol. 2, Pages 162-178 2, 162–178. https://doi.org/10.3390/OCEANS2010010

Utami, D.A., Reuning, L., Konechnaya, O., Schwarzbauer, J., 2021. Microplastics as a sedimentary component in reef systems: A case study from the Java Sea. Sedimentology. https://doi.org/10.1111/sed.12879

Valbo-Jørgensen, J., 2002. THE MRC MEKONG FISH DATABASE: An Information Base on Fish of a Major International River Basin ADD-INFO: Assessment of Data-limiteD INland Fish stOcks View project Climate change and inland fisheries View project, researchgate.net.

Valbo-Jørgensen, J., Coates, D., Hortle, K., 2009. Fish diversity in the Mekong River basin, in: TThe Mekong. Academic Press, pp. 161–196.

Van Cauwenberghe, L., Janssen, C.R., 2014. Microplastics in bivalves cultured for human consumption. Environ. Pollut. 193, 65–70. https://doi.org/10.1016/j.envpol.2014.06.010

van Emmerik, T., Strady, E., Kieu-Le, T.C., Nguyen, L., Gratiot, N., 2019. Seasonality of riverine macroplastic transport. Sci. Rep. 9. https://doi.org/10.1038/s41598-019-50096-1

Van Melkebeke, M., Janssen, C., De Meester, S., 2020. Characteristics and Sinking Behavior of Typical Microplastics including the Potential Effect of Biofouling: Implications for Remediation. Environ. Sci. Technol. 54, 8668–8680. https://doi.org/10.1021/acs.est.9b07378

Van Rijn, L., Kroon, A., 1993. Sediment transport by currents and waves, in: Proceedings of the Coastal Engineering Conference. American Society of Civil Engineers, pp. 2613–2628. https://doi.org/10.1061/9780872629332.199

van Wiechen, P.P.J., 2020a. Wave dissipation on a fringing coral reef An experimental study 154.

van Wiechen, P.P.J., 2020b. Wave dissipation on a complex coral reef: An experimental study. Delft University of Technology.

Varis, O., Kummu, M., Salmivaara, A., 2012. Ten major rivers in monsoon Asia-Pacific: An assessment of vulnerability. Appl. Geogr. 32, 441–454. https://doi.org/10.1016/J.APGEOG.2011.05.003

Vidyasakar, A., Neelavannan, K., Krishnakumar, S., Prabaharan, G., Sathiyabama Alias Priyanka, T., Magesh, N.S., Godson, P.S., Srinivasalu, S., 2018. Macrodebris and microplastic distribution in the beaches of Rameswaram Coral Island, Gulf of Mannar, Southeast coast of India: A first report. Mar. Pollut. Bull. 137, 610–616. https://doi.org/10.1016/j.marpolbul.2018.11.007

Vroom, R.J.E., Koelmans, A.A., Besseling, E., Halsband, C., 2017. Aging of microplastics promotes their ingestion by marine zooplankton. Environ. Pollut. 231, 987–996. https://doi.org/10.1016/j.envpol.2017.08.088

Vu, A. V, Hortle, K.G., Nguyen, D.N., 2021. Factors driving long term declines in inland fishery yields in the Mekong delta. Water (Switzerland) 13. https://doi.org/10.3390/w13081005

Waldschläger, K., Born, M., Cowger, W., Gray, A., Schüttrumpf, H., 2020a. Settling and rising velocities of environmentally weathered micro- and macroplastic particles. Environ. Res. 191. https://doi.org/10.1016/j.envres.2020.110192

Waldschläger, K., Brückner, M.Z.M., Carney Almroth, B., Hackney, C.R., Adyel, T.M., Alimi, O.S., Belontz, S.L., Cowger, W., Doyle, D., Gray, A., Kane, I., Kooi, M., Kramer, M., Lechthaler, S., Michie, L., Nordam, T., Pohl, F., Russell, C., Thit, A., Umar, W., Valero, D., Varrani, A., Warrier, A.K., Woodall, L.C., Wu, N., 2022. Learning from natural sediments to tackle microplastics challenges: A multidisciplinary perspective. Earth-Science Rev. 228, 104021. https://doi.org/10.1016/j.earscirev.2022.104021

Waldschläger, K., Lechthaler, S., Stauch, G., Schüttrumpf, H., 2020b. The way of microplastic through the environment – Application of the source-pathway-receptor model (review). Sci. Total Environ. 713, 136584. https://doi.org/10.1016/j.scitotenv.2020.136584

Waldschläger, K., Schüttrumpf, H., 2019. Effects of Particle Properties on the Settling and Rise Velocities of Microplastics in Freshwater under Laboratory Conditions. Environ. Sci. Technol. 53, 1958–1966. https://doi.org/10.1021/acs.est.8b06794

Wang, C., Xing, R., Sun, M., Ling, W., Shi, W., Cui, S., An, L., 2020. Microplastics profile in a typical urban river in Beijing. Sci. Total Environ. 743, 140708. https://doi.org/10.1016/J.SCITOTENV.2020.140708

Wang, W., Wairimu, A., Li, Z., Wang, J., 2016. Microplastics pollution in inland freshwaters of China : A case study in urban surface waters of Wuhan , China. Sci. Total Environ. https://doi.org/10.1016/j.scitotenv.2016.09.213

Wang, Z., Dou, M., Ren, P., Sun, B., Jia, R., Zhou, Y., 2021. Settling velocity of irregularly shaped microplastics under steady and dynamic flow conditions. Environ. Sci. Pollut. Res. 28, 62116–62132. https://doi.org/10.1007/s11356-021-14654-3

Watkins, L., Sullivan, P.J., Walter, M.T., 2019. A case study investigating temporal factors that influence microplastic concentration in streams under different treatment regimes. Environ. Sci. Pollut. Res. 26, 21797–21807. https://doi.org/10.1007/s11356-019-04663-8

Waycott, M., Duarte, C.M., Carruthers, T.J.B., Orth, R.J., Dennison, W.C., Olyarnik, S., Calladine, A., Fourqurean, J.W., Heck, K.L., Hughes, A.R., Kendrick, G.A., Kenworthy, W.J., Short, F.T., Williams, S.L., 2009. Accelerating loss of seagrasses across the globe threatens coastal ecosystems. Proc. Natl. Acad. Sci. U. S. A. 106, 12377–12381.

https://doi.org/10.1073/pnas.0905620106

Wild, C., Huettel, M., Klueter, A., Kremb, S.G., Rasheed, M.Y.M., Jørgensen, B.B., 2004. Coral mucus functions as an energy carrier and particle trap in the reef ecosystem. Nature 428, 66–70. https://doi.org/10.1038/nature02344

Wilson, S.K., Bellwood, D.R., Choat, J.H., Furnas, M., 2021. Detritus in the epilithic algal matrix and its use by coral reef fishes. Oceanogr. Mar. Biol. An Annu. Rev. Vol. 41 287–287. https://doi.org/10.1201/9780203180570-30

Windsor, F.M., Tilley, R.M., Tyler, C.R., Ormerod, S.J., 2019. Microplastic ingestion by riverine macroinvertebrates. Sci. Total Environ. 646, 68–74. https://doi.org/10.1016/j.scitotenv.2018.07.271

Winkler, A., Nessi, A., Antonioli, D., Laus, M., Santo, N., Parolini, M., Tremolada, P., 2020. Occurrence of microplastics in pellets from the common kingfisher (Alcedo atthis) along the Ticino River, North Italy. Environ. Sci. Pollut. Res. 27, 41731–41739. https://doi.org/10.1007/s11356-020-10163-x

Woodward, J., Jiawei, L., Rothwell, J., Hurley, R., 2021. Acute riverine microplastic contamination due to avoidable releases of untreated wastewater. Nat. Sustain. 4, 793–802.

Wright, S., Galloway, Tamara Susan, Wright, S.L., Thompson, R.C., Galloway, Tamara S, 2013. The physical impacts of microplastics on marine organisms: A review Investigating microplastic contamination in coastal waters. Artic. Environ. Pollut. https://doi.org/10.1016/j.envpol.2013.02

Xue, Z., Liu, J.P., Ge, Q., 2011. Changes in hydrology and sediment delivery of the Mekong River in the last 50 years: connection to damming, monsoon, and ENSO. Earth Surf. Process. Landforms 36, 296–308. https://doi.org/10.1002/esp.2036

Yan, M., Huayue, N., K., X., He, Y., Hu, Y., Huang, Y., Wang, J., 2019. Microplastic abundance, distribution and composition in the Pearl River along Guangzhou city and Pearl River estuary, China. Chemosphere 217, 879–886.

Ye, S., Andrady, A.L., 1991. Fouling of floating plastic debris under Biscayne Bay exposure conditions. Mar. Pollut. Bull. 22, 608–613. https://doi.org/10.1016/0025-326X(91)90249-R

Yukie Mato, †, Tomohiko Isobe, †, Hideshige Takada, *,†, Haruyuki Kanehiro, ‡, Chiyoko Ohtake, § and, Kaminuma§, T., 2000. Plastic Resin Pellets as a Transport Medium for Toxic Chemicals in the Marine Environment. https://doi.org/10.1021/ES0010498

Zalasiewicz, J., Waters, C.N., Ivar do Sul, J.A., Corcoran, P.L., Barnosky, A.D., Cearreta, A., Edgeworth, M., Gałuszka, A., Jeandel, C., Leinfelder, R., McNeill, J.R., Steffen, W., Summerhayes, C., Wagreich, M., Williams, M., Wolfe, A.P., Yonan, Y., 2016. The geological cycle of plastics and their use as a stratigraphic indicator of the Anthropocene. Anthropocene. https://doi.org/10.1016/j.ancene.2016.01.002

Zettler, E.R., Mincer, T.J., Amaral-Zettler, L.A., 2013a. Life in the “Plastisphere”: Microbial Communities on Plastic Marine Debris. Environ. Sci. Technol. 47, 7137–7146. https://doi.org/10.1021/es401288x

Zettler, E.R., Mincer, T.J., Amaral-Zettler, L.A., 2013b. Life in the “Plastisphere”: Microbial Communities on Plastic Marine Debris. Environ. Sci. Technol. 47, 7137–7146. https://doi.org/10.1021/es401288x

Zhang, F., Man, Y.B., Mo, W.Y., Man, K.Y., Wong, M.H., 2020. Direct and indirect effects of microplastics on bivalves, with a focus on edible species: A mini-review. Crit. Rev. Environ. Sci. Technol. 50, 2109–2143. https://doi.org/10.1080/10643389.2019.1700752

Zhang, H., 2017. Transport of microplastics in coastal seas. Estuar. Coast. Shelf Sci.

n

ˊ.

[Page intentionally left blank]

# List of Figures

[Page intentionally left blank]

# List of Tables

[Page intentionally left blank]

# Appendices

# Appendix A: Shifting settling regimes of microplastics – supplementary material

---

Script to detect particles in images aquired with LabSFLOC camera compute their size and settling velocity. Developed by Robert Fernadez. (October-November 2020, Reviewed March 2022) R.Fernandez@hull.ac.uk

This code has enough comments that any used can pick it up and understand each step.

Potential Improvements:

1. Adjust particle size based on how blurry they are (for out of focus particles)
2. Tracking that includes potential particle rotation as it settles (for example a fibre that starts vertically and ends horizontally).

## Contents



## Clean up

Clear alt variables in the workspace

```
clearvars
% Close all open figure windows
```

## Input values

Indicate if you want the code to display intermediate results by using a value of one (1). Use any other number or character to avoid this (code will run faster if intermediate results are not displayed).

```
intRes = 1;

   Specify threshold (area in pixels^2) to discard particles in detection routines

% This value might need to be revisited depending on particle size

%expected.
aT     7000;

% Specify image size (rows - number of pixels in the vertical direction, and
  cols - number of pixels in the horizontal direction).

   NOTE: When working with images, the coordinate (x,y) = (0,0), i.e. the

   origin of the image is always the top left corner. 'x' grows to the right(co
   lumns), and 'y' grows to the bottom(rows).

rows = 1448;co
ls = 1928;
```

## Input

The code assumes that the user chooses •.tit or •.jpg files. If a different file format is chosen it will crash. Get image series file - returns the names of all files selected by the user. If only one it is returned as a string. **If** multiple as a cell. For tracking, the user MUST select more than one image. Tracking requires an image pair (at least). path - returns the folder in which those files are stored (only single path is possible)

```
[file, path] = uigetfile('*.tif', '*.jpg', 'Select an image or an image series', 'MultiSelect', 'on');


  Get number of images (nImages) in the series selected by the user

  Check if the format of file is a cell (this means that the user selected
  multiple images)

if iscell(file)

    % If true, number of images is the number of columns of the cell
    nimages = size(file,2);

elseif file ~= 0

      If false, and the value isn't zero, convert the variable file to a cell (When only

    % one image chosen, file is a string. However, it is easier to turn into a cell here than to

    % deal with multiple formats later in the code
    file= {file};

    % Number of images
```

## Detection

The steps for detection are the following:

1. Load image
2. Invert image
3. Make image binary (speeds things up)
4. Determine properties of areas within image (particles)

```
      Create array (called structure in Matlab) to store results from all images in a given image series.

The first field in the structure is the image number (within the series) and the second field is another structure that holds the properties of all particles
detected in the image. (mpProps - microplastic properties)
Type 'doc struct' or 'help struct' in the Command Window for more information about this kind of variable.

allStats = struct('image', NaN, 'mpProps', NaN);

Loop through all images in the series. If user selects one image the code
      runs only once. Otherwise it runs as many times as the numbe of chosen images.

for          1 : nImages

Call function to detect particles in image and save thier properties in a structure called mpStats (microplastic statistics). The function is included at
the end of this file (scroll down).

mpStats = rf_DetectMPs(path,file{j});

% Call function to filter out paticles that do not meet the area threshold criteria. The function is included at the end of this file (scroll down). Any parti
```

```
cles with area smaller than aT (area
threhsold) are removed from the mpStats structure. mpStats =rf_FilterDetMPs (mpStats, aT);
% Add image number to allStats structure (one row 'j' per image) allStats(j).image = j;
% Save the properties of all particles in that image as a structure in
% the second column (or second field) .allStats(j) .mpProps = mpStats;
% Following lines of code for plotting purposes only (they slow down
the code and might be ignored by setting intRes to a value different than onewhen user knows what they are doing and trusts the code).
If user wants to display intermediate results (intRes = 1) at the beginning of the code.
if intRes == 1
% Grab centroids of all particles detected in the current image (image
% j in the series)
centroids = cat(1, mpStats.Centroid);
% Grab bounding boxes of all particles detected in the current image (image j in the series). The boxes have four values. The first value
is the top left 'x' (column) coordinate of the box; the second value is the top left 'y' (row) coordinate of the box; the third value indicates
the horizontal width of the box (number of columns); the fourth column indicates the vertical height of the box (number of rows).
boxes = cat (1, mpStats.BoundingBox);
% Get the 'x' (column) coordinates of all box corners
bx = [boxes (:,1) boxes(:,1) +boxes (:1 3) boxes(:,1) +boxes (:,3) boxes(:,1) boxes(:,1)];
% Get the 'y' (row) coordinates of all box corners
by = [boxes (:,2) boxes(:,2) boxes(:,2) +boxes (:,4) boxes(:,2) +boxes (:,4) boxes(:,2)];
% Clear figure (not needed when j = 1 but needed for j > 1)elf
% Make sure images are plotted in Figure 1figure(1)
% Display image j in the series andhold on (hold on makes sure that new items added to the plot are displayed over the contents already there. Otherwise, the
new line deletes the previous contents and onlyshows the plot/image corresponding to the last line of code).
imshow(imread(fullfile(path, file{j})), hold on
% Plot particle centroids over the image.
% Centroids will be cyan crosses given by '+c')plot(centroids(:,1)1 centroids(:,2), '+c')
% Plot the bounding boxes using solid lines
% Matlab will automatically asign different colors to different boxes. plot(bx', by', '-'I
% Pause execution for 0.1 seconds to give the user enough time to see
% what the code is doing.pause(0.1)
% Last line related to intermediate results plots that maybe left out
End
```

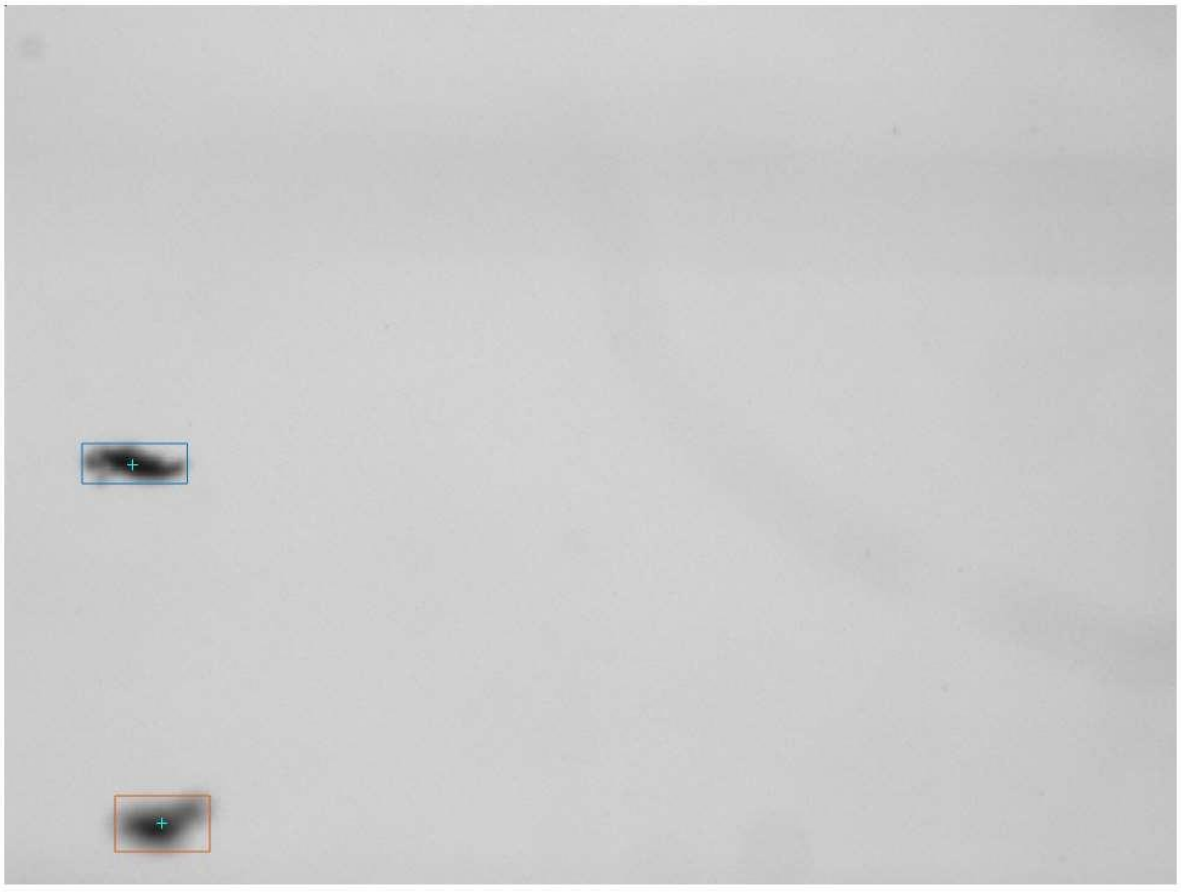

Figure A.1: Example of detection of microplastic particles by script

## Matching

Assumes particles settle without rotating. The steps for tracking are the following:
1. Read image pari
2. Grab first particle in image
3. Use bounding box of partile in Image 1 and extract a sub image (the size of the bounding box) from Image 1.
4. Compare to each particle in second image via cross-correlation
5. Identify matches and save relevent data.
6. Repeat with next particle in the image
7. Repeat with next image pair

```
    Create structure to save all information related to image pairs
    (allPairs). It contains the following fields:

    image1 - saves the number of the image within the series
    image2 - saves the number of the image within the series
    nParts1 - saves the number of particles in the first image
    nParts2 - saves the number of particles in the second image

    ccR - saves the cross correlation value (result of comparing the subimage
          extracted from image 1 with the subimages extracted from image 2). A

          positive value close to 1 means very good correlation (possible match). Smaller valuesand
          negative values indicate poor correlation (nomatch).

    file1 - stores the string containing the folder and file name of image to help ID
          later onwhen postprocessing

    file2 - stores the string containing the folder and file name of image to helpID
          later onwhen postprocessing

allPairs = struct('image1', NaN, 'image2', NaN, 'nParts1', NaN, 'nParts2', NaN, 'ccR', NaN, 'file1', NaN, 'file2', NaN);


    Loop through all image pairs (loop goes up to number of images minus one)
    NOTE: This loop could run slightly faster if all things corresponding to img2
    are assigned to img1 before next iteration (instead of re-reading the i
    mage and grabbing all values again).

    Would need to do img1 of j=1 before the loop and modify some code near
    the end of it.

if nimages>1

for i=1:nimages-1
```

```
% Grab bounding boxes of particles detected in image1 (and not filtered via aT)boxes1 = cat(1, allStats{j}.mpProps.BoundingBox);
% Grab bounding boxes of particles detected in image2 (and not filtered via aT)boxes2 = cat(1, allStats{j+1}.mpProps.BoundingBox);
Following lines of code for plotting purposes only (they slow down
the code and might be ignored by setting intRes to a value different than onewhen user knows what they are doing and trusts the code).
If user wants to display intermediate results (intRes = 1)
if intRes 1
        % Get
        bxl     the 'x' (column) coordinates for the corners of all boxes (particles) in image 1
                [boxes1(:,1) boxes1(:,1)+boxes1(:,3) boxes1(:,1)+boxes1(:,3) boxes1(:,1) boxes1{:,1)];the 'y' (row) coordinates for the corners of all boxes
                (particles) in image 1
        % Get   [boxes1(:,2) boxes1(:,2)+boxes1(:,4) boxes1(:,2)+boxes1(:,4) boxes1(:,2)];the 'x' (column) coordinates for the corners of all boxes
                (particles) in image 2
byl             [boxes2(:,1) boxes2(:,1)+boxes2(:,3) boxes2(:1l)+boxes2(:,3) boxes2(:,1) boxes2(:,1)];the 'y' (row) coordinates for the corners of all boxes
% Get           (particles) in image 2
bx2             [boxes2(:,2) boxes2(:,2) boxes2(:,2)+boxes2(:,4) boxes2(:,2)+boxes2(:,4) boxes2(:,2)];
% Getby2
```

```
% Open new figure window (Figure 2)figure (2)
% Clear figure (useless in first iteration but good to have for
% following iterations)elf
% Create a figure with two rows, one column, and work with the first rowsubplot 12 , 1, 11
% Show the first image and hold onimshow (img1) , hold on
% Plot centroids over image! as cyan crosses '+c 'plot (centroidsl (:, 1), centroidsl (:, 2), '+c')
% Plot bounding boxes over image 1 using cyan solid lines '-c'plot (bxl 1 , byl', '-c'}
% Move to second row (plot with 2 rows, 1 column, second row active)subplot (2 , 1, 2)
% Show image 2 and hold onimshow (img2) , hold on
% Plot centroids over image 2 as green stars '*g'plot (centroids 2 (:, 1), centroids2 (:, 2), '*g')
% Plot bounding boxes over image 2 using green dashed lines '--g'plot (bx 2', by 2', '--g'I
% Last liner elated to intermediate results plots that maybe left outend
% Determine number of identified particles in image (nPl) nPl = size (centroids1, 1);
% Determine number of identified particles in image (nP2)nP2 = size (centroids 2, 1);
Initialize matrix to store cross correlationr esults between
% particles in image one and potential matches (candidate particles) in
% image 2. Initial values are all zeros.R = zeros (nPl, nP2);
% Save imagel (j) number to allPairs structureallPairs (j) .image! = j;
% Save image2 (j+l) number to allPairs structureallPairs (j) . image2 = j+1;
% NOTE: The following two lines of code only work if running the code
% from Box. The '29' will need to be different if the code is moved to a different folder.
Save folder and file name of imagel (j) to allPairs structureallPairs (j). file1 = fullfile (path (29 : end), file{j});
% Save folder and file name of image2 (j+l) to allPairs structure allPairs (j) . file2 = fullfile (path (29 : end), file{ j+l ));
% Save number of particles in imagel (j) to allPairs structureallPairs (j). nParts1 = nPl;
% Save number of particles in image2 ( j+l ) to allPairs structure allPairs (j). nParts2 = nP2;

% Loop through all particles in image 1 {nPl)for k = 1 : nPl
% Determine size of bounding box of particle k in image lboxsz = [boxesl (k, 4) boxesl (k, 3)];
% Grab centroid coordinates of particle k in image lcntrdl = centroids! (k, :);
Determine the 'x, y' (column, row) coordinates for the sides of the box bounding particle k in imagel (image j)
Top row (y) - centroid position minus half the box height roundedtowards minus infinity (floor)
topl = floor (cntrdl (2)- ceil (boxsz (1)/2)); % y increases from top to bottom
% Bottom row (y) - centroid position plus half the box height
% rounded towards plus infinity (ceil)
bottoml = ceil (cntrdl (2)+ceil (boxsz (1)/2)); % y increases from top to bottom
% Left column (x) - centroid position minus half the box width rounded
% towards minus infinity (floor)
leftl = floor (cntrdl (1) - ceil (boxsz (2)/2));
% Right column (x) - centroid position plus half the box width rounded
% towards plus infinity (ceil)
rightl = ceil (cntrdl (1)+ceil (boxsz (2)/2));
% Verify that box is not touching imagel edges on any side If top side smaller than first row (y = 1) OR
If bottom side is larger than image number of rows (y = rows) OR
If left side is smaller than first column (x = 1) OR
If right side is larger than image number of columns (y cols)if topl < 1 II bottoml > rows II leftl < 1 II rightl > cols
% If true make subimgl equal to nans (Not a number NaN)subimgl = uint8 (nan (bottoml - topl +l, rightl - leftl +l));
else
If no side of bounding box near image edges
Extract sub image from imagel using the top-bottom, left-right coordinates.



subimgl = imgl (topl :bottoml , leftlrightl);

end


Following lines of code for plotting purposes only (they slow down
the code and might be ignored by setting intRes to a value different than one

when user knows what they are doing and trusts the code) . If user wants to display intermediate results (intRes = 1)
if intRes ="" 1

% Open new figure window - Figure 3figure (3)
% Clear figure (useless in first iteration but good to have for
% following iterations)elf
% Two rows, one column, go to first row

subplot (2,1,1)
% Show subimgl (small image containing particle extracted from
% image1 or black box = NaN if it was touching the edge of the original image)imshow (subimgl), hold on
% Last line related to intermediate results plots that maybe left out
end

% Loop through all particles in image2 (all candidates) for m = 1 : nP2
% Grab centroid paticles of particle m in imagecntrd2 = centroids2 (m, :);
Determine the 'x, y' (column, row) coordinates for the sides of the box bounding particle m in image2 (image j+l)
Top row (y) - centroid position minus half the box height roundedtowards minus infinity (floor)
top2 = floor (cntrd2 (2)-ceil (boxsz (1) /2)); % y increases from top to bottom
% Bottom row (y) - centroid position plus half the box height
% rounded towards plus infinity (ceil)
bottom2 = ceil (cntrd2 (2)+ceil (boxsz (1)/2)); % y increases from top to bottom
% Left column (x) - centroid position minus half the box widthr ounded
% towards minus infinity (floor)
left2 = floor (cntrd2 (1) - ceil (boxsz (2)/2));
% Right column (x) - centroid position plus half the box width rounded
% towards plus infinity (ceil)
right2 = ceil (cntrd2 (1) +ceil (boxsz (2)/2));
% Verify that boxis not touching image 2 edges on any side If top side smaller than first row(y = 1) OR
If bottom side is larger than image nl.lllber of rows (y = rows) OR
If left side is smaller than first column (x = 1) OR
If right side is larger than image nl.lllber of columns (y cols)if top2 < 1 II bottom2 > rows II left2 < 1 II right 2 > cols
% If true make subimg2 equal to nans (Not a nl.lllber NaN) subimg2 = uintB (nan (bottom 2- top2+1 , right 2- left 2+1));
else

If no side of bounding box near image edges
Extract sub image from image2 using the top- bottom,left-right coordinates.
subimg2 = img2 (top2 :bottom2, left2r: ight 2);

end


Following lines of code for plotting purposes only (they slow down
the code and might be ignored by setting intRes to a value different than one when user knows what they are doing and trusts the code).
If user wants to display intermediater esults (intRes = 1)
if intRes == 1
% Activate Figure 3 windowfigure (3)
% Two rows, one column, go to second rowsubplot (2,1, 2)
% Show subimg2 (small image containing particle extracted from
% image2 or black box = NaN if it was touching the edge of the original image)imshow (subimg2), hold on
```

```
% Pause code execution for 0.1 seconds to allow user to see
% what the code is doing.pause(0.1)
% Last linerelated to intermediater esults plots that maybe left out end
% Verify that subimgl and subimg2 have the same dimensionsif (size(subimgl) == size(subimg2))
% If true (subimgl and subimg2 have same size)
% Compute cross correlation between both subimages R(k,m) = corr2(subimgl, subimg2);
% Filter right away those particle pairs for which the
% cross correlation coefficient is les sthan minR (threshold to accept a pair of particles as a successful match)
If R < minR
if (R(k,m) <minR)
% Assign a NaN if R value suggests that particles are different. R(k,m) = NaN;
                    end
else

                    % If false (i.e. subimgl and subimg2 have different sizes)
                    % Assign NaN to the cross correlation value R(k,m) = NaN;
end

                % Clear variables before next iteration
                clear cntrd2 top2 bottom2 left2 right2 subimg2

            end


        % Clear variables before next iteration
        clear boxsz cntrdl topl bottoml leftl rightl subimgl

    end


Save all cross correlation results (matrix with nPl rows and nP2columns) to the allPairs structure.




        allPairs(j).ccR = R;

        % Clear variables before next iteration

        clear Rimgl img2 centroidsl centroids2 boxes! boxes2 bxl bx2 byl by2

end
end
```

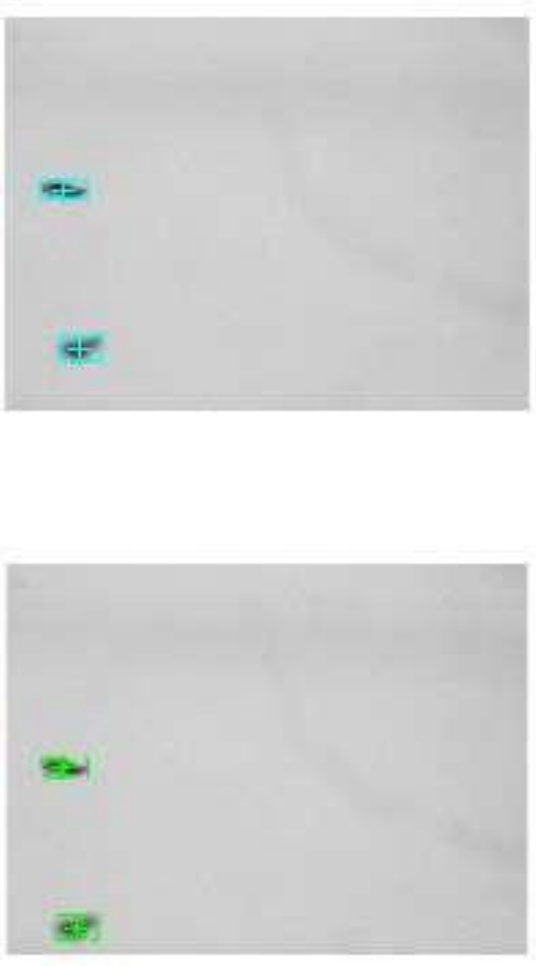

Figure A.2: Example of particles being matched by scrip

## Displacements and Areas

### Compte displacements of successfully matched particles and save their relevent details as results (mpTracks)

```
    Create matrix to save all information related to particle
    tracking(mpTracks). It contains the following columns:

    cxl - stores the 'x' coordinate (column) of a particle in
    image 1cyl - stores the 'y' coordinate (row) of a particle in
    image 1

    cx2 - stores the 'x' coordinate (column) of the same particle in
    imagecy2 - stores the 'y' coordinate (row) of the same particle
    in image 2dy - displacement in 'y' (associated to fall velocity)

    al - area of particle in image 1

    a2 - area of same particle in

image 2mpTracks = nan(l,7);



%Initialize results
variableresults = [NaN NaN]
;

% Loop through all image
pairsfor = 1:nimages-1

      Go through all pairs and compute displacements between frames
      .Find indices for matched microplastic particles (those
      locationswhere ccR is not NaN)
```

```
        % Grab centroids of particles detected in image 2

        centroids2 = cat(1,allStats(j+l).mpProps.Centroid);

        % Grab 'x' coordinate of centroids (for particle tracki
        ng)cxl = centroidsl(piml,1);

        cx2 = centroids2(pim2,1);

        % Grab 'y' coordinate of centroids to compute
        displacements cyl = centroidsl(piml,2);

        cy2 = centroids2(pim2,2);

        % Compute vertical displacements between matched particles (only in

        % 'y' not total displacements
        ).dy = cy2-cyl;

        % Grab area of particles detected in image!
        areasl = cat(l, allStats(j).mpProps.Area)
        ;

        % Grab area of particles detected in
        image2areas2 = cat(1,allStats(j+1).mpProps.
        Area);



        al = areasl(piml
        );a2 = areas2
        (pim2);

        % Concatenate intermediate results

        intResult = [cxl cyl cx2 cy2 dy al a2];

        % Get rid of particles with fall velocities smaller or equal to

        % zero (not moving or moving upwards).
```

## Tracking

### Go through all matched particles and identify if same particle is matched in more than one image pair (i.e. track it)

```
% Obtain total number of particle matches
mpTotal = size(mpTracks, 1);

% Add column to mpTracks to include particle idmpT
acks = [zeros(mpTotal,1) mpTracks];

% Initialize particle counter
mpCounter = 1;

% Give row 1 a particle ID of 1mp
Tracks(1,1)=1;


   The routine below has too many if-else statements and I am sure there is
   a more elegant solution. It started as a simple if statement but th
   ough debugging and having issues with certain image series it became messy.

   Loop through all particles to tack centroids
for  j=2:mpTotal

    % Find the column that has a cxl == cx2 (same 'centroid 'x' coordinate in current and previou image).posx
    = find(mpTracks(j,2) == mpTracks(:,4));

    % Find the row that has a cyl == cy2 (same 'centroid 'y' coordinate in current and previous image).if
    isempty(posx)

        % Increase the counter by one
        mpCounter = mpCounter + 1;

        % Assign new particle ID mp
        Tracks(j,1) = mpCounter;

    else

        posy = find(mpTracks(j,3) == mpTracks(:,5));

        % If no matches found or if ther ows for x,y do not matchif
        isempty(posy)

            % Increase the counter by one
            mpCounter = mpCounter + 1;

            % Assign new particle ID mpTr
            acks(j,1) = mpCounter;

          Else, if matches found
        elseif posx ~= posy

            % Increase the counter by one
```

## Independent Particle Results

### Get median displacement and median area for particles ifentifed in multiple image pairs

```
% Max number of individual particles detected
andmatchedmaxID == max (mpTracks(:,1));
```

```
% Create a figure to plot trajectories
figure(4)

set(gca,'ydir','reverse')
xlirn([0 cols]);

ylim([0 rows]); hold
on


% Loop through all particle IDs
for j = 1:maxID

    % Find all rows in rnpTracks corresponding to the same particle ID id
    = find(rnpTracks(:,1)==j);

    % Plot trajectory

    plot(rnpTracks(id, 2), rnpTracks(id,3), 'o')

    % Add plot labels

    xlabel('Image column (pixels]')
```

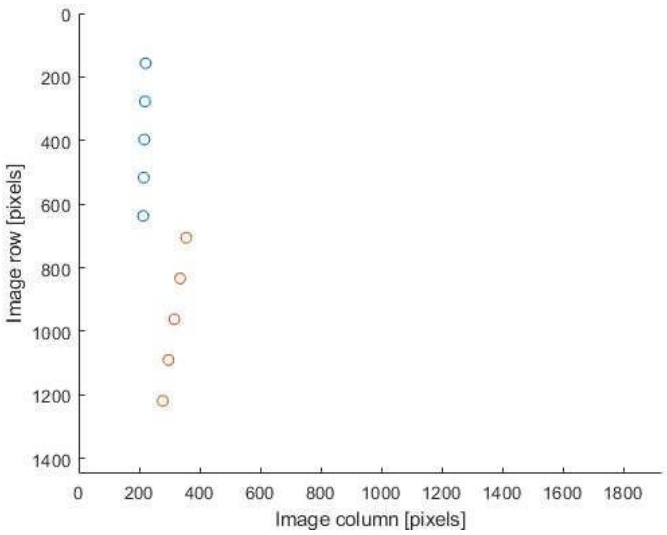


Figure A.3: Example of trajectory plot of particles by script

## Output

Write results to spreadsheet. Newer versions of Matlab prefer to use 'writematrix' instead of 'xlswrite' but my current version predates the change.

```
[outfile,outpath] = uiputfile('*.xlsx', 'Save Results', 'results.xlsx');if
outpath ~= 0

    outfilename = fullfile(outpath,outfile);
    xlswrite(outfilename, mpTracks);

    xlswrite(outfilename, mpSummary, 2)

    save(fullfile(outpath,outfile(1:end-5)), 'mpSummary', 'mpTracks', 'allStats', 'allPairs')
```

## Detection Function

The funcron recieves two strings:
Path-folder in which the image is strored
File-name of the image and an integer
After readking the image and makign it binary, the code determines the propertied of the partilces in the image by using Matlab's regeionprops function.

```
function [stats] = rf_DetectMPs(path, file)

%rf_DetectMPs finds particles in a grayscale image

    % Read greyscale image

    img = imread(fullfile(path, file));

    % Invert image (darker shades become lighter and vice versa)
    invimg = 255-img;

    % Convert image to black and white only

    BW = imbinarize(invimg, 'adaptive', 'Sensitivity', 0.3);

    %BW = imbinarize(invimg, 'global');s
      ubplot(1,3,1),     imshow(img)
      subplot(1,3,2),imshow(invimg)
```

## Post-Detection Filtering

Filter results of detected particles in images. Need to filter particles whose bounding box is near the edge of the image
Filter based on particle size first then bounding box

```
    areaThreshold - integer value used to filter out 'patides'
    misidentified by the code. Any particle with an area (in pixel^2)
    smaller than areaThreshold will be removed.


    Before returning the statistics (stats) of the particles, the codef
    ilters the results to remove misidentified particles.

function [stats] = rf_FilterDetMPs(stats, areaThreshold)

% Create an array function to apply to all entries in the stats structure
fun = @(x)    stats(x).Area < areaThreshold;

% Identify all stats entries that have an area smaller than
%   areaThreshold
```

*Published with MATLAE:m R2018a*

Table A.1: Overview of previous microplastic settling experiments

| Source | Setup | Polymer(s) | Particle size range (mm) | Shape | Clean/Biofilm | Salinity | Sinking rate |
|---|---|---|---|---|---|---|---|
| Ballent et al (2012) | 1m water column and video analysis | Non-buoyant high density preproduction (not specified) | ~5.0 | Pellets (spheres) | Unspecified (from a sample) | 36 | 28 mm/s |
| Kowalski et al (2016) | Atterberg cylinders of 40 cm height and 7.5 cm diameter and stopwatch measuring time to travel distance of 10cm | PS, PA, polymethyl methacrylate (PMMA), PET, polyoxymethylene (POM), PVC | 0.3-2.6 | Cylindrical, nodular, angular, think flakes, elongate | "Non-aged" (clean) | 0,15,36 | 91 × 10−3 ms/3 |
| Bagaev et al (2017) | 50ml glass vial filled with distilled water, time taken for particle to sink 20cm measured with a stopwatch | Synthetic fibres, taken from field samples | N/A for all tested but uses 8.0mm as an example | Fibres | Biofilm (field samples) | 0 | 0.9 ± 0.8 mm/s. |
| Kaiser et al (2017) | Atterberg cylinders of 40 cm height and 7.5 cm internal diameter at a temperature of about 20 ◦C. Time taken to travel 2 x 10cm distance was mesured | PS & PE | 1.0 | Cylindrical | Clean and biofilmed | 10,9.9,36 | 0.009-0.017m s-1 |
| Khatmullina & Isachenko (2017) | Glass column 110cm height and cross section of 18 x 18cm filled with distilled water with stop watch | Polycaprolactone (PCL) & aged fishing line | 0.15-0.71 | Spheres, cylinders &fishing line (fibres?) | Clean | 0 | 5-127mm/s |
| Mohlenkamp et al (2018) | 1m settling column. Aggregates (MP + diatom cells + river sediment) photographed every 2 seconds for 60 minutes. | Microbeads (polymer not specified) from cosmetics | 0.022-1.589 | Spherical, elliptical | Clean | 0,34 | 53-559m d-1 |
| Hoellein et al. (2019) | Experimental stream: mean width 48 cm (±1.8) and depth of 3.7 cm (±0.2), lined with a substrate of uniformly-sized pea gravel (D50 = 0.5 cm) with constant discharge 1.45 L/s | PP, PS, Acrylic | 1.0-3.0 | Pellets , fragments, fibres | Clean and biofilmed | n/a | 0.61 (±0.48) mm/s. |
| Kaiser et al (2019) | A camera recorded the trajectory of a particle through a sealed photometric cuvette (10 × 10 × 150 mm) jacketed by a water chamber for temperature control (100 mm high, 50 mm edge length, 1 mm wall thickness). | PA, PMMA, PET | 0.006-0.251 | Fragments | Clean | 0,15,36 | 0.42-117.68m/d |
| Waldschlgaer & Schüttrumpf (2019) | Plexiglass water column (20x20x100cm) with settling and rising velocity observed with digital camera | PE, PP, PS (EPS), PVC, PET, and PP&A-fibers | 0.3-5.0 | Fibres, pellets, spheres, fragments | Clean | 0 | 3.9-314mm/s |
| Van Melkebeke et al (2020) | Cylindrical settling column 45cm height, 10cm diameter, time to settle recorded with high dynamic range (HDR) camera at 100 frames/s | PET, HDPE, PP, PS, PE, PVC | 0.63-3.48 | Granular, film, fibre | Clean and biofilmed | 0 | 4.5-104.7mm/s |
| Waldschlgaer et al (2020) | Plexiglass water column (20x20x100cm) with settling and rising velocity observed filled with DI water with digital camera | PE,PP,PS,PVC, PET,EPS | 0.58-30.81 | Spheres, pellets, fragments and fibres | Biofilm (field samples) | 0 | 0.16-3.52cm/s |
| Anderson et al (2021) | Settling tubes 1m long with diameter of 50mm | PVC | 0.063-0.125 | Fragments | Clean | 9.4-15.6 | 0.09 ± 0.03 mm s21, |
| Elagami et al (2022) | Glass column of 18x18cm cross section and height 1.1m and high speed camera | PS, PA66, PVC, PCL, PLLA, PBAT | 0.15-2.2 | Fragments | Clean and biofilmed | 0 | 0.3-0.5mm/s |
| Ngyyen et al (2022) | 2x12x16 cm acrylic settling column with camera | PET | 1-6 | Fibres | Clean | 0 | 0.1-0.55mm/s |
| This study | LabSFLOC Plexiglass column with dimensions of 12cm x 12cm x 33cm combined with a LED light panel and high-resolution video camera | PET, PVC, NP&A | 0.02-4.94 | Fragments and fibres | Clean and biofilmed | 0,18,30 | 4-25.6mm/s |

Table A.2: Summary of statistical analysis (post hoc analysis with lmeans package, Tukey adjusted) between all variables and microplastic types

| Comparison | Microplastic type | | |
|---|---|---|---|
| | PET | PVC | NP&A fibres |
| BIOFOULING | | | |
| Clean vs Biofilm SAL0 | p<0.001 | - | - |
| Clean vs Biofilm SAL18 | p<0.001 | - | - |
| Clean vs Biofilm SAL30 | p<0.001 | p<0.001 | p=0.0116 |
| Clean vs Biofilm 0mg | p<0.0001 | p<0.001 | - |
| Clean vs Biofilm 100mg | p=0.0215 | - | - |
| Clean vs Biofilm 400mg | p<0.001 | - | p<0.0001 |
| Clean vs Biofilm 600mg | p<0.001 | p<0.001 | - |
| SALINITY | | | |
| Clean SAL0 vs Clean SAL18 | p=0.0108 | - | - |
| Clean SAL0 vs Clean SAL30 | - | p=0.301 | - |
| Clean SAL18 vs Clean SAL30 | p=0.0084 | - | - |
| Biofilm SAL0 vs Biofilm SAL18 | - | p=0.0167 | - |
| Biofilm SAL0 vs Biofilm SAL30 | p=0.0089 | - | - |
| Biofilm SAL18 vs Biofilm SAL30 | - | - | - |
| CLAY CONCENTRATION | | | |
| Clean 0mg vs 100mg | - | - | - |
| Clean 0mg vs 400mg | - | p=0.0142 | - |
| Clean 0mg vs 600mg | - | p<0.001 | - |
| Clean 100mg vs 400mg | - | - | p<0.0001 |
| Clean 100mg vs 600mg | - | - | - |
| Clean 400mg vs 600mg | - | - | - |
| Biofilmed 0mg vs 100mg | p=0.0001 | p=0.0001 | p=0.0058 |
| Biofilmed 0mg vs 400mg | - | p<0.0001 | p=0.0001 |
| Biofilmed 0mg vs 600mg | p=0.0270 | p=0.0181 | p=0.0008 |
| Biofilmed 100mg vs 400mg | - | - | - |
| Biofilmed 100mg vs 600mg | - | - | - |
| Biofilmed 400mg vs 600mg | | - | - |

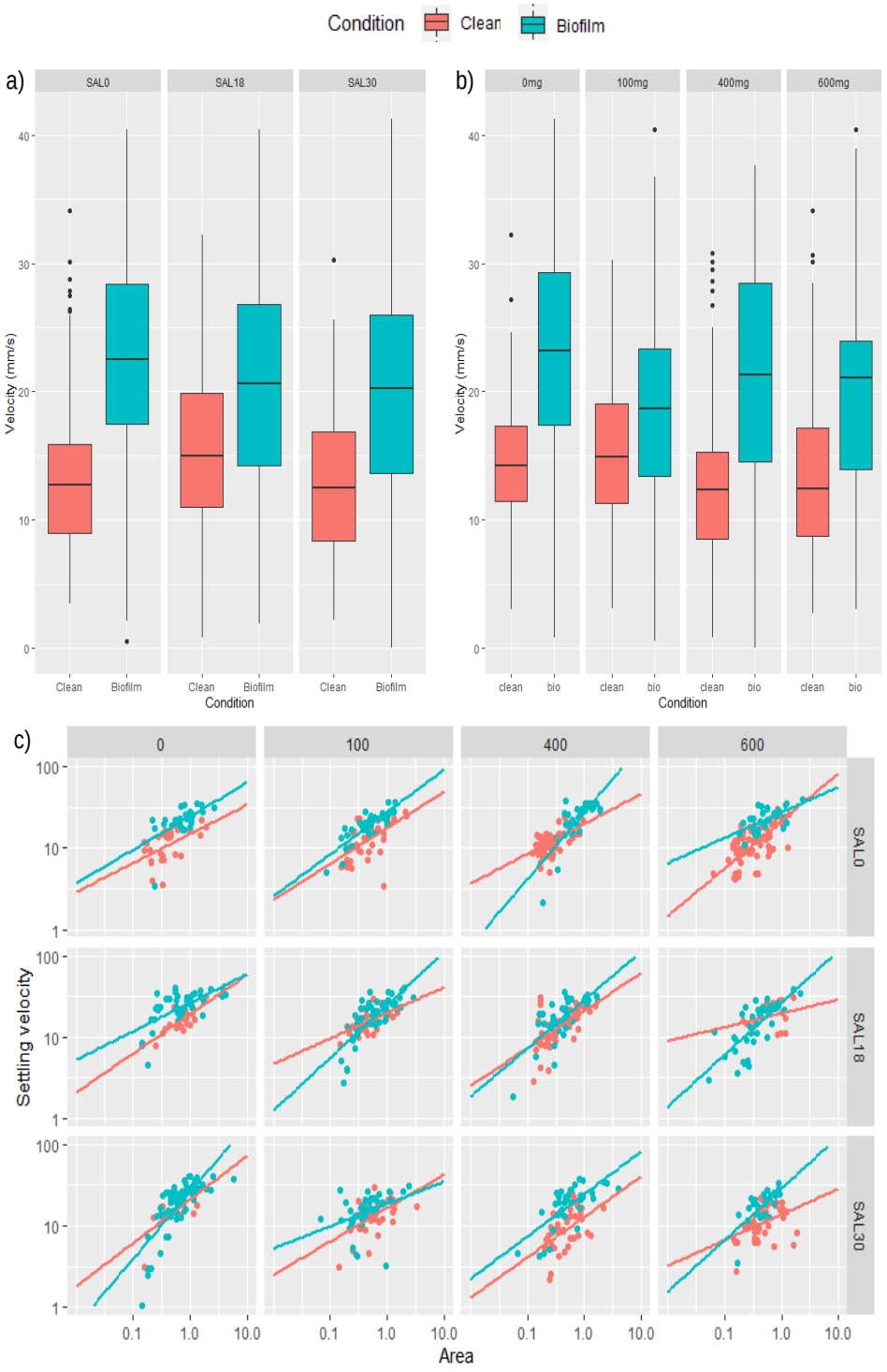


Figure A.4: The settling velocity of clean and biofilmed PET fragments a) under different salinities from SAL0-30, b) various sediment concentrations from 0-600mg/L and c) verses particle area under all salinity and clay conditions

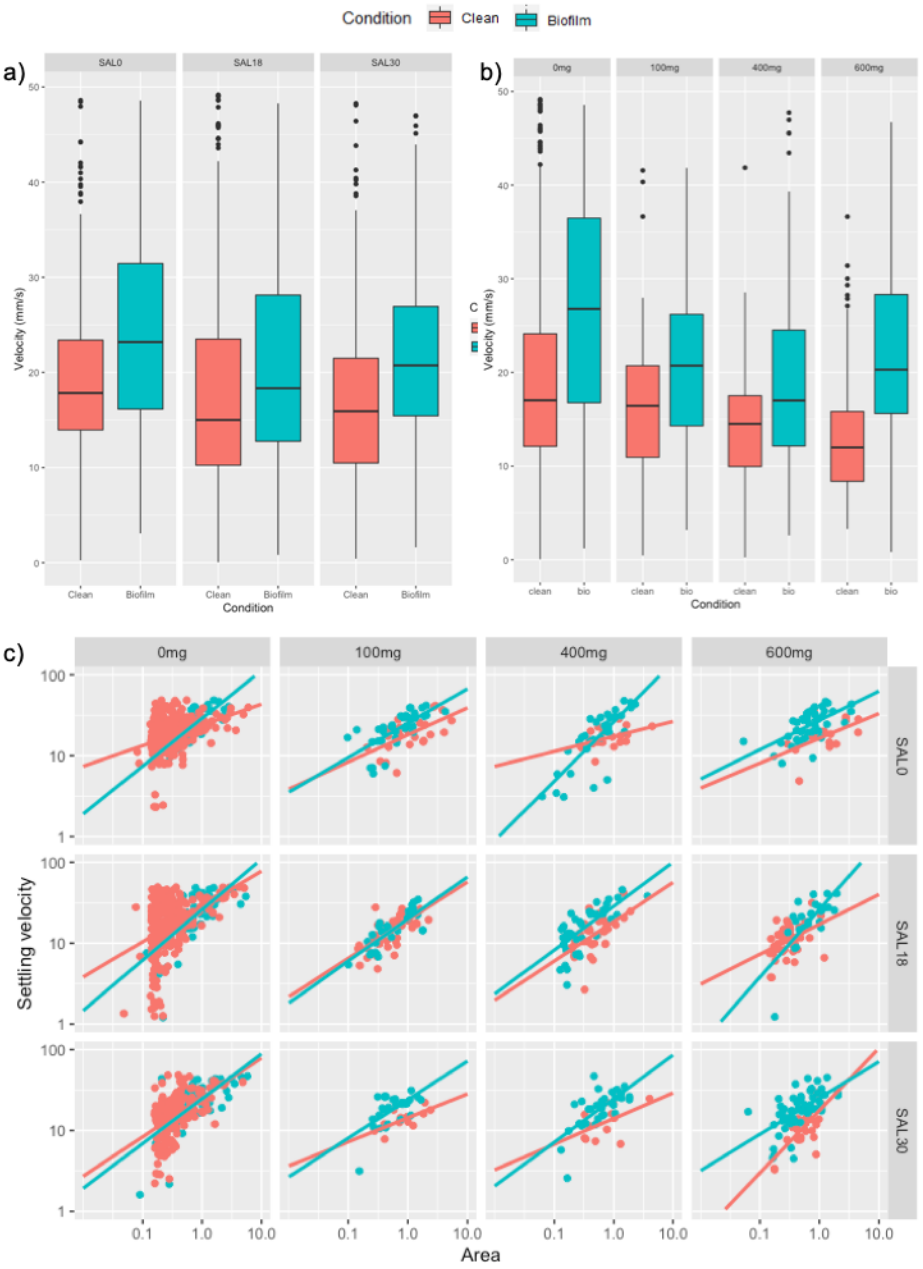


Figure A.5: The settling velocity of clean and biofilmed PVC fragments a) under different salinities from SAL0-30, b) various sediment concentrations from 0-600mg/L and c) verses particle area under all salinity and clay conditions

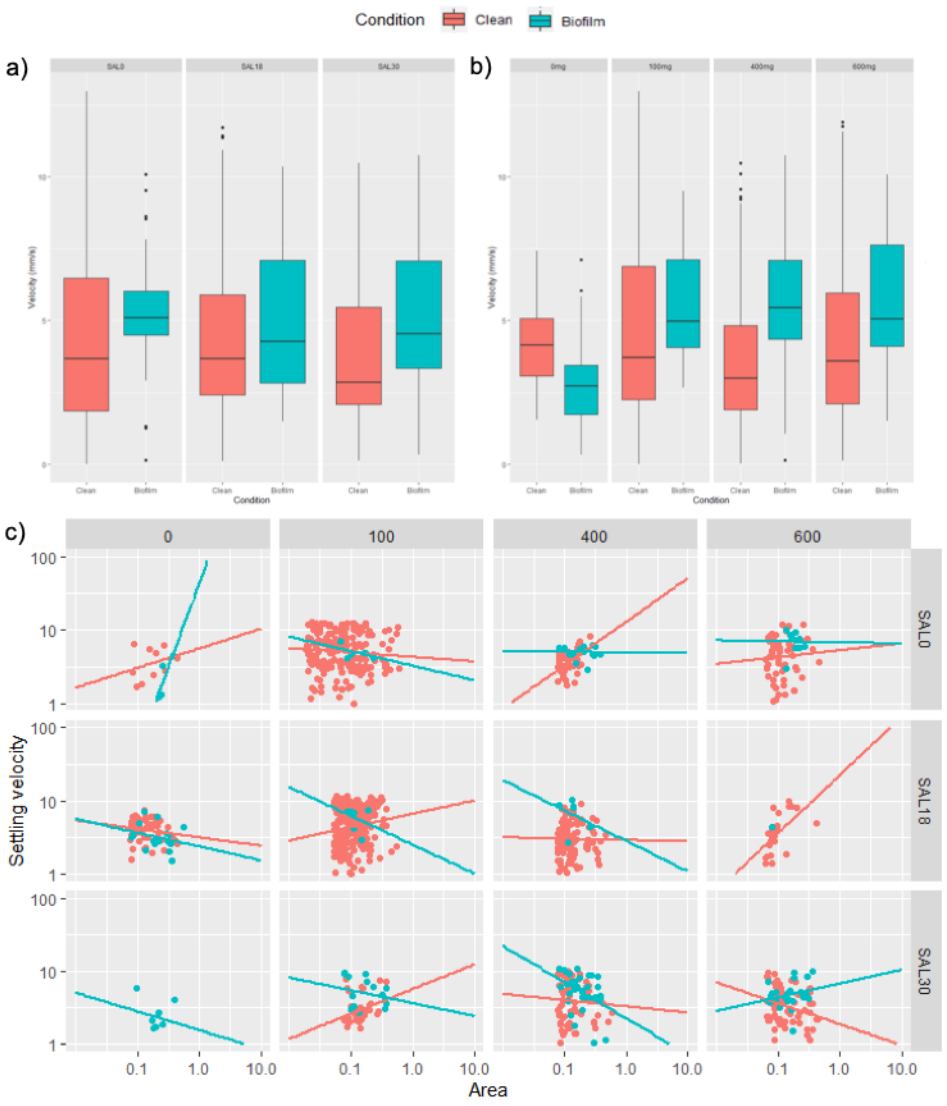


Figure A.6: The settling velocity of clean and biofilmed fibres a) under different salinities from SAL0-30, b) various sediment concentrations from 0-600mg/L and c) verses particle area under all salinity and clay conditions

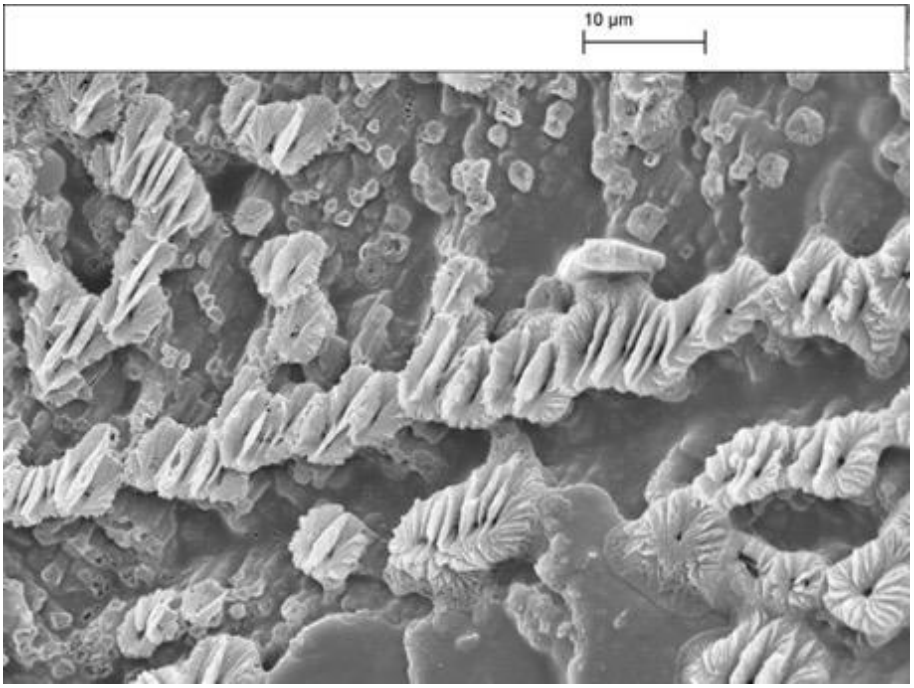


Figure A.7: Clean PET fragment after clay mixing

Figure A.8: Example of fibres clumping together: clean, SAL30, 600mg clay

[Page intentionally left blank]

# Appendix B: The transport and vertical distribution of microplastics in the Mekong River, Southeast Asia - Supplementary Material

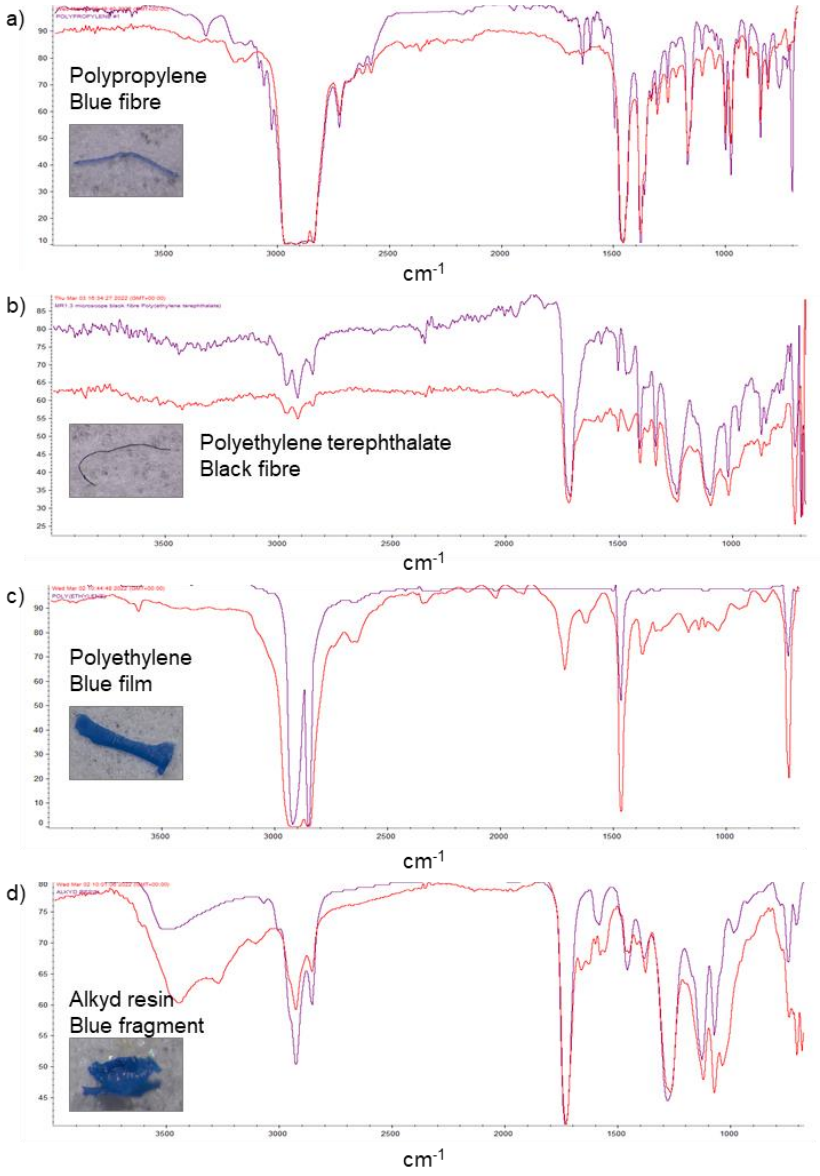


Figure B.1: Examples of FT-IR spectra of microplastics observed in samples a) polypropylene (PP) blue fibre b) polyethylene terephthalate (PET) black fibre, c) polyethylene (PE) blue film and d) alkyd resin classified as “other” blue fragment

[Page intentionally left blank]